Role of receptor activator of NF-kB ligand (RANKL) in adult lymph node homeostasis and identification of inhibitors

Mélanie Chypre

UNIVERSITÉ DE STRASBOURG

ÉCOLE DOCTORALE DES SCIENCES DE LA VIE ET DE LA SANTE

THÈSE présentée par :

Mélanie CHYPRE

Soutenue le : **10 Mai 2017**

pour obtenir le grade de : **Docteur de l'université de Strasbourg**

Discipline/ Spécialité : Aspects moléculaires et cellulaires de la biologie/Immunologie

---

Role of receptor activator of NF-kB ligand (RANKL) in adult lymph node homeostasis and identification of inhibitors

---

THÈSE dirigée par :

Dr. MUELLER Christopher	IBMC, CNRS UPR 3572

RAPPORTEURS :

Dr. DEJARDIN Emmanuel	Laboratory of Molecular Immunology and Signal Transduction, GIGA-Research, Université de Liège, Belgique
Dr. BARONE Francesca	Institute of Inflammation and Ageing, University of Birmingham, UK

EXAMINATEUR :

Dr. CHAN Susan	IGBMC, INSERM U964/ CNRS UMR7104, Illkirch-Graffenstaden

Remerciements

First of all, I would like to thank the members of my jury Dr. Francesca Barone (University of Birmingham, UK), Dr. Emmanuel Dejardin (University of Liège, Belgium) and Dr. Susan Chan (IGBMC, Strasbourg) for having accepted to evaluate my work.

Je remercie la société Prestwick Chemical (PC SAS) d'avoir continué à me soutenir financièrement et d'avoir ainsi rendu cette thèse possible. Je remercie plus particulièrement le Dr. Christophe Morice d'avoir suivi mon travail et d'avoir siégé au jury en tant que membre invité.

Je remercie le Pr. Sylviane Muller, directrice de l'unité Immunopathologie et chimie thérapeutique (UPR 3572), d'avoir accepté de m'accueillir dans son laboratoire.

Je tiens à remercier tout particulièrement mon directeur de thèse, le Dr. Christopher Mueller pour m'avoir encadré durant ces 3 années. J'ai parfois eu du mal à te suivre dans tes idées un peu folles, mais tu as su être là lorsque j'en avais besoin au milieu des multiples projets. Merci pour l'autonomie que tu m'as laissée et la confiance que tu m'as accordée dès les premiers jours dans ton équipe. Merci pour les team-meetings auxquels tu tiens tant, ce sont des moments d'échange d'idées qui sont importants pour faire vivre une équipe.

Merci à tous les membres passés et actuels de l'équipe. Merci à Vincent pour tes conseils surtout pour la cytométrie qui m'était totalement inconnue à mon arrivée ici. Merci à Janina et Farouk pour l'aide dans les nombreuses manips. Janina, j'ai beaucoup aimé t'encadrer pendant ton master, je souhaite à d'autres d'avoir un stagiaire aussi efficace que toi! Bonne chance pour la suite de ta thèse! Merci à Olga de m'avoir montré une grande partie des expériences avant son départ. Merci à Ben de m'avoir aussi montré certaines manips.

Merci à Monique et Delphine pour tout le travail que vous avez fait avec les multiples lignées de souris et injections en tout genre. C'était toujours un plaisir d'aller à l'animalerie avec vous. Merci à Astrid pour ton aide précieuse, les commandes et toutes les petites choses qui rendent nos manips possibles. Merci à Hayet d'assurer les stocks du labo avec Astrid et pour nos conversations en tout genre.

Merci à Isabelle pour ton aide dans l'organisation des missions et autres aspects logistiques.

Merci à Nathalie pour toutes les manips que l'on a faites ensemble, on a fini par réussir à le publier ce papier!

Table of content

List of abbreviations

A:

ACKR: atypical chemokine receptor

ADAM: a disintegrin and metalloproteinase

Ag: antigen

Aire: Autoimmune regulatory element

AMD: age-related macular degeneration

AP-1: activator protein 1

APC: antigen presenting cells

ARO: autosomal recessive osteopetrosis

B:

BEC: blood endothelial cells

BM: bone marrow

BMP-2 : bone morphogenic protein 2

C:

CCL: chemokine (C-C motif) ligand

CCR: chemokine (C-C motif) receptor

CHO: chinese ovary hamster

CI2MDP: dichloromethylene diphosphonate

CLCA: Chloride channel accessory 1

CLEVER-1: common lymphatic endothelial and vascular endothelial receptor-1

CRAC: calcium release activated channels

CRD: cysteine rich domains

CSF-1: colony stimulating factor-1

c-SRC: cellular sarcoma

CXCL: chemokine (C-X-C motif) ligand

CXCR: chemokine (C-X-C motif) receptor

D:

DAG: diacylglycerol

DAP: DNAX-activating protein

DC: dendritic cell

DcR1: decoy receptor 1

DcR2: decoy receptor 2

DD: death domain

DDH: death domain homologous

DNA: deoxyribonucleic acid

DR4: death receptor 4

DR5: death receptor 5

DT: diphtheria toxin

DTR: diphtheria toxin receptor

E:

E.coli: Escherichia coli

ECM: extracellular matrix

EGF: epidermal growth factor

ELISA: enzyme-linked immunosorbent assay

ER: endoplasmic reticulum

ERK: extracellular-signal-regulated kinase

F:

FADD: Fas-associated DD

FAE: follicle associated epithelia

FCRγ: Fc receptor common γ subunit

FDC: follicular dendritic cells

FEO: familial expansile osteolysis

FRC: fibroblastic reticular cells

G:

GAB2: growth factor receptor-bound protein 2-associated binding protein

GALT: gut-associated lymphoid tissues

Glu: glutamine

GPCR: G Protein coupled receptors

GRB2: growth factor receptor bound protein 2

GCTB: giant-cell tumor of the bone

H:

HDL: high density lipoprotein

HEV: high endothelial venules (HEV)

HSC: hematopoietic stem cells

I:

ICAM: InterCellular Adhesion Molecule

IDO : *indoleamine* 2,3-dioxygénase

IFN: interferon

IFNAR : interferon-α/β *receptor*

IFP : interstitial fluid pressure

Ig: immunoglobulin

IGF-1: insulin growth factor 1

IKK: IκB kinase

IL: interleukin

IRF : Interferon regulatory factor

IRF-7: Interferon-regulatory factor 7

IRI : ischemia reperfusion injury

ITAM: immunoreceptor tyrosine based activation motif

ITGA2b: integrin alpha-IIb

J:

JB: Jolkinolide B

JNK: c-Jun N-terminal kinase

K:

KO : knockout

L:

LCMV: lymphocytic choriomeningitis virus

LEC: lymphatic endothelial cells

LFA-1: Lymphocyte function-associated antigen 1

LGR4: leucine-rich repeat-containing G-protein-coupled receptor 4

LN: lymph node

LPS: lipopolysaccharide

LT: lymphotoxin

LXR: liver X receptor

M:

M cells: Microfold cells

mAb: monoclonal antibody

MAC-1 : Macrophage-1 antigen

MAdCAM-1: mucosal vascular addressin cell adhesion molecule 1

MALT: mucosal associated lymphoid tissues

MAP3K: MAPK kinase kinase

MAPK: mitogen activated protein kinase

MAPKK: MAP kinase kinase

MARCO: macrophage receptor with collagenous structure

MCM: medullary cord macrophages

MCMV: murine cytomegalovirus

M-CSF: macrophage colony-stimulating factor

MEC: mammary epithelial cells

MEK: MAPK/ERK kinase

MHC: major histocompatibility complex

MMM: metallophilic macrophages

MMP: matrix metalloproteinases

MR: mannose receptor

MRC: marginal reticular cells

MR-L: ligands for the cystein-rich domain of mannose receptor

mRNA: messenger RNA

MSM: medullary sinus macrophages

MSR1: Macrophage scavenger receptor 1

mTECs: medullary thymic epithelial cells

MZM: marginal zone macrophages

N:

NEMO : NF-kB Essential Modulator

NFAT: nuclear factor of activated T cells

NF-κB : nuclear factor-kappa B

NIK: NF-κB inducing kinase

NK: natural-killer

NO: nitric oxide

NRP2: neuropilin 2

O:

OB: osteoblasts

OC: osteoclasts

OCIF: osteoclastogenesis inhibitory factor

ODAR: osteoclast differentiation and activation receptor

ODF: osteoclast differentiation factor

ODFR: osteoclast differentiation factor receptor

ONJ: osteonecrosis of the jaw

OPG: osteoprotegerin

OPGL: OPG ligand

P:

PDB: Paget's disease of the bone

PDL: programmed death ligand

Pdpn: podoplanin

PI3K: phosphoinositide 3-kinase

PIP2: phosphatidylinositol 4,5 biphosphate

PIP3: phosphatidylinositol 1,4,5 triphosphate

PKB: protein kinase B

PLCγ: phospholipase C γ

PLVAP: plasmalemma vesicle-associated protein

PMA: phorbol myristate acetate

PNAD: Protein NH2-Terminal Asparagine Deamidase

PNAD: *Protein* NH2-Terminal Asparagine Deamidase

Pro: proline

Prox1: prospero homeobox 1

PRR: pattern recognition receptor

PTA: peripheral tissue restricted antigens

PTH: parathyroid hormone

R:

RA: rheumatoid arthritis

RANK: receptor activator of NF-κB

RANKL: receptor activator of NF-κB ligand

RBC : red blood cells

RIP1: receptor interacting serine/threonine kinase 1

RLN: regional lymph node

RNA: ribonucleic acid

RPM: red pulp macrophages

RRI: RANK receptor inhibitor

S:

S1P: sphingosine-1-phosphate (S1P)

S1PR1: sphingosine-1-phosphate receptor type 1

scFv : single chain fraction variable

SCS: subcapsular sinus

Siglec-1: sialic acid binding lectin

SIGN-R1: DC-SIGN-related protein 1

SLO: secondary lymphoid organs

SMC: smooth muscle cells

SRE: skeletal related events

SSM: subcapsular sinus macrophages

STAT1: signal transducer and activator of transcription 1

T:

TAB1: TAK1 binding protein

TACE: metalloprotease-desintegrin TNFα convertase

TAK1: TGF-β activated kinase

TAM: tumor-associated macrophages

TCR: T cell receptor

tEVs: tumor-derived extracellular vesicles

TGF-β: transforming growth factor β

THD: TNF homology domain

TLO: tertiary lymphoid organs

TLR: toll-like receptor

TM: transmembrane domain

TNF: tumor necrosis factor

TNFRSF: tumor necrosis factor receptor super family

TNFSF: tumor necrosis factor super family

TRADD: TNFR-associated DD

TRAF: TNFR-associated factors

TRAIL: TNF-related apoptosis-inducing ligand

TRANCE: TNF-related activation induced cytokine

TRANCE-R: TNF-related activation induced cytokine

TRAcP: Tartrate-resistant acid phosphatase

Treg: regulatory T cells

TSA: tissue specific antigens

U:

Ub: ubiquitin

V:

VCAM-1: Vascular cell adhesion *protein* 1

VE-cadherin: vascular endothelial cadherin

VEGF: vascular endothelial growth factor

VEGI: vascular endothelial cell growth inhibitor

VSV: vesicular stomatitis virus

VV: vaccinia virus

Résumé en Français

Introduction :

Le récepteur membranaire RANK (receptor activator of NF-κB), membre de la famille des récepteurs du TNF (tumor necrosis factor), est activé suite à l'interaction avec son ligand RANKL. Les deux molécules ont été découvertes pour leur implication dans l'homéostasie de l'os [1,2]. RANKL existe sous une forme soluble ou liée à la membrane cellulaire, comme les autres membres de la famille du TNF, il forme un homotrimère qui se lie à RANK induisant ainsi la trimérisation du récepteur. L'ostéoprotégérine (OPG) est un récepteur leurre qui se lie à RANKL et empêche l'activation de RANK. OPG se lie aussi avec une plus faible affinité à un autre ligand nommé TRAIL qui joue un rôle dans l'apoptose cellulaire. La stimulation de RANK conduit à l'activation de la cascade NF-κB, mais aussi de Akt, JNK, MAPK ou encore ERK [3].
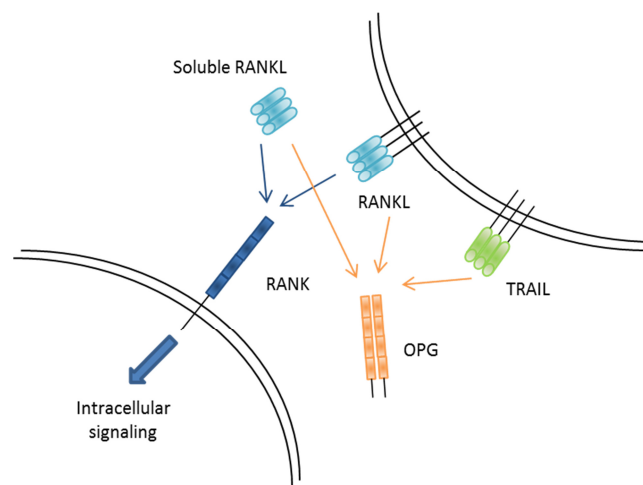
Figure 1: Représentation de l'interaction entre les membres de la triade RANK/RANKL/OPG. RANKL soluble ou lié à la membrane se lie à RANK ce qui induit une signalisation intracellulaire. OPG est un récepteur leurre qui se lit à RANKL empêchant l'activation de RANK. OPG se lie aussi à TRAIL, un ligand activant l'apoptose des cellules qui exprime le récepteur TRAIL-R.

RANK induit une différenciation des cellules de la lignée myéloïde en ostéoclastes, macrophages spécialisés dans la résorption de la matrice osseuse [3]. Ainsi, les souris déficientes pour RANK ou RANKL ont une plus grande densité osseuse et sont atteintes d'ostéopétrose [4,5]. A l'opposé, les souris déficientes pour OPG sont atteintes d'ostéoporose et présentent une plus faible densité

osseuse [6]. RANK joue également un rôle dans l'immunité, sa présence sur les cellules dendritiques a été observée dans les premières recherches décrivant ce récepteur mais un rôle *in vivo* reste à être démontré. RANK sur les cellules dendritiques interagit avec RANKL exprimé à la surface des cellules T activées et participe à la survie des cellules dendritiques [7]. RANK et RANKL sont également indispensables pour le développement des ganglions lymphatiques puisque l'absence de ces organes lymphoïdes secondaires a été observée chez les souris déficientes pour RANK et RANKL [4,5]. RANK active aussi la prolifération des cellules épithéliales, et joue donc un rôle dans la formation et la métastase des tumeurs [8,9].

Deux principales approches ont été développées pour cibler l'axe RANK/RANKL et ainsi inhiber les effets pathologiques de cette voie. L'une consiste à bloquer la signalisation induite par l'activation de RANK, l'autre consiste à bloquer l'interaction entre RANK et son ligand. Plusieurs molécules et peptides inhibant la signalisation induite par RANK ont été développés [10–15]. Ces molécules inhibent pour la plupart l'ostéoclastogenèse. Des peptides fusions tels que OPG-Fc et RANK-Fc ont également été développés pour empêcher RANKL de se lier au récepteur [16]. Des peptides basés sur la séquence responsable de la liaison à RANKL de OPG ou de RANK ont également été décrits [17–19]. D'autre part, à ce jour, un anticorps thérapeutique ciblant RANKL appelé denosumab est sur le marché pour le traitement de l'ostéoporose et la métastase osseuse de certains cancers. Cependant, à notre connaissance aucune petite molécule inhibant l'interaction entre RANK et son ligand n'a été décrite.

Le ganglion lymphatique est un organe lymphoïde secondaire important pour l'initiation de la réponse immunitaire. Il est composé de plusieurs types cellulaires incluant des cellules hématopoïétiques (exprimant CD45) et des cellules non-hématopoïétiques. Le ganglion lymphatique est divisé en trois parties, le cortex où l'on retrouve des follicules de lymphocytes B, le paracortex qui contient des lymphocytes T et la zone médullaire. Les cellules endothéliales lymphatiques forment les sinus sous-capsulaires et médullaires qui permettent la circulation de la lymphe et l'apport d'antigènes et des cellules présentatrices d'antigènes depuis les tissus périphériques. Dans la région sous-capsulaire, en bordure des follicules de cellules B se trouvent également les cellules marginales réticulaires qui expriment RANKL. Enfin, insérés entre les cellules endothéliales lymphatiques, se trouvent les macrophages CD169^{+} appelés macrophages sous-capsulaires. Ces macrophages jouent un rôle dans le transfert des antigènes de la lymphe vers les cellules B et sont aussi importants pour limiter la propagation des virus. Dans la partie médullaire, les macrophages du sinus médullaire expriment également CD169 et F4/80.
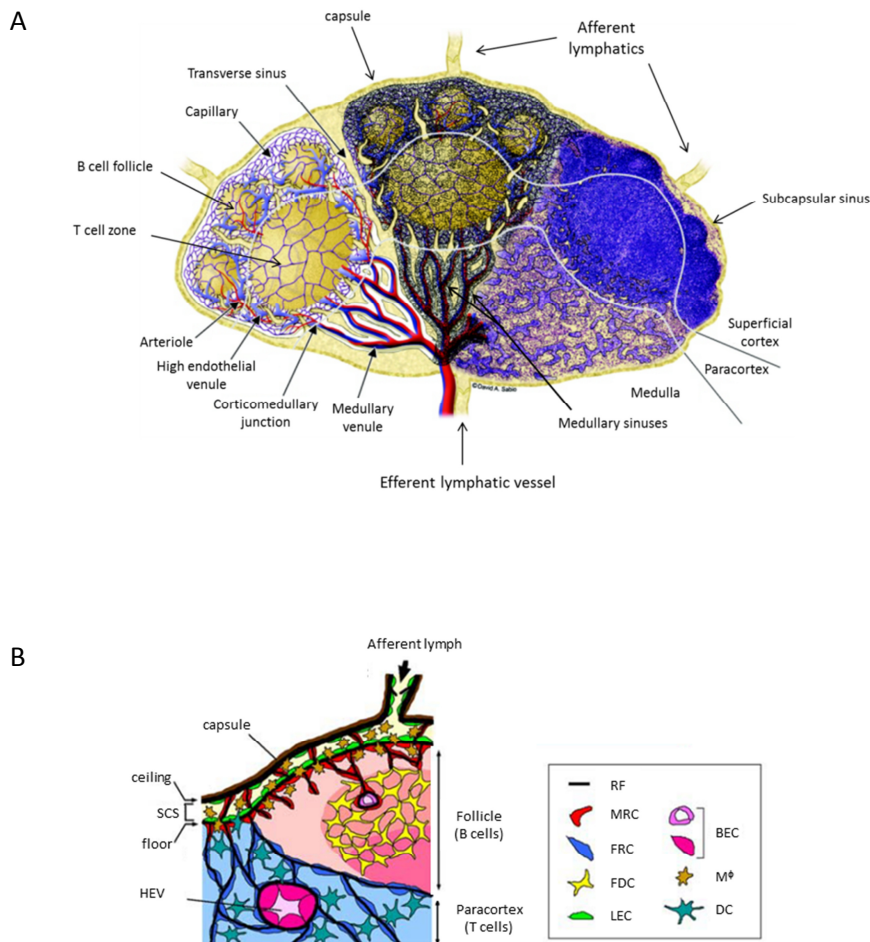
Figure 2: Représentation schématique de l'organisation du ganglion lymphatique. (**A**) Représentation d'un ganglion montrant l'organisation en trois zones, le cortex, le paracortex et la zone médullaire. Le ganglion contient plusieurs vaisseaux lymphatiques afférents et un vaisseau efférent. Gauche: représentation schématique du réseau vasculaire. Centre: réseau vasculaire représenté avec le réseau réticulaire formé par des cellules non-hématopoïétiques. Droite : section d'un ganglion lymphatique mésentérique de rat. Modifié d'après la référence [20]. (**B**) Représentation schématique de l'organisation cellulaire du ganglion lymphatique. Les cellules endothéliales lymphatiques (LEC) forment le sinus sous-capsulaire. Les macrophages CD169+ (M$^\phi$) sont insérés dans le sinus. Sous le sinus sous-capsulaire se trouvent les cellules marginales réticulaires (MRC). Les cellules folliculaires dendritiques (FDC) sont nécessaires au maintien de l'organisation du follicule B. Les cellules fibroblastiques réticulaires (FRC) forment un conduit de fibres réticulaires (RF) qui permet le transport des cellules et des molécules depuis le sinus sous-capsulaire jusqu'à la zone T. Les cellules dendritiques (DC) se trouvent dans la zone T. Les lymphocytes ne sont pas représentés pour simplifier la représentation. Modifié d'après la référence [21].

Notre équipe a précédemment montré que RANKL active la croissance du ganglion lymphatique par la prolifération des cellules endothéliales lymphatiques (LEC). Cet organe lymphatique présente aussi

un surnombre en lymphocytes B, cellules importantes dans la défense contre les agents infectieux mais aussi dans l'autoimmunité [22]. De plus, RANKL joue un rôle dans la différenciation des ostéoclastes mais peu de choses sont connues de son effet sur la différenciation d'autres sous-types de macrophages.

Ainsi, lors de ma thèse je me suis intéressée au rôle que joue RANKL dans l'homéostasie du ganglion lymphatique et plus précisément à son effet sur les LEC et sur la différenciation des macrophages CD169^{+} qui se trouvent dans le sinus sous-capsulaire et le sinus médullaire du ganglion. D'autre part, mon projet de thèse consiste aussi à développer de nouveaux outils permettant de cibler RANK et RANKL. Ainsi, j'ai caractérisé des anticorps ciblant RANK et j'ai criblé une librairie de petites molécules à la recherche d'inhibiteurs de l'interaction entre RANK et RANKL.

Résultats :

1. Développement d'outils ciblant RANK/RANKL

a. Caractérisation de deux anticorps anti-RANK : de nouveaux outils pour l'étude de ce récepteur

Notre laboratoire a développé un nouvel anticorps anti-RANK (RANK-02) en collaboration avec Medimmune. La séquence de reconnaissance de RANK de cet anticorps est basée sur une publication décrivant un ScFv (Single chain fraction variable) issu d'une expérience de phage display [23]. Cette publication a mis en évidence une activité inhibitrice de ce ScFv sur l'ostéoclastogenèse de cellules murines. Une partie de mes travaux a porté sur la caractérisation de cet anticorps aussi bien au niveau de son affinité pour RANK que de son effet biologique. Nous avons pu montrer que cet anticorps a une forte affinité pour les récepteurs RANK humain (hRANK) et murin (mRANK) (KD de l'ordre de 10^{-10} M). Dans cette étude, nous avons également comparé l'anticorps RANK-02 à un anticorps anti-RANK (R12-31) décris par Kamijo et al [24] mais qui n'avait pas été caractérisé pour son effet biologique. Cet anticorps se lie à mRANK avec la même affinité que RANK-02 mais semble avoir une affinité inférieure pour hRANK (KD de l'ordre de 10^{-8} M). Grâce à l'utilisation de lignées surexprimant RANK, nous avons pu comparer l'activité biologique de ces deux anticorps. Nous avons utilisé des cellules Jurkat JOM2 RANK:Fas qui expriment une protéine fusion composée du domaine extracellulaire de RANK et du domaine intracellulaire de Fas induisant ainsi la mort cellulaire lorsque RANK est activé. Nous avons également étudié l'activation de la signalisation de NF-κB grâce à une expérience de gène rapporteur dans des cellules HEK 293 exprimant RANK. R12-31 semble avoir un effet agoniste sur mRANK et hRANK. De manière opposée, RANK-02 semble avoir une faible activité antagoniste sur mRANK et une faible activité agoniste sur hRANK. Enfin, nous avons utilisé ces

anticorps sur des cellules primaires pour vérifier qu'ils permettent de mettre en évidence l'expression de RANK à la surface des cellules non transfectées. En utilisant la cytométrie en flux, nous avons pu montrer que les deux anticorps marquent RANK à la surface de cellules de Langerhans activées issues de peau humaine. L'utilisation d'un test ELISA compétitif a permis de mettre en évidence que RANK-02 semble se lier au même site que RANKL alors que R12-31 se lie sur un épitope différent. Ce travail de caractérisation de ces deux anticorps anti-RANK a fait l'objet d'une publication en premier auteur parue en Janvier 2016 dans Immunology Letters [25].

mAb	Affinité	Activité agoniste		Activité antagoniste		Blocage RANK-RANKL	
		Cellules JOM2	NF-κB	Cellules JOM2	NF-κB	mRANKL	hRANKL
	RANK humain						
R12-31	+	++	++	ND	ND	+-	-
RANK-02	++	+-	+-	ND	ND	++	+++
	RANK murin						
R12-31	++	++	++	ND	ND	+-	-
RANK-02	++	-	-	-+	-+	+	+

Tableau 1 : Récapitulatif des résultats obtenus lors de la comparaison des deux anticorps anti-RANK R12-31 et RANK-02. ++ = très bon, + = bon, +- = faible, - = absent, ND = non déterminé.

b. Criblage de petites molécules inhibant la liaison RANK-RANKL

Grâce au test ELISA et aux tests cellulaires développés pour l'étude des anticorps, j'ai pu évaluer des petites molécules pour leur capacité à inhiber la liaison de RANK à son ligand RANKL. J'ai criblé la Prestwick Chemical Library® (PCL) qui contient 1280 composés à l'aide du test ELISA compétitif. Cette librairie représente une grande diversité chimique de molécules déjà validées par la FDA pour certaines applications cliniques.

Suite au criblage, un hit (vertéporfine) avec une activité supérieure à 40% à 100µM a pu être confirmé. Cette molécule montre également une activité dose dépendante dans l'ELISA avec un IC50 de 0.4µM (**Fig 3**).
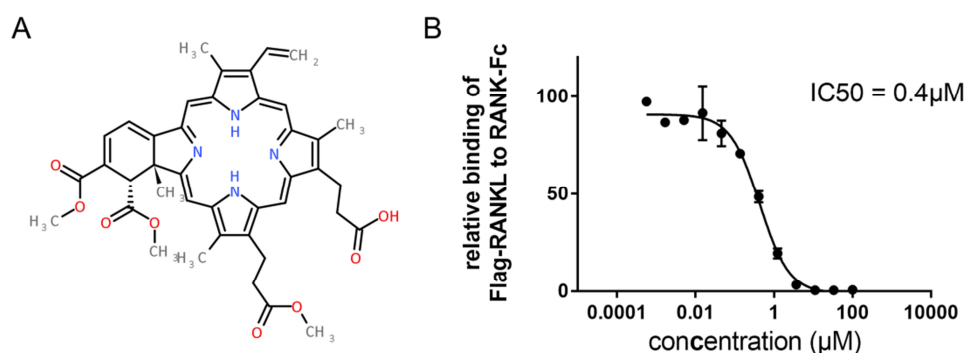
Figure 3: La vertéporfine inhibe l'interaction entre RANK et RANKL. (**A**) Structure de la vertéporfine (**B**) Dose-réponse de vertéporfine dans un test ELISA compétitif étudiant la liaison de RANKL à RANK. La quantité de hRANKL liée à hRANK a été mesurée. Les valeurs sont exprimées en pourcentage du contrôle positif (moyenne ± SD).

Nous avons par la suite testé 10 analogues structuraux de la vertéporfine à l'aide de l'ELISA. Parmi ces analogues, seulement deux n'avaient pas d'activité inhibitrice, quatre composés avaient un IC50 compris en 0.3 et 1.5µM, deux composés entre 2 et 8.5 µM et 2 composés une activité très moyenne due entre autre à une faible solubilité (**Fig 4**).
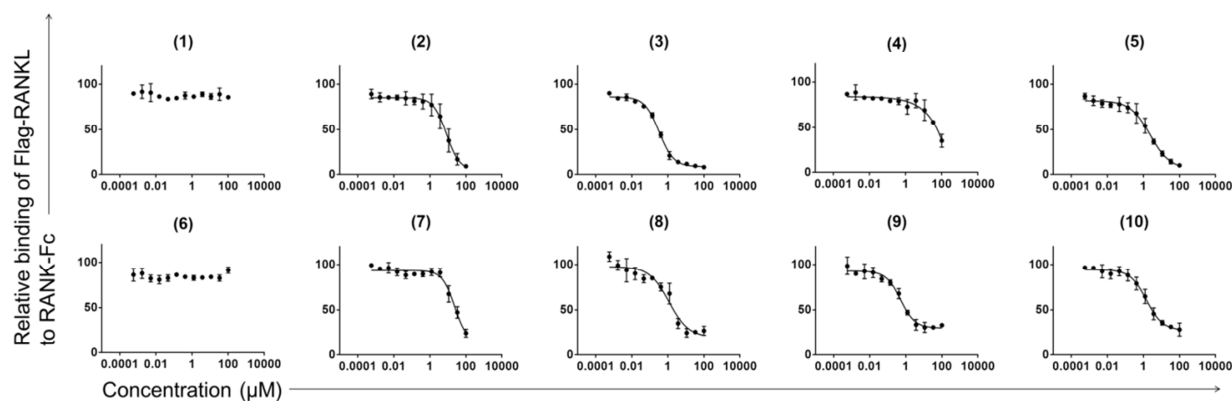
Figure 4: Evaluation de l'activité d'analogues de la vertéporfine. Dose-réponses d'analogues de la vertéporfine dans un test ELISA compétitif étudiant la liaison de RANKL à RANK. La quantité de hRANKL liée à hRANK a été mesurée. Les valeurs sont exprimées en pourcentage du contrôle positif (moyenne ± SD). Les chiffres 1 à 10 font référence aux molécules décrites dans le tableau 2.

n°	Nom	IC50 (µM)	n°	Nom	IC50 (µM)
1	Coproporphyrin I dihydrochloride	-	7	Protoporphyrin IX dimethyl ester	23.82
2	Chlorin e6	8.37	8	Pheophorbide a (mixture of diastereomers)	1.15
3	Hematoporphyrin IX dimethyl ester	0.32	9	Pyropheophorbide-a	0.51
4	Isohematoporphyrin IX	Ambiguous	10	Purpurin 18	1.45
5	Pyropheophorbide-a methyl ester	2.37			

Tableau 2: Description des analogues de la vertéporfine

J'ai par la suite testé ce hit dans un test cellulaire avec une lignée cellulaire exprimant une protéine fusion hRANK:Fas. Lorsque RANK est activé dans ces cellules cela induit la mort cellulaire via l'activation de Fas. La mort cellulaire peut ensuite être étudiée grâce à un marquage avec l'iodure de propidium qui marque les cellules mortes et une analyse par cytométrie en flux. Une activité inhibitrice de la vertéporfine à 10µM a pu être mise en évidence dans ces cellules. En testant les analogues à 10µM dans le test cellulaire, nous avons pu confirmer l'activité de cette famille de molécules pour l'inhibition de l'interaction entre RANK et son ligand RANKL. De plus, ces molécules ne semblent pas avoir un effet cytotoxique sur les cellules jurkat JOM2 (**Fig 5**).
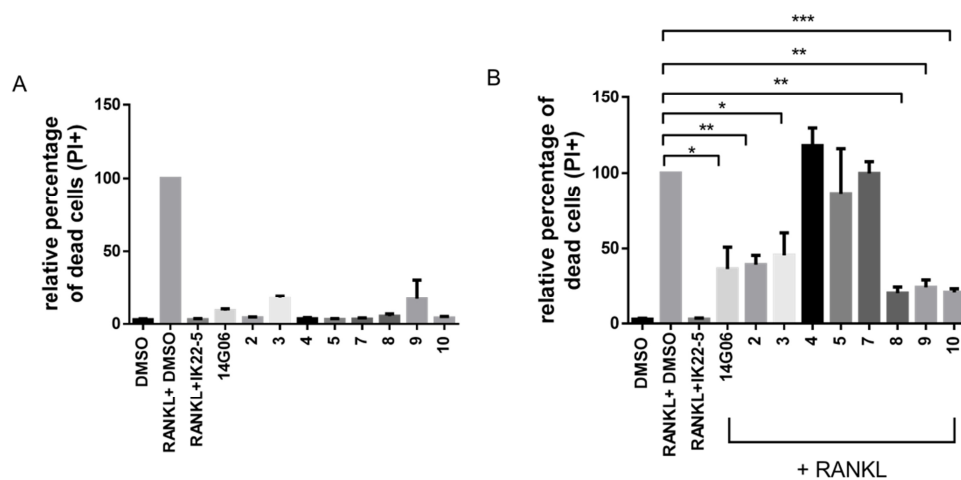
Figure 5: La vertéporfine et les analogues ont une faible cytotoxicité et inhibent l'activation de RANK dans les cellules Jurkat JOM2 hRANK:Fas. Les graphes représentent l'intensité de fluorescence moyenne (MFI) du marquage à l'iodure de propidium (PI) normalisée par rapport aux cellules traitées avec RANKL + 0.05% DMSO. (**A**) les cellules ont été traitées pendant 16h avec 10µM des molécules. (**B**) Les cellules ont été traitées avec 10µM des molécules et 1ng/ml de RANKL. L'anticorps anti-RANKL IK22-5 à 10µg/ml est un contrôle positif de l'inhibition de l'interaction RANK-RANKL. Moyenne ± SD. Un t test a été utilisé pour évaluer la significativité statistique. * $p < 0.05$ ** $p < 0.001$ ***$p < 0.001$

Finalement, nous avons testé la vertéporfine dans un test de différenciation des ostéoclastes. La vertéporfine à des doses de l'ordre du micromolaire inhibe efficacement l'ostéoclastogenèse induite par le traitement avec M-CSF et RANKL de la lignée cellulaire RAW 264.7 (**Fig 6**).
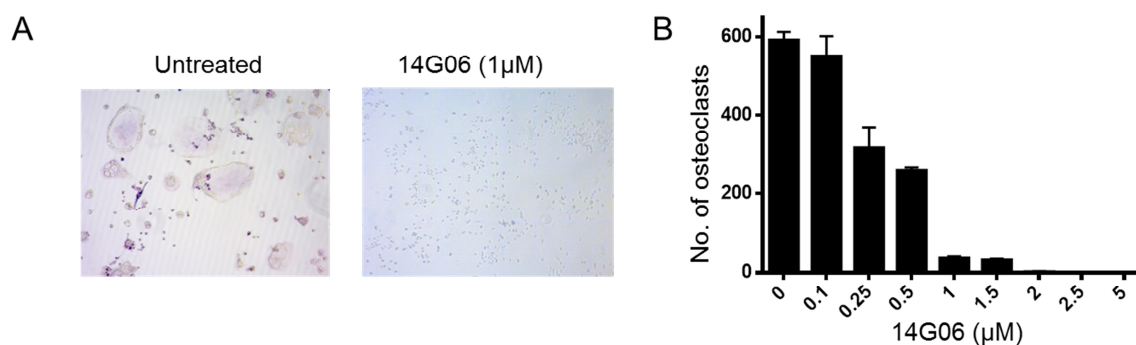
Figure 6: La vertéporfine inhibe l'ostéoclastogenèse. (A) Images de microscopie montrant l'effet de la vertéporfine sur la différenciation des cellules RAW 264.7 en culture avec M-CSF (25ng/ml) et RANKL (30ng/ml) pendant 4 jours en présence ou non de vertéporfine. La formation d'ostéoclastes est évaluée par un marquage de TRAcP et les cellules sont photographiées (x10). **(B)** le graphe représente le nombre d'ostéoclastes multinuclés (>3 noyaux) positifs pour TRAcP (moyenne ± SD en triplicats) après traitement avec différentes doses de vertéporfine.

Cette étude démontre qu'une petite molécule peut inhiber l'interaction entre RANK et son ligand. Cependant la vertéporfine est utilisée comme traitement en thérapie photodynamique de la

néovascularisation dans la dégénérescence maculaire liée à l'âge. Cette molécule induit donc une photosensibilité lorsqu'elle est injectée. Une étude plus approfondie des potentiels effets secondaires et de son effet *in vivo* est donc nécessaire.

2. Rôle de RANKL dans l'homéostasie du ganglion lymphatique

a. Mise en évidence d'un nouveau marqueur des cellules endothéliales lymphatiques (LEC) sous l'influence de RANKL : ITGA2b

ITGA2b est une molécule de surface qui forme un complexe avec ITGB3, l'intégrine α2bβ3. Cette intégrine est connue pour son expression par les mégacaryocytes et les plaquettes. Nous avons montré que ITGA2b est présente à la surface des cellules endothéliales lymphatiques (LEC) du ganglion lymphatique et que cela n'est pas dû à une contamination par des plaquettes (**Fig 7**).
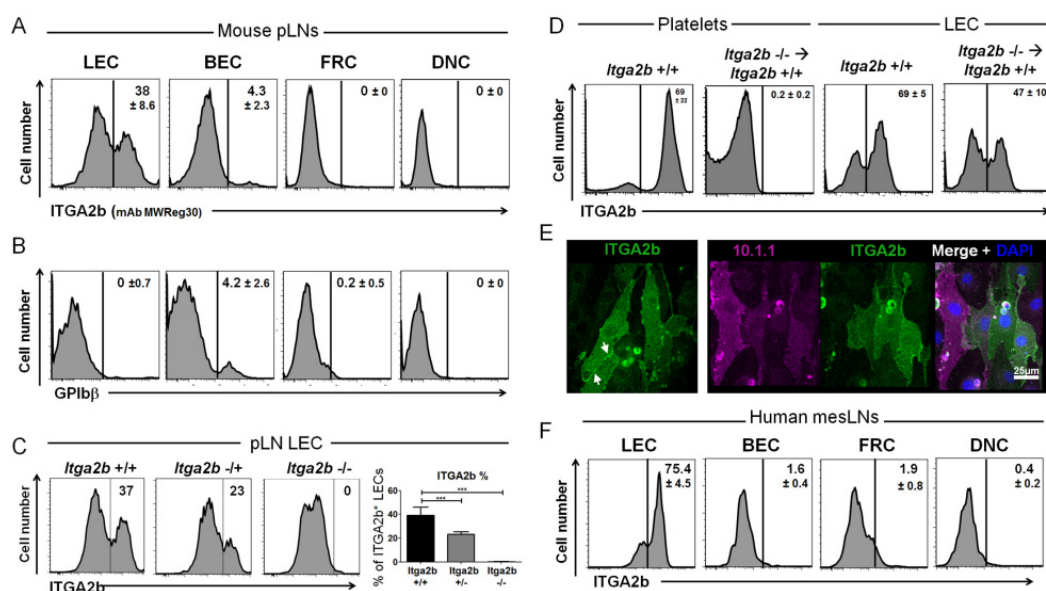
Figure 7 : Les cellules endothéliales lymphatiques du ganglion expriment ITGA2b. **(A)** Histogrammes de cytométrie en flux montrant l'expression de ITGA2b par les cellules stromales du ganglion lymphatique. LEC= cellules endothéliales lymphatiques ; BEC= cellules endothéliales vasculaires ; FRC= cellules fibroblastiques réticulaires ; DNC= cellules doubles négatives (gp38⁻CD31⁻). Le pourcentage de cellules marquées (moyenne ± SD n=13) est indiqué. **(B)** Histogrammes de cytométrie en flux montrant l'expression d'un marqueur spécifique des plaquettes (GPIbβ). Le pourcentage de cellules marquées (moyenne ± SD n=8) est indiqué. **(C)** Les histogrammes montrent l'expression de ITGA2b dans les LECs des souris WT contrôle et une expression réduite à absente dans les LECs des souris hétérozygotes ou homozygotes pour la délétion du gène *Itga2b*. Le pourcentage de cellules marquées (moyenne ± SD n=9) est indiqué. **(D)** Histogrammes montrant l'expression de ITGA2b par les plaquettes et les LECs dans des souris contrôles et dans des souris après transfert de moelle osseuse Itga2b $^{-/-}$ (n=8, n=4 pour les souris WT). Le pourcentage ± SD de cellules ITGA2b+ est indiqué. **(E)** Images de microscopie à fluorescence confocale de LECs triées et mises en culture montrant l'expression de mCLCA1 (clone 10.1.1, magenta) et ITGA2b (vert). **(F)** Histogrammes de cytométrie en flux montrant l'expression de ITGA2b dans les cellules stromales du ganglion lymphatique mésentérique d'embryon humain. Un t test a été utilisé pour calculer la significativité statistique. ***p<0.001.

Nous avons montré que ITGA2b est plus fortement exprimée par les LECs de la partie interne du sinus sous-capsulaire et par une partie des LECs de la zone médullaire. L'expression de cette molécule de surface illustre donc l'hétérogénéité des LECs au sein du ganglion lymphatique. De plus, nous avons démontré que l'expression de ITGA2b est sensible à RANKL. En effet, le pourcentage de LECs positives pour ITGA2b est augmenté dans des souris qui surexpriment RANKL et il est diminué dans des souris traitées avec un anticorps anti-RANKL ou dans des souris déficientes pour RANKL dans les cellules marginales réticulaires (**Fig 8**). L'expression de ITGA2b par les LECs semble également être sous le contrôle de la lymphotoxine. Ces résultats ont fait l'objet d'une publication en deuxième auteur dans PLoS ONE en Mars 2016 [26].
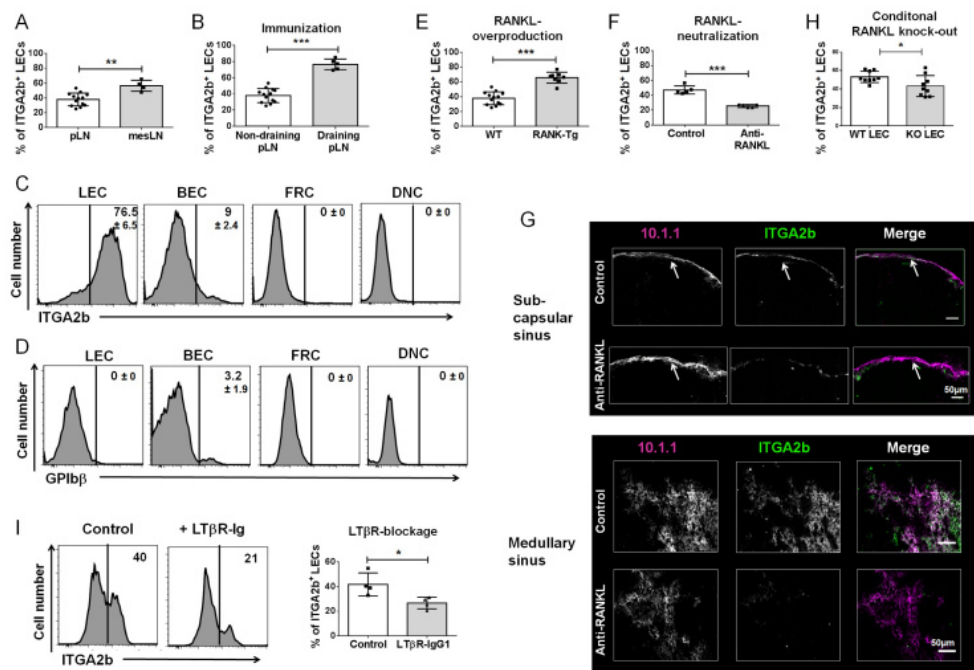
Figure 8: L'expression de ITGA2b par les LECs est sensible à RANKL et à la lymphotoxine.
(A) Pourcentage de LECs ITGA2b+ dans les ganglions lymphatiques périphériques (pLN) en comparaison avec les ganglions mésentériques (mLN) (moyenne ± SD n=6). **(B)** Les souris ont été immunisées avec *B.Pertussis* inactivées et l'expression de ITGA2b dans les LECs a été étudiée dans les ganglions drainants et non drainants. Le graphe montre le pourcentage de LECs ITGA2b+ (moyenne ± SD n=6) montrant une augmentation en réponse à l'immunisation. **(C)** Histogrammes de cytométrie en flux montrant l'expression de ITGA2b dans les cellules stromales des ganglions drainants après immunisation (moyenne ±SD n=6). **(D)** Histogrammes montrant l'expression de GPIBβ par les cellules stromales des ganglions drainants après immunisation (moyenne ±SD, n=6). **(E)** Pourcentage de LECs ITGA2b+ dans les ganglions lymphatiques des souris contrôles WT en comparaison avec des souris qui surexpriment RANKL (RANK-Tg) (moyenne ±SD, n=8). **(F)** Pourcentage de LECs ITGA2b+ dans les ganglions lymphatiques des souris contrôles en comparaison avec des souris traitées avec un anticorps anti-RANKL (moyenne ±SD, n=5). **(G)** Images de microscopie confocale de l'expression de ITGA2b (vert) par les LECs (10.1.1, magenta) dans les sinus sous-capsulaires et médullaires après traitement avec un anticorps anti-RANKL ou un isotype contrôle. **(H)** Pourcentage de LECs ITGA2b+ dans les ganglions

lymphatiques des souris contrôles en comparaison avec des souris déficientes pour RANKL dans les cellules marginales réticulaires (KO) (moyenne ±SD, n=9). **(I)** Pourcentage de LECs ITGA2b^{+} dans les ganglions lymphatiques des souris contrôles en comparaison avec des souris traitées avec LTβR-Ig (moyenne ±SD, n=3). Un t test a été utilisé pour calculer la significativité statistique. *p<0.5, **p < 0.01, ***p < 0.001.

b. <u>Rôle de RANKL dans l'activation des LECs et la présence des macrophages sous-capsulaires</u>

Les macrophages sous-capsulaires CD169^{+} sont insérés entre les cellules endothéliales lymphatiques dans le sinus sous-capsulaire. Ils sont importants pour la réponse immunitaire contre les virus et le transfert des antigènes aux lymphocytes B. Il a été précédemment montré que les souris déficientes pour RANK présentent une diminution de l'expression de CD169 dans la rate. Nous avons confirmé ces résultats avec des souris déficientes pour RANKL (**Fig 9A**). Comme ces souris ne développent pas de ganglions, nous avons injecté un anticorps anti-RANKL dans des souris WT. Nous avons observé une diminution du marquage CD169 dans la rate et dans les ganglions lymphatiques (**Fig 9B**). Nous avons également observé une diminution du nombre absolu de macrophages sous-capsulaires par cytométrie en flux (**Fig 9C**). Les injections de LTβR-Fc et de TNFR2-Fc servent respectivement de contrôle positif et de contrôle négatif pour la disparition des macrophages sous-capsulaires.
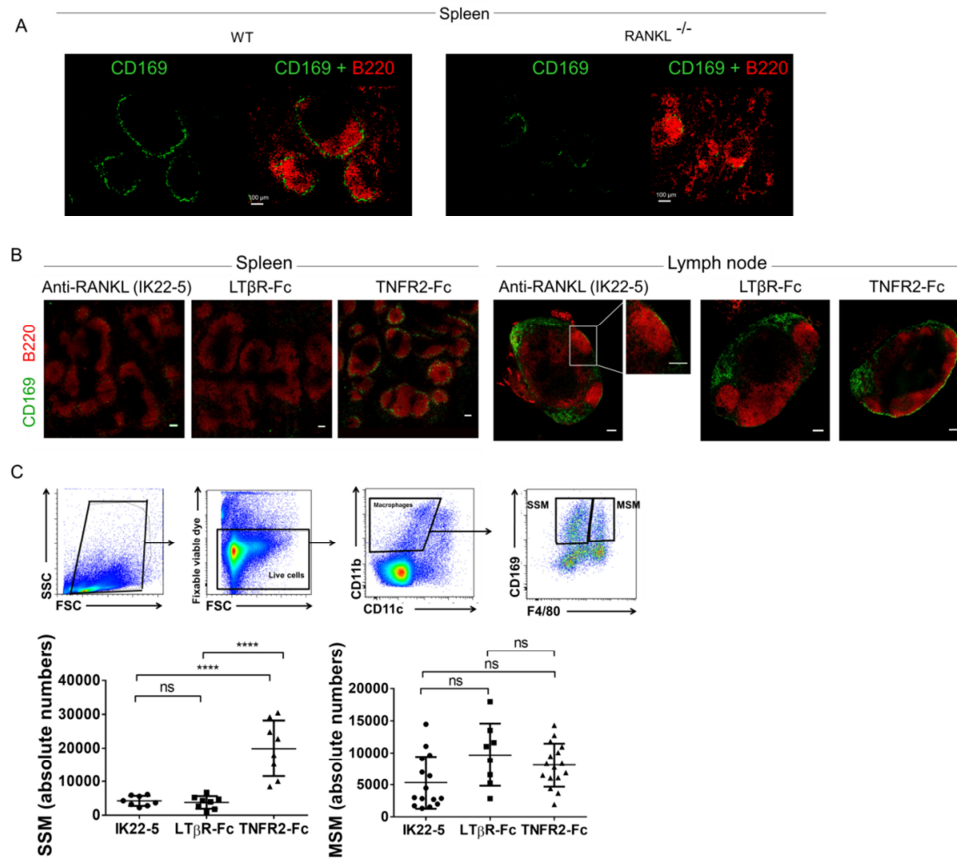
Figure 9: Effet de RANKL sur les macrophages exprimant CD169 dans la rate et le ganglion.
(A) Images de microscopie de sections de rate de souris WT et RANKL$^{-/-}$ marquées pour visualiser CD169 (vert) et B220 (rouge). **(B)** Images de microscopie de sections de rate ou de ganglions marquées pour visualiser CD169 (vert) et B220 (rouge) après traitement avec 20μg d'anticorps anti-RANKL IK22-5, LTβR-Fc ou TNFR2-Fc 3 fois par semaines pendant 3 semaines. Echelle = 100μm. **(C)** Stratégie de gating pour étudier les macrophages des ganglions par cytométrie en flux. Les graphes montrent le nombre absolu (moyenne ± SD) des macrophages sous-capsulaires (SSM) et des macrophages médulaires (MSM) après traitement avec anti-RANKL, LTβR-Fc, TNFR2-Fc. Les résultats pour les ganglions inguinaux et brachiaux analysés séparément sont représentés sur le même graphe. La significativité statistique a été calculée en utilisant un test ANOVA avec une correction de bonferroni. **** $p < 0.0001$

Les cellules marginales réticulaires (MRC) expriment de manière constitutive RANKL. Afin de mieux étudier l'effet de RANKL sur l'homéostasie du ganglion adulte, nous avons développé un modèle murin dans lequel les cellules marginales réticulaires (MRC) n'expriment pas RANKL dans le ganglion lymphatique adulte (**Fig 10**).
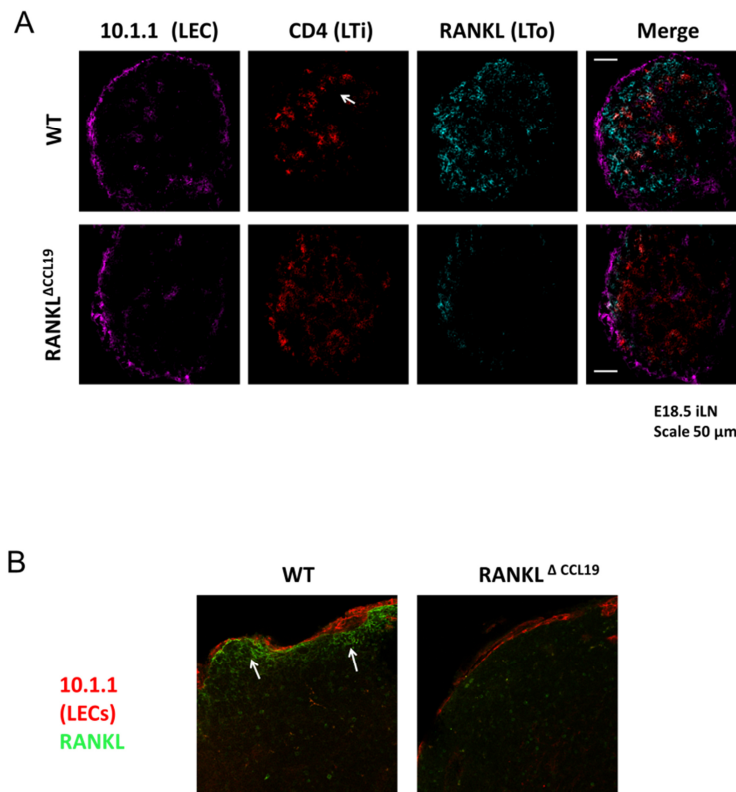
Figure 10: Absence de RANKL dans les souris RANKL^{ΔCcl19}. (A) Images de microscopie confocale de ganglion inguinaux de souris RANKL^{ΔCcl19} et de souris contrôles cre- au stade E18.5 marqué pour visualiser les cellules endothéliales lymphatiques (anticorps 10.1.1, purple), les cellules LTi (lymphoid inducer cells, marquée avec CD4, rouge) et RANKL (cyan). Echelle = 50µm. **(B)** Images de microscopie confocale de ganglion inguinaux de souris RANKL^{ΔCcl19} et de souris contrôles cre- adultes âgées de 8 semaines marqués pour visualiser RANKL (vert) et les cellules endothéliales lymphatiques (anticorps 10.1.1, rouge). Echelle = 50µm

Nous avons pu mettre en évidence que le nombre de macrophages sous-capsulaires est diminué en l'absence de RANKL provenant des cellules stromales. Les souris dépourvues de RANKL dans les MRCs montrent également un dysfonctionnement fonctionnel puisque le transfert d'antigène aux cellules B ne se fait pas correctement (**Fig 11**).
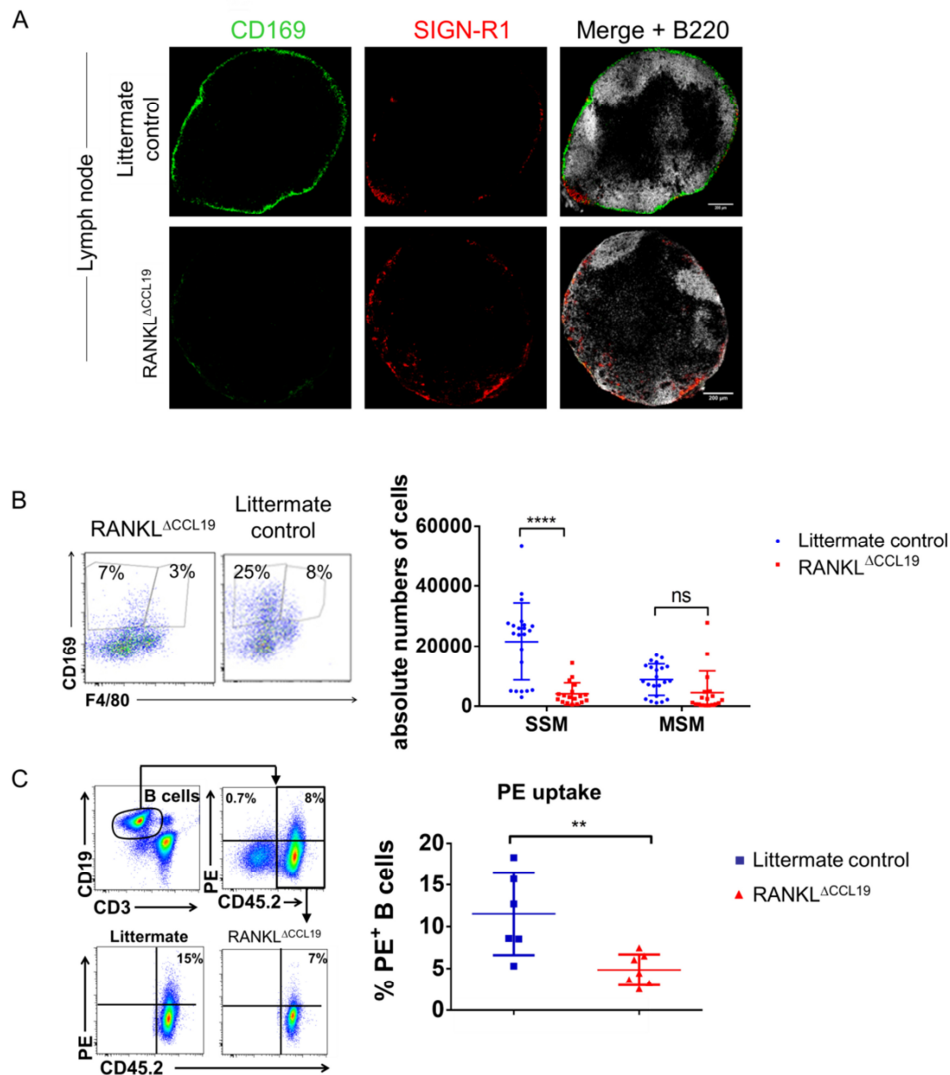
Figure 11: L'absence de RANKL provenant des cellules stromales affecte la différenciation des macrophages sous-capsulaires CD169⁺. **(A)** Images de microscopie d'une section de ganglion provenant de souris RANKL$^{\Delta Ccl19}$ et de souris contrôles marquées pour visualiser CD169 (vert), SIGN-R1 (rouge) et B220 (gris). Echelle = 200µm **(B)** Les graphes montrent la réduction de la population de macrophages CD169⁺ F4/80⁻ correspondant aux macrophages sous-capsulaires par cytométrie en flux. Le nombre absolu de cellules est représenté (moyenne ± SD). La significativité statistique a été calculée avec un test ANOVA avec une correction de bonferroni ***p<0.001. **(C)** Les graphes représentent la stratégie pour étudier la présence d'immunocomplexe PE-IC sur les lymphocytes B. Le pourcentage (moyenne ± SD) de lymphocytes B PE+ dans les souris RANKL$^{\Delta Ccl19}$ et les souris contrôle est représenté. La significativité statistique a été calculée en utilisant un test de Mann-Whitney **p<0.01.

Nous avons par la suite cherché à identifier le mécanisme par lequel RANKL agit sur les macrophages. J'ai étudié le phénotype de souris KO pour RANK dans les macrophages. Je n'ai pas pu observer de diminution des macrophages sous-capsulaires dans ces souris (**Fig 12A**). D'autre part, lors d'un transfert de cellules de foie fœtal provenant de souris RANK KO total dans des souris irradiées, nous avons pu observer que l'absence de RANK dans les précurseurs myéloïdes n'empêche pas la présence

de macrophages sous-capsulaires (**Fig 12B**). Ces observations nous permettent de conclure que RANKL n'a pas un effet direct sur RANK à la surface des macrophages (**Fig 12C**). Nous avons aussi étudié des souris déficientes pour RANK dans les MRC. Ces souris ne présentent pas d'anomalie dans les macrophages des ganglions (**Fig 12D**). Nous pouvons donc exclure un effet autocrine sur les MRCs (**Fig 12 E**).
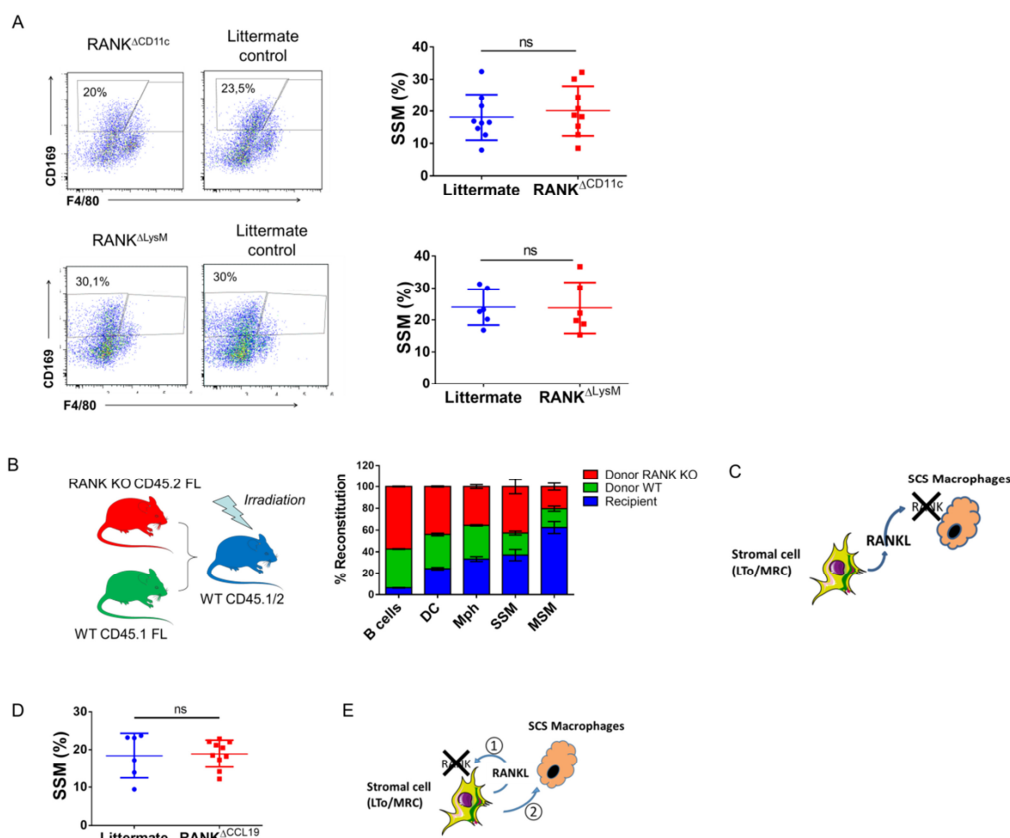
Figure 12: **RANKL n'agit pas directement sur les macrophages ou sur les MRC. (A)** Les graphes représentent le pourcentage (moyenne ±SD) de macrophages sous-capsulaires dans les souris RANK^ΔCD11c et RANK^ΔLysM ainsi que dans les souris contrôles cre-. **(B)** Le schéma représente le protocole pour le transfert de cellules de foie fétale. Le graphe montre le pourcentage de reconstitution (moyenne ±SD) en fonction de l'origine des cellules. **(C)** Représentation schématique résumant nos résultats montrant que RANKL n'agit pas directement sur les macrophages. **(D)** Le graphe montre le pourcentage (moyenne ±SD) de macrophages sous-capsulaires dans les souris RANK^ΔCCL19 et les souris contrôles cre-. **(E)** Représentation schématique montrant que RANKL n'a pas un effet autocrine sur les MRC. La significativité statistique a été calculée avec un test de Mann-Whitney.

Nous avons déjà montré que les LECs sont sensibles à RANKL et surexpriment ITGA2b et MAdCAM-1 en présence de RANKL [22,26]. Nous avons montré que RANK est exprimé par les LECs par qPCR (**Fig 13A**). Nous avons donc étudié comment les MRC, les LECs et les macrophages pourraient communiquer entre elles. Pour cela, nous avons injecté du RANKL-GST soluble et nous avons pu

observer que le phénotype des LECs (expression de MAdCAM et de ITGA2b) revient à un niveau normal dans les souris qui n'expriment pas RANKL dans les MRC (**Fig 13B**). Notre hypothèse est donc un mécanisme indirect entrainant la différenciation des macrophages sous-capsulaires passant par les LECs (**Fig 13C**).
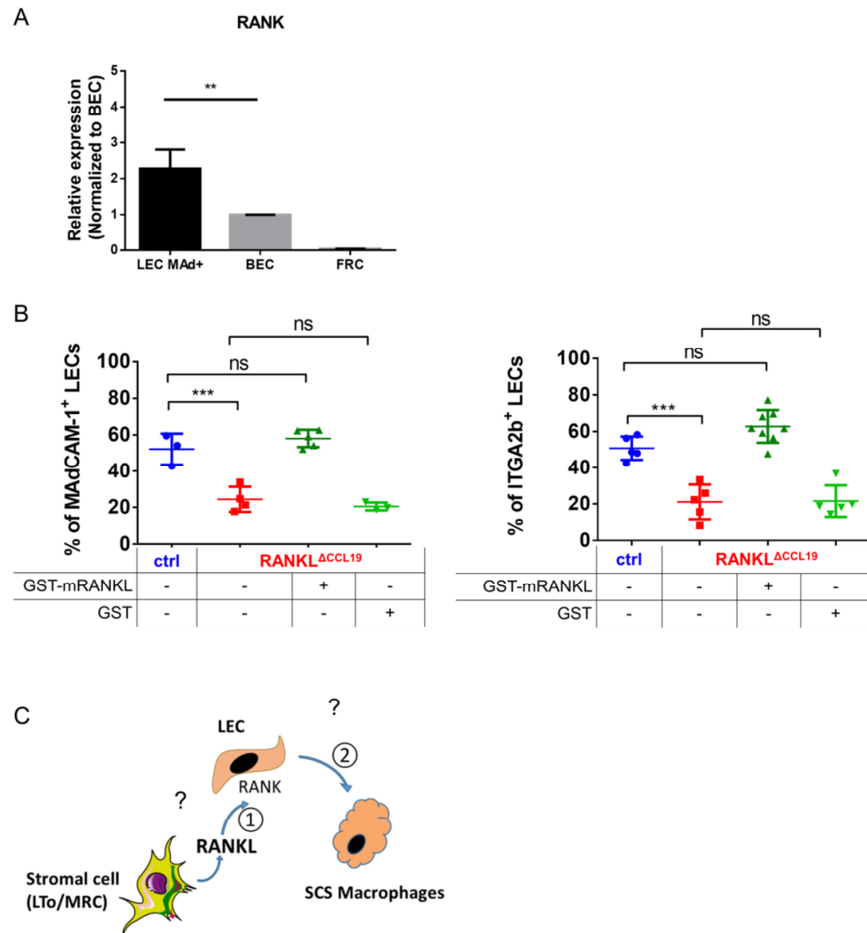
Figure 13: Les cellules endothéliales lymphatiques (LECs) sont sensibles à RANKL et l'expression de ITGA2b et de MAdCAM-1 peut être restaurée. (A) Expression relative de l'ARN messager de RANK (moyenne ± SD) dans les LECs, les cellules endothéliales vasculaires (BEC) et les cellules fibroblastiques réticulaires (FRC). La significativité statistique a été calculée en utilisant un test de Mann-Whitney. **p<0.01 **(B)** Le graphe représente le pourcentage (moyenne ± SD) de LECs MAdCAM-1$^+$ et ITGA2b$^+$ dans les souris RANKL$^{\Delta Ccl19}$ injectées ou non avec 100µg de GST-mRANKL ou de GST pendant 4 jours en comparaison avec les souris contrôles cre-. La significativité statistique a été calculée en utilisant un test ANOVA avec une correction de bonferroni. ***p<0.001 **(C)** Représentation schématique d'un possible mécanisme impliquant les LECs dans la différenciation des macrophages sous-capsulaires.

Conclusion et perspectives :

La triade RANK/RANKL/OPG joue un rôle dans différents processus biologiques. En particulier RANKL joue un rôle important dans des pathologies telles que le cancer, l'ostéoporose et l'autoimmunité. Il est donc intéressant de cibler l'interaction entre RANK et RANKL pour traiter ces pathologies. De plus, une bonne caractérisation des outils utilisés pour étudier RANK est importante pour la découverte de nouveaux rôles de cette molécule. Pendant cette thèse, j'ai identifié et caractérisé des molécules permettant de cibler RANK ou RANKL. Tout d'abord j'ai mis en place des tests *in vitro* permettant la caractérisation de deux anticorps anti-RANK. L'utilisation de ces tests m'a par la suite permis d'identifier une famille de petites molécules inhibant l'interaction entre RANK et RANKL.

L'utilisation de l'ELISA compétitif m'a permis de cribler la Prestwick Chemical Library® et d'identifier un hit : la vertéporfine. L'étude de 10 analogues nous a permis de confirmer l'activité de cette famille. Nous avons également montré que la vertéporfine et certains analogues inhibent l'activation de RANK dans un test cellulaire avec les cellules Jurkat JOM2 hRANK :Fas et enfin que la vertéporfine inhibe l'ostéoclastogenèse de cellules murines et humaines.

Ces molécules seraient donc d'intéressants inhibiteurs de la voie RANK/RANKL et de l'ostéoclastogenèse. Cependant la vertéporfine est utilisée en thérapie photodynamique et entraine donc une photosensibilité. Les potentiels effets secondaires et off-target de ces molécules doivent donc être mieux caractérisés avant d'envisager une utilisation thérapeutique.

Cette étude apporte tout de même la preuve que ces structures spécifiques sont capables d'inhiber l'interaction entre RANK et RANKL et pourrait permettre le développement d'autres molécules plus efficaces ayant moins d'effet indésirables.

D'autre part, nous avons mis en évidence l'importance de RANKL provenant des cellules stromales dans la région du sinus sous-capsulaire des ganglions lymphatiques. Cette chimiokine semble en effet affecter la différenciation des macrophages sous-capsulaires. Nous avons également mis en évidence que les LEC expriment des marqueurs d'activation dépendant de RANKL. Une coopération entre les MRC exprimant RANKL, les LEC qui sont sensibles à RANKL et les macrophages sous-capsulaires serait donc possible. Pour confirmer cela, nous sommes en train d'étudier des souris dans lesquels les LECs n'expriment pas RANK. D'autre part, l'analyse du transcriptome des LECs de souris RANKL[ΔCcl19] traitées ou non avec du RANKL recombinant nous permettrait d'identifier les facteurs responsables de la différenciation des macrophages. Nous avons donc trié les LECs de ces souris et nous avons réalisé un RNAseq. Les résultats sont en cours d'analyse. Enfin, les LEC et les SSM pouvant jouer un

rôle dans certaines conditions pathologiques, il serait intéressant d'étudier le rôle de RANKL dans des pathologies telles que les cancers et les maladies auto-immunes.
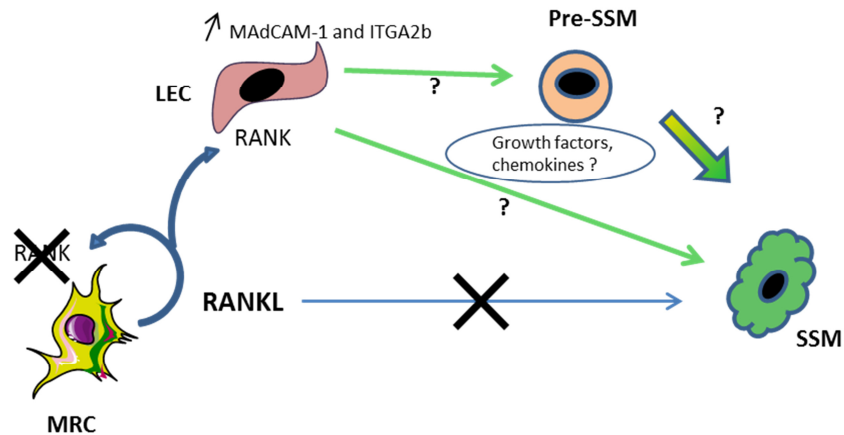
Figure 14 : Représentation schématique du mécanisme liant RANKL exprimé par les cellules stromales et la différenciation des macrophages sous-capsulaires (SSM). RANKL est exprimé par les MRCs dans le ganglion lymphatique. Nous avons montré que RANKL n'agit pas directement sur les macrophages ou sur les précurseurs myéloïdes. Nous avons également exclu une boucle autocrine de RANKL sur les MRCs. Nous avons observé que les LECs sont sensibles à RANKL. Nous avons donc comme hypothèse un mécanisme indirect passant par les LECs. RANKL aura ainsi un effet sur les LECs qui sécréteraient à leur tour des facteurs permettant la différenciation des macrophages. Ces facteurs restant à être identifiés.

Références :

1. Simonet WS, Lacey DL, Dunstan CR, Kelley M, Chang M-S, Lüthy R, et al. Osteoprotegerin: A Novel Secreted Protein Involved in the Regulation of Bone Density. Cell. 1997;89: 309–319. doi:10.1016/S0092-8674(00)80209-3

2. Tsuda E, Goto M, Mochizuki S, Yano K, Kobayashi F, Morinaga T, et al. Isolation of a Novel Cytokine from Human Fibroblasts That Specifically Inhibits Osteoclastogenesis. Biochem Biophys Res Commun. 1997;234: 137–142. doi:10.1006/bbrc.1997.6603

3. Wada T, Nakashima T, Hiroshi N, Penninger JM. RANKL–RANK signaling in osteoclastogenesis and bone disease. Trends Mol Med. 2006;12: 17–25. doi:10.1016/j.molmed.2005.11.007

4. Dougall WC, Glaccum M, Charrier K, Rohrbach K, Brasel K, Smedt TD, et al. RANK is essential for osteoclast and lymph node development. Genes Dev. 1999;13: 2412–2424.

5. Kong YY, Boyle WJ, Penninger JM. Osteoprotegerin ligand: a common link between osteoclastogenesis, lymph node formation and lymphocyte development. Immunol Cell Biol. 1999;77: 188–193. doi:10.1046/j.1440-1711.1999.00815.x

6. Bucay N, Sarosi I, Dunstan CR, Morony S, Tarpley J, Capparelli C, et al. osteoprotegerin-deficient mice develop early onset osteoporosis and arterial calcification. Genes Dev. 1998;12: 1260–1268.

7.   Wong BR, Josien R, Lee SY, Sauter B, Li H-L, Steinman RM, et al. TRANCE (Tumor Necrosis Factor [TNF]-related Activation-induced Cytokine), a New TNF Family Member Predominantly Expressed in T cells, Is a Dendritic Cell–specific Survival Factor. J Exp Med. 1997;186: 2075–2080. doi:10.1084/jem.186.12.2075

8.   Gonzalez-Suarez E, Jacob AP, Jones J, Miller R, Roudier-Meyer MP, Erwert R, et al. RANK ligand mediates progestin-induced mammary epithelial proliferation and carcinogenesis. Nature. 2010;468: 103–107. doi:10.1038/nature09495

9.   Schramek D, Sigl V, Penninger JM. RANKL and RANK in sex hormone-induced breast cancer and breast cancer metastasis. Trends Endocrinol Metab. 2011;22: 188–194. doi:10.1016/j.tem.2011.02.007

10. Ma X, Liu Y, Zhang Y, Yu X, Wang W, Zhao D. Jolkinolide B inhibits RANKL-induced osteoclastogenesis by suppressing the activation NF-κB and MAPK signaling pathways. Biochem Biophys Res Commun. 2014;445: 282–288. doi:10.1016/j.bbrc.2014.01.145

11. Chen Y, Sun J, Dou C, Li N, Kang F, Wang Y, et al. Alliin Attenuated RANKL-Induced Osteoclastogenesis by Scavenging Reactive Oxygen Species through Inhibiting Nox1. Int J Mol Sci. 2016;17. doi:10.3390/ijms17091516

12. Xiu Y, Xu H, Zhao C, Li J, Morita Y, Yao Z, et al. Chloroquine reduces osteoclastogenesis in murine osteoporosis by preventing TRAF3 degradation. J Clin Invest. 2014;124: 297–310. doi:10.1172/JCI66947

13. Lee C-C, Liu F-L, Chen C-L, Chen T-C, Chang D-M, Huang H-S. Discovery of 5-(2',4'-difluorophenyl)-salicylanilides as new inhibitors of receptor activator of NF-κB ligand (RANKL)-induced osteoclastogenesis. Eur J Med Chem. 2015;98: 115–126. doi:10.1016/j.ejmech.2015.05.015

14. Aggarwal B, Darnay B, Singh S. Inhibitors of receptor activator of NF-kappaB and uses thereof [Internet]. US20040167072 A1, 2004. Available: http://www.google.tl/patents/US20040167072

15. Kim H, Choi HK, Shin JH, Kim KH, Huh JY, Lee SA, et al. Selective inhibition of RANK blocks osteoclast maturation and function and prevents bone loss in mice. J Clin Invest. 2009;119: 813–825. doi:10.1172/JCI36809

16. Lacey DL, Boyle WJ, Simonet WS, Kostenuik PJ, Dougall WC, Sullivan JK, et al. Bench to bedside: elucidation of the OPG–RANK–RANKL pathway and the development of denosumab. Nat Rev Drug Discov. 2012;11: 401–419. doi:10.1038/nrd3705

17. Cheng X, Kinosaki M, Takami M, Choi Y, Zhang H, Murali R. Disabling of Receptor Activator of Nuclear Factor-κB (RANK) Receptor Complex by Novel Osteoprotegerin-like Peptidomimetics Restores Bone Loss in Vivo. J Biol Chem. 2004;279: 8269–8277. doi:10.1074/jbc.M309690200

18. Hur J, Ghosh A, Kim K, Ta HM, Kim H, Kim N, et al. Design of a RANK-Mimetic Peptide Inhibitor of Osteoclastogenesis with Enhanced RANKL-Binding Affinity. Mol Cells. 2016;39: 316–321. doi:10.14348/molcells.2016.2286

19. Ta HM, Nguyen GTT, Jin HM, Choi J, Park H, Kim N, et al. Structure-based development of a receptor activator of nuclear factor-κB ligand (RANKL) inhibitor peptide and molecular basis for osteopetrosis. Proc Natl Acad Sci. 2010;107: 20281–20286. doi:10.1073/pnas.1011686107

20. Willard-Mack CL. Normal Structure, Function, and Histology of Lymph Nodes. Toxicol Pathol. 2006;34: 409–424. doi:10.1080/01926230600867727

21. Katakai T, Suto H, Sugai M, Gonda H, Togawa A, Suematsu S, et al. Organizer-Like Reticular Stromal Cell Layer Common to Adult Secondary Lymphoid Organs. J Immunol. 2008;181: 6189–6200. doi:10.4049/jimmunol.181.9.6189

22. Hess E, Duheron V, Decossas M, Lézot F, Berdal A, Chea S, et al. RANKL Induces Organized Lymph Node Growth by Stromal Cell Proliferation. J Immunol. 2012;188: 1245–1254. doi:10.4049/jimmunol.1101513

23. Newa M, Lam M, Bhandari KH, Xu B, Doschak MR. Expression, Characterization, and Evaluation of a RANK-Binding Single Chain Fraction Variable: An Osteoclast Targeting Drug Delivery Strategy. Mol Pharm. 2014;11: 81–89. doi:10.1021/mp400188r

24. Kamijo S, Nakajima A, Ikeda K, Aoki K, Ohya K, Akiba H, et al. Amelioration of bone loss in collagen-induced arthritis by neutralizing anti-RANKL monoclonal antibody. Biochem Biophys Res Commun. 2006;347: 124–132. doi:10.1016/j.bbrc.2006.06.098

25. Chypre M, Seaman J, Cordeiro OG, Willen L, Knoop KA, Buchanan A, et al. Characterization and application of two RANK-specific antibodies with different biological activities. Immunol Lett. 2016;171: 5–14. doi:10.1016/j.imlet.2016.01.003

26. Cordeiro OG, Chypre M, Brouard N, Rauber S, Alloush F, Romera-Hernandez M, et al. Integrin-Alpha IIb Identifies Murine Lymph Node Lymphatic Endothelial Cells Responsive to RANKL. PLOS ONE. 2016;11: e0151848. doi:10.1371/journal.pone.0151848

INTRODUCTION

Chapter 1: The RANK/RANKL/OPG triad, a member of the TNF/TNFR superfamilies

1.1. TNFR and TNF superfamilies

The tumor necrosis factor (TNF) superfamily of receptors and ligands include several signal transducers which are important in biological processes such as development and maintenance of immune cells and secondary lymphoid organs. They also have other functions such as bone and mammary gland homeostasis, host defense, inflammation, and apoptosis [1]. In the 1970's, lymphotoxin (LT) and tumor necrosis factor (TNF) were the first members of the family to be identified as molecules causing the lysis of tumor cells [2,3]. In 1984, cDNA coding these two proteins were cloned. Strong homologies between TNF and LT were observed suggesting that they formed a new superfamily of genes [4,5]. Since then, 18 genes have been identified coding for 19 TNF superfamily ligands and 29 receptors were discovered [6] (**figure 1.1**).
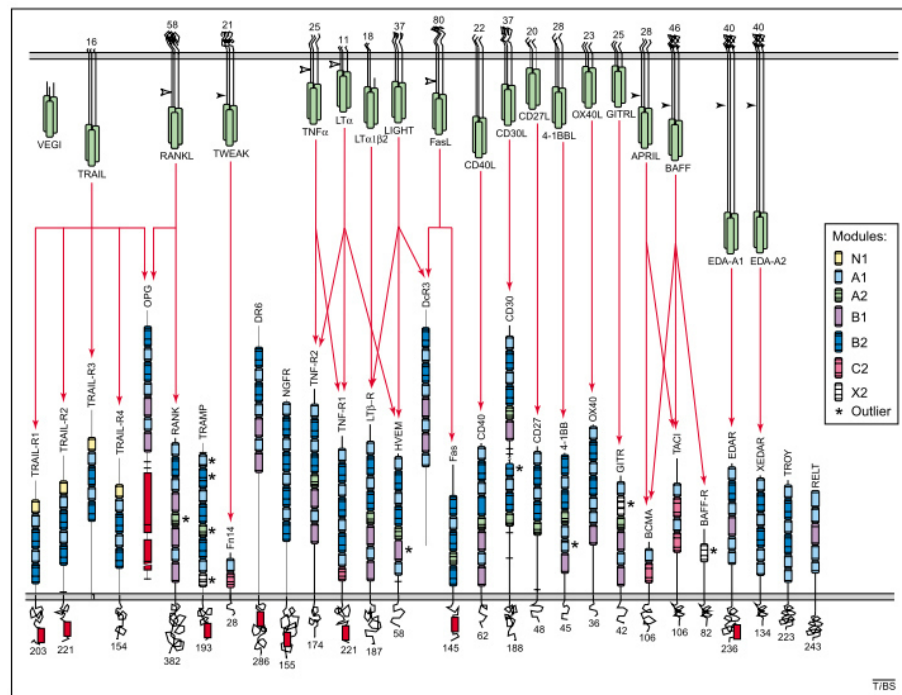
Figure 1.1: Members of the human TNF and TNFR superfamilies. Representation of the interaction between human tumor necrosis factor superfamily ligands (top) and their receptors (bottom). TNF ligands are all type II transmembrane proteins which can be cleaved as a soluble form by proteases. The arrows show the cleavage sites. The vascular endothelial cell growth inhibitor (VEGI) is an exception as it is directly expressed as a soluble protein. The green boxes represent the TNF homology domain (THD). The TNF receptors are type I or type III transmembrane proteins but can also be soluble. They are composed of cysteine rich domains (CRD) comprising a tandem pair of modules (A,B,C,X). The size of intracellular domain is indicated for ligands and receptors. The red boxes represent the death domains of TNFR. The red arrows show the known interactions between TNF ligands and receptors. After reference [6].

As type II transmembrane proteins, TNF superfamily ligands have an intracellular N terminus and an extracellular C terminus. Most ligands are membrane bound but they can be cleaved by proteolysis and secreted as a soluble form. Vascular endothelial cell-growth inhibitor (VEGI) is an exception as it is directly expressed as a soluble protein. All TNF family members contain a conserved C-terminal domain called "TNF homology domain" (THD) which has 20-30% sequence identity between family members. The THD folds into antiparallel β-sandwiches and is involved in receptor binding. TNF family ligands assemble into homotrimers containing three receptor binding sites [6]. LTβ cannot form homotrimers but rather forms heterotrimers with LTα. Receptor selectivity of the ligands is due to difference in length and residue composition of the surface loops connecting the THD β-strands [7].

TNFSF receptors are mostly type I transmembrane proteins, meaning that they have an extracellular N terminus and an intracellular C terminus. They are characterized by the presence of cysteine rich domains (CRDs) the number of which varies from one to four depending on the receptor. Each CRDs are formed of 2 modules called A,B,C or X depending on their folding and the number of disulfide bridges they contain [7]. These CRDs are located in the extracellular domain of the receptors and contain 3 disulfide bonds giving them an elongated shape. This specific shape enables the receptors to bind the ligands. Indeed, as TNFSF ligands assemble into homotrimers, the elongated shape of the receptors allows the binding between two ligand monomers. Moreover, different orientation of the CRDs are responsible for selectivity of the ligands [7].

Because TNFR lack intrinsic kinase activity, interaction of the intracellular domain with signaling molecules is required for receptor activation and signaling. TNFR can be separated in two types of receptors based on the signaling molecule they bind. Activating receptors such as RANK, CD40, CD30 or TNFR2, bind one or more TNFR-associated factors (TRAF). Depending on the TRAF protein, different signaling pathways can be induced such as NF-κB, mitogen activated protein kinases (MAPK) and JNK leading to cell growth and survival [1,8]. On the other hand, death receptors such as TRAILR1, TNFR1 or Fas contain an intracellular death domain (DD). This domain binds Fas-associated DD (FADD) or TNFR-associated DD (TRADD) proteins inducing caspase pathways and cell death [1]. Therefore, the signaling induced after TNFR superfamily members activation can lead to both beneficial and harmful effects [8]. TNF ligands family members have anticancer potential, regulate the immune system and protect against infection. On the other hand, they can promote tumour development, play a role in autoimmunity and are implicated in other diseases such as osteoporosis and chronic heart failure [8]. As they play a role in many physiopathological conditions, TNF family members represent interesting therapeutic targets. Indeed, several therapies targeting members of

the TNF family are currently approved or in clinical trials, many of them being protein-based drugs [9].

1.2. Discovery of RANK/RANKL/OPG

In the late 1990's, parallel work aimed at identifying new members of the TNF superfamily. Amgen Inc. generated several transgenic mice overexpressing cDNA related to TNF receptors. One of these mice presented severe osteopetrosis due to the lack of bone resorbing cells called osteoclasts. The protein encoded by this cDNA was named osteoprotegerin (OPG) [10]. Independently, a research team from the Snow Brand Milk Product co. reported the discovery of a molecule purified from human embryonic fibroblasts inhibiting osteoclastogenesis. This molecule was named osteoclastogenesis inhibitory factor (OCIF) [11]. After cloning of this gene both teams identified the corresponding ligand called respectively OPG ligand (OPGL) and osteoclast differentiation factor (ODF) [12,13]. Two other groups had discovered a member of the TNF ligand superfamily named respectively receptor activator of NF-κB ligand (RANKL) [14] and TNF-related activation induced cytokine (TRANCE) [15]. All these ligands (OPGL, OCIF, TRANCE and RANKL) discovered independently by four teams turned out to be identical. However, OPG was identified as a soluble decoy receptor lacking a transmembrane domain [10,16]. Anderson et al identified the cellular receptor called receptor activator of NF-κB (RANK) while sequencing cDNAs from human bone marrow derived dendritic cells. This group found that RANK had a partial homology to the extracellular domain of CD40, another member of the TNFRSF [14]. Therefore, RANK-RANKL-OPG system was identified in parallel by four teams describing two different roles for these molecules. RANK,RANKL and OPG are involved in osteoclastogenesis and bone homeostasis [12,13] and in T cell proliferation and activation by dendritic cells [14,15]. The biological implications of this triad will be detailed in the Chapter 2.

As described in this paragraph, different names were given to the members of the RANK-RANKL-OPG triad depending on the group where they were discovered. They are summarised in **table 1.1** together with their chromosomal location on human and mouse chromosomes. These molecules will be called RANKL, RANK and OPG in this thesis.

Nomenclature name	Other names	Human chromosome	Mouse chromosome
TNFSF11	RANKL (receptor activator of NF-κB ligand) [14] OPGL (osteoprotegerin ligand) [13] TRANCE (TNF-related activation induced cytokine) [15] ODF (osteoclast differentiation factor) [12]	13q14	14
TNFRSF11A	RANK (receptor activator of NF-κB) [14] ODFR (osteoclast differentiation factor receptor) [17] TRANCE-R (TNF-related activation induced cytokine receptor) [15] ODAR (osteoclast differentiation and activation receptor) [18]	18q22.1	1
TNFRSF11B	OPG (osteoprotegerin) [10] OCIF (osteoclastogenesis inhibitory factor) [11]	8q24	15

Table 1.1: Different names of RANK, RANKL and OPG and chromosomal location.

TRAIL (TNF-related apoptosis-inducing ligand) is another member of the TNF superfamily of ligands. DR4 (death receptor 4) and DR5 (death receptor 5) are binding TRAIL and induce cell apoptosis. Two other receptors bind TRAIL but do not contain cell death domain; they are called DcR1 (decoy receptor 1) and DcR2 (decoy receptor 2). OPG was also identified as a decoy receptor for TRAIL by Emery and co-workers in 1998 [19]. The known interactions between RANK, RANKL and OPG are summarized in **figure 1.2**.
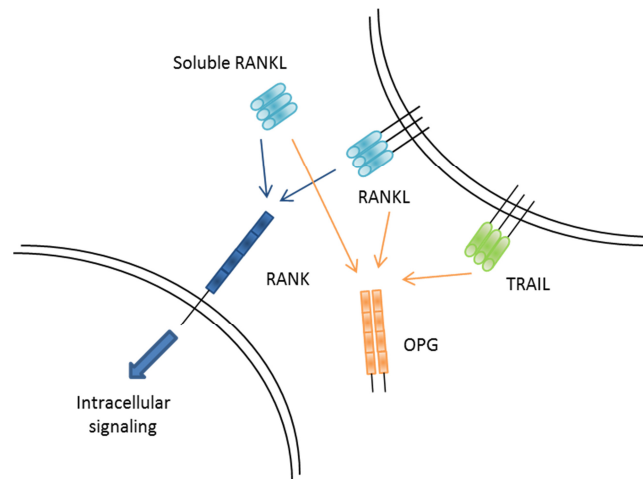
Figure 1.2: Representation of the interactions between the members of RANK/RANKL/OPG axis. Soluble or membrane bound RANKL binds RANK to induce intracellular signaling in RANK expressing cells. OPG is a soluble decoy receptor binding RANKL and preventing RANK activation. OPG also binds TRAIL, a ligand inducing apoptosis of the cells expressing a receptor for TRAIL.

1.3. Structure and signaling pathways of the RANK/RANKL/OPG triad

1.3.1. Structures of RANK/RANKL/OPG triad and regulation of their expression

a) RANKL

RANK ligand (RANKL) is a type II homotrimeric transmembrane protein and has homology with other TNFSF members such as TRAIL, FasL and TNFα. Murine RANKL is composed of 316 amino acids and has 85% of homology with human RANKL [14]. RANKL protein comprises a C-terminal extracellular receptor-interacting domain and a transmembrane domain. It is found both in membrane bound (45kDa) and soluble form (31 kDa). Indeed, metalloprotease-desintegrin TNFα convertase (TACE) can cleave the extracellular part and release soluble RANKL [20]. The matrix metalloproteinases MMP 14 and 7 together with a disintegrin and metalloproteinase (ADAM) 10 were also shown to cleave RANKL [21,22]. The murine RANKL ectodomain was crystallized in 2001 by Lam and colleagues [23] (**figure 1.3**). They found that RANKL forms homotrimers as it was already known for other members of the TNFSF. Monomers contain four surface loops (AA', CD, EF, DE loops) which play a role in the unicity and specificity of RANKL [23]. RANKL structure is highly comparable to TNF and TRAIL ligands, the main differences residing in these surface loops. In 2012, Nelson and colleagues crystallised RANKL-OPG and RANKL-RANK complexes. The important residues for binding were different between RANKL binding to OPG or RANK. DE loop seems to be important in both cases [24] (**figure 1.3**).

Two other isoforms of RANKL resulting from RNA splicing have been identified [25]. RANKL2 contains the transmembrane domain but presents a shorter intracellular domain. RANKL3 isoform lacks the transmembrane domain.

RANKL expression was observed in several tissues and cells including lymph nodes, spleen, T lymphocytes, osteoblasts, bone marrow, heart and skeletal muscle. During embryonic development, RANKL mRNA expression was also found in tissues such as brain, kidney, skin, liver and lung [14,15,26].
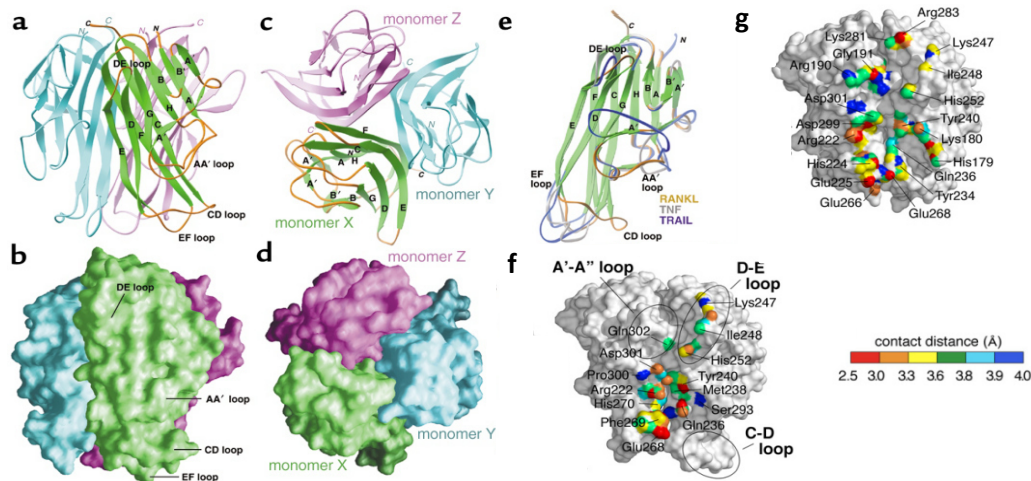
Figure 1.3 : Crystal structure of murine RANKL ectodomain. (a) Ribbon diagram of RANKL homotrimer. The β-strands of one monomer are shown in green and connecting loops in orange. The two other monomers are shown in blue and magenta. The C-terminus is on the top of the diagram and the membrane-distal region is at the bottom. **(b)** Surface of the homotrimer in the same orientation as in a. **(c)** Ribbon diagram of RANKL homotrimer with membrane-distal face forward. **(d)** Surface of the homotrimer in the same orientation as in c. **(e)** Comparison of RANKL monomer with TNF and TRAIL monomers. β-strands are colored in green and connecting loops of RANKL in orange. Connecting loops of TNF and TRAIL are respectively gray and blue. RANKL β-strands superimpose with the other TNFSF members but the structure differs in the connecting loops that are unique to RANKL. Key interaction residues between RANKL and OPG **(f)** and RANKL and RANK **(g)** are coloured depending on the distance according to the scale. Modified after references [23,24].

b)   RANK

RANK receptor is a type I transmembrane protein composed of 616 amino acids and four CRDs [14]. There is 85% homology between human and murine RANK. The cytoplasmic domain of RANK contains 382 amino acids and is the longest of the TNFR superfamily [6]. RANK protein is highly homologous to CD40 with 40% homology [14]. As other receptors of the TNFRSF, RANK lacks intrinsic kinase activity and TRAF proteins are recruited after activation to induce downstream signaling. The signaling pathways will be detailed in the following paragraph. Upon interaction with RANKL, RANK homo-trimerizes [27]. In 2010, Liu and colleagues crystallized the complex containing RANK extracellular domain and RANKL ectodomain. They observed the elongated shape formed by the four CRDs of RANK and conformational changes of the receptor after binding of RANKL. The structure of RANK-RANKL complex was similar to TNFβ(LTα)-TNFRSF1A and TRAIL-DR5 complexes but the CRD3 of RANK was differently oriented [28]. Ta and colleagues also showed that loop 3 is particularly important for RANK activity [29]. This loop is structurally distinct from other TNF-family members and represents the largest surface area binding RANKL. Nelson and colleagues crystallized the RANK-

RANKL complex in 2012 and were able to identify the key residues for RANK binding to RANKL [24] (**figure 1.4**).

Alternative splicing variants of RANK were identified. These truncated RANK proteins were shown to be less efficient in binding RANKL and activating downstream signaling *in vitro* [30,31]. The importance of these isoforms *in vivo* remains to be investigated.

RANK mRNA was found in several tissues including bone marrow, heart, lung, thymus, liver, bones, mammary glands, prostate, brain, liver, skeletal muscles and skin [14,32].
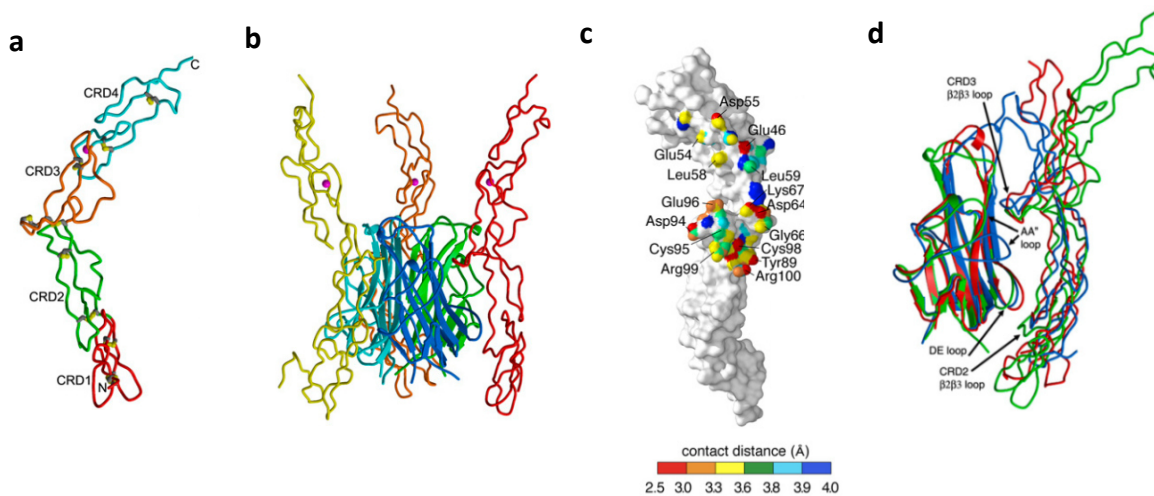
Figure 1.4: Crystal structures of RANK and RANK-RANKL complex. (a) Structure of RANK with the four cysteine-rich domains (CRD) represented in blue, orange, green and red. **(b)** Structure of the heterohexameric complex containing RANKL homotrimer represented by ribbon diagram in the center and the extracellular domain of three RANK receptors**. (c)** Molecular surface of RANK with the key interaction residues colored by distance according to the scale. **(d)** RANKL-RANK (green), TNFβ(LTα)-TNFRSF1A (red) and TRAIL-DR5 (blue) complexes superimposed showing the homology between these receptors. The difference in conformation of AA' and DE loops of the ligands and loops in CRD2 and CRD3 of the receptors are also shown. Modified after references [24,28].

c)   OPG

The OPG decoy receptor is also a highly conserved protein as the homology between rat and human OPG is approximately 94% while rat and mouse OPG show 85% homology [10]. Full length OPG is a 401 amino acid protein which is reduced to 380 amino acids due to signal peptidase cleavage [10,32]. This protein comprises four CRDs N-terminal domains, two death domain homologous (DDH) regions and a C-terminal heparin-binding domain [19,33]. OPG is secreted as a soluble receptor because it lacks a membrane-interacting domain [6]. Therefore, DDH are not able to induce apoptosis.

However, it was shown that expression of OPG:Fas fusion protein with Fas sequence inserted between CRDs and DDH of OPG is able to induce apoptosis [34]. The heparin binding domain was shown to bind syndecan 1, a heparan sulfate proteoglycan involved in cell adhesion and migration as well as cytoskeleton regulation [35]. OPG contains several N-linked glycosylation sites and is then secreted as a disulfide-linked homodimer [10,11,36]. Therefore, OPG protein presents two uncommon elements in the TNFR superfamily: (i) it covalently dimerizes and (ii) lacks a transmembrane domain.

It was shown that OPG binds RANKL with high affinity but also binds TRAIL, another TNFSF member, with low affinity [19]. Nelson et al crystalized the structure of RANKL-OPG complex in 2012. They identified key residues for interaction of OPG with RANKL. The RANKL binding cleft adopts a unique conformation to bind OPG which is different from RANKL bound to RANK (**figure 1.5**). Nelson and colleagues also showed that OPG binds RANKL with approximately 500 fold higher affinity than RANK [24]. OPG was found to be expressed in several tissues such as skin, liver, heart, lung, kidney, intestine, stomach, brain, mammary gland, prostate, spleen and bone [10,37].
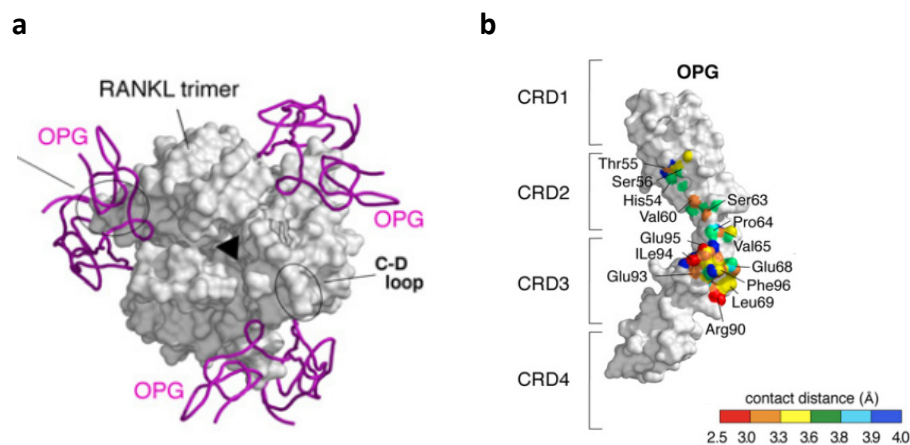
Figure 1.5: Crystal structure of OPG and RANKL complex. (a) Structure of RANKL trimer and OPG binding to three different binding cleft equally distributed on RANKL surface. **(b)** Molecular surface of OPG with the key interaction residues colored by distance according to the scale. Modified after reference [24].

As a summary of this paragraph, a schematic representation of RANK, RANKL and OPG proteins is presented in **figure 1.6**.
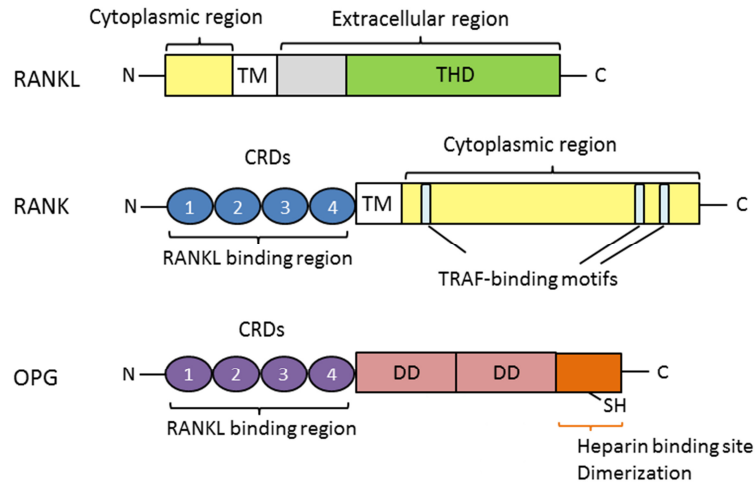
Figure 1.6: Schematic representation of RANKL, RANK and OPG proteins. Domains architecture of RANKL, RANK and OPG are represented. TM: transmembrane domain, THD: TNF homology domain, CRD: Cysteine rich domain, DD: death domain. Modified after references [24,33,34].

d) Regulation of RANK, RANKL and OPG expression

RANK, RANKL and OPG mRNA/protein levels can be both negatively and positively regulated by numerous factors. Most of these factors are associated with bone homeostasis. **Table 1.2** summarizes the main factors regulating RANK, RANKL and OPG expression.

	RANKL	OPG	RANK
Hormones			
Vitamin D3	↑	↑	↑
Parathyroid hormone	↑	↓	
Estradiol	-	↑	
Testosterone		↑	
Prolactin	↑	↓	
Cytokines			
TNFα	↑	↑	
TNFβ		↑	
IL-1α		↑	
IL-1β	↑	↑	
IL-4 + anti-CD3 *(T cells)*	↑		↑
IL-6	↑	↑	↓
IL-11	↑	↑	
IL-17	↑		
CD40L		↑	
M-CSF			↑
Growth factors			
TGF-β	↓	↑	↓
TGF-β + anti-CD3 *(T cells)*	↑		↑
BMP-2	↑	↑	
IGF-1	↑	↓	
VEGF			↑
Glucocorticoids			
Dexamethasone	↑	↓	↑
Hydrocortisone		↓	
Immunosuppressive molecules			
Rapamycin	↑	↓	
Cyclosporine A	↑	↓	
Tacrolimus	↑	↓	
Others			
Prostaglandin E2	↑	↓	↑
Calcium	↑	↑	
LPS	↑	↓	
Ionomycin *(T cells)*	↑		
PMA *(T cells)*	-		

Table 1.2: Factors modulating RANKL, OPG and RANK expression. Most results were obtained in studies using cells from osteoblasts or osteoclasts lineage; if otherwise the cell type concerned appears in parenthesis. Blank: not tested ↑: increased expression ↓: decreased expression –: unchanged . Abbreviations: TNF: tumor necrosis factor, IL: interleukin, TGF-β: Transforming growth factor β, BMP-2: Bone morphogenic protein 2, IGF-1: Insulin growth factor 1, VEGF: Vascular endothelial growth factor, LPS: lipopolysaccharide, PMA: Phorbol myristate acetate. Modified after references [38–40].

1.3.2. Signaling pathways induced by RANK

Binding of RANKL homotrimers to RANK induces trimerization of the receptor and intracytoplasmic signaling regulating cell activity differentiation and survival [32]. However, it was also observed that when RANK is overexpressed *in vitro*, it can self-assemble at the cell surface an induce signaling without RANKL binding [41]. Member of the activating receptors in the TNFRSF without a death domain, RANK binds five of the six known TRAF adaptors proteins. It was shown *in vitro* that TRAF 1, 2, 3 and 5 bind a membrane-distal motif on RANK intracellular domain while TRAF6 binds RANK in a different membrane-proximal region [42]. TRAF6 appears to be the most relevant adaptor for RANK signaling *in vivo* as TRAF6 knockout mice show increased bone mass and lack of lymph nodes [43]. On the other hand, TRAF2 and TRAF3 deficient mice did not develop osteopetrosis [44,45]. TRAF6 contains a distinct Pro-X-Glu-X-X-(aromatic/acidic residue) binding motif that differs from the other TRAF adaptor proteins [46]. Another protein called GRB2 (growth factor receptor-bound protein 2)-associated binding protein (GAB2) is also involved in RANK signaling activation [47]. Finally mutation in aminoacids 535 and 536 of RANK cytoplasmic region inhibited RANKL induced osteoclastogenesis but not TRAF6 signaling suggesting the existence of a signaling pathway independent of TRAF6 [48]. RANK downstream signaling includes different pathways which are summarized in **figure 1.7**.
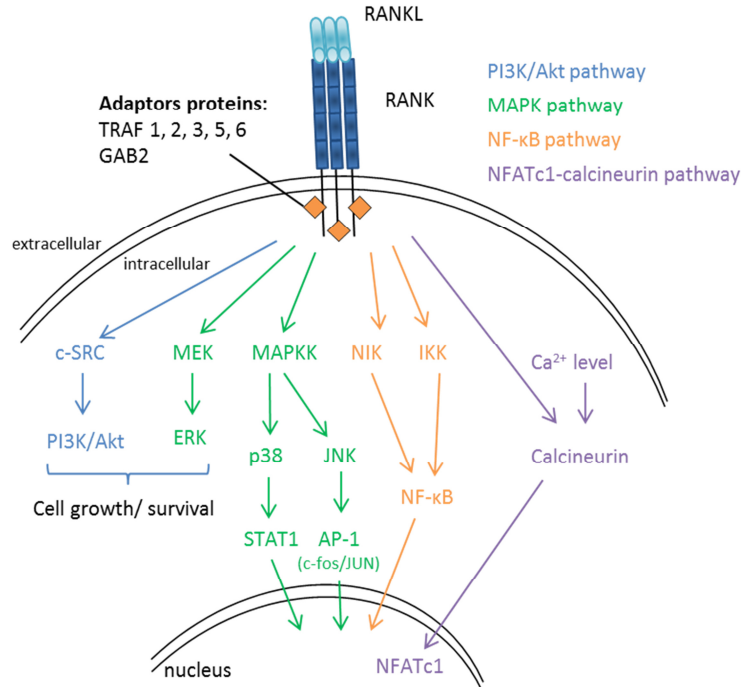
Figure 1.7: Schematic diagram of the downstream signaling pathways induced by RANK activation.
Abbreviations: TRAF: TNFR-associated factors, c-SRC: cellular sarcoma, PI3K: phosphoinositide 3-kinase, MAPK: mitogen activated protein kinase, MEK: MAPK/ERK kinase, ERK: extracellular-signal-regulated kinase, MAPKK: MAP kinase kinase, JNK: c-Jun N-terminal kinase, STAT1: signal transducer and activator of transcription 1, AP-

1: activator protein 1, NIK: NF-κB inducible kinase, IKK: IκB kinases complex, NFATc1: nuclear factor of activated T cells. Modified after references [27,49].

a)   NF-κB pathway

The NF-κB pathway was the first pathway induced by RANK that was identified and gave the name Receptor activator of NF-κB (RANK) [14]. Five NF-κB transcription factors are expressed in mammals. A first group of transcription factors contains RelA (p65), RelB and c-Rel. These are mature proteins that do not require proteolytic processing. A second group of transcription factors requires proteolytic processing from large precursors NF-κB1 (p105) and NF-κB2 (p100) to mature p50 and p52 proteins. Formation of NF-κB dimers is required to induce transcription activation. Indeed only RelA, RelB and c-Rel proteins contain a domain allowing transcription activation. NF-κB signaling has been divided in two main pathways: the canonical (classical) pathway and the non-canonical (alternative) pathway.

The canonical pathway usually involves RelA/p50 dimers which are retained in the cytoplasm by IκB proteins. Activation of the receptor leads to adaptor proteins recruitment such as TRAF6. TRAF ubiquitination induces the recruitment of an adaptor complex containing TAB2/TAB1 (TAK1 binding protein) and the mitogen activated kinase kinase (MAPKK) kinase TAK1 (TGF-β activated kinase). TAK1 activation induces the phosphorylation of IκB kinase (IKK) complex. In the canonical pathway, IKK complex is formed of IKKα and IKKβ catalytic subunits and IKKγ (NEMO, NF-κB essential modulator) negative regulatory subunit. Phosphorylation of IKKβ induces proteasomal degradation of IκB and translocation of RelA/p50 to the nucleus [39,50].

In the non-canonical pathway, receptor activation induces the recruitment of NF-κB inducing kinase (NIK). This kinase phosphorylates IKKα homodimers leading to proteolytic processing of RelB/p100 dimer into mature RelB/p52 transcription factor enabling nuclear translocation and transcription activation [39,50,51].

RANK, similarly to LTβR, can activate both canonical and non-canonical pathways leading to cell survival and differentiation [39,51–53].
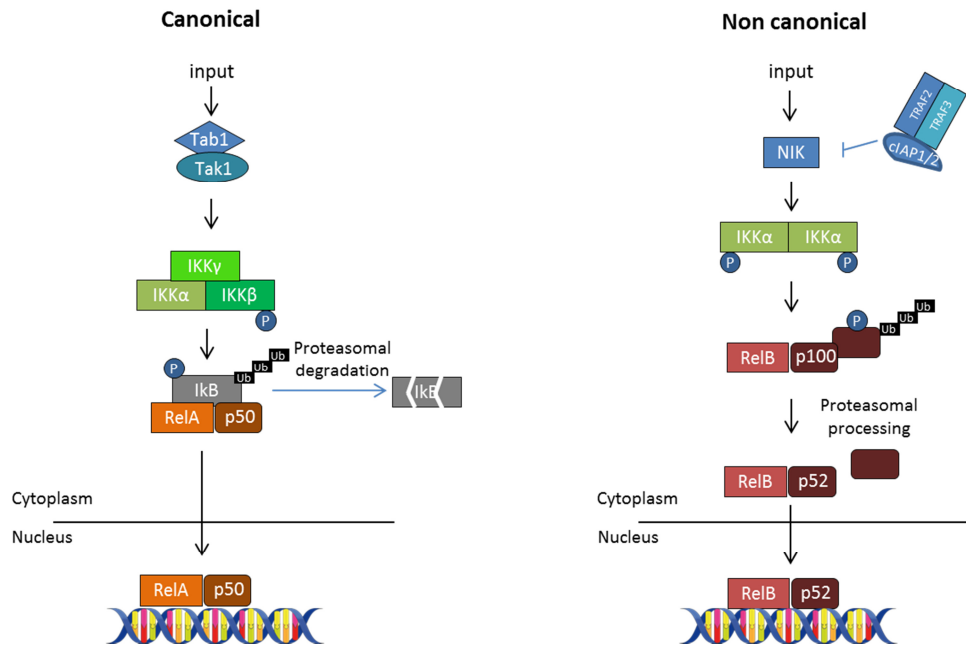
Figure 1.8: Canonical and non-canonical NF-κB pathways. The canonical pathway requires the recruitment of an adaptor complex containing TAB1/2 and TAK1. TAK1 phosphorylates IKKβ leading to IκB phosphorylation and proteasomal degradation. IκB degradation allows RelA/p50 dimer to translocate to the nucleus and activate gene transcription. The non-canonical pathway requires phosphorylation of IKKα by NIK. IKKα induces processing of RelB/p100 dimer into mature RelB/p52 dimer and translocation to the nucleus. Abbreviations: TAB: TAK1 binding protein, TAK1: TGF-β activated kinase 1, IKK: IκB kinase, NIK: NF-κB inducible kinase, Ub: ubiquitin. After reference [50,54].

b)   MAPK pathway

The family of mitogen-activated protein kinases (MAPK) contains the extracellular signal regulated kinases (ERK1/2), p-38-MAPK, c-Jun N-terminal kinases (JNK 1,2,3) and larger MAPKs (ERK 5,7,8). They are serine/threonine protein kinases responsible for a wide range of intracellular responses including cell differentiation, proliferation and apoptosis. ERK1/2, p38 and JNK signaling have been shown to be induced after RANK activation [27,39]. The MAPKs signaling pathway involves a cascade of phosphorylation leading to transcription factor activation or structural proteins phosphorylation. After receptor activation, MAP3K (MAPK kinase kinase) is activated leading to phosphorylation of the MAPK kinase (MAPKK). MAPKK in turn phosphorylates a MAPK inducing the cellular response. It has also been shown that p38 MAPK can be activated in a MAPKK independent manner via recruitment of TAK1/TAB1-2 complex by TRAF6 [55]. Activation of p38 via RANK signaling was shown to activate STAT-1 (signal transducer and activator of transcription 1) thus controlling gene expression [56]. JNK1 activation induces phosphorylation of c-Jun allowing the formation of AP-1 (activator protein 1) transcription factor heterodimer containing c-Fos and c-Jun [57]. The consequences of ERK1/2

pathway activation by RANKL are less clear but these kinases are known to be involved in cell proliferation [58].
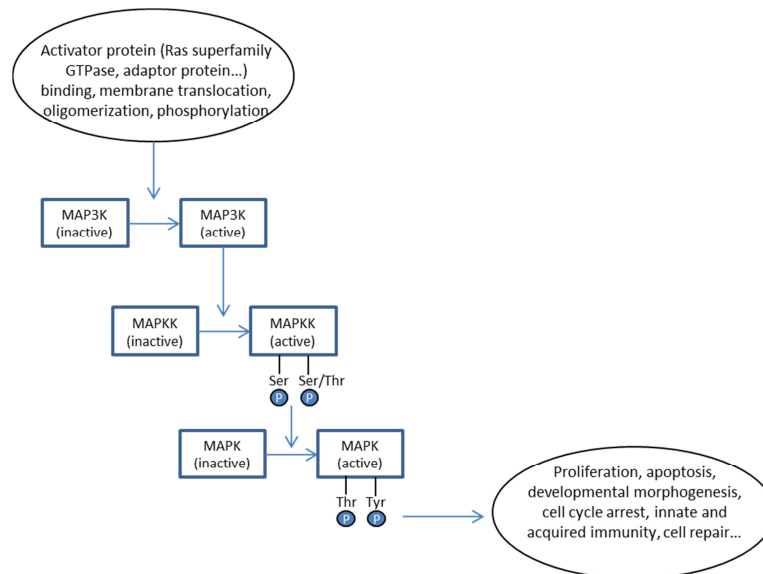
Figure 1.9: Phosphorylation cascade of the MAPKs pathway. After receptor activation activated MAP3K phosphorylates MAPKK which in turn phosphorylates the MAPKs ERK, p38 or JNK. Abbreviations: MAP3K: mitogen-activated protein kinase kinase kinase, MAPKK: MAP kinase kinase, MAPK: MAP kinase, Ser: serine, Thr: Threonine, Tyr: Tyrosine. Modified after reference [58].

c)   PKB/Akt pathway

Akt proteins are also called protein kinase B (PKB). Akt1/PKBα is ubiquitously expressed while Akt2/PKBβ is expressed by insulin sensitive tissues and Akt3/PKBγ is expressed in the brain and testis. Akt is activated by the phosphatidylinositol 3-kinase (PI3K) heterodimeric lipid kinase. PI3K phosphorylates Akt leading to stabilization and activation of the protein thus inducing cellular response [59]. It was shown that after RANKL stimulation TRAF6 recruits the c-Src kinase [60]. This kinase phosphorylates Cbl protein involved in recruitment of PI3K to the receptor complex [27]. Akt activates downstream signaling molecules leading to control of genes involved in cell survival, cell cycle, glucose metabolism and protein synthesis depending on the cell type [59].
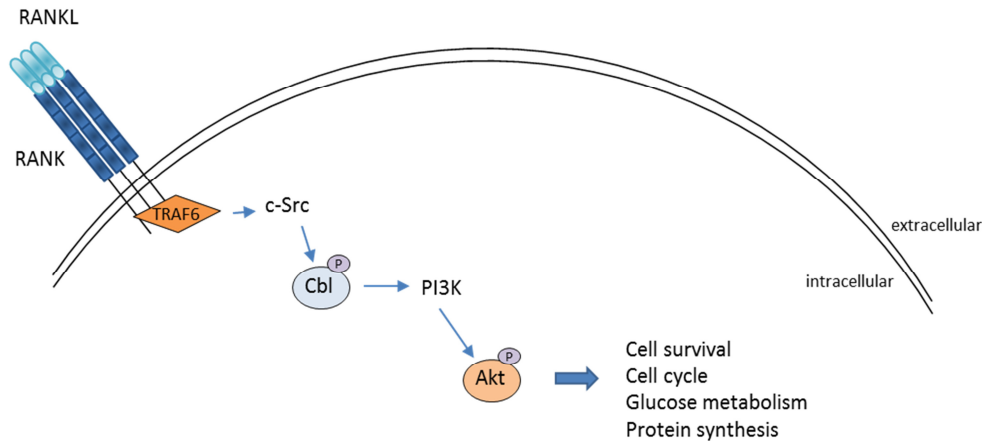
Figure 1.10: Akt signaling activation by RANKL. TRAF6 activates c-Src and recruitment of PI3K to the receptor complex via phosphorylation of Cbl. PI3K phosphorylates Akt thus inducing cellular response. Abbreviations: PI3K: phosphatidylinositol 3-kinase, TRAF: TNFR-associated factors, c-SRC: cellular sarcoma.

d)   NFATc1/calcineurin pathway

NFAT (Nuclear factor of activated T cells) transcription factors were discovered at first in T cells. This family contains five proteins named NFATc1, c2, c3, c4 and NFAT5 playing a role in many biological processes including cell differentiation. They are found in a hyperphosphorylated inactive form in the cytoplasm. Increase in Ca^{2+} intracellular levels activates calcineurin via the signaling intermediate calmodulin. Calcineurin activation induces NFAT dephosphorylation and nuclear translocation. NFAT proteins bind DNA response elements together with other transcription factor such as AP-1 hence cooperating with MAPKs pathway [61]. RANKL was shown to induce NFATc1 expression [62,63]. However, RANKL was not known to play a role in calcium influx. Koga and colleagues showed that RANK can phosphorylate the immunoreceptor tyrosine based activation motif (ITAM) on FCRγ (Fc receptor common γ subunit) and DAP (DNAX-activating protein) 12 [64]. ITAM phosphorylation leads to Syk kinase activation of phospholipase C γ (PLCγ) [65]. Activated PLC is recruited to the receptor and hydrolyses phosphatidylinositol 4,5 biphosphate (PIP2) into diacylglycerol (DAG) and phosphatidylinositol 1,4,5 triphosphate (PIP3). PIP3 further induces Ca^{2+} influx via membrane calcium channels. NFATc1 expression was also shown to be induced by p50 and RelA NF-κB components binding to NFATc1 promoter after RANK activation [66].
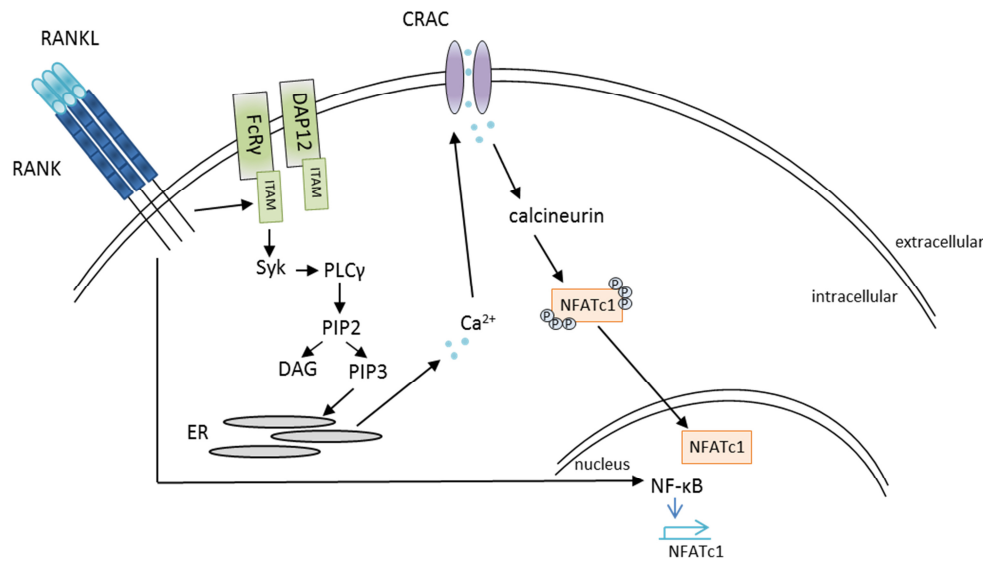
Figure 1.11: Regulation of NFATc1 pathway by RANKL. RANK activates ITAM thus inducing PLC pathway. PLC induces Ca^{2+} influx from endoplasmic reticulum increasing Ca^{2+} intracellular levels and activating NFATc1. RANK-induces NF-κB signaling which increases NFATc1 expression. Abbreviations: ER: endoplasmic reticulum, CRAC: calcium release activated channels, ITAM: immunoreceptor tyrosine based activation motif, FcRγ: Fc receptor common γ subunit, DAP12: DNAX-activating protein 12, PLCγ: phospholipase C γ, PIP2: phosphatidylinositol 4,5 biphosphate, DAG: diacylglycerol, PIP3: phosphatidylinositol 1,4,5 triphosphate. Modified after reference [27,67].

e) Crosstalk with interferon pathway

It was observed that RANK signaling can crosstalk with other signaling pathways including interferon pathway. IFNγ induces the degradation of TRAF6 in an ubiquitin-proteasome dependent mechanism consequently inhibiting RANK downstream signaling [68]. Moreover, RANKL stimulation induces the production of IFNβ but not IFNα in a mechanism involving c-Fos. IFNβ in turn negatively regulates RANKL induced c-Fos expression and NFATc1 induction in a STAT1 dependent manner creating a negative feeback loop [69]. The induction of IFNβ expression was shown to be mediated by IRF-7 (Interferon-regulatory factor 7) transcription factor in medullary thymic epithelial cells [70].
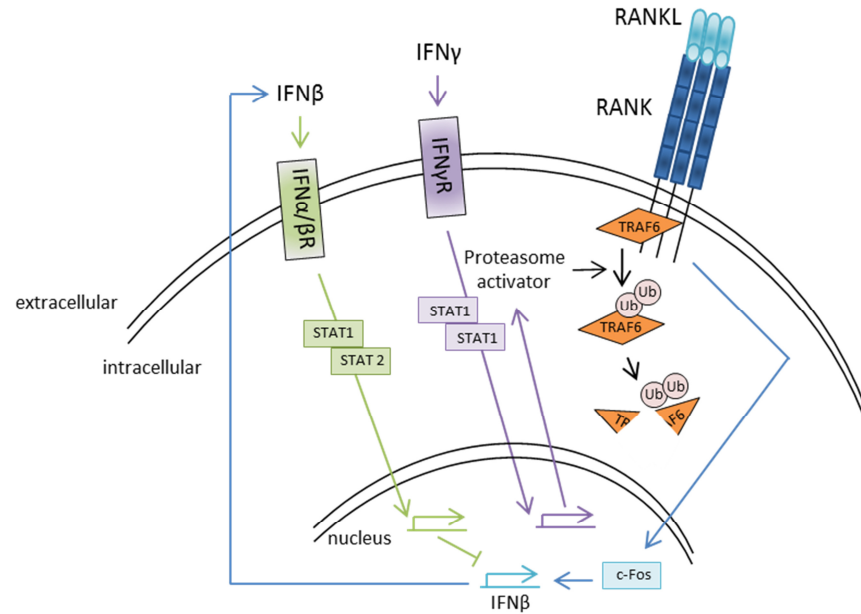
Figure 1.12: Crosstalk between RANK signaling and interferon signaling. IFNγ signaling induces TRAF6 degradation in an ubiquitin-proteasome dependent mechanism. RANK activation induces expression of IFNβ. In a negative feedback loop IFNβ in turn downregulates gene transcription activated by RANK. Modified after reference [27].

1.4. Conclusions

In the 1990's, four different groups discovered the RANK/RANKL/OPG triad. These proteins are part of the TNF and TNFR superfamilies of receptors and ligands. RANK binds RANKL but OPG acts as a decoy receptor binding RANKL and preventing RANK activation. Crystallization of RANKL in a complex with RANK and OPG provided detailed understanding of the residues and conformation required for binding. RANKL stimulation induces the recruitment of adaptor proteins leading to activation of different signaling pathways including canonical and non-canonical NF-κB, MAPK, Akt/PKB and calcineurin/NFATc1 pathways. Therefore, RANKL stimulation induces numerous cellular responses playing a role in a wide range of biological processes. RANK signaling pathway also crosstalks with interferon pathway in a mechanism negatively regulating RANK activation. Although RANK signaling pathways are not the subjects of my thesis, I described these different pathways in this chapter to highlight the potency of RANK signaling in cell activation. The biology of the RANK/RANKL/OPG triad will be detailed in the following chapter together with the therapeutic approaches used to target specifically RANK/RANKL axis.

1.5. <u>**References**</u>

1. Locksley RM, Killeen N, Lenardo MJ. The TNF and TNF Receptor Superfamilies: Integrating Mammalian Biology. Cell. 2001;104: 487–501. doi:10.1016/S0092-8674(01)00237-9

2. Granger GA, Shacks SJ, Williams TW, Kolb WP. Lymphocyte in vitro Cytotoxicity: Specific Release of Lymphotoxin-like Materials from Tuberculin-sensitive Lymphoid Cells. Nature. 1969;221: 1155–1157. doi:10.1038/2211155a0

3. Carswell EA, Old LJ, Kassel RL, Green S, Fiore N, Williamson B. An endotoxin-induced serum factor that causes necrosis of tumors. Proc Natl Acad Sci U S A. 1975;72: 3666–3670.

4. Gray PW, Aggarwal BB, Benton CV, Bringman TS, Henzel WJ, Jarrett JA, et al. Cloning and expression of cDNA for human lymphotoxin, a lymphokine with tumour necrosis activity. Nature. 1984;312: 721–724. doi:10.1038/312721a0

5. Pennica D, Nedwin GE, Hayflick JS, Seeburg PH, Derynck R, Palladino MA, et al. Human tumour necrosis factor: precursor structure, expression and homology to lymphotoxin. Nature. 1984;312: 724–729. doi:10.1038/312724a0

6. Bodmer J-L, Schneider P, Tschopp J. The molecular architecture of the TNF superfamily. Trends Biochem Sci. 2002;27: 19–26. doi:10.1016/S0968-0004(01)01995-8

7. Zhang G. Tumor necrosis factor family ligand–receptor binding. Curr Opin Struct Biol. 2004;14: 154–160. doi:10.1016/j.sbi.2004.03.003

8. Aggarwal BB. Signalling pathways of the TNF superfamily: a double-edged sword. Nat Rev Immunol. 2003;3: 745–756. doi:10.1038/nri1184

9. Croft M, Benedict CA, Ware CF. Clinical targeting of the TNF and TNFR superfamilies. Nat Rev Drug Discov. 2013;12: 147–168. doi:10.1038/nrd3930

10. Simonet WS, Lacey DL, Dunstan CR, Kelley M, Chang M-S, Lüthy R, et al. Osteoprotegerin: A Novel Secreted Protein Involved in the Regulation of Bone Density. Cell. 1997;89: 309–319. doi:10.1016/S0092-8674(00)80209-3

11. Tsuda E, Goto M, Mochizuki S, Yano K, Kobayashi F, Morinaga T, et al. Isolation of a Novel Cytokine from Human Fibroblasts That Specifically Inhibits Osteoclastogenesis. Biochem Biophys Res Commun. 1997;234: 137–142. doi:10.1006/bbrc.1997.6603

12. Yasuda H, Shima N, Nakagawa N, Yamaguchi K, Kinosaki M, Mochizuki S, et al. Osteoclast differentiation factor is a ligand for osteoprotegerin/osteoclastogenesis-inhibitory factor and is identical to TRANCE/RANKL. Proc Natl Acad Sci U S A. 1998;95: 3597–3602.

13. Lacey DL, Timms E, Tan H-L, Kelley MJ, Dunstan CR, Burgess T, et al. Osteoprotegerin Ligand Is a Cytokine that Regulates Osteoclast Differentiation and Activation. Cell. 1998;93: 165–176. doi:10.1016/S0092-8674(00)81569-X

14. Anderson DM, Maraskovsky E, Billingsley WL, Dougall WC, Tometsko ME, Roux ER, et al. A homologue of the TNF receptor and its ligand enhance T-cell growth and dendritic-cell function. Nature. 1997;390: 175–179. doi:10.1038/36593

15. Wong BR, Josien R, Lee SY, Sauter B, Li H-L, Steinman RM, et al. TRANCE (Tumor Necrosis Factor [TNF]-related Activation-induced Cytokine), a New TNF Family Member Predominantly Expressed in T cells, Is a Dendritic Cell–specific Survival Factor. J Exp Med. 1997;186: 2075–2080. doi:10.1084/jem.186.12.2075

16. Yasuda H, Shima N, Nakagawa N, Mochizuki S-I, Yano K, Fujise N, et al. Identity of Osteoclastogenesis Inhibitory Factor (OCIF) and Osteoprotegerin (OPG): A Mechanism by which OPG/OCIF Inhibits Osteoclastogenesis in Vitro. Endocrinology. 1998;139: 1329–1337. doi:10.1210/endo.139.3.5837

17. Nakagawa N, Kinosaki M, Yamaguchi K, Shima N, Yasuda H, Yano K, et al. RANK Is the Essential Signaling Receptor for Osteoclast Differentiation Factor in Osteoclastogenesis. Biochem Biophys Res Commun. 1998;253: 395–400. doi:10.1006/bbrc.1998.9788

18. Hsu H, Lacey DL, Dunstan CR, Solovyev I, Colombero A, Timms E, et al. Tumor necrosis factor receptor family member RANK mediates osteoclast differentiation and activation induced by osteoprotegerin ligand. Proc Natl Acad Sci U S A. 1999;96: 3540–3545.

19. Emery JG, McDonnell P, Burke MB, Deen KC, Lyn S, Silverman C, et al. Osteoprotegerin Is a Receptor for the Cytotoxic Ligand TRAIL. J Biol Chem. 1998;273: 14363–14367. doi:10.1074/jbc.273.23.14363

20. Lum L, Wong BR, Josien R, Becherer JD, Erdjument-Bromage H, Schlöndorff J, et al. Evidence for a Role of a Tumor Necrosis Factor-α (TNF-α)-converting Enzyme-like Protease in Shedding of TRANCE, a TNF Family Member Involved in Osteoclastogenesis and Dendritic Cell Survival. J Biol Chem. 1999;274: 13613–13618. doi:10.1074/jbc.274.19.13613

21. Hikita A, Yana I, Wakeyama H, Nakamura M, Kadono Y, Oshima Y, et al. Negative Regulation of Osteoclastogenesis by Ectodomain Shedding of Receptor Activator of NF-κB Ligand. J Biol Chem. 2006;281: 36846–36855. doi:10.1074/jbc.M606656200

22. Lynch CC, Hikosaka A, Acuff HB, Martin MD, Kawai N, Singh RK, et al. MMP-7 promotes prostate cancer-induced osteolysis via the solubilization of RANKL. Cancer Cell. 2005;7: 485–496. doi:10.1016/j.ccr.2005.04.013

23. Lam J, Nelson CA, Ross FP, Teitelbaum SL, Fremont DH. Crystal structure of the TRANCE/RANKL cytokine reveals determinants of receptor-ligand specificity. J Clin Invest. 2001;108: 971–979.

24. Nelson CA, Warren JT, Wang MW-H, Teitelbaum SL, Fremont DH. RANKL employs distinct binding modes to engage RANK and the osteoprotegerin decoy receptor. Struct Lond Engl 1993. 2012;20: 1971–1982. doi:10.1016/j.str.2012.08.030

25. Ikeda T, Kasai M, Utsuyama M, Hirokawa K. Determination of Three Isoforms of the Receptor Activator of Nuclear Factor-κB Ligand and Their Differential Expression in Bone and Thymus. Endocrinology. 2001;142: 1419–1426. doi:10.1210/endo.142.4.8070

26. Kartsogiannis V, Zhou H, Horwood NJ, Thomas RJ, Hards DK, Quinn JMW, et al. Localization of RANKL (receptor activator of NFκB ligand) mRNA and protein in skeletal and extraskeletal tissues. Bone. 1999;25: 525–534. doi:10.1016/S8756-3282(99)00214-8

27. Wada T, Nakashima T, Hiroshi N, Penninger JM. RANKL–RANK signaling in osteoclastogenesis and bone disease. Trends Mol Med. 2006;12: 17–25. doi:10.1016/j.molmed.2005.11.007

28. Liu C, Walter TS, Huang P, Zhang S, Zhu X, Wu Y, et al. Structural and Functional Insights of RANKL–RANK Interaction and Signaling. J Immunol. 2010;184: 6910–6919. doi:10.4049/jimmunol.0904033

29. Ta HM, Nguyen GTT, Jin HM, Choi J, Park H, Kim N, et al. Structure-based development of a receptor activator of nuclear factor-κB ligand (RANKL) inhibitor peptide and molecular basis for osteopetrosis. Proc Natl Acad Sci. 2010;107: 20281–20286. doi:10.1073/pnas.1011686107

30. Mukai S, Kitazawa R, Ishii J, Kondo T, Hakozaki A, Horiuchi K, et al. Identification and analysis of function of a novel splicing variant of mouse receptor activator of NF-κB. Mol Cell Biochem. 2011;350: 29–38. doi:10.1007/s11010-010-0679-z

31. Sirinian C, Papanastasiou AD, Zarkadis IK, Kalofonos HP. Alternative splicing generates a truncated isoform of human TNFRSF11A (RANK) with an altered capacity to activate NF-κB. Gene. 2013;525: 124–129. doi:10.1016/j.gene.2013.04.075

32. Walsh MC, Choi Y. Biology of the RANKL–RANK–OPG system in immunity, bone, and beyond. Inflammation. 2014;5: 511. doi:10.3389/fimmu.2014.00511

33. Théoleyre S, Kwan Tat S, Vusio P, Blanchard F, Gallagher J, Ricard-Blum S, et al. Characterization of osteoprotegerin binding to glycosaminoglycans by surface plasmon resonance: Role in the interactions with receptor activator of nuclear factor κB ligand (RANKL) and RANK. Biochem Biophys Res Commun. 2006;347: 460–467. doi:10.1016/j.bbrc.2006.06.120

34. Yamaguchi K, Kinosaki M, Goto M, Kobayashi F, Tsuda E, Morinaga T, et al. Characterization of Structural Domains of Human Osteoclastogenesis Inhibitory Factor. J Biol Chem. 1998;273: 5117–5123. doi:10.1074/jbc.273.9.5117

35. Mosheimer BA, Kaneider NC, Feistritzer C, Djanani AM, Sturn DH, Patsch JR, et al. Syndecan-1 Is Involved in Osteoprotegerin-Induced Chemotaxis in Human Peripheral Blood Monocytes. J Clin Endocrinol Metab. 2005;90: 2964–2971. doi:10.1210/jc.2004-1895

36. Kwon BS, Wang S, Udagawa N, Haridas V, Lee ZH, Kim KK, et al. TR1, a new member of the tumor necrosis factor receptor superfamily, induces fibroblast proliferation and inhibits osteoclastogenesis and bone resorption. FASEB J. 1998;12: 845–854.

37. Schoppet M, Preissner KT, Hofbauer LC. RANK Ligand and Osteoprotegerin. Arterioscler Thromb Vasc Biol. 2002;22: 549–553. doi:10.1161/01.ATV.0000012303.37971.DA

38. Walsh MC, Choi Y. Biology of the TRANCE axis. Cytokine Growth Factor Rev. 2003;14: 251–263. doi:10.1016/S1359-6101(03)00027-3

39. Leibbrandt A, Penninger JM. RANK/RANKL: Regulators of Immune Responses and Bone Physiology. Ann N Y Acad Sci. 2008;1143: 123–150. doi:10.1196/annals.1443.016

40. Arai F, Miyamoto T, Ohneda O, Inada T, Sudo T, Brasel K, et al. Commitment and Differentiation of Osteoclast Precursor Cells by the Sequential Expression of C-Fms and Receptor Activator of Nuclear Factor κb (Rank) Receptors. J Exp Med. 1999;190: 1741–1754.

41. Kanazawa K, Kudo A. Self-Assembled RANK Induces Osteoclastogenesis Ligand-Independently. J Bone Miner Res. 2005;20: 2053–2060. doi:10.1359/JBMR.050706

42. Galibert L, Tometsko ME, Anderson DM, Cosman D, Dougall WC. The Involvement of Multiple Tumor Necrosis Factor Receptor (TNFR)-associated Factors in the Signaling Mechanisms of Receptor Activator of NF-κB, a Member of the TNFR Superfamily. J Biol Chem. 1998;273: 34120–34127. doi:10.1074/jbc.273.51.34120

43. Naito A, Azuma S, Tanaka S, Miyazaki T, Takaki S, Takatsu K, et al. Severe osteopetrosis, defective interleukin-1 signalling and lymph node organogenesis in TRAF6-deficient mice. Genes Cells. 1999;4: 353–362. doi:10.1046/j.1365-2443.1999.00265.x

44. Xu Y, Cheng G, Baltimore D. Targeted Disruption of TRAF3 Leads to Postnatal Lethality and Defective T-Dependent Immune Responses. Immunity. 1996;5: 407–415. doi:10.1016/S1074-7613(00)80497-5

45. Yeh W-C, Shahinian A, Speiser D, Kraunus J, Billia F, Wakeham A, et al. Early Lethality, Functional NF-κB Activation, and Increased Sensitivity to TNF-Induced Cell Death in TRAF2-Deficient Mice. Immunity. 1997;7: 715–725. doi:10.1016/S1074-7613(00)80391-X

46. Ye H, Arron JR, Lamothe B, Cirilli M, Kobayashi T, Shevde NK, et al. Distinct molecular mechanism for initiating TRAF6 signalling. Nature. 2002;418: 443–447. doi:10.1038/nature00888

47. Wada T, Nakashima T, Oliveira-dos-Santos AJ, Gasser J, Hara H, Schett G, et al. The molecular scaffold Gab2 is a crucial component of RANK signaling and osteoclastogenesis. Nat Med. 2005;11: 394–399. doi:10.1038/nm1203

48. Kim H, Choi HK, Shin JH, Kim KH, Huh JY, Lee SA, et al. Selective inhibition of RANK blocks osteoclast maturation and function and prevents bone loss in mice. J Clin Invest. 2009;119: 813–825. doi:10.1172/JCI36809

49. Baud'huin M, Lamoureux F, Duplomb L, Rédini F, Heymann D. RANKL, RANK, osteoprotegerin: key partners of osteoimmunology and vascular diseases. Cell Mol Life Sci. 2007;64: 2334–2350. doi:10.1007/s00018-007-7104-0

50. Mowla SN, Perkins ND, Jat PS. Friend or foe: emerging role of nuclear factor kappa-light-chain-enhancer of activated B cells in cell senescence. OncoTargets Ther. 2013;6: 1221–1229. doi:10.2147/OTT.S36160

51. Dejardin E. The alternative NF-κB pathway from biochemistry to biology: Pitfalls and promises for future drug development. Biochem Pharmacol. 2006;72: 1161–1179. doi:10.1016/j.bcp.2006.08.007

52. Mizukami J, Takaesu G, Akatsuka H, Sakurai H, Ninomiya-Tsuji J, Matsumoto K, et al. Receptor Activator of NF-κB Ligand (RANKL) Activates TAK1 Mitogen-Activated Protein Kinase Kinase Kinase through a Signaling Complex Containing RANK, TAB2, and TRAF6. Mol Cell Biol. 2002;22: 992–1000. doi:10.1128/MCB.22.4.992-1000.2002

53. Remouchamps C, Boutaffala L, Ganeff C, Dejardin E. Biology and signal transduction pathways of the Lymphotoxin-αβ/LTβR system. Cytokine Growth Factor Rev. 2011;22: 301–310. doi:10.1016/j.cytogfr.2011.11.007

54. Yang C, Davis JL, Zeng R, Vora P, Su X, Collins LI, et al. Antagonism of Inhibitor of Apoptosis Proteins Increases Bone Metastasis via Unexpected Osteoclast Activation. Cancer Discov. 2013;3: 212–223. doi:10.1158/2159-8290.CD-12-0271

55. Ge B, Gram H, Padova FD, Huang B, New L, Ulevitch RJ, et al. MAPKK-Independent Activation of p38α Mediated by TAB1-Dependent Autophosphorylation of p38α. Science. 2002;295: 1291–1294. doi:10.1126/science.1067289

56. Kwak HB, Lee SW, Jin HM, Ha H, Lee SH, Takeshita S, et al. Monokine induced by interferon-γ is induced by receptor activator of nuclear factor κB ligand and is involved in osteoclast adhesion and migration. Blood. 2005;105: 2963–2969. doi:10.1182/blood-2004-07-2534

57. David J-P, Sabapathy K, Hoffmann O, Idarraga MH, Wagner EF. JNK1 modulates osteoclastogenesis through both c-Jun phosphorylation-dependent and -independent mechanisms. J Cell Sci. 2002;115: 4317–4325. doi:10.1242/jcs.00082

58. Kyriakis JM, Avruch J. Mammalian Mitogen-Activated Protein Kinase Signal Transduction Pathways Activated by Stress and Inflammation. Physiol Rev. 2001;81: 807–869.

59. Shiojima I, Walsh K. Role of Akt Signaling in Vascular Homeostasis and Angiogenesis. Circ Res. 2002;90: 1243–1250. doi:10.1161/01.RES.0000022200.71892.9F

60. Wong BR, Besser D, Kim N, Arron JR, Vologodskaia M, Hanafusa H, et al. TRANCE, a TNF Family Member, Activates Akt/PKB through a Signaling Complex Involving TRAF6 and c-Src. Mol Cell. 1999;4: 1041–1049. doi:10.1016/S1097-2765(00)80232-4

61. Hogan PG, Chen L, Nardone J, Rao A. Transcriptional regulation by calcium, calcineurin, and NFAT. Genes Dev. 2003;17: 2205–2232. doi:10.1101/gad.1102703

62. Takayanagi H, Kim S, Koga T, Nishina H, Isshiki M, Yoshida H, et al. Induction and Activation of the Transcription Factor NFATc1 (NFAT2) Integrate RANKL Signaling in Terminal Differentiation of Osteoclasts. Dev Cell. 2002;3: 889–901. doi:10.1016/S1534-5807(02)00369-6

63. Fu J, Tao YD, Chen J, Zhang Y, He J. Role of RANKL in the regulation of NFATc1 and c-Src mRNA expression in osteoclast-like cells. Mol Med Rep. 2016;13: 5163–5168.

64. Koga T, Inui M, Inoue K, Kim S, Suematsu A, Kobayashi E, et al. Costimulatory signals mediated by the ITAM motif cooperate with RANKL for bone homeostasis. Nature. 2004;428: 758–763. doi:10.1038/nature02444

65. Mao D, Epple H, Uthgenannt B, Novack DV, Faccio R. PLCγ2 regulates osteoclastogenesis via its interaction with ITAM proteins and GAB2. J Clin Invest. 2006;116: 2869–2879. doi:10.1172/JCI28775

66. Asagiri M, Sato K, Usami T, Ochi S, Nishina H, Yoshida H, et al. Autoamplification of NFATc1 expression determines its essential role in bone homeostasis. J Exp Med. 2005;202: 1261–1269. doi:10.1084/jem.20051150

67. Medyouf H, Ghysdael J. The calcineurin/NFAT signaling pathway: A NOVEL therapeutic target in leukemia and solid tumors. Cell Cycle. 2008;7: 297–303. doi:10.4161/cc.7.3.5357

68. Takayanagi H, Ogasawara K, Hida S, Chiba T, Murata S, Sato K, et al. T-cell-mediated regulation of osteoclastogenesis by signalling cross-talk between RANKL and IFN-γ. Nature. 2000;408: 600–605. doi:10.1038/35046102

69. Takayanagi H, Kim S, Matsuo K, Suzuki H, Suzuki T, Sato K, et al. RANKL maintains bone homeostasis through c-Fos-dependent induction of interferon-β. Nature. 2002;416: 744–749. doi:10.1038/416744a

70. Otero DC, Baker DP, David M. IRF7-Dependent IFN-β Production in Response to RANKL Promotes Medullary Thymic Epithelial Cell Development. J Immunol. 2013;190: 3289–3298. doi:10.4049/jimmunol.1203086

Chapter 2: Biology of RANK/RANKL/OPG triad and current therapeutic strategies targeting the triad

2.1. RANK/RANKL/OPG triad in bone homeostasis and pathologies

Bone is necessary for protection of vital organs, locomotive activity, calcium storage and is also a source of hematopoietic stem cells necessary for immune cell development. Bone remodeling is a continuous process replacing old bone with new bone matrix thus maintaining size, shape and quality of the skeleton. Two main cell types are involved in bone remodeling: osteoblasts (OBs) and osteoclasts (OCs) [1]. OCs have a myeloid origin and resorb mineralized bone by secreting digestive acids. On the other hand, OBs have a mesenchymal origin and are filling the holes with new bone matrix [1]. This continuous cycle is required to maintain skeletal strength and a source of hematopoietic stem cells in the bone marrow. Imbalanced activity of these two cell types can lead to osteopetrosis (increase of bone mass) or osteoporosis (decrease of bone mass) (**figure 2.1**). The bone homeostasis process can be impaired by a wide range of factors including hormonal changes, cytokines and growth factors [1]. (see Chapter 1 table 1.1)
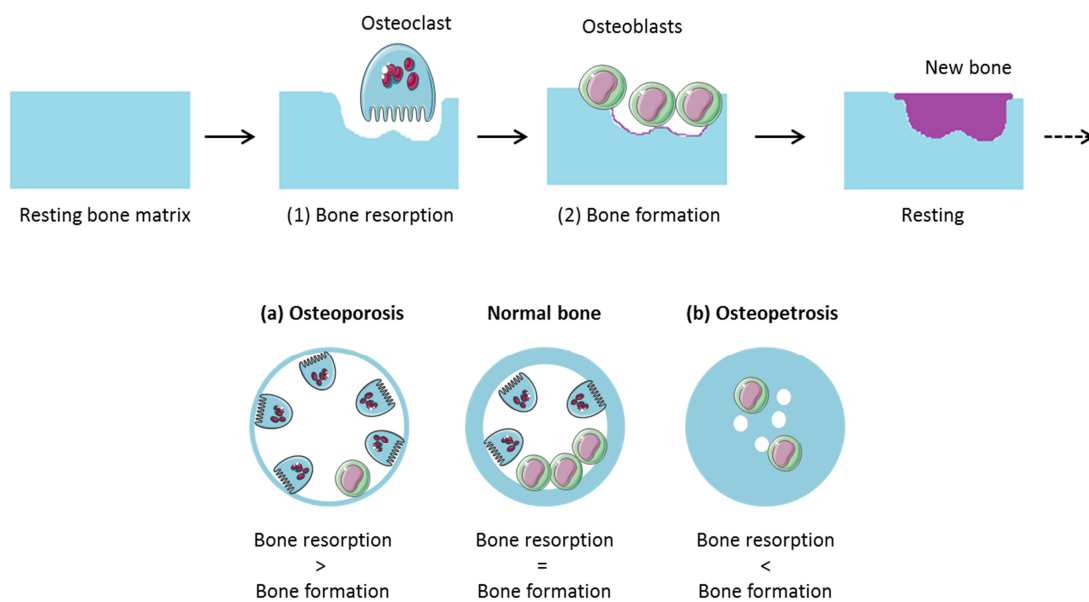
Figure 2.1: Bone remodeling cycle and involvement in diseases. Schematic representation of bone cycle. The first step in bone remodeling is resorption of existing bone matrix by osteoclasts (1). In a second step, osteoblasts produce new bone matrix to fill the lacunae formed after resorption (2). This continuous cycle enables constant renewal of bone matrix maintaining size, shape and quality of the skeleton. Increased bone resorption compared to bone formation leads to osteoporosis and thinner bone matrix (a). On the opposite when osteoblasts are more active, bone formation increase leads to osteopetrosis and thicker bone matrix (b). Modified after reference [2].

Early studies showed that OCs differentiation is induced by RANKL [3] and the role of RANK-RANKL in bone biology has since been extensively studied. It was shown that both macrophage colony-stimulating factor (M-CSF) and RANKL are required for OC precursor proliferation and differentiation [4,5]. Both RANKL and RANK deficient mice present severe osteopetrosis due to a lack of osteoclasts [6,7] whereas osteoporosis occurs in OPG deficient mice [8,9]. RANKL is expressed by OBs and bone marrow stromal cells while RANK is expressed by both OC precursors and mature OC (**figure 2.2**). Oligomerization of RANKL *in vitro* mimics the effect of membrane-bound RANKL. It was observed that soluble RANKL is less efficient than oligomers in inducing osteoclastogenesis *in vitro* [10]. Hence, cell-cell interaction and membrane bound expression of RANKL on OBs might be required for osteoclastogenesis.
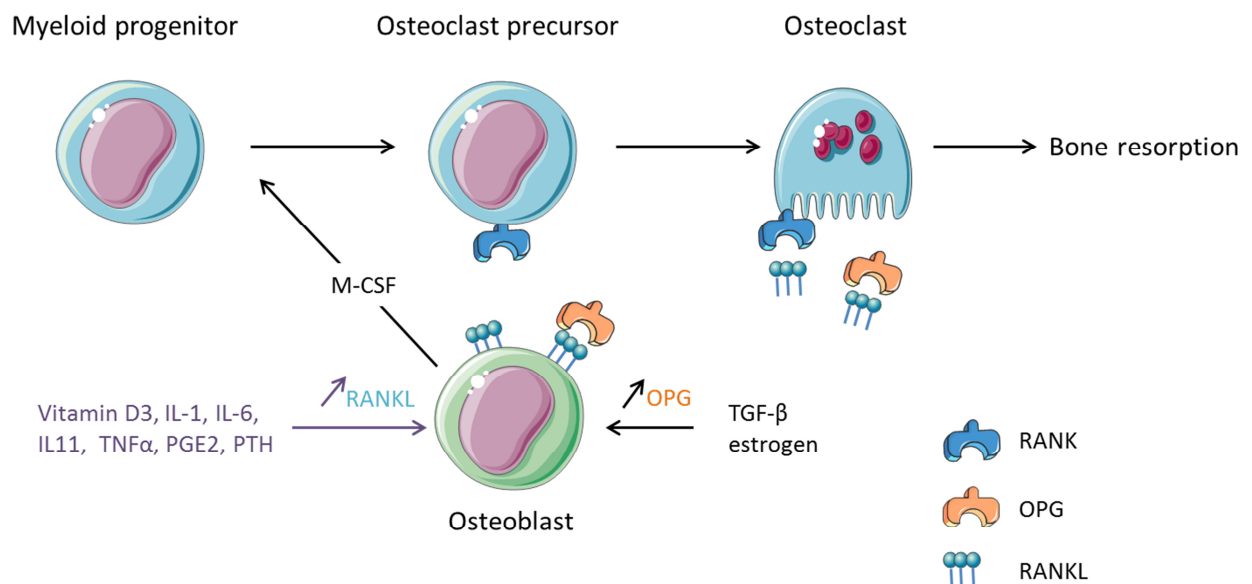
Figure 2.2: Role of RANK-RANKL-OPG triad in osteoclast differentiation. Several calcitropic factors such as vitamin D3, IL-1 and TNFα induce the expression of RANKL and macrophage colony stimulating factor (M-CSF) by osteoblasts. M-CSF promotes the development of RANK-expressing osteoclast precursors from myeloid progenitors. Osteoblast expressing RANKL then activate precursor differentiation into plurinucleated mature osteoclasts. TGF-β and estrogen negatively regulate osteoclastogenesis by inducing OPG expression on osteoblasts. Modified after reference [5].

Several factors acting on expression of the RANK/RANKL/OPG triad are involved in the systemic regulation of osteoclastogenesis. These molecules such as parathyroid hormone (PTH), vitamin D3, prostaglandin E2, IL-1β, TNFα and estrogen were already described in chapter 1. In particular, estrogen negatively regulates osteoclastogenesis by inducing OPG expression by OBs. On the other hand IL-1, IL-6 and IL-11 are known to induce RANKL expression on OBs [4]. Moreover, TNFα induces RANK expression on OC precursors as well as RANKL expression on OBs [11].

After RANK stimulation, different signaling pathways are activated (see Chapter 1) inducing osteoclast differentiation, proliferation and survival. Osteopetrosis and defect in bone-remodeling was observed in TRAF6-deficient mice [12] showing the important relationship between RANK and this signaling adaptor. The NF-κB pathway is important for osteoclastogenesis as p50/p52 double KO mice show arrested differentiation of osteoclasts [13]. Moreover, IKKβ and IKKγ are required for osteoclast differentiation underlining the predominant importance of the canonical NF-kB pathway in this process [14]. On the other hand, the alternative NF-κB pathway was also shown to promote osteoclastogenesis and mitochondrial biogenesis in osteoclasts in response to RANKL [15]. JNK1 [16], Akt/PKB [17], ERK1/2 [17] and p38 MAPK [18] pathways are also activated in osteoclasts. NF-κB and Akt/PKB pathways lead to expression of NFATc1 transcription factor. Moreover, as described in the previous chapter, RANK can induce ITAM activation and NFATc1 translocation to the nucleus [19]. NFATc1 is critical for osteoclasts differentiation as NFATc1 deficient mice showed impaired osteoclast development [20].

OPG is negatively regulating osteoclastogenesis but some pathways induced by RANK signaling can also lead to negative regulation of osteoclasts differentiation. The de-ubiquitinase CYLD was shown to negatively regulate RANKL induced osteoclastogenesis by preventing ubiquitinated TRAF6 to be recruited to IKK complex [21]. Moreover, IFNβ production is induced by RANKL stimulation. A negative regulatory loop inhibits RANKL-induced osteoclastogenesis via activation of the IFNAR1 receptor by IFNβ. Mice deficient in IFNAR1 show osteoporosis and increased OC development [22,23]. T cells can also negatively regulate osteoclastogenesis by secreting IFNγ [24]. Finally, the formation of a complex containing TRAF3 on the intracellular domain of RANK was shown to inhibit NF-κB pathway [25].

Some pathological conditions are linked with the role of RANKL in osteoclastogenesis. First of all, in line with the findings in mice, mutations in RANK and OPG were identified in patients with severe rare bone disorders [26]. Indeed, paget's disease and familial expansile osteolysis (FEO) are rare autosomal dominant conditions in which osteolytic lesions and enhanced bone remodeling are observed. Mutations disrupting functions of RANK signal peptide and inducing RANK constitutive activity were linked to FEO and Paget's disease of the bone (PDB) [26]. Besides inherited bone diseases, acquired bone pathologies such as osteoporosis are more common. Osteoporosis is characterized by predisposition to fracture and bone weakening due to exacerbated OCs activity compared to new bone formation [4]. Post-menopausal women are at high risk of osteoporosis because their estrogen levels naturally decrease. Bone remodeling process is accelerated in these women as shown by higher expression of both markers for bone formation and resorption [27,28]. Postmenopausal women showed higher expression of RANKL on the cell surface of pre-osteoblasts

compared to premenopausal or estrogen-treated postmenopausal women [28]. Estrogen effect on osteoclastogenesis have also been linked with decreased expression of inflammatory cytokines such as IL-1, IL-6 and TNFα which have been shown to regulate RANKL and OPG expression (see chapter 1) [29]. Therefore, the RANK-RANKL-OPG triad under the control of estrogen clearly plays a role in postmenopausal osteoporosis. Moreover, breast cancer or prostate cancer patients under hormone ablation therapy may also present osteoporosis due to increased RANKL expression.

The leucine-rich repeat-containing G-protein-coupled receptor 4 (LGR4) was recently identified as a new receptor for RANKL playing a role in osteoclastogenesis. It was shown that LGR4 extracellular domain binds RANKL and negatively regulates osteoclast differentiation via Gq signaling [30]. Therefore, tuning of osteoclast differentiation appears to be a complex mechanism and deserves further investigation.

2.2. RANK/RANKL/OPG triad in the immune system

2.2.1. B and T lymphocytes

By generating mice deficient for RANK and RANKL, Dougall and colleagues [6] and Kong and colleagues [7] respectively showed that RANK and RANKL are important for lymphoid development. Firstly, both RANK and RANKL deficient mice presented a decreased number of B lymphocytes in the spleen with a reduced number of mature IgM^+IgD^+ and $B220^+IgM^+$ B cells [6,7]. Kong and co-workers also showed that RANKL plays a role in the development of B cell precursors from $B220^+CD43^+CD25^-$ pro-B cells to $B220^+CD43^-CD25^+$ pre-B cells [7]. The importance of RANK for B cell development was also seen in humans as mutations in *Rank* leads to hypogammaglobulinemia in patients with severe autosomal-recessive osteopetrosis (ARO) presenting a defect in immunoglobulin production [31,32]. OPG also seems to play a role in B cell development and function. Indeed, accumulation of B cells in the spleen and higher *in vitro* proliferation of pro B cells after IL-7 stimulation was seen in OPG deficient mice [33]. It was shown that B cells express OPG after CD40 stimulation [34]. Taken together, these observations are in favour of a role for the RANK/RANKL/OPG axis in B cells development. The B cells defect observed can be due to a decreased bone marrow cellularity due to severe osteopetrosis in these mice [6,7]. In contrast, a recent study of mice with a B cell specific RANK deletion showed normal B cells development in these mice [35]. Normal antibody secretion, Ig class switch recombination and somatic mutation was also observed in B cell RANK KO mice [35]. According to this study, the effective role of RANK signaling in B cells remains unclear but does not

appear to be essential for B cell development. This suggests rather a role for these genes in bone marrow hematopoiesis.

T cell development was also investigated in mice lacking RANK and RANKL. The proportion of CD4$^+$CD8$^+$ immature cells and mature CD4$^+$ or CD8$^+$ T cells were normal in both RANKL and RANK deficient mice [6,7]. Normal expression of differentiation markers and TCR-CD3 complex was observed in RANKL deficient mice [7]. However, decreased thymic cellularity and size as well as impaired early thymocyte development was reported in 4 weeks old RANKL deficient mice [7]. Though, thymus of newborns and thymocytes from fetal thymic cultures were normal. From these studies, the implication of RANK signaling in T cell development remains unclear but might not be essential. On the other hand, RANK is required for the development of invariant γδ T cells [36].

2.2.2. Dendritic cells and adaptive immune response

Dendritic cells (DCs) are professional antigen presenting cells of the same lineage as osteoclasts. These cells are specialized in the capture of antigen and presentation to T cells. Therefore they play an important role in immune surveillance and adaptive immunity. RANK expression was detected on the surface of mature bone marrow-derived DCs as well as on fresh lymph node (LN), splenic DCs and mucosal DCs [37,38]. On the other hand, RANKL is not expressed by naïve T cells but after stimulation with anti-CD3/CD28 antibodies; both CD4$^+$ and CD8$^+$ activated T cells express RANKL on their surface [39]. It was shown *in vitro* that RANKL acts as a survival factor on bone marrow-derived DCs and that RANKL stimulation of DCs stimulates T cell proliferation [37] (**figure 2.3**). In the same study, Wong and colleagues showed that RANK activation leads to increased expression of the pro-survival protein Bcl-xl [37]. Moreover, anti-apoptotic signaling pathways such as Akt, NF-κB and ERK are activated after RANK stimulation [5]. The relevance of this anti-apoptotic effect *in vivo* is of great interest for immunotherapy. DC "vectors" survive longer when pre-treated with RANKL [40]. Moreover, RANKL could act as an "adjuvant" since mice injected with antigen-pulsed mature DCs pre-treated with RANKL *ex-vivo* showed increased DCs numbers and survival [41]. The increased T cell response was probably also due to a modification of cytokine production by DCs. Indeed, RANKL-stimulated DCs express pro-inflammatory cytokines IL-1 and IL-6 as well as T cell differentiation and proliferation factors such as IL-12 and IL-15 [39,42]. Conversely, it was also demonstrated that DCs activated with RANKL can lead to anti-inflammatory response and induce tolerance in a model of oral administration of antigens [38]. Williamson and colleagues showed that splenic DCs express pro-inflammatory IL-12 in response to RANK stimulation while DCs of Peyer's patches express the anti-

inflammatory cytokine IL-10 [38]. This difference between mucosal and peripheral DCs might be explained by the fact that intestinal DCs play an important role in counteracting immune response against the microbiome or food antigens thus preventing autoimmunity.

Additionally, RANK is expressed on Langerhans cells, the dendritic cells of the skin epidermis and RANKL also acts as a survival factor for these cells [43].

In spite of all these findings, there is little experimental proof that RANKL regulates DC development. Indeed, both RANK and RANKL deficient mice do not show impaired DC development [6,7]. Only a decreased number of LCs in RANKL deficient mice was observed by Barbaroux and colleagues [43]. Moreover, mice treated with recombinant OPG did not present dramatic impairments in innate or adaptive immunity [44]. This could be explained by the redundancy of RANK/RANKL system with CD40/CD40L. In fact, neutralization of RANKL *in vivo* in CD40 deficient mice leads to impaired CD4$^+$ T cells proliferation in response to viral or parasitic infection [42,45]. This anti-viral response is more severely inhibited in CD40 deficient mice than in normal mice, showing the redundancy of RANK/RANKL and CD40/CD40L. Moreover, CD40 was shown to be increased in DCs after RANKL stimulation [37] and treatment of DCs *in vitro* with CD40L increased RANK expression [46]. Even if there are similarities between these two signaling pathways, the RANK/RANKL system does not affect the expression of DC markers such as MHC class II, CD80, CD86, CD54 [46].

OPG has also been shown to be expressed by DCs [34] and it can bind the TNF superfamily ligand TRAIL, a well-known apoptotic factor expressed by activated T cells to induce DC death [47]. Therefore the balance between RANKL and TRAIL expression by activated T cells would contribute to death or survival of DCs and control the immune response (**figure 2.3**). However the low affinity of OPG for TRAIL compared to RANKL leaves the question open regarding the effective role of TRAIL *in vivo*. OPG expression is upregulated in DCs after CD40 stimulation [34].

Knowing that RANKL is under sex hormonal regulation, the effect of RANKL on DCs may explain the gender differences observed regarding immunity and the higher occurrence of autoimmune disorders in women. Moreover, the fact that RANKL induces survival and increases efficacy of DCs could be useful for antitumor vaccination or autoimmune disease treatment.
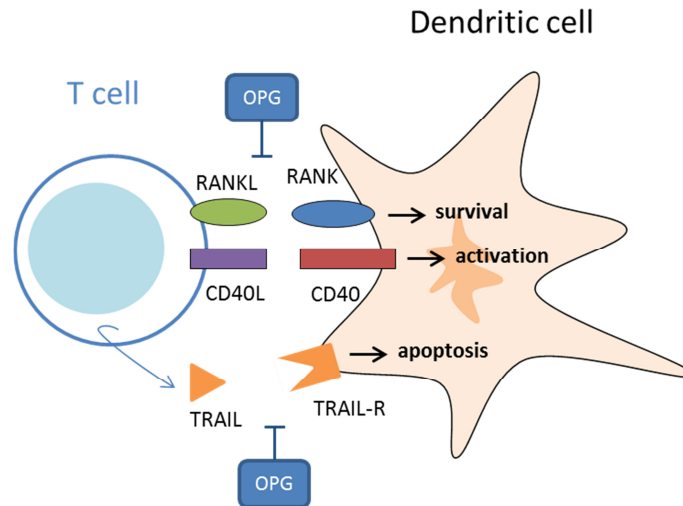
Figure 2.3: Role of the RANK/RANKL/OPG triad in interaction between dendritic cells and T cells. Activated T cells express RANKL and induce dendritic cell survival by inducing RANK signaling. OPG can inhibit this mechanism. The CD40/CD40L pathway is redundant with RANK/RANKL as it has similar effect on DCs. Activated T cells also produce TRAIL and can induce apoptosis of DCs. OPG binds TRAIL and could therefore play a role in the balance between survival and apoptosis of DCs. Modified after reference [5].

2.2.3. Lymph node development and growth

Studies of RANKL and RANK-deficient mice showed absence or abnormalities in lymphoid organs including LN, spleen and Peyer's patches. The mice failed to develop LNs but retained spleen and Peyer's patches [6,7,48,49]. Moreover, when pregnant monkeys were treated with anti-RANKL antibody denosumab, infants monkeys also show impaired LN formation [50].

During embryogenesis, a rudimentary lymph node anlage is composed of lymphoid tissue organizer (LTo) cells expressing RANKL. These cells recruit RANK expressing lymphoid tissue inducer (LTi) cells to cluster in the forming LN. LTi cells then activate LTβR expressing LTo cells thanks to expression of lymphotoxin α/β (LTα/β). This leads to the development of mature LTo cells. This mechanism induces a feed-back loop in which mature LTo cells express RANK/RANKL, trigger LTi growth and induce tissue organization [51,52] (**figure 2.4**). It was observed that the non-canonical NF-κB pathway induced both by LTβR and RANK play an important role in this process [14,53].

Lymphocyte recruitment is also an important step in LN development. Postnatally, RANKL induces LN growth by inducing proliferation and chemokines production of non-hematopoietic cells [54]. RANKL induction of chemokines secretion such as CXCL13 could be responsible for B cell recruitment and organization in LN. Indeed, reduced B cell numbers in LN were observed after RANKL neutralization [55]. The organization and function of adult LN will be described in the following chapter.
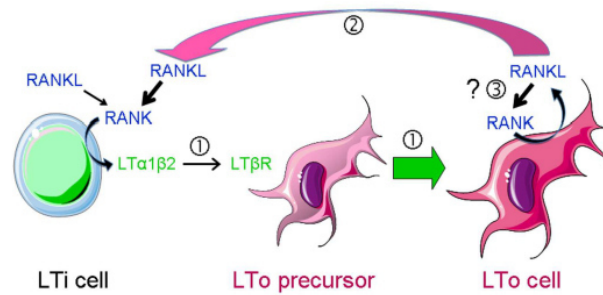
Figure 2.4: Role of RANKL in lymph node development. During embryogenesis, lymphoid tissue organizer cells (LTo) are recruited to the forming lymph node anlage. LTo cells recruit RANK expressing lymphoid tissue inducer (LTi) cells. LTi cells stimulate the development of mature LTo cells by activating LTβR. Mature LTo cells produce RANKL and attract a large number of LTi cells. This creates an amplification loop between LTo and LTi cells enabling the development of a complete lymph node. After reference [51].

2.2.4. Central and peripheral tolerance

An important role for RANK-RANKL has also been established in central tolerance. The thymus is a primary lymphoid organ where developing T cells are educated and T cells expressing a potentially self-reactive TCR are eliminated. Moreover, generation of immunosuppressive T cells is also occurring in the thymus participating in preventing autoimmune diseases. Medullary thymic epithelial cells (mTEC) are non-hematopoietic cells in the medullary area of the thymus. They play a crucial role in negatively selecting T cells. During embryogenesis, it was shown that RANK signaling is necessary for mTEC development. Moreover, a cooperation between RANK and CD40 is essential in postnatal development of mTECs [56]. RANK, together with LTβR and CD40, induces expression of the autoimmune regulator (AIRE) and tissue specific antigens (TSA) in mTECs [57]. Consequently, lack of RANK signaling leads to autoimmune phenotypes. Autoantibodies where found in the sera of immunodeficient mice after transplantation of RANK-deficient thymic stroma [58]. TRAF6 deficient mice showed impaired mTEC development [59]. The non-canonical NF-κB pathway seems to play a crucial role in mTEC development as RelB deficient mice and *aly/aly* mice having a dysfunctional mutation in NIK gene lack mTECs [60,61]. Finally, crosstalk between RANK and IFNβ pathways has been shown to be important for the development of AIRE[+] mTECs [62].

It was also observed that expression of RANKL in the skin can regulate peripheral tolerance. Indeed, RANKL controls the pool of regulatory T cells (Treg) in the skin. Tregs are CD4^{+}CD25^{+}Foxp3^{+} cells playing an important role in maintaining self-tolerance and suppressing immune responses to self-antigens in allergies or autoimmune diseases [63]. RANKL binds RANK on LCs in the dermis and promotes their survival. Activation of LCs by RANKL enhances Treg proliferation and immune response against self-antigens [64]. Therefore, local stimulation of the RANK/RANKL axis in the skin

could be a therapeutic strategy to treat allergies or systemic autoimmunity. RANKL is also required for induction of Treg differentiation in other organs. It was shown in a mouse type I diabetes model that RANKL prevents CD8^{+} T cells destruction of pancreatic beta islet. Ablation of RANKL signals lead to a decreased number of Tregs in pancreatic tissues and rapid progression of diabetes [65]. Finally, RANKL also controls Treg function in the intestine and plays an important role in preventing the development of colitis [66].

Table 2.1 summarizes the different roles of RANK/RANKL/OPG axis in the immune system.

Enhancement of immunity	Inhibition of immunity
Regulation of B lymphocytes (remains unclear) and γδ T cells development.	Development of medullary thymic epithelial cells (mTECs), which mediate T-cell self-tolerance
Lymph node organogenesis	Generation of regulatory T cells (Tregs)
Increased dendritic cell (DC) survival, cytokine expression and migration	Induction of T-cell tolerance and deletion
Enhanced induction of T cell response	

Table 2.1: Roles of RANK/RANKL in the immune system. Modified after reference [67].

2.2.5. Role of the RANK/RANKL/OPG triad in osteoimmunology, the example of rheumatoid arthritis

The osteoimmunology field studies the interaction between bone and the immune system. RANKL is one of the major cytokines playing a role in these interactions. Rheumatoid arthritis (RA) is one of the most studied diseases involving interaction between bone and the immune system. The pathologic mechanisms involved in RA are common between several diseases. RA patients suffer from chronic inflammation of the synovial joints leading to bone and cartilage destruction and joint pain. It was shown that RANKL is responsible for bone destruction in RA and increased levels are found in the synovium of patients [68,69]. RANKL appears to be mainly expressed by synovial fibroblasts and its expression can be increased by inflammatory cytokines such as IL-1, IL-6 and TNFα [70]. Moreover, RA disease points out the important role of T cells in osteoclastogenesis. Indeed, IL-17 producing T cells (Th17) express RANKL and induce osteoclastogenesis and bone destruction. Moreover, IL-17 production induces RANKL expression by synovial fibroblasts and osteoclast differentiation [70] (**figure 2.5**). RANKL expressing Th17 cells might also increase the activity of mature osteoclasts and not only act on the differentiation of osteoclasts precursors [71]. Moreover, a recent study in a

mouse model of antibody-induced arthritis showed that exogenous IFNβ improves bone loss by inhibiting RANKL signaling [72].
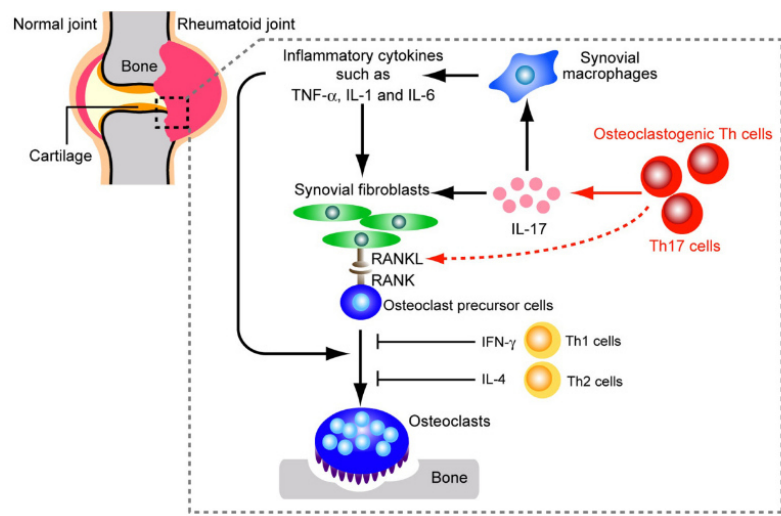
Figure 2.5: Role of RANKL in rheumatoid arthritis. RANKL is expressed by synovial fibroblasts under inflammatory conditions including secretion of IL-1, IL-6 and TNFα. IL-17 produced by Th17 cells also induces expression of RANKL by synovial fibroblasts. Th17 cells express RANKL and play a role in osteoclasts differentiation and maturation. After reference [70].

The example of rheumatoid arthritis shows the importance of the interaction between T cells and the bone environment in the development of severe bone diseases. It was also recently observed that B cells express RANKL and play a role in osteoclastogenesis in a model of estrogen loss after ovariectomy in mouse [73]. Moreover, RANKL is produced by pro-inflammatory FcRL4+ B cells in the synovium of RA patients   [74,75]. These observations pave the way to discovery of new mechanism involving immune cells in bone disorders.

2.3. RANKL/RANKL/OPG triad in other tissues

2.3.1   Mammary glands

Lobulo-alveolar mammary structures mainly form during pregnancy under the control of hormones. It was shown that RANK and RANKL deficiency leads to impaired development of these mammary structures and lactating mammary gland resulting in death of newborns [76,77]. RANK is expressed in mammary gland while mammary epithelial cells (MECs) express RANKL. RANKL expression by MECs increases during pregnancy and after the first days of lactation [76]. Impaired proliferation of MECs and increased apoptosis is observed in RANKL KO mice and can be reversed with RANKL treatment. It was shown that this is due to a lack of Akt/PKB pathway activation [76]. The non-canonical NF-κB

pathway has also been shown to be involved in MEC proliferation via upregulation of cyclin D1 by IKKα [78]. Overall hormonal regulation of RANKL is required for terminal differentiation of MECs and the formation of a functional milk secreting mammary gland.

2.3.2 Skin and hair follicles

As previously mentioned, RANK is expressed in human and mouse by LCs in the skin [43,64]. RANKL is expressed by inflamed or activated keratinocytes in mouse. Human keratinocytes also express RANKL and higher levels are observed in inflammatory conditions such as psoriasis [43,64,79]. Loser and colleagues showed that UV exposure induces RANKL expression in the skin via a vitamin D3 dependent signaling [64]. In RANKL deficient mice, the number of LCs is decreased and their proliferation is impaired [43]. Thus keratinocytes play a role in regulating LCs homeostasis. As described previously, RANKL activation of LCs was shown to increase the number of peripheral regulatory T cells [64]. RANKL deficient mice also show impaired hair renewal and epidermal homeostasis. Indeed, it was observed in our group that these mice cannot initiate a new growth phase (anagen) of the hair follicle and show arrested epidermal homeostasis [80]. On the contrary, transgenic mice with overexpression of RANKL presented increased hair follicle activity and epidermal growth. Moreover, RANK is expressed by hair follicle stem cells and in the basal layer of the epidermis [80]. Together these results highlight the role of RANK-RANKL axis in both hair and epidermis renewal.

2.3.3 Microfold cells in the intestine

Microfold (M) cells are intestinal epithelial-derived cells incorporated in the epithelia covering the gut-associated lymphoid tissues (GALT) such as Peyer's patches. They represent approximately 10% of the follicle associated epithelia (FAE) under steady-state conditions (**figure 2.6**). M cells are specialized in phagocytosis and transcytosis of antigens from the gut lumen to antigen presenting cells. Hence, these cells play an important role in mucosal immunity [81].

It was shown that stromal cells in the subepithelial dome of FAE express membrane bound RANKL [82]. Study of RANKL deficient mice and administration of recombinant RANKL *in vivo* showed that RANKL plays a critical role in the differentiation of RANK expressing enterocytes into M cells [49]. Indeed, RANKL deficient mice do not develop M cells. As stromal cells are expressing membrane bound RANKL, cell/cell contact and special FAE microarchitecture is probably needed for M cell

differentiation [83]. RANKL upregulates the transcription factor Spi-B which is required for maturation of M cells [84].
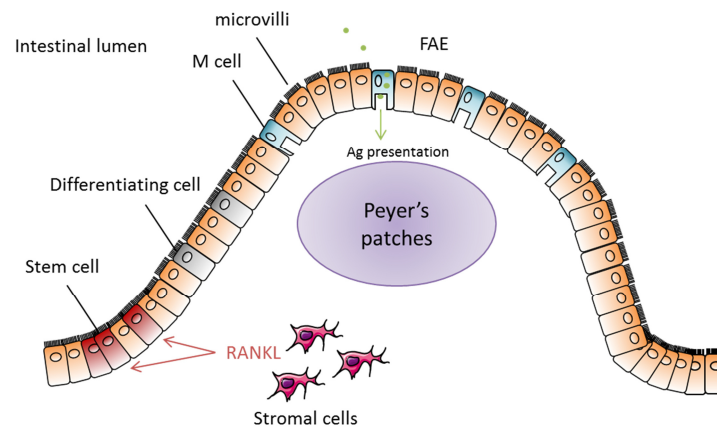
Figure 2.6: Microfold cells and the follicle associated epithelia. Microfold cells (M cells) are inserted in the follicle associated epithelia (FAE) covering Peyer's patches. They transfer antigen (Ag) from the intestinal lumen to antigen presenting cells in Peyer's patches. Stromal cells in the subepithelial dome produce RANKL and induce differentiation of stem cells into mature M cells. Modified after references [81,85].

2.3.4   Blood endothelial cells

Angiogenesis involves proliferation of blood endothelial cells (BEC), migration and tube formation. It was observed that RANKL induces angiogenesis of human endothelial cells in a pathway involving Src and phospholipase C (PLC) [86]. BECs express RANK, RANKL and OPG [87,88]. Induction of RANK signaling in BEC promotes their survival via the PI3K/Akt pathway [88]. It was proposed that smooth muscle cells surrounding the blood vessels secrete soluble RANKL and stimulate endothelial cells in a paracrine manner [88]. Moreover, expression of OPG by BECs prevents apoptosis by blocking TRAIL induced signaling [89]. Expression of OPG by BECs can be upregulated via activation of integrin $\alpha v\beta 3$ in a NF-κB dependent pathway. This mechanism induces BEC proliferation and migration [90,91]. In inflammatory conditions RANKL induces the expression of the adhesion molecules ICAM-1 and VCAM-1 in a pathway involving NF-κB, PLC, PI3K and PKC. These adhesion molecules enhance adhesion of leukocytes and their recruitment from circulating blood to the site of inflammation [92]. Finally, OPG deficient mice develop vascular calcification indicating a role for RANKL in vessel wall homeostasis [8].

2.4. The RANK/RANKL/OPG triad and cancers

RANK-RANKL-OPG have been shown to be involved in several cancers including breast and prostate cancer, multiple myeloma, renal and hepatocellular carcinomas and melanoma [93]. Indeed, several

studies showed that they play a role in migration and metastasis of epithelial cells. RANK signaling in breast cancer has been well studied. It was observed both in mice and humans that RANKL induces mammary epithelial cell proliferation in early steps of tumorigenesis as well as migration and metastasis of breast cancer cells [94–97]. It was shown that the alternative NF-κB pathway activated by RANK controls nuclear exclusion of p27 and induces mammary tumorigenesis [98]. Human breast adenocarcinomas with high RANK mRNA levels were associated with high pathological grade, high proliferation, increased metastasis and consequently a decreased overall survival [97]. Moreover, it was shown in this study that RANK overexpression in human mammary cells can lead to activation of the signaling pathway without RANKL stimulation leading to an increase in $CD44^+CD24^-$ stem cells and epithelial to mesenchymal transition [97]. Hormone replacement therapy could influence cancer development as progesterone increases RANKL expression in mammary gland and participates in early mammary tumorigenesis [94,95].

In osteosarcoma, increased RANK expression was associated with low response to chemotherapy [99]. RANK levels were also increased in advanced metastatic melanoma and was shown to maintain melanoma-initiating cells [100]. High RANK/RANKL/OPG levels are associated with prostate cancer metastasis [101]. Overall, activation of RANK signalling is of bad prognosis in many cancers.

Another important role of the RANK/RANKL/OPG system is its involvement in bone tumors and bone metastasis of several cancers. As described before in this paragraph, RANK signaling induces proliferation of epithelial cells and initiates cancer development. Prostate and breast cancer as well as multiple myeloma can develop bone metastases. This is linked with bad prognosis, pathological complications (skeletal related events) and bone pain [93]. RANK/RANKL can participate in both the promotion of metastasis and the induction of osteolysis, facilitating tumor establishment. An increased level of RANKL was seen in bone stromal cells of multiple myeloma patients, together with bone pain and excessive osteoclast activity [102]. Breast cancer cell lines are capable of increasing RANKL expression and decreasing OPG expression on stromal osteoblasts leading to osteoclastogenesis [103]. Moreover, prostate cancer cells produce soluble RANKL inducing osteoclastogenesis and OPG prevents prostate cancer tumor metastases to the bone [104]. Overall bone metastases create what is called a "vicious cycle". Metastasis of cancer cells to the bone modifies bone turnover leading to osteolysis. In turn, the bone matrix produces growth factors such as TGF-β or insulin like growth factors which stimulates tumor cells growth. Tumor growth further enhances secretion of factors that are stimulating bone destruction. This cycle enables tumor establishment and growth in bones [93] (**figure 2.7**).
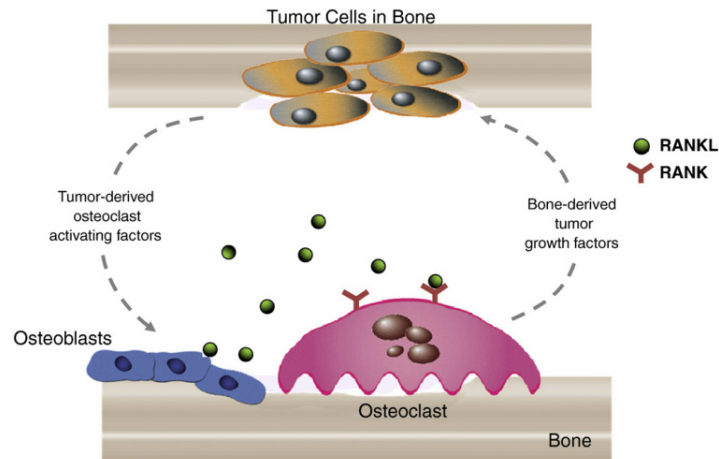
Figure 2.7: The "vicious cycle" of cancer metastases in the bone. Metastatic tumor cells induce osteoclastogenesis and bone destruction. Bone matrix in turn secretes tumor-growth factors further enhancing development of tumors cells in the bone. After reference [105].

Another aspect of RANK and RANKL molecules involvement in cancer is their role in immune cells. Indeed, immune cells expressing RANK or RANKL are present in the tumor microenvironment but their role is still unclear and might be dependent on the context. As an example, tumor-associated macrophages (TAM) where shown to express RANK in breast adenocarcinomas [95,97]. Moreover, RANKL inhibition could have a beneficial effect in inducing anti-tumor immunity. Indeed we have already described in this chapter the importance of RANKL in modulating central tolerance. Thus RANKL inhibition could lead to persistence of tumor-specific effector T cells [106]. Moreover, RANKL expressing Tregs are infiltrating mammary tumors and induce pulmonary metastasis [96]. Finally, it was observed that RANK signaling enhances tumour antigen presentation by DCs and CD8^{+} T cells anti-tumor response [107]. Therefore, the role of RANK/RANKL axis in the crosstalk between tumor cells and immune cells in the context of oncogenesis is of great importance and deserves further investigations to be better understood.

2.5. Therapeutic approaches targeting RANK/RANKL/OPG triad

As described earlier in this chapter, the RANK-RANKL-OPG axis is involved in many pathological conditions. Therefore, therapeutic targeting of this pathway is a main axis of research. In this paragraph I will describe the two main strategies used to target RANK-RANKL system: (i) targeting of RANK downstream signaling pathway and (ii) targeting of RANK/RANKL interaction. This paragraph will end with the description of denosumab, a fully humanized mouse monoclonal antibody targeting RANKL and approved for specific human treatment.

2.5.1 Small molecules and peptides targeting RANK downstream signaling

One of the strategies to improve pathological conditions due to exacerbated RANK activation consists in targeting RANK downstream signaling. Many studies have been performed *in vitro* and in animal models using various synthetic small molecules, phytopharmaceuticals as well as peptides. The main goal of these studies was to inhibit osteoclastogenesis and bone degradation. There are numerous studies therefore I will only describe here some examples to illustrate the broad types of molecules targeting RANK signaling that were studied.

Phytopharmaceuticals are molecules naturally present in plants which are studied for their potential therapeutic applications. Jolkinolide B (JB) is isolated from the root of *Euphorbia fischeriana* Steub and is classically used in traditional Chinese medicine. It was observed that JB prevents IκBα degradation and phosphorylation of mitogen-activated kinases (MAPKs) downstream of RANK in an *in vitro* model of osteoclast differentiation from bone marrow macrophages [108]. Additionally, alliin (S-allyl-L-cysteine sulfoxides), the major component of aged garlic extract, was shown to impair RANKL-induced osteoclastogenesis *in vitro* via a mechanism involving inhibition of c-Fos and NFATc1 pathways [109]. Flavonoids are plant metabolites often studied for their therapeutic applications. Herbacetin is a type of flavonoid which inhibits osteoclastogenesis *in vitro* and *in vivo*. It was shown to suppress IκBα and JNK phosphorylation and to decrease c-fos and NFATc1 mRNA levels [110].

Synthetic molecules were also observed to have beneficial effects on osteoclasts differentiation. 5-(2',4'-difluorophenyl)-salicylanilide derivatives were shown to inhibit osteoclastogenesis *in vitro* by inhibiting c-Fos and NFATc1 expression [111]. Chloroquine is an anti-malarial agent also used in autoimmune diseases. It was observed that chloroquine increased TRAF3 expression in osteoclasts thus reducing the expression of NFATc1 and inhibiting osteoclasts differentiation *in vitro* and *in vivo* [25]. Small molecules called ABD compounds were studied in the context of rheumatoid arthritis. It was shown that they inhibit RANKL induced activation of the MAPKs ERK and JNK. This mechanism protected mice from inflammatory arthritis, joint destruction and systemic bone loss [112].

Finally, peptides targeting RANK signaling pathway were also developed. A peptide composed of the TRAF6 binding site to RANK was shown to prevent RANK signaling induction by RANKL in a mechanism disrupting interaction between endogenous TRAF6 and RANK intracellular domain. This peptide successfully inhibited osteoclastogenesis *in vitro* and *in vivo*. This discovery is part of a US patent deposit by Aggarwal and colleagues [113] however since its patent deposition in 2004 the peptide has not been tested in clinical trials. Moreover, a peptide called RANK receptor inhibitor (RRI) was designed to target a motif on the RANK intracellular domain that was found to induce signaling in a TRAF6 independent manner. The peptide blocked osteoclastogenesis *in vitro* and

reduced inflammation-induced bone destruction as well as ovariectomy-induced bone loss in mice [114].

2.5.2   Antibodies, fusion proteins and peptides targeting RANK/RANKL

Targeting RANK signaling is a strategy which can lead to several adverse effects because kinases and transcription factors involved are common with other receptors. Therefore, another strategy consists in blocking the interaction between RANKL and RANK. Many peptides or proteins were developed and tested both in animal models and patients.

First of all, several peptides and proteins targeting RANKL were developed. Native OPG was used to block RANKL *in vivo* in mice but high doses administered subcutaneously (>10-30 mg/kg) were needed to suppress bone resorption. Indeed, the carboxyl terminus of native OPG contains heparin-binding region that alters half-life of the protein and leads to poor pharmacokinetic and pharmacodynamic properties [115]. Therefore native OPG was not used in patients. Efforts were made to develop recombinant conjugates or fusion proteins lacking the C-terminal heparin binding domain of OPG. Among the many fusion proteins that were produced, a protein produced by Amgen Inc. in *Escherichia coli* containing the residues 22-194 of human OPG fused to IgG1 human Fc region showed good activity. This Fc-OPG protein was 200 times more active than native OPG *in vivo*, displayed a longer half-life and was therefore the first version of OPG tested in humans in 1998 [50]. One single dose injection lead to a rapid (12h), dose dependent decline in bone turnover and the effects were measurable up to 6 weeks after the injection [116]. As a backup for this Fc-OPG, Amgen Inc also developed an alternative OPG-Fc protein (AMGN-0007) produced in Chinese ovary hamster (CHO) mammalian cells. This protein showed three to tenfold higher efficacy and tenfold longer half-life, thus the development of   AMGN-0007 was continued at the expense of Fc-OPG. AMGN-0007 phase I trial revealed better pharmacokinetic/pharmacodynamic than Fc-OPG produced in *E. Coli* [117]. However, one patient receiving AMGN-007 developed an immune response against OPG which represented a safety risk if a neutralizing immune response against endogenous OPG would occur. Moreover, OPG also targets TRAIL and could inhibit TRAIL in tumor surveillance and apoptosis [118]. Therefore the development of OPG-Fc constructs was discontinued.

Another strategy developed by Immunex, similar to the one used for etanercept (TNFR2-Fc), consisted in developing a fusion protein containing the extracellular domain of RANK and the Fc part of human IgG1 (RANK-Fc). This protein bound specifically RANKL and no other TNF ligands. However injections in primates revealed the presence of activating autoantibodies. Thus   RANK-Fc development was stopped due to potential risk of immune response to endogenous RANK in patients

[50]. IK22-5, an anti-RANKL antibody was developed by Kamijo and colleagues and reduced bone loss in a collagen-induced arthritis mouse model [119]. RANK-Fc [65,95,120], OPG-Fc [121–123] and IK22-5 remain interesting tools to study RANKL blockage *in vivo* in animal models.

Several peptides based on either OPG or RANK sequences were tested *in vitro* and in animal models and showed inhibitory effect on osteoclast differentiation. Naidu et al developed a peptide from site directed mutagenesis of OPG. Using one of OPG binding site sequence Leu113-Arg122 and mutations, this group identified the peptide YR-11 (YLEIEFSLKHR). This peptide inhibited RANK-RANKL binding thus reducing osteoclast differentiation *in vitro* and ameliorating bone loss and inflammation in a model of adjuvant induced arthritis in rats [124]. OP3-4 is an OPG-like peptidomimetic. It was shown to inhibit osteoclastogenesis *in vitro* and bone loss in an osteoporosis animal model [125]. OP3-4 also limited bone loss in an adjuvant-induced arthritis model but did not decrease inflammation [126]. This peptide binds specifically to RANKL and not to TRAIL and also prevents myeloma associated bone diseases [127].

RANK-mimetic peptides based on the finding that loop3 of RANK is important for the binding of RANKL were also developed. These peptides reduced RANKL-induced osteoclastogenesis *in vitro* and *in vivo* [128,129]. The peptide WP9QY known to bind TNFα was shown to bind also RANKL and inhibit osteoclast differentiation [130]. Finally, the discovery of LGR4 as a new receptor for RANKL brought the possibility to use the soluble LGR4 extracellular domain to target RANKL and prevent binding to RANK [30].

Antibodies and antibody fragments targeting RANK were also developed. R12-31 anti-RANK antibody was described by Kamijo and colleagues together with IK22-5 anti-RANKL antibody. R12-31 was shown to prevent RANKL binding to RANK but no further biological effect was described [119]. In 2014, Newa and colleagues developed a RANK specific single chain fraction variable (scFv) inhibiting osteoclastogenesis *in vitro* [131]. These proteins targeting RANK require further investigation to understand their potential use in animal models or patients.

2.5.3 Denosumab: a fully human anti-RANKL antibody with clinical applications

a)   Development of denosumab

Denosumab is a fully humanized mouse IgG2κ antibody obtained from foot pad immunization with human RANKL of the IgG2 XenoMouse [50]. This antibody was developed by Amgen Inc. The IgG2 isotype was preferred because it is known to have limited effector function that could be harmful to RANKL-expressing cells. Moreover, the strategy using anti-RANKL antibodies rather than antibodies targeting RANK was preferred to avoid unexpected receptor agonism that could be a concern [50]. In the XenoMouse model, the murine IgG genes are not expressed and have been replaced by human orthologs. Immunization of these mice resulted in an immune response with production of specific fully human IgGs binding RANKL [132]. Primary screens of hybridoma used enzyme-linked immunosorbent assay (ELISA) to analyse the binding to human and murine RANKL. Secondary screens tested the capacity of monoclonal antibodies to actually block recombinant soluble human RANKL using Biacore [50]. One of these IgGs (AMG 162) was cloned from lymph node lymphocytes and expressed in CHO cells. Production of large-scale purified antibody was then performed to obtain clinical grade batches [133]. Denosumab was shown to bind both soluble and membrane-bound human RANKL with high affinity (Kd = 3 pM) but not mouse or rat RANKL. More precisely, denosumab binds the DE loop on RANKL [50]. Moreover, the binding of denosumab is specific to RANKL as it has no affinity for TRAIL or other TNF family members such as TNFα, TNFβ and CD40L [134]. However, crossreactivity of denosumab with cynomolgus RANKL was shown and enabled the first *in vivo* trials to be done in cynomolgus monkeys. Single-dose treatment of monkeys proved that denosumab inhibited bone resorption and osteoclast activity. The fact that denosumab was not active in mouse or rat but only in monkey accelerated the clinical development of this molecule as the first preclinical trials were directly done in primates [50]. In patients, denosumab was safer and more efficient than OPG-Fc. Indeed, better effect on bone turnover was observed at lower doses and the effect last longer than OPG-Fc [118,135] (**figure 2.8**). Therefore, clinical trials for OPG-Fc (AMGN-0007) were discontinued in favour of denosumab.
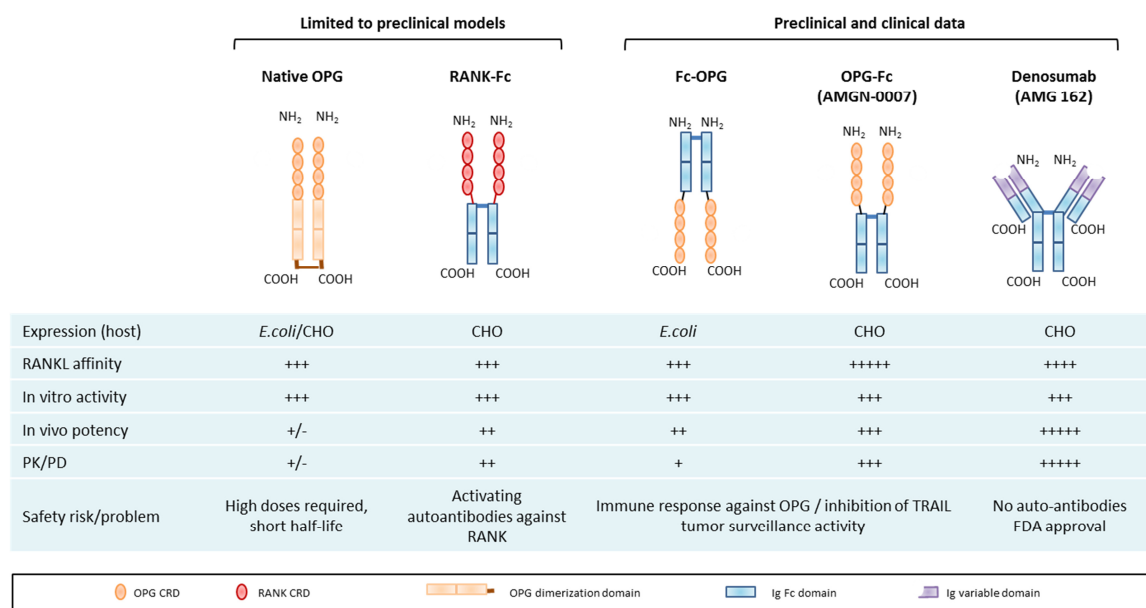
	Native OPG	RANK-Fc	Fc-OPG	OPG-Fc (AMGN-0007)	Denosumab (AMG 162)
Expression (host)	*E.coli*/CHO	CHO	*E.coli*	CHO	CHO
RANKL affinity	+++	+++	+++	+++++	++++
In vitro activity	+++	+++	+++	+++	+++
In vivo potency	+/-	++	++	+++	+++++
PK/PD	+/-	++	+	+++	+++++
Safety risk/problem	High doses required, short half-life	Activating autoantibodies against RANK	Immune response against OPG / inhibition of TRAIL tumor surveillance activity		No auto-antibodies FDA approval

Figure 2.8: Summary of the strategies developed by Amgen and Immunex Inc. leading to denosumab approval. Several inhibitors of RANKL were developed and tested in animal models and clinical trials. The table summarizes with +/- rating the results of the teams evaluating these different inhibitors on their affinity, activity and potency. Native OPG was the less efficient inhibitor and required treatment with high doses. The RANKL binding domain of RANK fused to immunoglobulin Fc (RANK-Fc) was more potent than native OPG. Nonetheless it leads to the development of autoantibodies against RANK. A recombinant OPG formed by amino-terminal immunoglobulin Fc fused to the RANKL binding domain of OPG (Fc-OPG) was the first recombinant form of OPG to be tested in humans. A more potent form of recombinant OPG with the immunoglobulin Fc in the C-terminal region (OPG-Fc) was then developed. However, immune response against OPG was observed in one patient. Denosumab, a fully human anti-RANKL monoclonal antibody was finally developed and tested in clinical trials. This antibody showed longer half-life and was more efficient than OPG-Fc. No safety issues were observed with denosumab treatment. Abbreviations: *E.coli*: Escherichia coli; CHO: Chinese hamster ovary cell. Modified after reference [50].

b)   Clinical indications of denosumab

Denosumab is approved for use in post-menopausal osteoporosis treatment since 2010, treatment of bone metastasis from solid tumors since 2011 and male osteoporosis since 2012. In 2013, the FDA (US Food and Drug Administration) also approved denosumab use for specific cases of giant cell tumor of bone. The half-life of this antibody is 28 days.

For treatment of post-menopausal osteoporosis, the commercial name of denosumab is Prolia. It is administered sub-cutaneously at a dose of 60mg every 6 months [67]. Before approval, several clinical trials enabled the establishment of the doses needed for a beneficial role of denosumab treatment in osteoporosis patients. A first single dose phase I trial in healthy post-menopausal women showed the activity of denosumab in decreasing born turnover markers [118]. In a phase II trial several doses were tested in post-menopausal women with low bone density. This study

determined that the treatment with 60mg every 6 months was the most efficient [136]. Finally, phase III trials allowed the comparison between denosumab, placebo and bisphosphonate, an established anti-resorptive agent. The FREEDOM trial demonstrated that treatment every 6 months during 3 years reduced fracture risks compared to placebo [137].

But did RANKL blockage lead to harmful side effects? Due to the biology of RANK-RANKL axis, blocking RANKL could lead to higher incidence of cancers or infections. Moreover, the anti-resorptive activity of denosumab could lead to hypocalcemia as bone degradation is also a source of calcium. Additionally, it is known that inhibition of osteoclastogenesis can lead to osteonecrosis of the jaw (ONJ) [138]. Therefore incidence of cancer, infection, hypocalcemia and ONJ are potential side effects that were investigated in clinical trials. In the FREEDOM trial, increased occurrence of these four side effects were not observed [137]. Despite the absence of difference in the total occurrence of infections, higher number of patients requiring hospitalisation was observed in the denosumab group. Moreover, rare cases of cellulitis were reported [139]. Development of ONJ in two patients was observed in the study extension [140]. In a recent study, denosumab treatment of osteoporotic women did not influence insulin resistance and development of diabetes [141]. However, treatment with denosumab can induce pain in the back, general musculoskeletal pain, increase cholesterol and bladder inflammation [139]. Moreover, occurrence of dermatitis and eczema were higher in denosumab treated patients [139]. Despite these observed side effects, the risk/benefit ratio was favorable and denosumab was approved for use in post-menopausal women with high risk of fracture in 2010 with a risk evaluation and mitigation strategy. The potential risk might be evaluated before treatment depending on patient condition and patients treated with denosumab should be closely monitored. The results of a study evaluating the effects of denosumab after 10 years of treatment were published in 2015 [142]. The occurrence of adverse events was not increased with long term administration of denosumab. Moreover, the treatment was still efficiently reducing bone loss after 10 years of treatment.

A phase III trial was also conducted on men with prostate cancer undergoing androgen deprivation therapy. This study showed reduced risk of fracture after denosumab treatment [143]. Therefore denosumab is also approved for male osteoporosis in the context of hormone ablation therapy.

For the prevention of skeletal-related events (SRE) from bone metastasis of solid tumors, the commercial name of denosumab is Xgeva. It is administered sub-cutaneously at a dose of 120mg every 4 months [67]. Before denosumab, zoledronic acid was used to reduce the appearance of bone metastasis but this treatment impairs renal function. Three phase III studies were included in a meta-analysis to compare the effect of denosumab to zoledronic acid. It was observed that denosumab was more efficient than zoledronic acid in reducing the incidence of SRE and a decreased bone pain

was observed in patients treated with denosumab. Moreover, the time to appearance of SRE was delayed with denosumab [144]. The mAb did not induce new cancer development, infections or ONJ. However, in these clinical trials denosumab showed increased risk of hypocalcemia. This side effect can be counteracted by calcium supplementation of patients. Despite adverse effects in few patients among the cohort, the risk/benefit ratio was also favorable for the use of denosumab in preventing SRE development.

Denosumab was evaluated in the treatment of giant tumour cell of the bone (GTCB), a rare primary bone tumor. It was observed that treatment reduced progression of this cancer. However the risk-benefit balance remains to be investigated depending on the patient population [145]. Therefore, denosumab is approved for use only in patients with unresectable tumor or at high risk of morbidity if undergoing surgery [146].

The effect of denosumab on rheumatoid arthritis patients was also investigated in recent clinical trials [147–150]. It was observed that treatment decreased bone loss in rheumatoid arthritis patients without safety issues. Higher incidence of infections was not observed in the patients [151]. Moreover, ONJ incidence was not observed and one case of hypocalcemia was   reported [147].

Beside the positive effects of denosumab in treating osteoporosis, bone metastasis of solid tumors and rheumatoid arthritis, the potential adverse effects on the immune system deserve to be studied. Indeed, as we discussed in this chapter the RANK/RANKL/OPG axis is involved in many mechanisms of the immune system. Therefore, blockage of RANKL could decrease monocyte or DCs survival, affect T cell activation or central tolerance for example. As described previously, the risk/benefit ratio was favorable in clinical trials. Infection incidence remained low although denosumab had more or less effect on the occurrence of infections depending on the study. On the other hand, there is little evidence that RANKL inhibition has immunomodulatory effect. Indeed, blocking RANKL in animal models of inflammatory arthritis reduced bone loss but did not change inflammatory parameters [126,152]. Moreover, denosumab decreased bone loss in RA patients but did not change disease activity [150]. Additionally, OPG treatment in mice did not affect the immune response to mycobacterial infection [44]. In humans, loss of function mutation in the RANK/RANKL/OPG axis has no effect on the development of immunity [153]. This could be due to the redundancy with other pathways such as CD40/CD40L as we discussed previously. RANK signaling might be essential during embryonic development illustrated by its requirement for lymph node formation and RANKL inhibitors treatment should be avoided in pregnant women. In adults, redundancy with other TNF superfamily members might limit the effect of RANKL inhibitors on the immune system. Overall, the

implication of RANKL in immune responses deserves further attention to fully understand the possible effects of anti-RANKL therapy.

2.6. Conclusions

The RANK/RANKL/OPG axis was primary studied for its role in osteoclastogenesis and bone homeostasis. Both RANK and RANKL deficient mice show severe osteopetrosis. However, these mice also show an absence of lymph nodes and impaired mammary gland development. Therefore RANK signaling is required for different biological processes. RANKL is required for LN development, stimulation of DC survival by T cells, and might have a role in mature B lymphocyte formation. Moreover, RANKL plays a role in inflammation-induced bone destruction such as in rheumatoid arthritis. RANKL also plays a crucial role in the development of central and peripheral tolerance. Finally, RANKL is required for skin homeostasis, M cell development and endothelial cell activation and maintenance of vessels wall homeostasis. Many strategies have been tested to block the adverse effect of RANKL in pathological conditions however few therapeutic molecules were tested in clinical trials. Inhibition of RANK intracellular signaling by small molecules or peptides is a strategy that was tested *in vitro* and in animal models. On the other hand, inhibition of RANK-RANKL interaction is of great interest and this strategy led to the approval of the anti-RANKL monoclonal antibody denosumab. This antibody is the first-in-class, first-in-pathway treatment for osteoporosis and SRE of solid malignancies. However, treatments with monoclonal antibodies require subcutaneous injections and are more expensive than therapies with small molecules. To date there is no evidence that a small molecule inhibiting RANK-RANKL interaction was discovered. Therefore, identification of such a molecule could be of great interest and could allow oral delivery of RANKL inhibitors.

2.7. References

1. Hadjidakis DJ, Androulakis II. Bone Remodeling. Ann N Y Acad Sci. 2006;1092: 385–396. doi:10.1196/annals.1365.035

2. Jimi E, Hirata S, Osawa K, Terashita M, Kitamura C, Fukushima H. The Current and Future Therapies of Bone Regeneration to Repair Bone Defects. Int J Dent. 2012;2012: e148261. doi:10.1155/2012/148261

3. Lacey DL, Timms E, Tan H-L, Kelley MJ, Dunstan CR, Burgess T, et al. Osteoprotegerin Ligand Is a Cytokine that Regulates Osteoclast Differentiation and Activation. Cell. 1998;93: 165–176. doi:10.1016/S0092-8674(00)81569-X

4. Walsh MC, Choi Y. Biology of the RANKL–RANK–OPG system in immunity, bone, and beyond. Inflammation. 2014;5: 511. doi:10.3389/fimmu.2014.00511

5. Theill LE, Boyle WJ, Penninger JM. RANK-L AND RANK: T Cells, Bone Loss, and Mammalian Evolution. Annu Rev Immunol. 2002;20: 795–823. doi:10.1146/annurev.immunol.20.100301.064753

6. Dougall WC, Glaccum M, Charrier K, Rohrbach K, Brasel K, Smedt TD, et al. RANK is essential for osteoclast and lymph node development. Genes Dev. 1999;13: 2412–2424.

7. Kong Y-Y, Yoshida H, Sarosi I, Tan H-L, Timms E, Capparelli C, et al. OPGL is a key regulator of osteoclastogenesis, lymphocyte development and lymph-node organogenesis. Nature. 1999;397: 315–323. doi:10.1038/16852

8. Bucay N, Sarosi I, Dunstan CR, Morony S, Tarpley J, Capparelli C, et al. osteoprotegerin-deficient mice develop early onset osteoporosis and arterial calcification. Genes Dev. 1998;12: 1260–1268.

9. Mizuno A, Amizuka N, Irie K, Murakami A, Fujise N, Kanno T, et al. Severe Osteoporosis in Mice Lacking Osteoclastogenesis Inhibitory Factor/Osteoprotegerin. Biochem Biophys Res Commun. 1998;247: 610–615. doi:10.1006/bbrc.1998.8697

10. Nakashima T, Kobayashi Y, Yamasaki S, Kawakami A, Eguchi K, Sasaki H, et al. Protein Expression and Functional Difference of Membrane-Bound and Soluble Receptor Activator of NF-κB Ligand: Modulation of the Expression by Osteotropic Factors and Cytokines. Biochem Biophys Res Commun. 2000;275: 768–775. doi:10.1006/bbrc.2000.3379

11. Kitaura H, Kimura K, Ishida M, Kohara H, Yoshimatsu M, Takano-Yamamoto T. Immunological Reaction in TNF-α-Mediated Osteoclast Formation and Bone Resorption In Vitro and In Vivo. J Immunol Res. 2013;2013: e181849. doi:10.1155/2013/181849

12. Lomaga MA, Yeh W-C, Sarosi I, Duncan GS, Furlonger C, Ho A, et al. TRAF6 deficiency results in osteopetrosis and defective interleukin-1, CD40, and LPS signaling. Genes Dev. 1999;13: 1015–1024.

13. Franzoso G, Carlson L, Xing L, Poljak L, Shores EW, Brown KD, et al. Requirement for NF-κB in osteoclast and B-cell development. Genes Dev. 1997;11: 3482.

14. Dejardin E. The alternative NF-κB pathway from biochemistry to biology: Pitfalls and promises for future drug development. Biochem Pharmacol. 2006;72: 1161–1179. doi:10.1016/j.bcp.2006.08.007

15. Zeng R, Faccio R, Novack DV. Alternative NF-κB Regulates RANKL-Induced Osteoclast Differentiation and Mitochondrial Biogenesis via Independent Mechanisms. J Bone Miner Res. 2015;30: 2287–2299. doi:10.1002/jbmr.2584

16. David J-P, Sabapathy K, Hoffmann O, Idarraga MH, Wagner EF. JNK1 modulates osteoclastogenesis through both c-Jun phosphorylation-dependent and -independent mechanisms. J Cell Sci. 2002;115: 4317–4325. doi:10.1242/jcs.00082

17. Wong BR, Besser D, Kim N, Arron JR, Vologodskaia M, Hanafusa H, et al. TRANCE, a TNF Family Member, Activates Akt/PKB through a Signaling Complex Involving TRAF6 and c-Src. Mol Cell. 1999;4: 1041–1049. doi:10.1016/S1097-2765(00)80232-4

18. Li X, Udagawa N, Itoh K, Suda K, Murase Y, Nishihara T, et al. p38 MAPK-mediated signals are required for inducing osteoclast differentiation but not for osteoclast function. Endocrinology. 2002;143: 3105–3113. doi:10.1210/endo.143.8.8954

19. Koga T, Inui M, Inoue K, Kim S, Suematsu A, Kobayashi E, et al. Costimulatory signals mediated by the ITAM motif cooperate with RANKL for bone homeostasis. Nature. 2004;428: 758–763. doi:10.1038/nature02444

20. Asagiri M, Sato K, Usami T, Ochi S, Nishina H, Yoshida H, et al. Autoamplification of NFATc1 expression determines its essential role in bone homeostasis. J Exp Med. 2005;202: 1261–1269. doi:10.1084/jem.20051150

21. Jin W, Chang M, Paul EM, Babu G, Lee AJ, Reiley W, et al. Deubiquitinating enzyme CYLD negatively regulates RANK signaling and osteoclastogenesis in mice. J Clin Invest. 2008;118: 1858–1866. doi:10.1172/JCI34257

22. Takayanagi H, Kim S, Matsuo K, Suzuki H, Suzuki T, Sato K, et al. RANKL maintains bone homeostasis through c-Fos-dependent induction of interferon-β. Nature. 2002;416: 744–749. doi:10.1038/416744a

23. Takayanagi H, Kim S, Taniguchi T. Signaling crosstalk between RANKL and interferons in osteoclast differentiation. Arthritis Res. 2002;4: S227–S232. doi:10.1186/ar581

24. Takayanagi H, Ogasawara K, Hida S, Chiba T, Murata S, Sato K, et al. T-cell-mediated regulation of osteoclastogenesis by signalling cross-talk between RANKL and IFN-γ. Nature. 2000;408: 600–605. doi:10.1038/35046102

25. Xiu Y, Xu H, Zhao C, Li J, Morita Y, Yao Z, et al. Chloroquine reduces osteoclastogenesis in murine osteoporosis by preventing TRAF3 degradation. J Clin Invest. 2014;124: 297–310. doi:10.1172/JCI66947

26. Hughes AE, Ralston SH, Marken J, Bell C, MacPherson H, Wallace RGH, et al. Mutations in TNFRSF11A, affecting the signal peptide of RANK, cause familial expansile osteolysis. Nat Genet. 2000;24: 45–48. doi:10.1038/71667

27. Ebeling PR, Atley LM, Guthrie JR, Burger HG, Dennerstein L, Hopper JL, et al. Bone turnover markers and bone density across the menopausal transition. J Clin Endocrinol Metab. 1996;81: 3366–3371. doi:10.1210/jcem.81.9.8784098

28. Eghbali-Fatourechi G, Khosla S, Sanyal A, Boyle WJ, Lacey DL, Riggs BL. Role of RANK ligand in mediating increased bone resorption in early postmenopausal women. J Clin Invest. 2003;111: 1221–1230. doi:10.1172/JCI200317215

29. Pacifici R. Estrogen, cytokines, and pathogenesis of postmenopausal osteoporosis. J Bone Miner Res. 1996;11: 1043–1051. doi:10.1002/jbmr.5650110802

30. Luo J, Yang Z, Ma Y, Yue Z, Lin H, Qu G, et al. LGR4 is a receptor for RANKL and negatively regulates osteoclast differentiation and bone resorption. Nat Med. 2016;22: 539–546. doi:10.1038/nm.4076

31. Guerrini MM, Sobacchi C, Cassani B, Abinun M, Kilic SS, Pangrazio A, et al. Human Osteoclast-Poor Osteopetrosis with Hypogammaglobulinemia due to TNFRSF11A (RANK) Mutations. Am J Hum Genet. 2008;83: 64–76. doi:10.1016/j.ajhg.2008.06.015

32. Crockett JC, Mellis DJ, Scott DI, Helfrich MH. New knowledge on critical osteoclast formation and activation pathways from study of rare genetic diseases of osteoclasts: focus on the RANK/RANKL axis. Osteoporos Int. 2010;22: 1–20. doi:10.1007/s00198-010-1272-8

33. Yun TJ, Tallquist MD, Aicher A, Rafferty KL, Marshall AJ, Moon JJ, et al. Osteoprotegerin, a Crucial Regulator of Bone Metabolism, Also Regulates B Cell Development and Function. J Immunol. 2001;166: 1482–1491. doi:10.4049/jimmunol.166.3.1482

34. Yun TJ, Chaudhary PM, Shu GL, Frazer JK, Ewings MK, Schwartz SM, et al. OPG/FDCR-1, a TNF Receptor Family Member, Is Expressed in Lymphoid Cells and Is Up-Regulated by Ligating CD40. J Immunol. 1998;161: 6113–6121.

35. Perlot T, Penninger JM. Development and Function of Murine B Cells Lacking RANK. J Immunol. 2012;188: 1201–1205. doi:10.4049/jimmunol.1102063

36. Roberts NA, White AJ, Jenkinson WE, Turchinovich G, Nakamura K, Withers DR, et al. Rank Signaling Links the Development of Invariant γδ T Cell Progenitors and Aire+ Medullary Epithelium. Immunity. 2012;36: 427–437. doi:10.1016/j.immuni.2012.01.016

37. Wong BR, Josien R, Lee SY, Sauter B, Li H-L, Steinman RM, et al. TRANCE (Tumor Necrosis Factor [TNF]-related Activation-induced Cytokine), a New TNF Family Member Predominantly Expressed in T cells, Is a Dendritic Cell–specific Survival Factor. J Exp Med. 1997;186: 2075–2080. doi:10.1084/jem.186.12.2075

38. Williamson E, Bilsborough JM, Viney JL. Regulation of Mucosal Dendritic Cell Function by Receptor Activator of NF-κB (RANK)/RANK Ligand Interactions: Impact on Tolerance Induction. J Immunol. 2002;169: 3606–3612. doi:10.4049/jimmunol.169.7.3606

39. Josien R, Wong BR, Li H-L, Steinman RM, Choi Y. TRANCE, a TNF Family Member, Is Differentially Expressed on T Cell Subsets and Induces Cytokine Production in Dendritic Cells. J Immunol. 1999;162: 2562–2568.

40. Zhong L, Granelli-Piperno A, Choi Y, Steinman RM. Recombinant adenovirus is an efficient and non-perturbing genetic vector for human dendritic cells. Eur J Immunol. 1999;29: 964–972. doi:10.1002/(SICI)1521-4141(199903)29:03<964::AID-IMMU964>3.0.CO;2-P

41. Josien R, Li H-L, Ingulli E, Sarma S, R.Wong B, Vologodskaia M, et al. Trance, a Tumor Necrosis Factor Family Member, Enhances the Longevity and Adjuvant Properties of Dendritic Cells in Vivo. J Exp Med. 2000;191: 495–502.

42. Bachmann MF, Wong BR, Josien R, Steinman RM, Oxenius A, Choi Y. TRANCE, a Tumor Necrosis Factor Family Member Critical for CD40 Ligand–independent T Helper Cell Activation. J Exp Med. 1999;189: 1025–1031.

43. Barbaroux J-BO, Beleut M, Brisken C, Mueller CG, Groves RW. Epidermal Receptor Activator of NF-κB Ligand Controls Langerhans Cells Numbers and Proliferation. J Immunol. 2008;181: 1103–1108.

44. Stolina M, Dwyer D, Ominsky MS, Corbin T, Van G, Bolon B, et al. Continuous RANKL Inhibition in Osteoprotegerin Transgenic Mice and Rats Suppresses Bone Resorption without Impairing Lymphorganogenesis or Functional Immune Responses. J Immunol. 2007;179: 7497–7505. doi:10.4049/jimmunol.179.11.7497

45. Padigel UM, Kim N, Choi Y, Farrell JP. TRANCE-RANK Costimulation is Required for IL-12 Production and the Initiation of a Th1-Type Response to Leishmania major Infection in CD40L-Deficient Mice. J Immunol. 2003;171: 5437–5441. doi:10.4049/jimmunol.171.10.5437

46. Anderson DM, Maraskovsky E, Billingsley WL, Dougall WC, Tometsko ME, Roux ER, et al. A homologue of the TNF receptor and its ligand enhance T-cell growth and dendritic-cell function. Nature. 1997;390: 175–179. doi:10.1038/36593

47. Emery JG, McDonnell P, Burke MB, Deen KC, Lyn S, Silverman C, et al. Osteoprotegerin Is a Receptor for the Cytotoxic Ligand TRAIL. J Biol Chem. 1998;273: 14363–14367. doi:10.1074/jbc.273.23.14363

48. Kim D, Mebius RE, MacMicking JD, Jung S, Cupedo T, Castellanos Y, et al. Regulation of Peripheral Lymph Node Genesis by the Tumor Necrosis Factor Family Member Trance. J Exp Med. 2000;192: 1467–1478. doi:10.1084/jem.192.10.1467

49. Knoop KA, Kumar N, Butler BR, Sakthivel SK, Taylor RT, Nochi T, et al. RANKL Is Necessary and Sufficient to Initiate Development of Antigen-Sampling M Cells in the Intestinal Epithelium. J Immunol. 2009;183: 5738–5747. doi:10.4049/jimmunol.0901563

50. Lacey DL, Boyle WJ, Simonet WS, Kostenuik PJ, Dougall WC, Sullivan JK, et al. Bench to bedside: elucidation of the OPG–RANK–RANKL pathway and the development of denosumab. Nat Rev Drug Discov. 2012;11: 401–419. doi:10.1038/nrd3705

51. Mueller CG, Hess E. Emerging Functions of RANKL in Lymphoid Tissues. Front Immunol. 2012;3. doi:10.3389/fimmu.2012.00261

52. Cupedo T, Mebius RE. Cellular Interactions in Lymph Node Development. J Immunol. 2005;174: 21–25. doi:10.4049/jimmunol.174.1.21

53. Remouchamps C, Boutaffala L, Ganeff C, Dejardin E. Biology and signal transduction pathways of the Lymphotoxin-αβ/LTβR system. Cytokine Growth Factor Rev. 2011;22: 301–310. doi:10.1016/j.cytogfr.2011.11.007

54. Hess E, Duheron V, Decossas M, Lézot F, Berdal A, Chea S, et al. RANKL Induces Organized Lymph Node Growth by Stromal Cell Proliferation. J Immunol. 2012;188: 1245–1254. doi:10.4049/jimmunol.1101513

55. Sugiyama M, Nakato G, Jinnohara T, Akiba H, Okumura K, Ohno H, et al. Expression pattern changes and function of RANKL during mouse lymph node microarchitecture development. Int Immunol. 2012;24: 369–378. doi:10.1093/intimm/dxs002

56. Akiyama T, Shimo Y, Yanai H, Qin J, Ohshima D, Maruyama Y, et al. The Tumor Necrosis Factor Family Receptors RANK and CD40 Cooperatively Establish the Thymic Medullary Microenvironment and Self-Tolerance. Immunity. 2008;29: 423–437. doi:10.1016/j.immuni.2008.06.015

57. Akiyama T, Shinzawa M, Qin J, Akiyama N. Regulations of gene expression in medullary thymic epithelial cells required for preventing the onset of autoimmune diseases. T Cell Biol. 2013;4: 249. doi:10.3389/fimmu.2013.00249

58. Rossi SW, Kim M-Y, Leibbrandt A, Parnell SM, Jenkinson WE, Glanville SH, et al. RANK signals from CD4+3– inducer cells regulate development of Aire-expressing epithelial cells in the thymic medulla. J Exp Med. 2007;204: 1267–1272. doi:10.1084/jem.20062497

59. Akiyama T, Maeda S, Yamane S, Ogino K, Kasai M, Kajiura F, et al. Dependence of Self-Tolerance on TRAF6-Directed Development of Thymic Stroma. Science. 2005;308: 248–251. doi:10.1126/science.1105677

60. Burkly L, Hession C, Ogata L, Reilly C, Marconl LA, Olson D, et al. Expression of relB is required for the development of thymic medulla and dendritic cells. Nature. 1995;373: 531–536. doi:10.1038/373531a0

61. Weih F, Carrasco D, Durham SK, Barton DS, Rizzo CA, Ryseck R-P, et al. Multiorgan inflammation and hematopoietic abnormalities in mice with a targeted disruption of RelB, a member of the NF-κB/Rel family. Cell. 1995;80: 331–340. doi:10.1016/0092-8674(95)90416-6

62. Otero DC, Baker DP, David M. IRF7-Dependent IFN-β Production in Response to RANKL Promotes Medullary Thymic Epithelial Cell Development. J Immunol. 2013;190: 3289–3298. doi:10.4049/jimmunol.1203086

63. Sakaguchi S. Naturally arising Foxp3-expressing CD25+CD4+ regulatory T cells in immunological tolerance to self and non-self. Nat Immunol. 2005;6: 345–352. doi:10.1038/ni1178

64. Loser K, Mehling A, Loeser S, Apelt J, Kuhn A, Grabbe S, et al. Epidermal RANKL controls regulatory T-cell numbers via activation of dendritic cells. Nat Med. 2006;12: 1372–1379. doi:10.1038/nm1518

65. Green EA, Choi Y, Flavell RA. Pancreatic Lymph Node-Derived CD4+CD25+ Treg Cells: Highly Potent Regulators of Diabetes that Require TRANCE-RANK Signals. Immunity. 2002;16: 183–191. doi:10.1016/S1074-7613(02)00279-0

66. Totsuka T, Kanai T, Nemoto Y, Tomita T, Okamoto R, Tsuchiya K, et al. RANK-RANKL Signaling Pathway Is Critically Involved in the Function of CD4+CD25+ Regulatory T Cells in Chronic Colitis. J Immunol. 2009;182: 6079–6087. doi:10.4049/jimmunol.0711823

67. Cheng ML, Fong L. Effects of RANKL-Targeted Therapy in Immunity and Cancer. Front Oncol. 2014;3. doi:10.3389/fonc.2013.00329

68. Gravallese EM, Manning C, Tsay A, Naito A, Pan C, Amento E, et al. Synovial tissue in rheumatoid arthritis is a source of osteoclast differentiation factor. Arthritis Rheum. 2000;43: 250–258. doi:10.1002/1529-0131(200002)43:2<250::AID-ANR3>3.0.CO;2-P

69. Takayanagi H, Iizuka H, Juji T, Nakagawa T, Yamamoto A, Miyazaki T, et al. Involvement of receptor activator of nuclear factor κB ligand/osteoclast differentiation factor in osteoclastogenesis from synoviocytes in rheumatoid arthritis. Arthritis Rheum. 2000;43: 259–269. doi:10.1002/1529-0131(200002)43:2<259::AID-ANR4>3.0.CO;2-W

70. Okamoto K, Takayanagi H. Regulation of bone by the adaptive immune system in arthritis. Arthritis Res Ther. 2011;13: 219. doi:10.1186/ar3323

71. Kikuta J, Wada Y, Kowada T, Wang Z, Sun-Wada G-H, Nishiyama I, et al. Dynamic visualization of RANKL and Th17-mediated osteoclast function. J Clin Invest. 2013;123: 866–873. doi:10.1172/JCI65054

72. Zhao R, Chen N-N, Zhou X-W, Miao P, Hu C-Y, Qian L, et al. Exogenous IFN-beta regulates the RANKL-c-Fos-IFN-beta signaling pathway in the collagen antibody-induced arthritis model. J Transl Med. 2014;12. doi:10.1186/s12967-014-0330-y

73. Onal M, Xiong J, Chen X, Thostenson JD, Almeida M, Manolagas SC, et al. Receptor Activator of Nuclear Factor κB Ligand (RANKL) Protein Expression by B Lymphocytes Contributes to Ovariectomy-induced Bone Loss. J Biol Chem. 2012;287: 29851–29860. doi:10.1074/jbc.M112.377945

74. Yeo L, Lom H, Juarez M, Snow M, Buckley CD, Filer A, et al. Expression of FcRL4 defines a pro-inflammatory, RANKL-producing B cell subset in rheumatoid arthritis. Ann Rheum Dis. 2015;74: 928–935. doi:10.1136/annrheumdis-2013-204116

75. Yeo L, Toellner K-M, Salmon M, Filer A, Buckley CD, Raza K, et al. Cytokine mRNA profiling identifies B cells as a major source of RANKL in rheumatoid arthritis. Ann Rheum Dis. 2011;70: 2022–2028. doi:10.1136/ard.2011.153312

76. Fata JE, Kong Y-Y, Li J, Sasaki T, Irie-Sasaki J, Moorehead RA, et al. The Osteoclast Differentiation Factor Osteoprotegerin-Ligand Is Essential for Mammary Gland Development. Cell. 2000;103: 41–50. doi:10.1016/S0092-8674(00)00103-3

77. Kim N-S, Kim H-J, Koo B-K, Kwon M-C, Kim Y-W, Cho Y, et al. Receptor Activator of NF-κB Ligand Regulates the Proliferation of Mammary Epithelial Cells via Id2. Mol Cell Biol. 2006;26: 1002–1013. doi:10.1128/MCB.26.3.1002-1013.2006

78. Cao Y, Bonizzi G, Seagroves TN, Greten FR, Johnson R, Schmidt EV, et al. IKKα Provides an Essential Link between RANK Signaling and Cyclin D1 Expression during Mammary Gland Development. Cell. 2001;107: 763–775. doi:10.1016/S0092-8674(01)00599-2

79. Toberer F, Sykora J, Göttel D, Ruland V, Hartschuh W, Enk A, et al. Tissue microarray analysis of RANKL in cutaneous lupus erythematosus and psoriasis. Exp Dermatol. 2011;20: 600–602. doi:10.1111/j.1600-0625.2011.01303.x

80. Duheron V, Hess E, Duval M, Decossas M, Castaneda B, Klopper JE, et al. Receptor activator of NF-?B (RANK) stimulates the proliferation of epithelial cells of the epidermo-pilosebaceous unit. Proc Natl Acad Sci U S A. 2011;108: 5342–5347. doi:10.1073/pnas.1013054108

81. Mabbott NA, Donaldson DS, Ohno H, Williams IR, Mahajan A. Microfold (M) cells: important immunosurveillance posts in the intestinal epithelium. Mucosal Immunol. 2013;6: 666–677. doi:10.1038/mi.2013.30

82. Taylor RT, Patel SR, Lin E, Butler BR, Lake JG, Newberry RD, et al. Lymphotoxin-Independent Expression of TNF-Related Activation-Induced Cytokine by Stromal Cells in Cryptopatches, Isolated Lymphoid Follicles, and Peyer's Patches. J Immunol. 2007;178: 5659–5667. doi:10.4049/jimmunol.178.9.5659

83. Knoop KA, Butler BR, Kumar N, Newberry RD, Williams IR. Distinct Developmental Requirements for Isolated Lymphoid Follicle Formation in the Small and Large Intestine: RANKL Is Essential Only in the Small Intestine. Am J Pathol. 2011;179: 1861–1871. doi:10.1016/j.ajpath.2011.06.004

84. Lau W de, Kujala P, Schneeberger K, Middendorp S, Li VSW, Barker N, et al. Peyer's Patch M Cells Derived from Lgr5+ Stem Cells Require SpiB and Are Induced by RankL in Cultured "Miniguts." Mol Cell Biol. 2012;32: 3639–3647. doi:10.1128/MCB.00434-12

85. figure M cells [Internet]. [cited 2 Feb 2017]. Available: http://leib.rcai.riken.jp/riken/research-e.html

86. Kim Y-M, Kim Y-M, Lee YM, Kim H-S, Kim JD, Choi Y, et al. TNF-related Activation-induced Cytokine (TRANCE) Induces Angiogenesis through the Activation of Src and Phospholipase C (PLC) in Human Endothelial Cells. J Biol Chem. 2002;277: 6799–6805. doi:10.1074/jbc.M109434200

87. Collin-Osdoby P. Regulation of Vascular Calcification by Osteoclast Regulatory Factors RANKL and Osteoprotegerin. Circ Res. 2004;95: 1046–1057. doi:10.1161/01.RES.0000149165.99974.12

88. Kim H-H, Shin HS, Kwak HJ, Ahn KY, Kim J-H, Lee HJ, et al. RANKL regulates endothelial cell survival through the phosphatidylinositol 3'-kinase/Akt signal transduction pathway. FASEB J. 2003; doi:10.1096/fj.03-0215fje

89. Pritzker LB, Scatena M, Giachelli CM. The Role of Osteoprotegerin and Tumor Necrosis Factor-related Apoptosis-inducing Ligand in Human Microvascular Endothelial Cell Survival. Mol Biol Cell. 2004;15: 2834–2841. doi:10.1091/mbc.E04-01-0059

90. Malyankar UM, Scatena M, Suchland KL, Yun TJ, Clark EA, Giachelli CM. Osteoprotegerin Is an αvβ3-induced, NF-κB-dependent Survival Factor for Endothelial Cells. J Biol Chem. 2000;275: 20959–20962. doi:10.1074/jbc.C000290200

91. Kobayashi-Sakamoto M, Isogai E, Hirose K, Chiba I. Role of αv integrin in osteoprotegerin-induced endothelial cell migration and proliferation. Microvasc Res. 2008;76: 139–144. doi:10.1016/j.mvr.2008.06.004

92. Min J-K, Kim Y-M, Kim SW, Kwon M-C, Kong Y-Y, Hwang IK, et al. TNF-Related Activation-Induced Cytokine Enhances Leukocyte Adhesiveness: Induction of ICAM-1 and VCAM-1 via TNF Receptor-Associated Factor and Protein Kinase C-Dependent NF-κB Activation in Endothelial Cells. J Immunol. 2005;175: 531–540. doi:10.4049/jimmunol.175.1.531

93. González-Suárez E, Sanz-Moreno A. RANK as a therapeutic target in cancer. FEBS J. 2016;283: 2018–2033. doi:10.1111/febs.13645

94. Schramek D, Leibbrandt A, Sigl V, Kenner L, Pospisilik JA, Lee HJ, et al. Osteoclast differentiation factor RANKL controls development of progestin-driven mammary cancer. Nature. 2010;468: 98–102. doi:10.1038/nature09387

95. Gonzalez-Suarez E, Jacob AP, Jones J, Miller R, Roudier-Meyer MP, Erwert R, et al. RANK ligand mediates progestin-induced mammary epithelial proliferation and carcinogenesis. Nature. 2010;468: 103–107. doi:10.1038/nature09495

96. Tan W, Zhang W, Strasner A, Grivennikov S, Cheng JQ, Hoffman RM, et al. Tumour-infiltrating regulatory T cells stimulate mammary cancer metastasis through RANKL-RANK signalling. Nature. 2011;470: 548–553. doi:10.1038/nature09707

97. Palafox M, Ferrer I, Pellegrini P, Vila S, Hernandez-Ortega S, Urruticoechea A, et al. RANK Induces Epithelial–Mesenchymal Transition and Stemness in Human Mammary Epithelial Cells and Promotes Tumorigenesis and Metastasis. Cancer Res. 2012;72: 2879–2888. doi:10.1158/0008-5472.CAN-12-0044

98. Zhang W, Tan W, Wu X, Poustovoitov M, Strasner A, Li W, et al. A NIK-IKKα Module Expands ErbB2-Induced Tumor-Initiating Cells by Stimulating Nuclear Export of p27/Kip1. Cancer Cell. 2013;23: 647–659. doi:10.1016/j.ccr.2013.03.012

99. Mori K, Le Goff B, Berreur M, Riet A, Moreau A, Blanchard F, et al. Human osteosarcoma cells express functional receptor activator of nuclear factor-kappa B. J Pathol. 2007;211: 555–562. doi:10.1002/path.2140

100.   Kupas V, Weishaupt C, Siepmann D, Kaserer M-L, Eickelmann M, Metze D, et al. RANK Is Expressed in Metastatic Melanoma and Highly Upregulated on Melanoma-Initiating Cells. J Invest Dermatol. 2011;131: 944–955. doi:10.1038/jid.2010.377

101.   Chen G, Sircar K, Aprikian A, Potti A, Goltzman D, Rabbani SA. Expression of RANKL/RANK/OPG in primary and metastatic human prostate cancer as markers of disease stage and functional regulation. Cancer. 2006;107: 289–298. doi:10.1002/cncr.21978

102.   Hameed A, Brady JJ, Dowling P, Clynes M, O'Gorman P. Bone Disease in Multiple Myeloma: Pathophysiology and Management. Cancer Growth Metastasis. 2014;2014: 33–42. doi:10.4137/CGM.S16817

103.   Thomas RJ, Guise TA, Yin JJ, Elliott J, Horwood NJ, Martin TJ, et al. Breast Cancer Cells Interact with Osteoblasts to Support Osteoclast Formation. Endocrinology. 1999;140: 4451–4458. doi:10.1210/endo.140.10.7037

104.   Zhang J, Dai J, Qi Y, Lin D-L, Smith P, Strayhorn C, et al. Osteoprotegerin inhibits prostate cancer–induced osteoclastogenesis and prevents prostate tumor growth in the bone. J Clin Invest. 2001;107: 1235–1244.

105.   Lipton A, Goessl C. Clinical development of anti-RANKL therapies for treatment and prevention of bone metastasis. Bone. 2011;48: 96–99. doi:10.1016/j.bone.2010.10.161

106.   Khan IS, Mouchess ML, Zhu M-L, Conley B, Fasano KJ, Hou Y, et al. Enhancement of an anti-tumor immune response by transient blockade of central T cell tolerance. J Exp Med. 2014;211: 761–768. doi:10.1084/jem.20131889

107.   Wiethe C, Dittmar K, Doan T, Lindenmaier W, Tindle R. Enhanced Effector and Memory CTL Responses Generated by Incorporation of Receptor Activator of NF-κB (RANK)/RANK Ligand Costimulatory Molecules into Dendritic Cell Immunogens Expressing a Human Tumor-Specific Antigen. J Immunol. 2003;171: 4121–4130. doi:10.4049/jimmunol.171.8.4121

108.   Ma X, Liu Y, Zhang Y, Yu X, Wang W, Zhao D. Jolkinolide B inhibits RANKL-induced osteoclastogenesis by suppressing the activation NF-κB and MAPK signaling pathways. Biochem Biophys Res Commun. 2014;445: 282–288. doi:10.1016/j.bbrc.2014.01.145

109.   Chen Y, Sun J, Dou C, Li N, Kang F, Wang Y, et al. Alliin Attenuated RANKL-Induced Osteoclastogenesis by Scavenging Reactive Oxygen Species through Inhibiting Nox1. Int J Mol Sci. 2016;17. doi:10.3390/ijms17091516

110.   Li L, Sapkota M, Kim S, Soh Y. Herbacetin inhibits RANKL-mediated osteoclastogenesis in vitro and prevents inflammatory bone loss in vivo. Eur J Pharmacol. 2016;777: 17–25. doi:10.1016/j.ejphar.2016.02.057

111.   Lee C-C, Liu F-L, Chen C-L, Chen T-C, Chang D-M, Huang H-S. Discovery of 5-(2',4'-difluorophenyl)-salicylanilides as new inhibitors of receptor activator of NF-κB ligand (RANKL)-induced osteoclastogenesis. Eur J Med Chem. 2015;98: 115–126. doi:10.1016/j.ejmech.2015.05.015

112.   Coste E, Greig IR, Mollat P, Rose L, Gray M, Ralston SH, et al. Identification of small molecule inhibitors of RANKL and TNF signalling as anti-inflammatory and antiresorptive agents in mice. Ann Rheum Dis. 2015;74: 220–226. doi:10.1136/annrheumdis-2013-203700

113.   Aggarwal B, Darnay B, Singh S. Inhibitors of receptor activator of NF-kappaB and uses thereof [Internet]. US20040167072 A1, 2004. Available: http://www.google.tl/patents/US20040167072

114.   Kim H, Choi HK, Shin JH, Kim KH, Huh JY, Lee SA, et al. Selective inhibition of RANK blocks osteoclast maturation and function and prevents bone loss in mice. J Clin Invest. 2009;119: 813–825. doi:10.1172/JCI36809

115.   Tomoyasu A, Goto M, Fujise N, Mochizuki S, Yasuda H, Morinaga T, et al. Characterization of Monomeric and Homodimeric Forms of Osteoclastogenesis Inhibitory Factor. Biochem Biophys Res Commun. 1998;245: 382–387. doi:10.1006/bbrc.1998.8443

116.   Bekker PJ, Holloway D, Nakanishi A, Arrighi M, Leese PT, Dunstan CR. The Effect of a Single Dose of Osteoprotegerin in Postmenopausal Women. J Bone Miner Res. 2001;16: 348–360. doi:10.1359/jbmr.2001.16.2.348

117.   Body J-J, Greipp P, Coleman RE, Facon T, Geurs F, Fermand J-P, et al. A Phase I study of AMGN-0007, a recombinant osteoprotegerin construct, in patients with multiple myeloma or breast carcinoma related bone metastases. Cancer. 2003;97: 887–892. doi:10.1002/cncr.11138

118.   Bekker PJ, Holloway DL, Rasmussen AS, Murphy R, Martin SW, Leese PT, et al. A Single-Dose Placebo-Controlled Study of AMG 162, a Fully Human Monoclonal Antibody to RANKL, in Postmenopausal Women. J Bone Miner Res. 2004;19: 1059–1066. doi:10.1359/JBMR.040305

119.   Kamijo S, Nakajima A, Ikeda K, Aoki K, Ohya K, Akiba H, et al. Amelioration of bone loss in collagen-induced arthritis by neutralizing anti-RANKL monoclonal antibody. Biochem Biophys Res Commun. 2006;347: 124–132. doi:10.1016/j.bbrc.2006.06.098

120.   Sordillo EM, Pearse RN. RANK-Fc: A therapeutic antagonist for RANK-L in myeloma. Cancer. 2003;97: 802–812. doi:10.1002/cncr.11134

121.   Bargman R, Posham R, Boskey A, Carter E, DiCarlo E, Verdelis K, et al. High- and low-dose OPG-Fc cause osteopetrosis-like changes in infant mice. Pediatr Res. 2012;72: 495–501. doi:10.1038/pr.2012.118

122.   Ominsky MS, Kostenuik PJ, Cranmer P, Smith SY, Atkinson JE. The RANKL inhibitor OPG-Fc increases cortical and trabecular bone mass in young gonad-intact cynomolgus monkeys. Osteoporos Int. 2007;18: 1073–1082. doi:10.1007/s00198-007-0363-7

123.   Schett G, Redlich K, Hayer S, Zwerina J, Bolon B, Dunstan C, et al. Osteoprotegerin protects against generalized bone loss in tumor necrosis factor–transgenic mice. Arthritis Rheum. 2003;48: 2042–2051. doi:10.1002/art.11150

124.   Naidu VGM, Dinesh Babu KR, Thwin MM, Satish RL, Kumar PV, Gopalakrishnakone P. RANKL targeted peptides inhibit osteoclastogenesis and attenuate adjuvant induced arthritis by

inhibiting NF-κB activation and down regulating inflammatory cytokines. Chem Biol Interact. 2013;203: 467–479. doi:10.1016/j.cbi.2012.12.016

125.   Cheng X, Kinosaki M, Takami M, Choi Y, Zhang H, Murali R. Disabling of Receptor Activator of Nuclear Factor-κB (RANK) Receptor Complex by Novel Osteoprotegerin-like Peptidomimetics Restores Bone Loss in Vivo. J Biol Chem. 2004;279: 8269–8277. doi:10.1074/jbc.M309690200

126.   Kato G, Shimizu Y, Arai Y, Suzuki N, Sugamori Y, Maeda M, et al. The inhibitory effects of a RANKL-binding peptide on articular and periarticular bone loss in a murine model of collagen-induced arthritis: a bone histomorphometric study. Arthritis Res Ther. 2015;17: 251. doi:10.1186/s13075-015-0753-8

127.   Heath DJ, Vanderkerken K, Cheng X, Gallagher O, Prideaux M, Murali R, et al. An Osteoprotegerin-like Peptidomimetic Inhibits Osteoclastic Bone Resorption and Osteolytic Bone Disease in Myeloma. Cancer Res. 2007;67: 202–208. doi:10.1158/0008-5472.CAN-06-1287

128.   Hur J, Ghosh A, Kim K, Ta HM, Kim H, Kim N, et al. Design of a RANK-Mimetic Peptide Inhibitor of Osteoclastogenesis with Enhanced RANKL-Binding Affinity. Mol Cells. 2016;39: 316–321. doi:10.14348/molcells.2016.2286

129.   Ta HM, Nguyen GTT, Jin HM, Choi J, Park H, Kim N, et al. Structure-based development of a receptor activator of nuclear factor-κB ligand (RANKL) inhibitor peptide and molecular basis for osteopetrosis. Proc Natl Acad Sci. 2010;107: 20281–20286. doi:10.1073/pnas.1011686107

130.   Aoki K, Saito H, Itzstein C, Ishiguro M, Shibata T, Blanque R, et al. A TNF receptor loop peptide mimic blocks RANK ligand–induced signaling, bone resorption, and bone loss. J Clin Invest. 2006;116: 1525–1534. doi:10.1172/JCI22513

131.   Newa M, Lam M, Bhandari KH, Xu B, Doschak MR. Expression, Characterization, and Evaluation of a RANK-Binding Single Chain Fraction Variable: An Osteoclast Targeting Drug Delivery Strategy. Mol Pharm. 2014;11: 81–89. doi:10.1021/mp400188r

132.   Green LL. Antibody engineering via genetic engineering of the mouse: XenoMouse strains are a vehicle for the facile generation of therapeutic human monoclonal antibodies. J Immunol Methods. 1999;231: 11–23. doi:10.1016/S0022-1759(99)00137-4

133.   Kearns AE, Khosla S, Kostenuik PJ. Receptor Activator of Nuclear Factor κB Ligand and Osteoprotegerin Regulation of Bone Remodeling in Health and Disease. Endocr Rev. 2008;29: 155–192. doi:10.1210/er.2007-0014

134.   Kostenuik PJ, Nguyen HQ, McCabe J, Warmington KS, Kurahara C, Sun N, et al. Denosumab, a Fully Human Monoclonal Antibody to RANKL, Inhibits Bone Resorption and Increases BMD in Knock-In Mice That Express Chimeric (Murine/Human) RANKL. J Bone Miner Res. 2009;24: 182–195. doi:10.1359/jbmr.081112

135.   Schwarz EM, Ritchlin CT. Clinical development of anti-RANKL therapy. Arthritis Res Ther. 2007;9: S7. doi:10.1186/ar2171

136.   McClung MR, Lewiecki EM, Cohen SB, Bolognese MA, Woodson GC, Moffett AH, et al. Denosumab in Postmenopausal Women with Low Bone Mineral Density. N Engl J Med. 2006;354: 821–831. doi:10.1056/NEJMoa044459

137.   Cummings SR, Martin JS, McClung MR, Siris ES, Eastell R, Reid IR, et al. Denosumab for Prevention of Fractures in Postmenopausal Women with Osteoporosis. N Engl J Med. 2009;361: 756–765. doi:10.1056/NEJMoa0809493

138.   Allen MR, Burr DB. The Pathogenesis of Bisphosphonate-Related Osteonecrosis of the Jaw: So Many Hypotheses, So Few Data. J Oral Maxillofac Surg. 2009;67: 61–70. doi:10.1016/j.joms.2009.01.007

139.   Bridgeman MB, Pathak R. Denosumab for the Reduction of Bone Loss in Postmenopausal Osteoporosis: A Review. Clin Ther. 2011;33: 1547–1559. doi:10.1016/j.clinthera.2011.10.008

140.   Papapoulos S, Chapurlat R, Libanati C, Brandi ML, Brown JP, Czerwiński E, et al. Five years of denosumab exposure in women with postmenopausal osteoporosis: Results from the first two years of the FREEDOM extension. J Bone Miner Res. 2012;27: 694–701. doi:10.1002/jbmr.1479

141.   Lasco A, Morabito N, Basile G, Atteritano M, Gaudio A, Giorgianni GM, et al. Denosumab Inhibition of RANKL and Insulin Resistance in Postmenopausal Women with Osteoporosis. Calcif Tissue Int. 2016;98: 123–128. doi:10.1007/s00223-015-0075-5

142.   Mallarkey G, Reid DM. Osteoporosis therapeutics: recent developments at ASBMR. Ther Adv Musculoskelet Dis. 2016;8: 3–7. doi:10.1177/1759720X15623489

143.   Smith MR, Saad F, Coleman R, Shore N, Fizazi K, Tombal B, et al. Denosumab and bone-metastasis-free survival in men with castration-resistant prostate cancer: results of a phase 3, randomised, placebo-controlled trial. The Lancet. 2012;379: 39–46. doi:10.1016/S0140-6736(11)61226-9

144.   Peddi P, Lopez-Olivo MA, Pratt GF, Suarez-Almazor ME. Denosumab in patients with cancer and skeletal metastases: A systematic review and meta-analysis. Cancer Treat Rev. 2013;39: 97–104. doi:10.1016/j.ctrv.2012.07.002

145.   Xu SF, Adams B, Yu XC, Xu M. Denosumab and giant cell tumour of bone—a review and future management considerations. Curr Oncol. 2013;20: e442–e447. doi:10.3747/co.20.1497

146.   Singh AS, Chawla NS, Chawla SP. Giant-cell tumor of bone: treatment options and role of denosumab. Biol Targets Ther. 2015;9: 69–74. doi:10.2147/BTT.S57359

147.   Takeuchi T, Tanaka Y, Ishiguro N, Yamanaka H, Yoneda T, Ohira T, et al. Effect of denosumab on Japanese patients with rheumatoid arthritis: a dose–response study of AMG 162 (Denosumab) in patients with RheumatoId arthritis on methotrexate to Validate inhibitory effect on bone Erosion (DRIVE)—a 12-month, multicentre, randomised, double-blind, placebo-controlled, phase II clinical trial. Ann Rheum Dis. 2016;75: 983–990. doi:10.1136/annrheumdis-2015-208052

148.   McHugh J. Rheumatoid arthritis: Bone-healing effects of denosumab in RA. Nat Rev Rheumatol. 2016;12: 692–692. doi:10.1038/nrrheum.2016.189

149.   Chiu YG, Ritchlin CT. Denosumab: targeting the RANKL pathway to treat rheumatoid arthritis. Expert Opin Biol Ther. 2017;17: 119–128. doi:10.1080/14712598.2017.1263614

150.   Cohen SB, Dore RK, Lane NE, Ory PA, Peterfy CG, Sharp JT, et al. Denosumab treatment effects on structural damage, bone mineral density, and bone turnover in rheumatoid arthritis: A

twelve-month, multicenter, randomized, double-blind, placebo-controlled, phase II clinical trial. Arthritis Rheum. 2008;58: 1299–1309. doi:10.1002/art.23417

151.   Curtis JR, Xie F, Yun H, Saag KG, Chen L, Delzell E. Risk of Hospitalized Infection Among Rheumatoid Arthritis Patients Concurrently Treated With a Biologic Agent and Denosumab. Arthritis Rheumatol. 2015;67: 1456–1464. doi:10.1002/art.39075

152.   Kong Y-Y, Feige U, Sarosi I, Bolon B, Tafuri A, Morony S, et al. Activated T cells regulate bone loss and joint destruction in adjuvant arthritis through osteoprotegerin ligand. Nature. 1999;402: 304–309. doi:10.1038/46303

153.   Ferrari-Lacraz S, Ferrari S. Effects of RANKL inhibition on inflammation and immunity. IBMS BoneKEy. 2009;6: 116–126. doi:10.1138/20090369

Chapter 3: Lymphatic endothelial cells and the lymphatic system

The lymphatic system was first identified in the seventeenth century [1]. It consists of a broad drainage network that helps recycling body fluid. The lymphatic system comprises lymphatic vessels draining lymph as well as lymph nodes (LN). Lymph is derived from interstitial fluids that leak out of blood capillaries. It contains gases, nutrients, signaling molecules, antigens and migrating cells. Lymphatic vessels formed by lymphatic endothelial cells (LEC) allow a unidirectional transport of the lymph from peripheral tissues to the LN. In this chapter, I will describe the lymphatic vasculature and the LN organization. I will then focus on LEC heterogeneity of phenotype and function in LNs as well as in peripheral tissues.

3.1. **The lymphatic vasculature structure and function**

In adults, about 20 liters of protein-poor fluid leaks from blood capillaries into extravascular spaces every day. Approximately 90% of this fluid is resorbed locally but the two remaining liters returns to blood circulation via lymph vessels [2]. Lymphatic vessels transport migrating cells and soluble antigens to the LNs thus play a crucial role for the immune response [3,4]. They are also associated with absorption of lipids from the intestinal tract. Indeed, it was shown that lymphatic vessel integrity is required for the functional maintenance of the intestine and the LNs [5]. The lymph circulation is unidirectional starting from lymph capillaries to collecting lymphatics and finally back to the inferior vena cava through the thoracic duct [4] (**figure 3.1**).
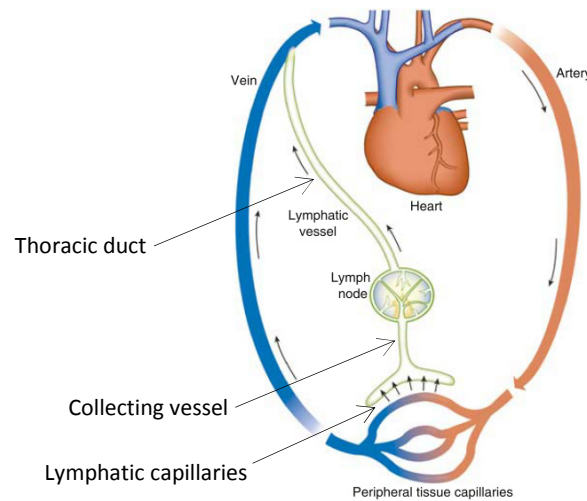
Figure 3.1: Schematic representation of the lymphatic and blood vasculature. The lymphatic vasculature is linear and open-ended. Cells, molecules and fluids leaking from blood capillaries into interstitial tissues are collected by lymphatic capillaries. The lymphatic capillaries then converge into larger collecting vessels that form the LN afferent vessels. Lymph is finally transported back to the blood circulation via the thoracic duct. After reference [6].

Blind-ended capillary lymphatic vessels first absorb interstitial fluids. In these capillaries, LECs form discontinuous button-like junctions allowing the entrance of fluids and immune cells [7] **(figure 3.3)**. VE-cadherin expression is required for maintenance of junction integrity. A thin discontinuous basement membrane surrounds lymphatic capillaries. Anchoring to the extracellular matrix (ECM) enables lymphatic cells to detect changes in interstitial pressure. When this interstitial fluid pressure increases, stretching of the ECM occurs leading to opening of the intercellular junctions and entry of cells and fluids in the capillaries **(figure 3.2)**.
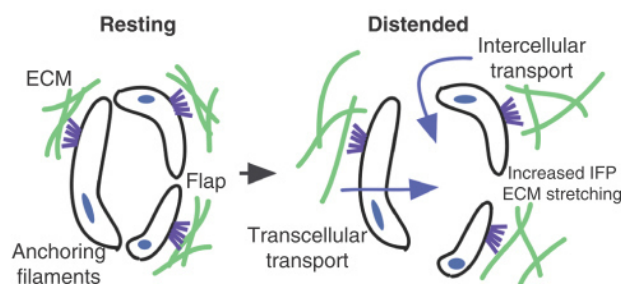

Figure 3.2: Representation of lymphatic capillaries opening. When interstitial fluid pressure (IFP) increases, the extracellular matrix (ECM) stretches allowing intercellular transport of fluids and migrating cells. After reference [8].

Lymphatic capillaries are responsible for the transmigration of immune cells from the peripheral tissues to the lymph. Dendritic cells (DC) enter the lymphatic vessels through already existing gaps in the basement membranes of the vessels [9]. LEC forming the capillaries express high levels of CCL21,

a chemokine binding the receptor CCR7 on DCs. The formation of CCL21 gradients in the interstitium would attract DCs to lymphatic vessels [10]. Moreover, intraluminal gradients of CCL21 have been shown to promote the migration of DCs toward collecting vessels once inside the capillaries [11]. Recirculating memory T cells [12] and neutrophils [13] are other immune cells that use the CCR7 dependent mechanism to enter the lymphatic capillaries. In the skin, another mean for entry of DCs in dermal lymphatics is the interaction between CXCL12 expressing LECs and CXCR4 on DCs [14]. Finally, LECs express the semaphorin3A which bind plexinA1/neuropilin 1 (Plwa1/Nrp1) on DCs and promote entry in the lymphatics [15].
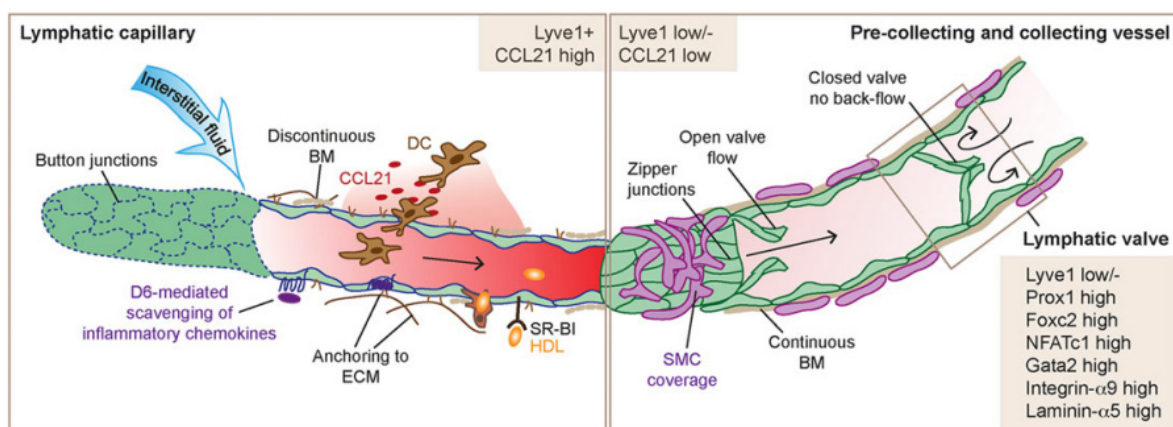

Figure 3.3: Schematic representation of lymphatic capillaries and collecting vessels. LECs forming the lymphatic capillaries express high levels of Lyve1 and CCL21. They form button like junctions, allowing entry of cells and interstitial fluids. They are surrounded by a discontinuous basement membrane (BM) and filaments allow anchoring to extracellular matrix (ECM). CCL21 allows recruitment of dendritic cells (DC) inside the vessels. Expression of HDL receptor SR-BI participates in regulating tissue cholesterol. Expression of D6 scavenging receptor reduces adherence of inflammatory cells and prevents capillary congestion during inflammation. Collecting vessels express low levels of Lyve1 and CCL21. They form impermeable zipper like junctions and are specialised for the transport of cells and fluids. They are surrounded by smooth muscle cells (SMC) and continuous basement membrane. Collecting vessels also contain valves allowing unidirectional transport of the lymph. After reference [16].

After entering lymphatic capillaries, the lymph flows through larger collecting vessels. LECs of these vessels form zipper-like junctions **(figure 3.3)**. Moreover, they are surrounded by perivascular smooth muscle cells and a continuous basement membrane creating impermeable vessels [7]. Therefore, the collecting lymphatic vessels are specialized for transport. They express low levels of CCL21 and thus are not well equipped for transmigration of immune cells in steady state [16]. Transport of lymph is a passive mechanism dependent on smooth muscle cells contraction as well as respiratory movements and contraction of skeletal muscles [17]. The presence of valve leaflets

formed by specialized LECs with a spindle like morphology ensures the unidirectional lymph flow. The opening and closing of the valves relies on the difference of pressure between the two sides. The valves allow lymph flow at pressure equilibrium **(figure 3.3)**. These LECs share a gene expression profile with venous valve endothelial cells [18]. They express Integrin α-9, laminin α5 and the transcription factors Foxc2, GATA2 and NFATC1. Foxc2 and NFATC1 are required for valve formation [19–21]. The separation between lymphatic capillaries and larger collecting vessels is not well understood. Pre-collecting vessels containing valves but surrounded by few smooth muscle cells are linking lymphatic capillaries and collecting vessels [16].

Lymphatic vasculature expresses markers that differentiate them from blood endothelial cells. LECs express prospero homeobox 1 (Prox-1), the transmembrane glycoprotein podoplanin (Pdpn or gp38), vascular endothelial growth factor 3 (Vegfr3) and neuropilin 2 (Nrp2) which both bind VEGF-C in a similar manner [16]. Prox-1 is a transcription factor that plays a role in LECs fate determination [22]. It is expressed in a subset of venous endothelial cells and forms primitive lymph sacs. It was observed in zebrafish that differentiation of LECs from Prox-1 positive blood endothelial cells (BECs) is due to asymmetric division of these cells. After division, one of the daughter cell upregulates Prox-1 while the other downregulates Prox-1 and remains BEC [23]. Gp38, also called podoplanin, is a mucin-type transmembrane protein that was first identified on LECs but is expressed by many other cell types including fibroblastic reticular cells (FRC), alveolar epithelial cells, keratinocytes and kidney podocytes. It is known to bind the C-type lectin receptor CLEC-2 on platelets and immune cells. This interaction is required for development and function of lymphatic vasculature and LN [24–27]. It also plays a role in maintenance of blood-lymphatic separation [28]. The hyaluronan receptor Lyve1 is also described as a marker of LEC [29]. However, high expression of Lyve1 was reported in lymphatic capillaries while lymphatic collecting vessels and lymphatic valves express lower levels of Lyve1 [30]. In addition, Lyve1 is expressed by some macrophages closely related to lymph vessels in embryos, tumors and lymph node medullary sinus [31–33]. CLCA1 is a member of CLCA family involved in calcium-dependent chloride ion transport and was also shown to be specific of LECs [34]. Antibodies targeting Prox-1, Lyve1 and CLCA1 are currently used to visualize lymphatic vessels [22,34,35].

A study by Malhotra et al, in the context of the immunological genome (ImmGen) project, published transcriptional profiling of LN cells [36]. In this study they identified molecules expressed exclusively by LECs. For instance within the family of integrins, *Itga2b* and *Itgb3* were expressed only by LECs. ITGA2b (CD41 or glycoprotein IIb) pairs exclusively with ITGB3 (CD61 or glycoprotein IIIa). The ITGA2b/ITGB3 complex is well known to be expressed by megakaryocytes and platelets and plays a role in blood clotting [37]. However, further investigations are required to further characterize ITGA2b/ITGB3 expression and function in LECs.

Finally, LECs also express endothelial markers shared with blood endothelial cells such as VE cadherin, claudin5, PECAM-1 (CD31) and the angiopoietin receptor Tie2 [16]. CD31 is a classical marker of all endothelial cells. But this adhesion molecule is also carried by platelets and some blood leucocytes. It has a role in cell-cell adhesion but can also induce intracellular signaling [38].

3.2. The lymph nodes

LNs play a critical role in filtration of lymph and thus its immune surveillance. Mice have 22 LNs and about 450 have been identified in humans [39]. The human body contains 250 LNs in abdomen and pelvis region, 100 in the thorax and 60 to 70 in the head and neck area [40]. The structure of these secondary lymphoid organs is similar between species in mammals. In large vertebrates, lymph usually flows through a series of nodes before reaching the collecting duct.

Lymph arrives in LN via afferent lymphatics, is channelled through the LN sinuses to the parenchyma and finally exits via efferent vessels. LNs consist of a collecting point hence it usually has several afferent vessels and one efferent vessel. LNs are organized in lobules which are separated by open communicating sinuses in small animals such as rats. In larger animals, fibrous radial bands called trabeculae separate the lobules. However, murine LNs are generally formed of one single lobule [39] **(figure 3.4)**. These secondary lymphoid organs are located at strategic positions in the body and act as filters to detect antigens and prevent systemic infection. Indeed, all factors and cells needed for the initiation of immune responses are in close contact inside LN. Furthermore, they also play a role in resolution of immune responses and maintenance of tolerance.
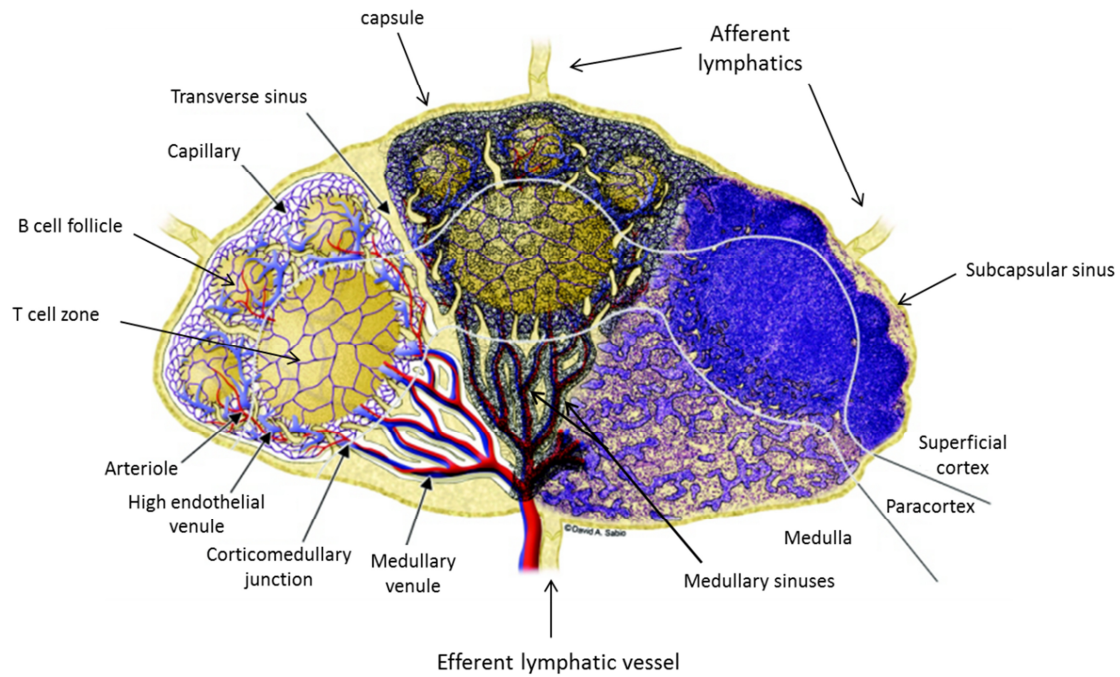
Figure 3.4: Schematic representation of LN organization. Representation of a LN with 3 lobules showing the organization in cortex, paracortex and medulla areas. Each lobule has one afferent lymphatic vessel and a single efferent vessel. Left lobule: schematic representation of the blood vascular network. Center lobule: blood vascular network together with the reticular network formed by non-hematopoietic cells. Right lobule: section from a rat mesenteric LN. Modified after reference [39].

LNs are well organized organs containing 3 major compartments: the cortex, the paracortex and the medulla. Each compartment contains different cell types from both haematopoietic and non-hematopoietic origin that form the complex microarchitecture of a functional LN. Non-hematopoietic cells are characterized by their lack of expression of CD45. They are mainly endothelial and mesenchymal cells while cell from hematopoietic origin comprise lymphocytes as well as DCs and macrophages. The LN is contained in a capsule composed of connective tissue including collagen fibers. Under the capsule lies the subcapsular sinus (SCS) into where lymph from afferent vessels flows. The two layers of LECs forming the SCS are called the "ceiling" and the "floor" of the sinus. In the "floor" layer, CD169^{+} macrophages responsible for the uptake of antigens into the LN are inserted between LECs. Under the SCS lies the cortex. It contains B cell follicles where follicular dendritic cells (FDCs) maintain the follicle architecture, enabling B cells to stay in close contact. Disturbed organization of the follicles correlates with reduced immunocompetence thus this specific configuration of B cells is required for the immune function of LNs [41]. Between the follicles and the floor LECs, marginal reticular cells (MRCs) form a reticulum that sustains the SCS. MRCs express RANKL as well as CXCL13 and CCL19 [42–44]. High endothelial venules (HEV) are also present in the cortex. They are specialized vascular endothelial cells that express Protein NH2-Terminal Asparagine

Deamidase (PNAD) and CCL21, facilitating lymphocyte entry into the LN [44]. In the paracortex, the T cell zone is more diffuse compared to the cell-dense B cell follicles. This zone contains CD4$^+$ and CD8$^+$ T cells, DCs and fibroblastic reticular cells (FRCs). FRCs contribute to the architecture of the T zone [44]. Finally, the medulla contains lymphocytes, blood vessels and the medullary sinus where macrophages can be found. Medullary sinus and efferent lymphatics allow lymphocyte exit from the LN and their return to the blood stream. **(figure 3.4 and 3.5)**
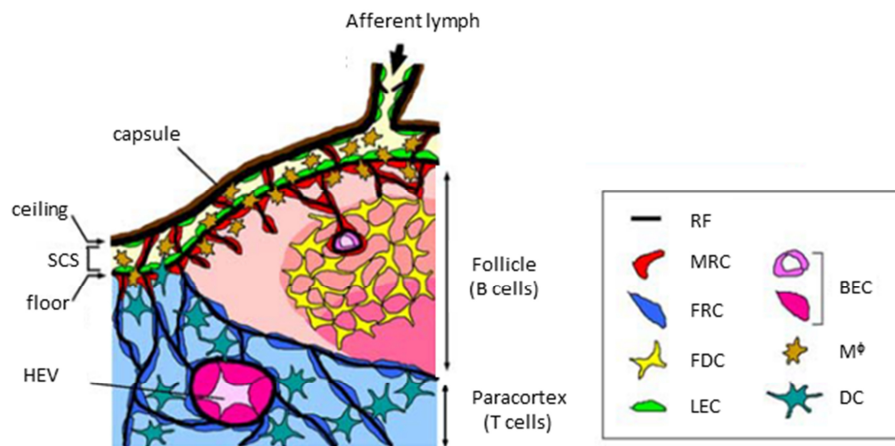
Figure 3.5: Schematic representation of the cell organization in the LN. LECs form the subcapsular sinus. CD169$^+$ macrophages (M$^\phi$) are inserted in the floor of the sinus. Underneath the subcapsular sinus lies a layer of reticular cells called marginal reticular cells (MRC). Follicular dendritic cells (FDC) are required for the organization of B cell follicles. Fibroblastic reticular cells (FRC) form a conduit of reticular fibers (RF) allowing the transport of cells and molecules from the subcapsular sinus to the T cell zone. Dendritic cells (DC) are found in the T cells zone. Lymphocytes are not represented to simplify the representation. After reference [43].

The antigens arriving into the LN can be proteins, lipids, sugars, microorganisms, debris or apoptotic cells. They arrive in the LN passively through the lymph flow or actively transported by cells. Self-antigens carried by tissue-resident antigen-presenting cells (APCs) are also transported to the LN [45]. APCs encounter pathogens in the periphery and then migrate to LNs to increase the chance of meeting the appropriate lymphocyte [46]. On the other hand, free antigen is recognized and processed by LN resident APCs.

LNs are constituted of numerous cell types, I will focus on LECs in the following paragraphs and on macrophages in the next chapter, the two main cell populations I was interested in during my thesis.

3.3. <u>Lymph node LEC heterogeneity and function</u>

As described in the paragraph 3.1, markers have been identified for LECs. A combination of two markers to identify LN non-hematopoietic cells by flow cytometry was introduced by Link et al [47].

After gating on CD45- cells, staining for CD31 and podoplanin gp38 allows the gating of four different populations. LECs are double positive for CD31 and gp38 **(figure 3.6)**.
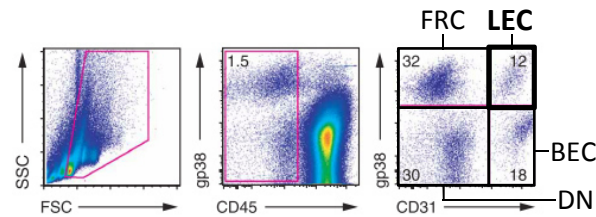

Figure 3.6: Identification of LN LECs by flow cytometry. After gating on CD45^{-} cells, staining for CD31 and podoplanin (gp38) allows the identification of four different populations. LECs are double positive for CD31 and gp38. The other lymph node stromal cells consist of blood endothelial cells (BEC) which are CD31^{+}gp38^{-}, fibroblastic reticular cells (FRC) which are CD31[-]gp38^{+} and double negative (DN) cells. After reference [47].

Despite these common markers, LN LECs represent a heterogeneous population depending on their localization in the LN and also show differences with peripheral tissue lymphatics. In this paragraph I will review the main differences between subcapsular sinus LEC and medullary sinus LECs as well as their main functions.

3.3.1 LECs forming the subcapsular sinus

The "floor" of the subcapsular sinus is formed by LECs that filter the entry of small molecules and cells in the LN parenchyma. This layer is highly selective as molecules with a size > 70kDa or a radius > 4nm cannot enter the parenchyma [48]. Chemokines, cytokines and other small molecules can also enter the conduit formed by fibroblastic reticular cells. This conduit is a network composed of tubular collagen which allows crosstalk between lymph and blood in the HEV. The mechanism for exclusion of large molecules has not been clear for a long time. Recently, it was shown that LN LECs express the plasmalemma vesicle-associated protein (PLVAP, also called PV-1 or MECA-32). This expression was specific to LN LECs as skin LECs do not express PLVAP. This protein forms a physical sieve in the floor sinus bridging the sinus with the conduits. Thus, the diaphragm formed by PLVAP in endothelial cells would regulate the entry of antigens but also lymphocytes into the parenchyma [49]. Floor LECs also play a role in entry of DCs in the LN. As in peripheral lymphatics, SCS LECs express CCL21. Engagement of CCR7 on DCs by CCL21 promotes DCs entry into the LN [50]. However, entry of T cells in the parenchyma is CCR7 independent and would rather rely on PLVAP diaphragms [49,51]. The ceiling LECs uniquely express CCRL1 (ACKR4), a scavenging receptor for CCL21 [52]. Thus, a chemokine gradient is created from the ceiling of the SCS to the parenchyma promoting DCs affinity for floor LECs. Moreover, CCL1 is expressed by SCS LECs and also promotes cell entry in the

LN by interacting with CCR8 [53]. Additionally, it was recently shown that Macrophage scavenger receptor 1 (MSR1) is carried by SCS LECs and regulates lymphocytes entry in the LN [54]. Finally, it was observed that SCS LECs uniformly express MAdCAM-1 compared to medullary sinus LECs; nonetheless the function remains unclear [55]. **(figure3.7)**
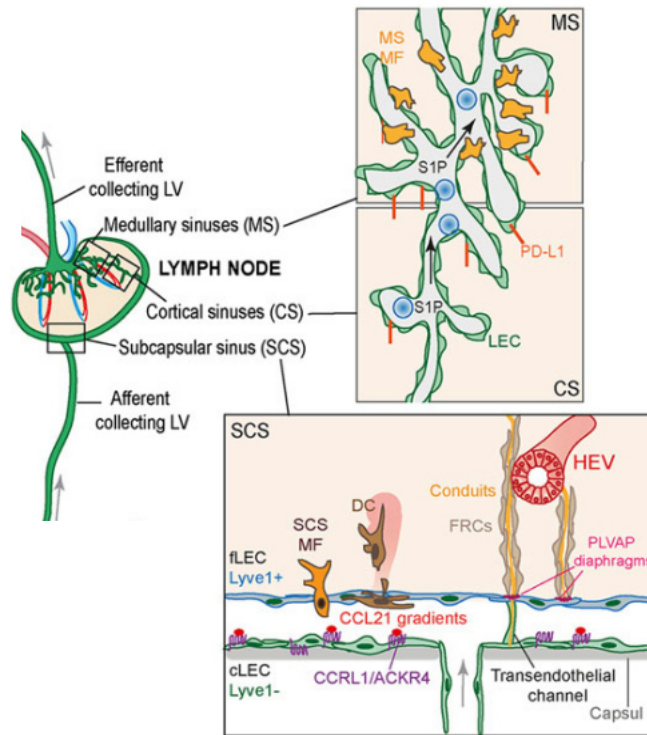

Figure 3.7: Representation of LN lymphatic vessels. Subcapsular sinus (SCS) is formed by two layers of LECs: the floor (fLEC) and the ceiling (cLEC). cLEC express CCRL1 scavenger receptor for CCL21 as well as low levels of Lyve1. fLEC express high levels of Lyve1 and the chemokine CCL21 allowing entry of tissue-derived dendritic cells (DC) in a CCR7 dependent manner. CD169^{+} subcapsular sinus macrophages (SCS MF) are inserted in the floor layer. Antigens and molecules can enter the parenchyma and rich high endothelial venules (HEV) via the conduit formed by fibroblastic reticular cells (FRC). PLVAP diaphragms control the size of the substances entering the LN. LECs forming the medullary sinuses (MS) and cortical sinuses (CS) have a distinct phenotype compared to SCS LECs. They play a role in egress of immune cells from the LN through the expression of sphingosine-1-phosphate (S1P). Medullary sinus macrophages (MS MF) are inserted into MS layer and are distinct from the SCS MF. MS and CS also play a role in tolerance as LECs of these vessels express PDL-1, an immune check point molecule. Modified after reference [16].

3.3.2   LECs forming the medullary and cortical sinuses

Most lymph fluid does not enter the conduits in the parenchyma but crosses the LN through medullary and cortical sinuses. These sinuses play a role in lymphocyte egress from the LN into the efferent lymph. Medullary and cortical LECs are the only cell type in LNs to produce sphingosine-1-phosphate (S1P) which promotes egress of lymphocytes from the LN. S1P binds the sphingosine-1-

phosphate receptor type 1 (S1PR1) expressed by T cells [56–58]. Integrin-α9 was also shown to regulate S1P secretion by LECs [59]. Moreover, lymphocytes adhere to LECs prior to leaving the LN and possible adherence molecules involved in this phenomenon could be CLCA1 and Mannose receptor (MR). CLCA1 was shown to bind LFA-1 and MAC-1 lymphocytes molecules [34]. MR is expressed by human lymphatic endothelium and can bind L-selectin on lymphocytes [60]. Moreover, the common lymphatic endothelial and vascular endothelial receptor-1 (CLEVER-1) is also expressed by LECs and was shown to play a role in lymphocyte trafficking [61]. The importance of these three molecules *in vivo* remains to be investigated. Finally, it was observed that T cells can enter the LN paracortex via medullary sinuses in a CCR7 dependent manner [51]. **(figure 3.7)**

3.3.3   Antigen presentation by LN LECs and peripheral tolerance

Besides regulating entry and egress of lymphocytes and DCs, LECs also share some characteristics with antigen presenting cells (APCs). Indeed LECs express both MHC class I [62,63] and MHC class II [36,64] molecules.

Expression of MHC II is restricted to LN LECs compared to tissue lymphatics LECs, showing the different immune function of these cells [64–66]. Tewalt et al have shown that MHC-II is functional on LECs as peptide-pulsed LECs induce proliferation of CD4^{+} T cells [67]. On the other hand, Nörder et al showed that LECs interact with CD4^{+} T cells via MHC-II and LFA-1 (CD58) but were not able to induce T cell proliferation [68]. Therefore, further investigation is required to understand the role of LECs in regulating CD4^{+} T cells activation and differentiation.

LECs are also capable of antigen endocytosis and MHC-I cross-presentation even if they do it less efficiently than professional APCs [62]. However, LECs do not express costimulatory molecules such as CD80, 4-1BBL and OX40L [64] but they express the Programmed death ligand (PDL-1) immune check point. It was also observed that LECs express peripheral tissue-restricted antigens (PTA). Therefore, antigen presentation by LECs would play a role in peripheral tolerance. Indeed, it was shown that deletion of CD8^{+} T cells can be induced by LECs [64,69]. The presentation of PTA by LECs promotes peripheral tolerance in a way that is similar to medullary thymic epithelial cells (mTECs). However, the expression of PTA is not dependent on the Autoimmune regulatory element (Aire). It was shown *in vivo* that tyrosinase presentation by LN LECs to tyrosinase-specific T cells arrests their proliferation and leads to their deletion in a mechanism that is independent of the Aire [63]. Therefore, T cell deletion by LECs probably relies on lack of costimulation and signaling via PD-L1:PD-1 pathway [64] (**figure 3.8**). PTA and PDL-1 are more abundant in LN LECs than tissue lymphatics with a higher expression in medullary and cortical sinus LECs [70]. Moreover, LECs express different patterns of PTA compared to FRCs or BECs showing that these cells play a specific role in tolerance [63,71].

Another proposed mechanism is the transfer of antigens from LEC to DCs that would present peripheral tissue antigens (PTA) via MHC-II molecule. This mechanism is similar to mTEC antigens transfer to thymic DCs thus inducing anergy of CD4^{+} T cells [67,72]. Whether LEC PTA presentation is involved in other immunological processes than T cell deletion remains to be investigated. Taken together, it is likely that dysregulation of peripheral tolerance induction by LN LECs could lead to autoimmune diseases.

Finally, the capture of antigen by LECs may also play a protective role in vaccination and viral infection. Indeed, LN LECs may store antigens for a longer period of time after the peak of T cell response. Tamburini and colleagues showed that T cell response induces proliferation of LECs and capture of persisting antigens. In this process, LECs can archive antigens for weeks and further activate memory CD8^{+} T cells with the help of DCs therefore increasing immune protection [73].
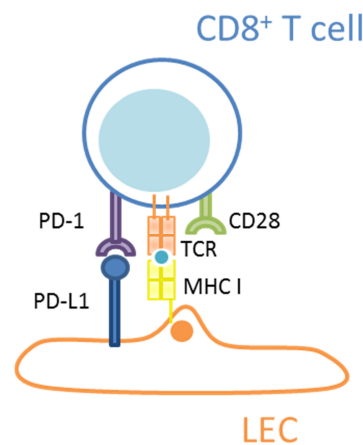

Figure 3.8: Schematic representation of tolerance induction by LECs. LECs present endogenous peripheral tissue antigens (PTAs) through MHC class I molecule to naïve CD8+ T cells. Expression of PD-L1 by LECs and absence of costimulatory molecules binding CD28 leads to T cell deletion. Modified after reference [74].

3.4.   Peripheral tissue LECs heterogeneity and function

Lymphatics in peripheral tissues are important for body fluid homeostasis and transport of antigens from the tissues to LN. Here I will describe some newly identified peripheral lymphatics as well as lymphatics with an essential function for the intestine, lungs and skin.

The ciliary body and the anterior segment of the eye contain lymphatic vessels while there is no vasculature in the cornea. The draining of aqueous humour is achieved by Schlemm's canal. Cells forming this vessel express Prox-1, integrin-α9, Vegfr3 and CCL21 therefore they have a lymphatic vessels phenotype. However, they do not express Lyve1 and gp38 [75,76].

It was thought for a long time that lymphatic vessels were absent from the brain. However, recent studies showed the presence of lymphatic vessels in the meninges. These vessels express Prox-1, Lyve1 and CCL21 and thus have a lymphatic capillary phenotype. They drain cerebrospinal fluid and allow transport of antigens and immune cells to the cervical LN [77,78].

The lung is an important organ for the defense against airborne particles and microbes. Moreover, lungs respond to injury or systemic changes by flooding of fluids. Thus lymphatic vasculature is essential for lungs to drain these fluids and keep the lungs dry. Moreover, lymph clears the substances entering the lung epithelium and enables pulmonary immune response. When the vessels are not needed because of low fluid volume in the lung, they are collapsed. When there is an increase in fluid volume the lymphatic vessels swell and increase in size [79].

Skin is also an important barrier to protect the body from external threats. The skin is composed of the epidermis, the dermis and a subcutaneous layer of adipose tissue. The lymphatic capillaries are found in the dermis where they allow entry of immune cells and antigens from the skin epithelium. Lymphatic vessels in the dermis are divided in two plexus. Lymph first enters the superficial plexus located in the dermal papillae and then flows vertically in the deep lymphatic plexus and larger collecting vessels that will finally bring the lymph to skin draining LN **(figure 3.9)** [8].
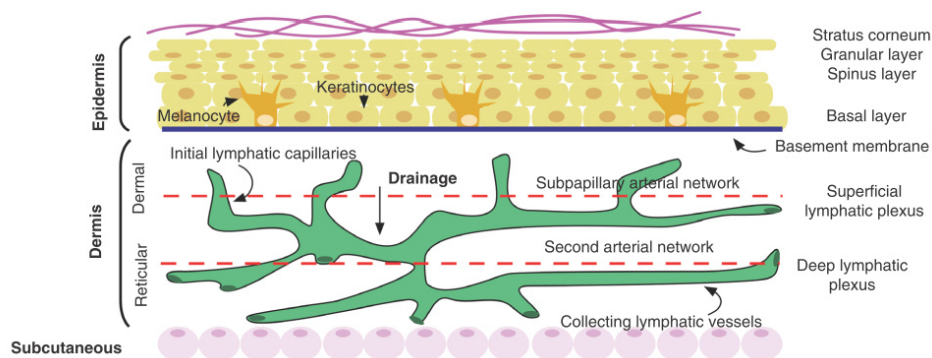

Figure 3.9: Skin lymphatic vasculature. Lymphatic vessels in the skin are located in the dermis. Two lymphatic plexus can be distinguished, the superficial lymphatic plexus in the dermis papillae and the deep lymphatic plexus located around the second arterial network. After reference [8].

The intestinal lymphatic system plays a particular role in fat absorption and metabolism as well as the intestinal immune response. There are two independent vessel networks in the intestine: lymphatics that drain the muscular layer of the intestine and the capillaries that drain the intestinal villi. The latter are called the lacteals **(figure 3.10)**. These networks connect to larger collecting vessels in the mesentery to join the mesenteric LN. The lacteals allow the uptake of chylomicrons,

huge triglyceride-loaded particles with a diameter up to 1µm. This mechanism leads to delivery of dietary fat to the blood. The mechanism is still not well understood but might involve intracellular transport across LECs as well as transport through intercellular junctions. In the lacteals, LECs are continuously proliferating even under steady state conditions and form a mix of button-like junctions and zipper-like junctions [80]. Lacteals are similar to dermal capillaries in the skin and express high levels of Lyve1 and CCL21 [16]. The lymphatic vessels in the intestinal villi and mucosa recruit tissue-derived DCs and enable them to reach mesenteric LNs. Intestinal lymphatics are crucial for induction of oral tolerance against food antigens and microbiota [81].
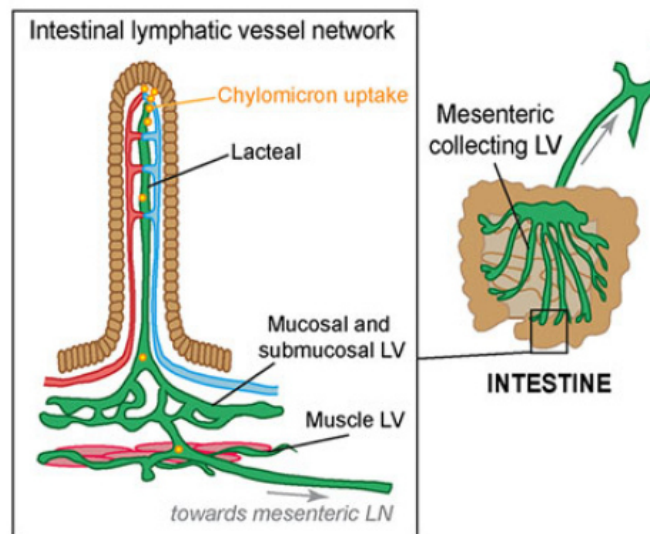
Figure 3.10: Representation of the lymphatic vessels in the intestine. Lacteals are specialized lymphatic capillaries of the intestine. They uptake chylomicrons, particles formed of dietary triglycerides. They also are responsible for the transport of antigens and immune cells to the mesenteric LN, playing a role both in oral tolerance and immune response against pathogens. The lymphatic vessels in the muscular part of the intestine form a separated network. LV: lymphatic vessel. Modified after reference [16].

Other lymphatic vessels outside the intestine also play a role in fat metabolism. Indeed, lymphatics are required for removal of cholesterol from the tissues and transport to the liver. Lymphatic capillaries express the HDL receptor SR-BI **(figure 3.2)**. This mechanism prevents atherosclerosis [16].

3.5. LECs in inflammation and pathological conditions

3.5.1   Role of LECs in inflammation

LECs express toll like receptors (TLR) as well as receptors for inflammatory cytokines such as IFN type I and II receptors and TNFR1 [36,82,83]. It was shown *in vitro* that stimulation of LECs with TLR agonists and TNFα induces production of chemokines [47,82–84]. These treatments also induce

upregulation of ICAM-1 and VCAM-1 promoting DCs adherence. However, this was not shown *in vivo* [82,83,85]. Inflammatory signals also increase the expression of CCR7 on DCs thus enhancing their recruitment to lymphatic vessels and entry in LN [4]. On the other hand, peripheral LECs express the atypical chemokine receptor D6 (ACKR2). This receptor binds inflammatory chemokines such as CCL2 and CCL5 thus limiting inflammatory leukocyte adhesion, preventing vessel congestion and improper circulation of APCs [86,87]. Increased ACKR2 expression was observed in inflammation-associated diseases such as psoriasis, chronic obstructive pulmonary diseases and inflammatory bowel disease [88].

Differentiation, proliferation and sprouting of LECs to form new vessels is called lymphangiogenesis. During inflammation, lymphangiogenesis is induced by different factors stimulating VEGFR2, VEGFR3 and LTβR expressed by LECs [89–91]. Inflammatory factors induce the NF-κB pathway in LECs leading to Prox-1 activation. Prox-1 in turn increases expression of VEGFR3 hence promoting lymphangiogenesis [92]. An interesting crosstalk have been demonstrated with macrophages modulating lymphangiogenesis during inflammation through secretion of growth factors such as VEGF-C/D and VEGF-A [93]. Scavenging of inflammatory chemokines by ACKR2 regulates the proximity of macrophages to lymphatic vessels thus controlling lymphatic vasculature density in inflammatory conditions [88]. Additionally, macrophages progenitors can transdifferentiate into Lyve-1 expressing LECs and participate in lymph vessels growth [92,94]. Lymphangiogenesis increases the lymph flow and participates in attracting innate and adaptive immune cells to support immune responses. Indeed, it was observed that increased fluid flow induces CCL21 secretion by LECs and higher expression of ICAM-1 and E-selectin on LECs surface [95]. In a synergistic mechanism, activation of CCR7 signaling in turn increases affinity of LFA-1 on DCs for ICAM-1 on LECs promoting DCs transmigration [96] (**figure 3.11**). Interaction between ICAM-1 and LFA-1 also increases T cells entrance and crawling inside lymph vessels [97]. During inflammation, lymphocytes accumulate leading to cellular expansion of the LN. When inflammation is prolonged and to return to steady state, lymphangiogenesis of the cortical and medullary sinuses promotes lymphocytes egress [98]. It was shown that IL-7 is produced by FRC and LEC and plays an important role in lymphatic vessel remodeling in a paracrine and autocrine manner [99,100]. To limit LN expansion, LECs can suppress T cell activation by DCs in inflammatory conditions (**figure 3.11**). ICAM-1 binds Mac1 on DCs which inhibits their maturation and consequently T cell activation [101]. Moreover, LECs secrete molecules suppressing T cell activation such as a indoleamine 2,3-dioxygenase (IDO) and nitric oxide (NO) in response to IFNγ or TNFα [68,102]. Therefore a negative regulatory loop between activated T cells in close contact with LECs limits activated T cells expansion in LNs during inflammation (**figure 3.11**). Finally, IFNγ produced by T cells also plays a role in regression of the lymphatic network after inflammation [94].
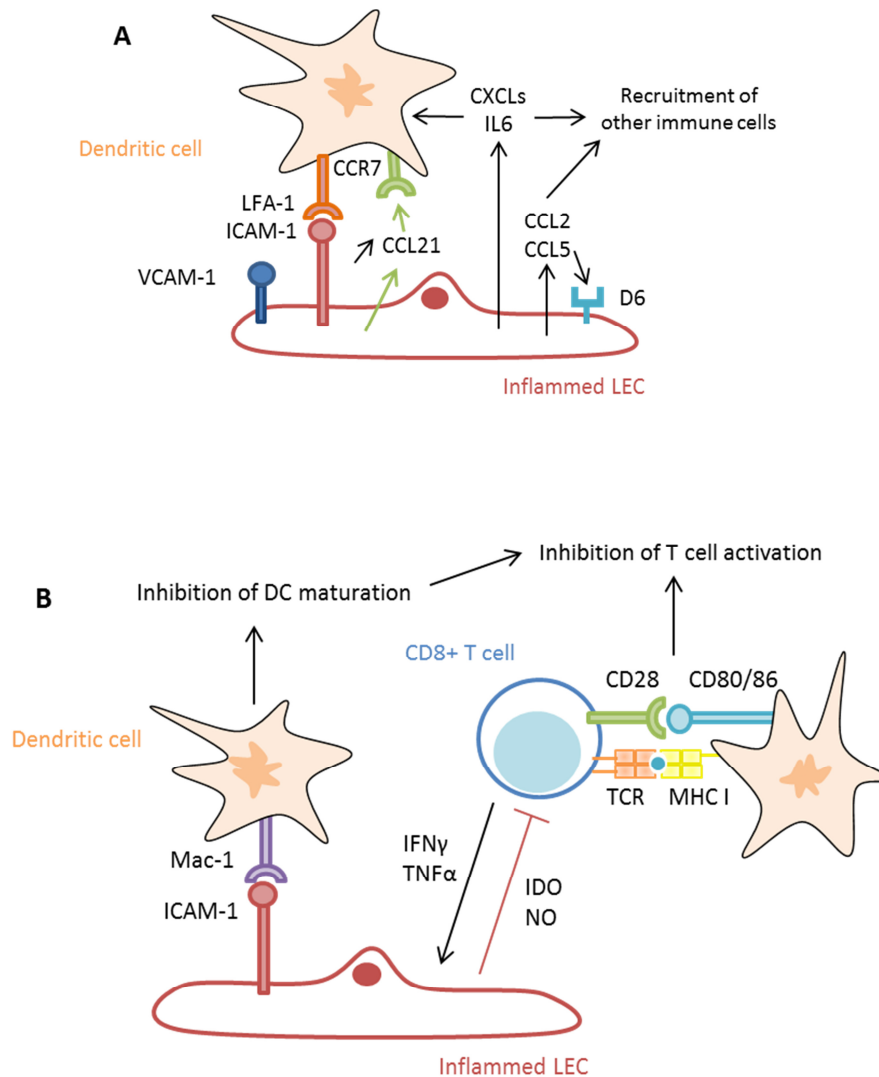
Figure 3.11: Role of inflammed LECs in recruitment of immune cells and control of T cell activation.
(A) Under inflammatory conditions LECs upregulate adhesion molecules such as VCAM-1 and ICAM-1 promoting recruitment of dendritic cells via binding to LFA-1. Increased expression of chemokines induces the recruitment of DCs and other immune subsets. D6 (ACKR2) acts as a decoy receptor to regulate adhesion of immune cells to LECs and prevent congestion of lymphatic vessels. **(B)** LECs also regulate the inflammatory process by suppressing T cell activation. ICAM-1 interacts with Mac-1 and inhibits maturation of DCs thus preventing activation of T cells by DCs. Pro-inflammatory cytokines (IFNγ, TNFα) induce the production of indoleamine 2,3-dioxygenase (IDO) and nitric oxide (NO) by LECs. These molecules suppress T cell activation. After reference [74].

Lymphangiogenesis also plays a role in clearance of immune cells from peripheral tissues in an inflammatory context. However, chronic inflammation can lead to aberrant accumulation of lymphocytes and formation of ectopic lymphoid structures called tertiary lymphoid organs (TLO). In these structures, expression of homeostatic chemokines favours a cellular organization similar to LNs, including formation of lymph vessels [92]. It was shown that IL-7 is required for early lymphatic vessel expansion in TLO [103]. Moreover, it was thought that LTα/β plays a role in development of

73

TLO. Targeting of LTβR pathway has prooved to be efficient in resolving these structure in autoimmune disease models and LTα overexpression leads to the formation of these stuctures [104–106]. However, in a mouse model of resolving TLO, a second wave of lymphangiogenesis was recently observed to depend of LTβR signaling and promotes egress of leukocytes from inflammed tissues and resorption of the ectopic lymphoid stuctures [103]. Lymphangiogenesis is thus required to resolve inflammatory TLO and targeting of LTβR pathway might not always be beneficial. On the other hand, ectopic expression of CCL21 by newly formed lymphatic vesssels can also promote recruitment of immune cells to the inflammed tissues and persistence of inflammatory process [92]. Maintenance of TLO can then be harmful as it is the case in autoimmune diseases and transplants rejection. Chronic inflammatory factors also promote lymphangiogenesis in dermal lymphatics and around islet cells in type 2 diabetes. This phenomenon contributes to impaired wound healing [94].

3.5.2   Role of LECs in Lymphedema

Lymphedema is forming when lymph is accumulating in peripheral tissues due to reduced capacity of transport by lymphatic vessels or too high volumes of lymph compared to transport capacity. This pathological condition induces susceptibility to infection, inflammation and fibrosis [4,107]. There are two types of lymphedema. The primary lymphedema is congenital and is due to failure of superficial or subcutaneous vessels in transporting the lymph back to the blood vasculature [107]. This congenital form of lymphedema appears in several diseases linked to mutations in genes including VEGFR-3, FOXC2, SOX18 and NEMO [4]. The latest is showing the importance of NF-κB signaling in LECs. The secondary lymphedema is a form of acquired lymphedema which has two main origins. The parasites *Wucheria bancrofti* and *Brugia malayi* are transmitted by mosquitoes bite and lead to development of lymphatic filariasis also called elephantiasis disease [108]. Moreover surgical ablation of LNs in cancers such as breast cancer can induce damage in surrounding lymphatic vessels leading to lymphedema [4]. There is currently no cure for lymphedema but VEGF-C, angiopoietin-1 and fibroblast growth factor 2 have been shown to induce beneficial effect in lymphedema animal models [109].

3.5.3   Role of LECs in cancers

Tumour cells and cells from the tumoral microenvironment produce growth factors including VEGF-C and VEGF-D which induce lymphangiogenesis. Induction of LEC proliferation and migration leads to enlargement of initial and collecting vessels around and inside tumours. Increased lymphangiogenesis is also observed in tumour-draining LNs. These phenomena promote cell entry in

the lymphatic vasculature thus spread of tumor cells in the body and metastasis [110]. In addition to VEGF-C and VEGF-D, other factors have been identified to play a role in tumor associated lymphangiogenesis. NRP2 blockage decreased LEC migration and tumour metastasis in animal models [111]. Moreover, prostaglandin increased lymphatic vessel formation and tumor dissemination [112]. On the other hand, TGF-β was shown to be a negative regulator of lymphangiogenesis in cancer [113]. Tumor-induced lymphangiogenesis also relies on interaction of LECs with the extracellular matrix. Indeed, LECs express integrin α4β1 which interact with fibronectin and induces lymph vessel growth [114]. LECs represent a heterogeneous population and tumour LECs have a distinct molecular profile from other normal and activated tissue LECs [115]. The mechanisms for this cell plasticity are not well understood to date. Furthermore, tumour cells express CCR7, CXCR4 and CCR8 thus enabling entry into lymphatics and the LN in the same way as immune cells [110]. Finally, presentation of tumor antigens by LECs can also have a tumor promoting effect. It was observed that LECs from tumor-draining LNs present tumor antigens via MHC-I and induce apoptosis of tumor-specific CD8$^+$ T cells [62]. Moreover, LECs from tumor-associated lymphatic vessels were shown to express PDL1 and play a role in T-cell inhibition [116].

Besides the many markers of lymphatic endothelium previously described, only Lyve1 and gp38 are currently used to monitor lymphatic vessels in tumour samples from patients [110]. Lymphatic remodeling and lymphangiogenesis has been shown to correlate with patient outcome. Therefore, targeting lymphangiogenesis is a strategy to decrease metastatic events and modulate immune response to cancer cells. Inhibitors of lymphangiogenesis promoting factors are already approved in some cancers and preclinical and clinical studies are still ongoing (for review see [110]).

3.6. <u>Conclusion</u>

Interstitial fluids leak from blood capillaries and are absorbed by lymphatic capillaries. Lymph is then transported to the LN through collecting vessels and brought back to the blood circulation via the thoracic duct. LNs are well organized lymphoid organs filtrating lymph. Antigens and APCs transit to the LN where presentation to T or B cells occurs. Therefore, LNs allow initiation and resolution of immune response as well as maintenance of tolerance. They are composed of immune cells and non-hematopoietic cells responsible for the architecture of the LN. LECs are forming the lymphatic vessels. They show a different phenotype depending on their localization in the tissues and in the LNs. As described in this chapter, LECs express multiple chemokines and adhesion molecules and play various roles in the peripheral tissues and LNs. LN LECs especially play a role in trafficking of DCs and T cells in and out of the LN. They express chemokines such as CCL21 attracting DCs. Moreover, LN

LECs present peripheral tissue antigens to T cells and induce tolerance. The expression of chemokines and adhesion molecules is inducible by inflammatory factors and can participate both in recruiting immune cells and regulating inflammation by suppressing T cell activation. Moreover, LECs proliferation and sprout leads to lymphangiogenesis that has beneficial and harmful effect. Indeed, formation of new lymphatic vessels is required for clearance of immune cells from inflamed tissues and return to steady-state in LN. However, lymphangiogenesis also promotes cancer dissemination. Several studies showed that LEC plasticity could be modulated as a treatment for lymphatic related diseases. However, the precise underlying mechanisms remain unknown. Overall, LECs were shown to interact with many cell types through direct contact or molecules secretions but further studies are required to understand the full potential of LECs.

As described in Chapter 2, RANK was shown to be expressed by endothelial cells from the blood vasculature but it is still not clear whether LECs express RANK. A first study from our group showed that RANKL overexpression in mice leads to activation of LECs with higher expression of MAdCAM-1 and VCAM1 [117]. Moreover, proliferation of LECs was induced in this animal model. Therefore, the detailed role of RANKL in modulating LECs phenotype and the consequences on LN cells function remains to be investigated more precisely.

3.7. References

1. Asellio G (1581-1626) A. De lactibus, sive lacteis venis, quarto vasorum mesaraicorum genere, novo invento Gasparis Asellii ... Dissertatio. Qua sententiæ anatomicæ multæ, vel perperam receptæ convelluntur, vel parum perceptæ illustrantur. Lugduni Batavorum, ex officinâ Johannis Maire, M D CXL.; 1640.

2. von Andrian UH, Mempel TR. Homing and cellular traffic in lymph nodes. Nat Rev Immunol. 2003;3: 867–878. doi:10.1038/nri1222

3. Oliver G. Lymphatic vasculature development. Nat Rev Immunol. 2004;4: 35–45. doi:10.1038/nri1258

4. Jurisic G, Detmar M. Lymphatic endothelium in health and disease. Cell Tissue Res. 2009;335: 97–108. doi:10.1007/s00441-008-0644-2

5. Jang JY, Koh YJ, Lee S-H, Lee J, Kim KH, Kim D, et al. Conditional ablation of LYVE-1+ cells unveils defensive roles of lymphatic vessels in intestine and lymph nodes. Blood. 2013;122: 2151–2161. doi:10.1182/blood-2013-01-478941

6. Cueni LN, Detmar M. New Insights into the Molecular Control of the Lymphatic Vascular System and its Role in Disease. J Invest Dermatol. 2006;126: 2167–2177. doi:10.1038/sj.jid.5700464

7. Baluk P, Fuxe J, Hashizume H, Romano T, Lashnits E, Butz S, et al. Functionally specialized junctions between endothelial cells of lymphatic vessels. J Exp Med. 2007;204: 2349–2362. doi:10.1084/jem.20062596

8. Lund AW, Medler TR, Leachman SA, Coussens LM. Lymphatic Vessels, Inflammation, and Immunity in Skin Cancer. Cancer Discov. 2016;6: 22–35. doi:10.1158/2159-8290.CD-15-0023

9. Pflicke H, Sixt M. Preformed portals facilitate dendritic cell entry into afferent lymphatic vessels. J Exp Med. 2009;206: 2925–2935. doi:10.1084/jem.20091739

10. Weber M, Hauschild R, Schwarz J, Moussion C, Vries I de, Legler DF, et al. Interstitial Dendritic Cell Guidance by Haptotactic Chemokine Gradients. Science. 2013;339: 328–332. doi:10.1126/science.1228456

11. Russo E, Teijeira A, Vaahtomeri K, Willrodt A-H, Bloch JS, Nitschké M, et al. Intralymphatic CCL21 Promotes Tissue Egress of Dendritic Cells through Afferent Lymphatic Vessels. Cell Rep. 2016;14: 1723–1734. doi:10.1016/j.celrep.2016.01.048

12. Bromley SK, Yan S, Tomura M, Kanagawa O, Luster AD. Recirculating Memory T Cells Are a Unique Subset of CD4+ T Cells with a Distinct Phenotype and Migratory Pattern. J Immunol. 2013;190: 970–976. doi:10.4049/jimmunol.1202805

13. Beauvillain C, Cunin P, Doni A, Scotet M, Jaillon S, Loiry M-L, et al. CCR7 is involved in the migration of neutrophils to lymph nodes. Blood. 2011;117: 1196–1204. doi:10.1182/blood-2009-11-254490

14. Kabashima K, Shiraishi N, Sugita K, Mori T, Onoue A, Kobayashi M, et al. CXCL12-CXCR4 Engagement Is Required for Migration of Cutaneous Dendritic Cells. Am J Pathol. 2007;171: 1249–1257. doi:10.2353/ajpath.2007.070225

15. Takamatsu H, Takegahara N, Nakagawa Y, Tomura M, Taniguchi M, Friedel RH, et al. Semaphorins guide the entry of dendritic cells into the lymphatics by activating myosin II. Nat Immunol. 2010;11: 594–600. doi:10.1038/ni.1885

16. Ulvmar MH, Mäkinen T. Heterogeneity in the lymphatic vascular system and its origin. Cardiovasc Res. 2016;111: 310–321. doi:10.1093/cvr/cvw175

17. Jurisic G, Detmar M. Lymphatic endothelium in health and disease. Cell Tissue Res. 2009;335: 97–108. doi:10.1007/s00441-008-0644-2

18. Bazigou E, Makinen T. Flow control in our vessels: vascular valves make sure there is no way back. Cell Mol Life Sci. 2013;70: 1055–1066. doi:10.1007/s00018-012-1110-6

19. Bazigou E, Xie S, Chen C, Weston A, Miura N, Sorokin L, et al. Integrin-α9 Is Required for Fibronectin Matrix Assembly during Lymphatic Valve Morphogenesis. Dev Cell. 2009;17: 175–186. doi:10.1016/j.devcel.2009.06.017

20. Norrmén C, Ivanov KI, Cheng J, Zangger N, Delorenzi M, Jaquet M, et al. FOXC2 controls formation and maturation of lymphatic collecting vessels through cooperation with NFATc1. J Cell Biol. 2009;185: 439–457. doi:10.1083/jcb.200901104

21. Kazenwadel J, Betterman KL, Chong C-E, Stokes PH, Lee YK, Secker GA, et al. GATA2 is required for lymphatic vessel valve development and maintenance. J Clin Invest. 2015;125: 2979–2994. doi:10.1172/JCI78888

22. Wigle JT, Oliver G. Prox1 Function Is Required for the Development of the Murine Lymphatic System. Cell. 1999;98: 769–778. doi:10.1016/S0092-8674(00)81511-1

23. Koltowska K, Lagendijk AK, Pichol-Thievend C, Fischer JC, Francois M, Ober EA, et al. Vegfc Regulates Bipotential Precursor Division and Prox1 Expression to Promote Lymphatic Identity in Zebrafish. Cell Rep. 2015;13: 1828–1841. doi:10.1016/j.celrep.2015.10.055

24. Astarita JL, Acton SE, Turley SJ. Podoplanin: emerging functions in development, the immune system, and cancer. Front Immunol. 2012;3. doi:10.3389/fimmu.2012.00283

25. Cueni LN, Chen L, Zhang H, Marino D, Huggenberger R, Alitalo A, et al. Podoplanin-Fc reduces lymphatic vessel formation in vitro and in vivo and causes disseminated intravascular coagulation when transgenically expressed in the skin. Blood. 2010;116: 4376–4384. doi:10.1182/blood-2010-04-278564

26. Bénézech C, Nayar S, Finney BA, Withers DR, Lowe K, Desanti GE, et al. CLEC-2 is required for development and maintenance of lymph nodes. Blood. 2014;123: 3200–3207. doi:10.1182/blood-2013-03-489286

27. Acton SE, Astarita JL, Malhotra D, Lukacs-Kornek V, Franz B, Hess PR, et al. Podoplanin-Rich Stromal Networks Induce Dendritic Cell Motility via Activation of the C-type Lectin Receptor CLEC-2. Immunity. 2012;37: 276–289. doi:10.1016/j.immuni.2012.05.022

28. Hess PR, Rawnsley DR, Jakus Z, Yang Y, Sweet DT, Fu J, et al. Platelets mediate lymphovenous hemostasis to maintain blood-lymphatic separation throughout life. J Clin Invest. 2014;124: 273–284. doi:10.1172/JCI70422

29. Banerji S, Ni J, Wang S-X, Clasper S, Su J, Tammi R, et al. LYVE-1, a New Homologue of the CD44 Glycoprotein, Is a Lymph-specific Receptor for Hyaluronan. J Cell Biol. 1999;144: 789–801. doi:10.1083/jcb.144.4.789

30. Mäkinen T, Adams RH, Bailey J, Lu Q, Ziemiecki A, Alitalo K, et al. PDZ interaction site in ephrinB2 is required for the remodeling of lymphatic vasculature. Genes Dev. 2005;19: 397–410. doi:10.1101/gad.330105

31. Harvey NL, Gordon EJ. Deciphering the roles of macrophages in developmental and inflammation stimulated lymphangiogenesis. Vasc Cell. 2012;4: 15. doi:10.1186/2045-824X-4-15

32. Ran S, Montgomery KE. Macrophage-Mediated Lymphangiogenesis: The Emerging Role of Macrophages as Lymphatic Endothelial Progenitors. Cancers. 2012;4: 618–657. doi:10.3390/cancers4030618

33. Grigorova IL, Schwab SR, Phan TG, Pham THM, Okada T, Cyster JG. Cortical sinus probing, S1P1-dependent entry and flow-based capture of egressing T cells. Nat Immunol. 2009;10: 58–65. doi:10.1038/ni.1682

34. Furuya M, Kirschbaum SB, Paulovich A, Pauli BU, Zhang H, Alexander JS, et al. Lymphatic endothelial mCLCA1 is a ligand for leukocyte LFA-1 and Mac-1. J Immunol Baltim Md 1950. 2010;185: 5769–5777. doi:10.4049/jimmunol.1002226

35. Prevo R, Banerji S, Ferguson DJP, Clasper S, Jackson DG. Mouse LYVE-1 Is an Endocytic Receptor for Hyaluronan in Lymphatic Endothelium. J Biol Chem. 2001;276: 19420–19430. doi:10.1074/jbc.M011004200

36. Malhotra D, Fletcher AL, Astarita J, Lukacs-Kornek V, Tayalia P, Gonzalez SF, et al. Transcriptional profiling of stroma from inflamed and resting lymph nodes defines immunological hallmarks. Nat Immunol. 2012;13: 499–510. doi:10.1038/ni.2262

37. Lefkovits J, Plow EF, Topol EJ. Platelet Glycoprotein IIb/IIIa Receptors in Cardiovascular Medicine. N Engl J Med. 1995;332: 1553–1559. doi:10.1056/NEJM199506083322306

38. Liu L, Shi G-P. CD31: beyond a marker for endothelial cells. Cardiovasc Res. 2012;94: 3–5. doi:10.1093/cvr/cvs108

39. Willard-Mack CL. Normal Structure, Function, and Histology of Lymph Nodes. Toxicol Pathol. 2006;34: 409–424. doi:10.1080/01926230600867727

40. Standring S. Gray's Anatomy: The Anatomical Basis of Clinical Practice. Elsevier Health Sciences; 2015.

41. Junt T, Scandella E, Ludewig B. Form follows function: lymphoid tissue microarchitecture in antimicrobial immune defence. Nat Rev Immunol. 2008;8: 764–775. doi:10.1038/nri2414

42. Katakai T. Marginal reticular cells: a stromal subset directly descended from the lymphoid tissue organizer. Front Immunol. 2012;3. doi:10.3389/fimmu.2012.00200

43. Katakai T, Suto H, Sugai M, Gonda H, Togawa A, Suematsu S, et al. Organizer-Like Reticular Stromal Cell Layer Common to Adult Secondary Lymphoid Organs. J Immunol. 2008;181: 6189–6200. doi:10.4049/jimmunol.181.9.6189

44. Mueller SN, Germain RN. Stromal cell contributions to the homeostasis and functionality of the immune system. Nat Rev Immunol. 2009;9: 618–629. doi:10.1038/nri2588

45. Turley SJ, Fletcher AL, Elpek KG. The stromal and haematopoietic antigen-presenting cells that reside in secondary lymphoid organs. Nat Rev Immunol. 2010;10: 813–825. doi:10.1038/nri2886

46. Koning JJ, Mebius RE. Interdependence of stromal and immune cells for lymph node function. Trends Immunol. 2012;33: 264–270. doi:10.1016/j.it.2011.10.006

47. Link A, Vogt TK, Favre S, Britschgi MR, Acha-Orbea H, Hinz B, et al. Fibroblastic reticular cells in lymph nodes regulate the homeostasis of naive T cells. Nat Immunol. 2007;8: 1255–1265. doi:10.1038/ni1513

48. Gretz JE, Norbury CC, Anderson AO, Proudfoot AEI, Shaw S. Lymph-Borne Chemokines and Other Low Molecular Weight Molecules Reach High Endothelial Venules via Specialized Conduits While a Functional Barrier Limits Access to the Lymphocyte Microenvironments in Lymph Node Cortex. J Exp Med. 2000;192: 1425–1440. doi:10.1084/jem.192.10.1425

49. Rantakari P, Auvinen K, Jäppinen N, Kapraali M, Valtonen J, Karikoski M, et al. The endothelial protein PLVAP in lymphatics controls the entry of lymphocytes and antigens into lymph nodes. Nat Immunol. 2015;16: 386–396. doi:10.1038/ni.3101

50. Tal O, Lim HY, Gurevich I, Milo I, Shipony Z, Ng LG, et al. DC mobilization from the skin requires docking to immobilized CCL21 on lymphatic endothelium and intralymphatic crawling. J Exp Med. 2011;208: 2141–2153. doi:10.1084/jem.20102392

51. Braun A, Worbs T, Moschovakis GL, Halle S, Hoffmann K, Bölter J, et al. Afferent lymph-derived T cells and DCs use different chemokine receptor CCR7-dependent routes for entry into the lymph node and intranodal migration. Nat Immunol. 2011;12: 879–887. doi:10.1038/ni.2085

52. Ulvmar MH, Werth K, Braun A, Kelay P, Hub E, Eller K, et al. The atypical chemokine receptor CCRL1 shapes functional CCL21 gradients in lymph nodes. Nat Immunol. 2014;15: 623–630. doi:10.1038/ni.2889

53. Qu C, Edwards EW, Tacke F, Angeli V, Llodrá J, Sanchez-Schmitz G, et al. Role of CCR8 and Other Chemokine Pathways in the Migration of Monocyte-derived Dendritic Cells to Lymph Nodes. J Exp Med. 2004;200: 1231–1241. doi:10.1084/jem.20032152

54. Iftakhar-E-Khuda I, Fair-Mäkelä R, Kukkonen-Macchi A, Elima K, Karikoski M, Rantakari P, et al. Gene-expression profiling of different arms of lymphatic vasculature identifies candidates for manipulation of cell traffic. Proc Natl Acad Sci. 2016;113: 10643–10648. doi:10.1073/pnas.1602357113

55. Rouhani SJ, Eccles JD, Tewalt EF, Engelhard VH. Regulation of T-cell Tolerance by Lymphatic Endothelial Cells. J Clin Cell Immunol. 2014;5. doi:10.4172/2155-9899.1000242

56. Pham THM, Baluk P, Xu Y, Grigorova I, Bankovich AJ, Pappu R, et al. Lymphatic endothelial cell sphingosine kinase activity is required for lymphocyte egress and lymphatic patterning. J Exp Med. 2010;207: 17–27. doi:10.1084/jem.20091619

57. Pappu R, Schwab SR, Cornelissen I, Pereira JP, Regard JB, Xu Y, et al. Promotion of Lymphocyte Egress into Blood and Lymph by Distinct Sources of Sphingosine-1-Phosphate. Science. 2007;316: 295–298. doi:10.1126/science.1139221

58. Matloubian M, Lo CG, Cinamon G, Lesneski MJ, Xu Y, Brinkmann V, et al. Lymphocyte egress from thymus and peripheral lymphoid organs is dependent on S1P receptor 1. Nature. 2004;427: 355–360. doi:10.1038/nature02284

59. Ito K, Morimoto J, Kihara A, Matsui Y, Kurotaki D, Kanayama M, et al. Integrin α9 on lymphatic endothelial cells regulates lymphocyte egress. Proc Natl Acad Sci. 2014;111: 3080–3085. doi:10.1073/pnas.1311022111

60. Irjala H, Johansson E-L, Grenman R, Alanen K, Salmi M, Jalkanen S. Mannose Receptor Is a Novel Ligand for L-Selectin and Mediates Lymphocyte Binding to Lymphatic Endothelium. J Exp Med. 2001;194: 1033–1042.

61. Irjala H, Elima K, Johansson E-L, Merinen M, Kontula K, Alanen K, et al. The same endothelial receptor controls lymphocyte traffic both in vascular and lymphatic vessels. Eur J Immunol. 2003;33: 815–824. doi:10.1002/eji.200323859

62. Lund AW, Duraes FV, Hirosue S, Raghavan VR, Nembrini C, Thomas SN, et al. VEGF-C Promotes Immune Tolerance in B16 Melanomas and Cross-Presentation of Tumor Antigen by Lymph Node Lymphatics. Cell Rep. 2012;1: 191–199. doi:10.1016/j.celrep.2012.01.005

63. Cohen JN, Guidi CJ, Tewalt EF, Qiao H, Rouhani SJ, Ruddell A, et al. Lymph node–resident lymphatic endothelial cells mediate peripheral tolerance via Aire-independent direct antigen presentation. J Exp Med. 2010;207: 681–688. doi:10.1084/jem.20092465

64. Tewalt EF, Cohen JN, Rouhani SJ, Guidi CJ, Qiao H, Fahl SP, et al. Lymphatic endothelial cells induce tolerance via PD-L1 and lack of costimulation leading to high-level PD-1 expression on CD8 T cells. Blood. 2012;120: 4772–4782. doi:10.1182/blood-2012-04-427013

65. Amatschek S, Kriehuber E, Bauer W, Reininger B, Meraner P, Wolpl A, et al. Blood and lymphatic endothelial cell-specific differentiation programs are stringently controlled by the tissue environment. Blood. 2007;109: 4777–4785. doi:10.1182/blood-2006-10-053280

66. Tripp CH, Haid B, Flacher V, Sixt M, Peter H, Farkas J, et al. The lymph vessel network in mouse skin visualised with antibodies against the hyaluronan receptor LYVE-1. Immunobiology. 2008;213: 715–728. doi:10.1016/j.imbio.2008.07.025

67. Rouhani SJ, Eccles JD, Riccardi P, Peske JD, Tewalt EF, Cohen JN, et al. Roles of lymphatic endothelial cells expressing peripheral tissue antigens in CD4 T-cell tolerance induction. Nat Commun. 2015;6: 6771. doi:10.1038/ncomms7771

68. Nörder M, Gutierrez MG, Zicari S, Cervi E, Caruso A, Guzmán CA. Lymph node-derived lymphatic endothelial cells express functional costimulatory molecules and impair dendritic cell-induced allogenic T-cell proliferation. FASEB J. 2012;26: 2835–2846. doi:10.1096/fj.12-205278

69. Cohen JN, Tewalt EF, Rouhani SJ, Buonomo EL, Bruce AN, Xu X, et al. Tolerogenic Properties of Lymphatic Endothelial Cells Are Controlled by the Lymph Node Microenvironment. PLoS ONE. 2014;9: e87740. doi:10.1371/journal.pone.0087740

70. Tewalt EF, Cohen JN, Rouhani SJ, Engelhard VH. Lymphatic endothelial cells - key players in regulation of tolerance and immunity. Front Immunol. 2012;3. doi:10.3389/fimmu.2012.00305

71. Fletcher AL, Lukacs-Kornek V, Reynoso ED, Pinner SE, Bellemare-Pelletier A, Curry MS, et al. Lymph node fibroblastic reticular cells directly present peripheral tissue antigen under steady-state and inflammatory conditions. J Exp Med. 2010;207: 689–697. doi:10.1084/jem.20092642

72. Koble C, Kyewski B. The thymic medulla: a unique microenvironment for intercellular self-antigen transfer. J Exp Med. 2009;206: 1505–1513. doi:10.1084/jem.20082449

73. Tamburini BA, Burchill MA, Kedl RM. Antigen capture and archiving by lymphatic endothelial cells following vaccination or viral infection. Nat Commun. 2014;5: 3989. doi:10.1038/ncomms4989

74. Card CM, Yu SS, Swartz MA. Emerging roles of lymphatic endothelium in regulating adaptive immunity. J Clin Invest. 2014;124: 943–952. doi:10.1172/JCI73316

75. Aspelund A, Tammela T, Antila S, Nurmi H, Leppänen V-M, Zarkada G, et al. The Schlemm's canal is a VEGF-C/VEGFR-3–responsive lymphatic-like vessel. J Clin Invest. 2014;124: 3975–3986. doi:10.1172/JCI75395

76. Park D-Y, Lee J, Park I, Choi D, Lee S, Song S, et al. Lymphatic regulator PROX1 determines Schlemm's canal integrity and identity. J Clin Invest. 2014;124: 3960–3974. doi:10.1172/JCI75392

77. Aspelund A, Antila S, Proulx ST, Karlsen TV, Karaman S, Detmar M, et al. A dural lymphatic vascular system that drains brain interstitial fluid and macromolecules. J Exp Med. 2015;212: 991–999. doi:10.1084/jem.20142290

78. Louveau A, Smirnov I, Keyes TJ, Eccles JD, Rouhani SJ, Peske JD, et al. Structural and functional features of central nervous system lymphatic vessels. Nature. 2015;523: 337–341. doi:10.1038/nature14432

79. Schraufnagel DE. Lung lymphatic anatomy and correlates. Pathophysiology. 2010;17: 337–343. doi:10.1016/j.pathophys.2009.10.008

80. Bernier-Latmani J, Cisarovsky C, Demir CS, Bruand M, Jaquet M, Davanture S, et al. DLL4 promotes continuous adult intestinal lacteal regeneration and dietary fat transport. J Clin Invest. 2015;125: 4572–4586. doi:10.1172/JCI82045

81. Pabst O, Mowat AM. Oral tolerance to food protein. Mucosal Immunol. 2012;5: 232–239. doi:10.1038/mi.2012.4

82. Pegu A, Qin S, Junecko BAF, Nisato RE, Pepper MS, Reinhart TA. Human Lymphatic Endothelial Cells Express Multiple Functional TLRs. J Immunol. 2008;180: 3399–3405. doi:10.4049/jimmunol.180.5.3399

83. Garrafa E, Imberti L, Tiberio G, Prandini A, Giulini SM, Caimi L. Heterogeneous expression of toll-like receptors in lymphatic endothelial cells derived from different tissues. Immunol Cell Biol. 2011;89: 475–481. doi:10.1038/icb.2010.111

84. Kataru RP, Kim H, Jang C, Choi DK, Koh BI, Kim M, et al. T Lymphocytes Negatively Regulate Lymph Node Lymphatic Vessel Formation. Immunity. 2011;34: 96–107. doi:10.1016/j.immuni.2010.12.016

85. Sawa Y, Ueki T, Hata M, Iwasawa K, Tsuruga E, Kojima H, et al. LPS-induced IL-6, IL-8, VCAM-1, and ICAM-1 Expression in Human Lymphatic Endothelium. J Histochem Cytochem. 2008;56: 97–109. doi:10.1369/jhc.7A7299.2007

86. Lee KM, McKimmie CS, Gilchrist DS, Pallas KJ, Nibbs RJ, Garside P, et al. D6 facilitates cellular migration and fluid flow to lymph nodes by suppressing lymphatic congestion. Blood. 2011;118: 6220–6229. doi:10.1182/blood-2011-03-344044

87. Graham GJ. D6 and the atypical chemokine receptor family: Novel regulators of immune and inflammatory processes. Eur J Immunol. 2009;39: 342–351. doi:10.1002/eji.200838858

88. Bonavita O, Mollica Poeta V, Setten E, Massara M, Bonecchi R. ACKR2: An Atypical Chemokine Receptor Regulating Lymphatic Biology. Front Immunol. 2017;7. doi:10.3389/fimmu.2016.00691

89. Kim KE, Koh Y-J, Jeon B-H, Jang C, Han J, Kataru RP, et al. Role of CD11b+ Macrophages in Intraperitoneal Lipopolysaccharide-Induced Aberrant Lymphangiogenesis and Lymphatic Function in the Diaphragm. Am J Pathol. 2009;175: 1733–1745. doi:10.2353/ajpath.2009.090133

90. Flister MJ, Wilber A, Hall KL, Iwata C, Miyazono K, Nisato RE, et al. Inflammation induces lymphangiogenesis through up-regulation of VEGFR-3 mediated by NF-κB and Prox1. Blood. 2010;115: 418–429. doi:10.1182/blood-2008-12-196840

91. Mounzer RH, Svendsen OS, Baluk P, Bergman CM, Padera TP, Wiig H, et al. Lymphotoxin-alpha contributes to lymphangiogenesis. Blood. 2010;116: 2173–2182. doi:10.1182/blood-2009-12-256065

92. Buckley CD, Barone F, Nayar S, Bénézech C, Caamaño J. Stromal cells in chronic inflammation and tertiary lymphoid organ formation. Annu Rev Immunol. 2015;33: 715–745. doi:10.1146/annurev-immunol-032713-120252

93. Ji R-C. Macrophages are important mediators of either tumor- or inflammation-induced lymphangiogenesis. Cell Mol Life Sci. 2011;69: 897–914. doi:10.1007/s00018-011-0848-6

94. Kim H, Kataru RP, Koh GY. Inflammation-associated lymphangiogenesis: a double-edged sword? J Clin Invest. 2014;124: 936–942. doi:10.1172/JCI71607

95. Miteva DO, Rutkowski JM, Dixon JB, Kilarski W, Shields JD, Swartz MA. Transmural Flow Modulates Cell and Fluid Transport Functions of Lymphatic Endothelium. Circ Res. 2010;106: 920–931. doi:10.1161/CIRCRESAHA.109.207274

96. Eich C, de Vries IJM, Linssen PC, de Boer A, Boezeman JB, Figdor CG, et al. The lymphoid chemokine CCL21 triggers LFA-1 adhesive properties on human dendritic cells. Immunol Cell Biol. 2011;89: 458–465. doi:10.1038/icb.2010.103

97. Teijeira A, Hunter MC, Russo E, Proulx ST, Frei T, Debes GF, et al. T Cell Migration from Inflamed Skin to Draining Lymph Nodes Requires Intralymphatic Crawling Supported by ICAM-1/LFA-1 Interactions. Cell Rep. 2017;18: 857–865. doi:10.1016/j.celrep.2016.12.078

98. Tan KW, Yeo KP, Wong FHS, Lim HY, Khoo KL, Abastado J-P, et al. Expansion of Cortical and Medullary Sinuses Restrains Lymph Node Hypertrophy during Prolonged Inflammation. J Immunol. 2012;188: 4065–4080. doi:10.4049/jimmunol.1101854

99. Onder L, Narang P, Scandella E, Chai Q, Iolyeva M, Hoorweg K, et al. IL-7–producing stromal cells are critical for lymph node remodeling. Blood. 2012;120: 4675–4683. doi:10.1182/blood-2012-03-416859

100. Iolyeva M, Aebischer D, Proulx ST, Willrodt A-H, Ecoiffier T, Häner S, et al. Interleukin-7 is produced by afferent lymphatic vessels and supports lymphatic drainage. Blood. 2013;122: 2271–2281. doi:10.1182/blood-2013-01-478073

101. Podgrabinska S, Kamalu O, Mayer L, Shimaoka M, Snoeck H, Randolph GJ, et al. Inflamed lymphatic endothelium suppresses dendritic cell maturation and function via Mac–/ICAM-1-dependent mechanism. J Immunol Baltim Md 1950. 2009;183: 1767–1779. doi:10.4049/jimmunol.0802167

102. Lukacs-Kornek V, Malhotra D, Fletcher AL, Acton SE, Elpek KG, Tayalia P, et al. Regulated release of nitric oxide by nonhematopoietic stroma controls expansion of the activated T cell pool in lymph nodes. Nat Immunol. 2011;12: 1096–1104. doi:10.1038/ni.2112

103. Nayar S, Campos J, Chung MM, Navarro-Núñez L, Chachlani M, Steinthal N, et al. Bimodal Expansion of the Lymphatic Vessels Is Regulated by the Sequential Expression of IL-7 and Lymphotoxin α1β2 in Newly Formed Tertiary Lymphoid Structures. J Immunol Author Choice. 2016;197: 1957–1967. doi:10.4049/jimmunol.1500686

104. Gatumu MK, Skarstein K, Papandile A, Browning JL, Fava RA, Bolstad AI. Blockade of lymphotoxin-beta receptor signaling reduces aspects of Sjögren's syndrome in salivary glands of non-obese diabetic mice. Arthritis Res Ther. 2009;11: R24. doi:10.1186/ar2617

105. Lee Y, Chin RK, Christiansen P, Sun Y, Tumanov AV, Wang J, et al. Recruitment and Activation of Naive T Cells in the Islets by Lymphotoxin β Receptor-Dependent Tertiary Lymphoid Structure. Immunity. 2006;25: 499–509. doi:10.1016/j.immuni.2006.06.016

106. Remouchamps C, Boutaffala L, Ganeff C, Dejardin E. Biology and signal transduction pathways of the Lymphotoxin-αβ/LTβR system. Cytokine Growth Factor Rev. 2011;22: 301–310. doi:10.1016/j.cytogfr.2011.11.007

107. Ji RC. Characteristics of lymphatic endothelial cells in physiological and pathological conditions. Histol Histopathol. 2005;20: 155–175.

108. Melrose WD. Lymphatic filariasis: new insights into an old disease. Int J Parasitol. 2002;32: 947–960. doi:10.1016/S0020-7519(02)00062-0

109. Saito Y, Nakagami H, Kaneda Y, Morishita R. Lymphedema and Therapeutic Lymphangiogenesis. BioMed Res Int. 2013;2013. doi:10.1155/2013/804675

110. Stacker SA, Williams SP, Karnezis T, Shayan R, Fox SB, Achen MG. Lymphangiogenesis and lymphatic vessel remodelling in cancer. Nat Rev Cancer. 2014;14: 159–172. doi:10.1038/nrc3677

111. Caunt M, Mak J, Liang W-C, Stawicki S, Pan Q, Tong RK, et al. Blocking Neuropilin-2 Function Inhibits Tumor Cell Metastasis. Cancer Cell. 2008;13: 331–342. doi:10.1016/j.ccr.2008.01.029

112. Karnezis T, Shayan R, Caesar C, Roufail S, Harris NC, Ardipradja K, et al. VEGF-D Promotes Tumor Metastasis by Regulating Prostaglandins Produced by the Collecting Lymphatic Endothelium. Cancer Cell. 2012;21: 181–195. doi:10.1016/j.ccr.2011.12.026

113. Oka M, Iwata C, Suzuki HI, Kiyono K, Morishita Y, Watabe T, et al. Inhibition of endogenous TGF-β signaling enhances lymphangiogenesis. Blood. 2008;111: 4571–4579. doi:10.1182/blood-2007-10-120337

114. Garmy-Susini B, Avraamides CJ, Schmid MC, Foubert P, Ellies LG, Barnes L, et al. Integrin α4β1 signaling is required for lymphangiogenesis and tumor metastasis. Cancer Res. 2010;70: 3042–3051. doi:10.1158/0008-5472.CAN-09-3761

115. Clasper S, Royston D, Baban D, Cao Y, Ewers S, Butz S, et al. A Novel Gene Expression Profile in Lymphatics Associated with Tumor Growth and Nodal Metastasis. Cancer Res. 2008;68: 7293–7303. doi:10.1158/0008-5472.CAN-07-6506

116. Dieterich LC, Ikenberg K, Cetintas T, Kapaklikaya K, Hutmacher C, Detmar M. Tumor-Associated Lymphatic Vessels Upregulate PDL1 to Inhibit T-Cell Activation. Front Immunol. 2017;8. doi:10.3389/fimmu.2017.00066

117. Hess E, Duheron V, Decossas M, Lézot F, Berdal A, Chea S, et al. RANKL Induces Organized Lymph Node Growth by Stromal Cell Proliferation. J Immunol. 2012;188: 1245–1254. doi:10.4049/jimmunol.1101513

Chapter 4: CD169^{+} macrophages in secondary lymphoid tissues and beyond

Macrophages are highly phagocytic cells that internalize and degrade pathogens and particulate antigens. In the XIXth century, Metchnikoff discovered these cells and named them macrophages from the Greek "large eaters" [1]. Macrophages were classified based on their ontogeny and phagocytic properties in what is called the mononuclear phagocytic system [2]. They are characterised by their dependence on colony stimulating factor-1 (CSF-1) [3,4] and the expression of the integrin CD11b (also called Mac1) [5]. They are present in tissue where they acquire specialized properties according to the function of their tissue of residence. Therefore, there is a great heterogeneity among the macrophage population. In some tissues, macrophages represent 10-15% of the total cell number [6]. In this chapter, I will focus on CD169^{+} macrophages, a subtype of macrophages with a great plasticity. This cell type plays an important role in secondary lymphoid tissues such as lymph nodes (LN) and spleen but also in other tissues.

4.1. Characteristics of macrophages in secondary lymphoid tissues

4.1.1 Phenotypic markers of lymphoid tissues macrophages

In addition to CD11b, several markers are used to define lymphoid tissues macrophages.

CD169 is also called sialoadhesin or sialic acid binding lectin 1 (siglec-1). It is part of the sialic acid binding immunoglobulin-like lectin (Siglec) family that contains 17 Ig domains in the extracellular region. This molecule does not have a tyrosine-based signaling motif as other members of the family. Therefore, CD169 plays a role in cell-cell interactions rather than signaling. CD169 on macrophages enables the interaction with other immune cells or microbial particles both in a sialic acid dependent and a sialic acid independent binding manner [7]. CD169 can also mediate endocytosis of toxins and antigens [8,9].

F4/80 has 7 transmembrane EGF-like domains. It is thus part of the EGF-TM7 family of molecules, members of a G Protein coupled receptors (GPCR) subfamily: the adhesion-GPCRs. Present on murine macrophages, it has both an adhesion and a signaling role, however the exact signaling mechanism remains to be discovered [10].

Other markers such as SIGN-R1, MARCO, the mannose receptor (MR) CD206 and CD68 are also used to characterize macrophages from lymphoid tissues. SIGN-R1 is a type II C-type lectin homologous to human DC-SIGN [11]. This protein binds mannose and fucose and is therefore essential for pathogen

recognition. The class A scavenger receptor MARCO is a type II transmembrane collagenous protein. This receptor plays a role in phagocytosis and endocytosis of pathogens [12,13] but also in adhesion of macrophages to B cells [14]. MR is a lectin-like endocytic receptor that recognizes several viruses and parasites. Ligands for the cystein-rich domain of MR (MR-L) are also used as markers of LN and splenic macrophages [15]. Finally, the glycoprotein CD68 is a pan macrophages marker [15].

The use of these markers and the localization of macrophages in lymphoid tissues allowed the characterization of different resident macrophage populations in LNs and spleen. They will be described in the next paragraphs.

4.1.2   LN macrophages

a)   Subcapsular sinus macrophages (SSM)

Macrophages located below the LN subcapsular sinus were identified in early studies as poorly phagocytic cells which can quickly capture small amounts of lymph-borne antigens [16,17]. They are called SSMs that refers to Subcapsular Sinus Macrophages. It was discovered later that these cells express low levels of lysosomal proteins, explaining the poor degradative activity of SSM [18].

SSMs are characterised as $CD169^{hi}CD11c^{lo}CD11b^{+}F4/80^{-}$ cells [18] and also express ligands for the cysteine-rich domain of MR (MR-L) [19]. These cells are lining the border to the B cell follicles and appear intercalated between the floor lymphatic endothelial cells. They capture particulate antigens from the lymph and transfer them to follicular B cells [18,20–22] . Moreover, SSM express VCAM-1 and ICAM-1 [20]. Knowing that these adhesion molecules play a role in B cells adhesion and formation of immunological synapse [23], this could contribute to antigen transfer to B cells.

b)   Medullary sinus macrophages (MSM)

Macrophages associated with the LN medullary sinus walls were also identified in early studies [24]. They are called MSMs for Medullary Sinus Macrophages. They are highly phagocytic and can acquire large amounts of antigens [17,24,25]. They also express higher amounts of lysosomal proteins such as LAMP-1 and 2 compared to SSMs [18]. Their poor selectivity allows them to take up any particulate antigen [26]. A proof of the more active phagocytic activity compared to SSMs is that MSMs disappear before SSM after dichloromethylene diphosphonate (CI2MDP)-containing liposome treatment [27]. MSMs also play an important role in survival and clearance of short lived plasma cells [15].

In addition to CD169 marker, MSM are characterised by the expression of F4/80, they are therefore labeled as CD169^{hi}CD11c^{lo}CD11b^{+}F4/80^{+} cells [18]. However, some studies depicted them as expressing lower levels of CD169 than SSM [28]. MSM also express the C-type lectin SIGN-R1, the class A scavenger receptor MARCO, MR and LYVE-1 [3,15]. Overall, MSMs harbour a more mature macrophage phenotype compared to SSMs.

c)   Medullary cord macrophages (MCM)

Medullary cord macrophages (MCM) are located in the parenchyma surrounding medullary sinuses of the LNs called the medullary cord. They do not express CD169 but express the macrophages markers CD11b and F4/80 and are therefore characterized as CD169^{-}CD11c^{lo}CD11b^{+}F4/80^{+} cells [3,18]. MCM have a lower phagocytic activity than MSM as they contain smaller lysosomes [25]. These macrophages are mainly responsible for the clearance of apoptotic plasma cells [3].

d)   Interfollicular macrophages

The interfollicular region, situated between B cell follicles shows a great heterogeneity regarding macrophage populations. SSMs are able to penetrate this region but cells showing the same characteristics as MSMs (SIGN-R1, MARCO, F4/80 expression) are also present. In 2002, Geijtenbeek and colleagues observed heterogeneous expression of SIGN-R1 in the subcapsular area which appears to be in this interfollicular region [11]. The role of macrophages in this region remains to be investigated in more details but they seem also to play a role in antigen transfer to B cells and DCs [3].
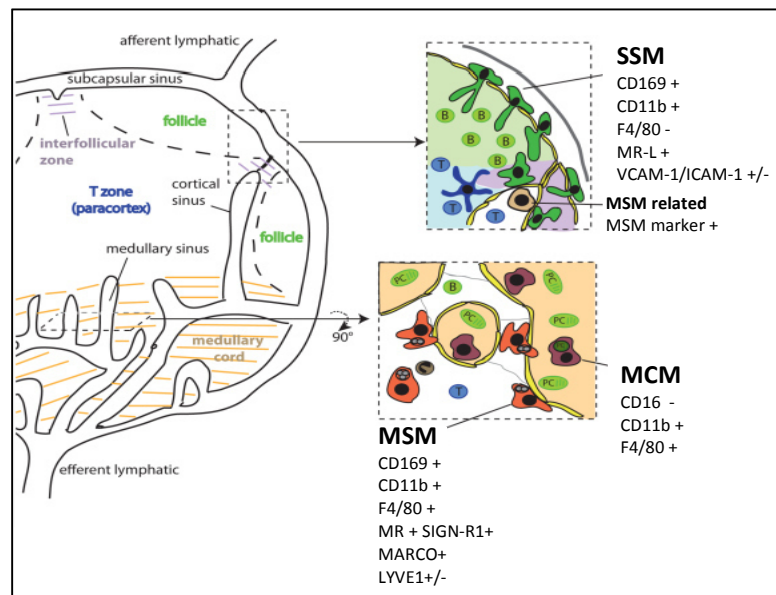
Figure 4.1: Localization and characteristics of LN macrophage populations. Subcapsular sinus macrophages (SSM) lie in the floor of the subcapsular sinus between lymphatic endothelial cells surrounding the B cell follicle. Medullary sinus macrophages (MSM) and medullary cord macrophages (MCM) are found in the LN medulla. Interfollicular regions contain both SSM and macrophages with the same characteristics as MSM. Characteristic markers of each population are indicated. Modified after reference [3].

4.1.3   Splenic macrophages

The main function of the spleen is to filter blood allowing the clearance of apoptotic erythrocytes and the elimination of pathogens. The spleen is divided into two parts: the red pulp containing erythrocytes and the white pulp containing lymphocytes. The border between the red pulp and the white pulp is called the marginal zone. This zone represents an important transit area for cells coming from blood flow and entering the white pulp [29]. Macrophage populations are found in the different areas of the spleen and will be described in this paragraph (**figure 4.2**).
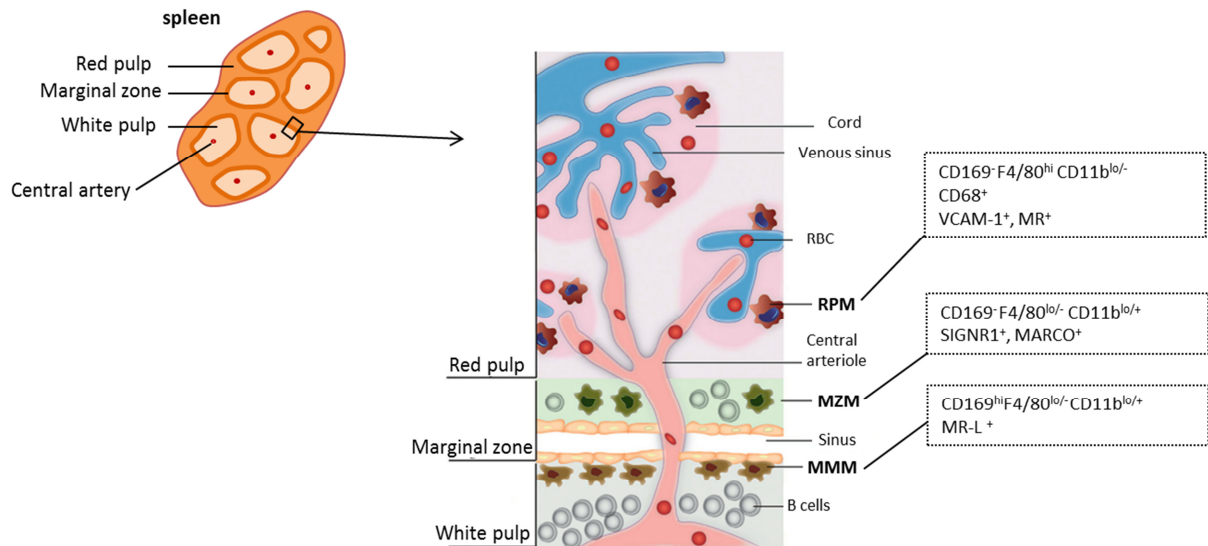
Figure 4.2: Localization and characteristics of splenic macrophage populations. The spleen has distinct red pulp and white pulp regions separated by the marginal zone. Red pulp macrophages (RPM) reside in the cords of the red pulp. They are directly in contact with red blood cells (RBCs). In the outer layer of the marginal zone, marginal zone macrophages (MZM) are directly in contact with blood-borne antigens. Marginal metallophilic macrophages (MMM) are found in the inner layer of the marginal zone, surrounding the white pulp. They are responsible for uptake of antigens from the blood flow and transfer to B cells in the white pulp. Modified after references [30,31].

a) Marginal metallophilic macrophages (MMM)

Marginal metallophilic macrophages (MMM) reside at the border of B cell follicles forming the white pulp, next to endothelial cells forming the inner ring of the marginal zone sinus. They express intermediate levels of CD11b.The expression of CD11c is not clear as there is discrepancy between studies showing absence or presence of CD11c staining in MMMs [32,33]. These macrophages are characterized by high expression of CD169 [34] and low expression of F4/80 [30]. They also express ligands for the cysteine-rich region of MR [19]. They are able to enter the B cell follicle during an immune response [19,35]. Due to their similarity of markers and function, MMM are thought to be the splenic counterpart of LN SSM. Knowledge brought by several studies on MMM might therefore apply to SSM. The detailed function of these cells will be described later in this chapter.

b) Marginal zone macrophages (MZM)

Marginal zone macrophages (MZM) form the outer ring of the marginal zone, residing between the marginal sinus and the red pulp. It was shown in one study by Eloranta and colleagues that they do not express CD11c [32]. They are characterized by the expression of SIGN-R1 [11,36] and MARCO [37] but do not express CD169 and express low levels of F4/80 [30]. These macrophages also have access

to the blood circulation and are responsible for antigen uptake and interaction with B cells from the marginal zone [35]. They are more phagocytic than MMMs [38].

c) Red pulp macrophages

Red pulp macrophages (RPM) highly express F4/80, CD68, VCAM-1 and MR, express intermediate to low levels of CD11b and do not express CD169 [28,39]. They are mainly involved in phagocytosis of dead erythrocytes and iron homeostasis. They also mediate regulation of serum glycoproteins and uptake of pathogens via MR [28].

4.1.4 Mucosal lymphoid tissues macrophages

There is little knowledge about macrophages associated with mucosal lymphoid tissues. As describe in chapter 2, M cells are responsible for the transfer of antigens from the gut lumen to peyer's patches. F4/80^{+} macrophages were not found in peyer's patches but in the lamina propria of small and large intestine [40]. CD169^{+} macrophages were also found in intestinal tissues and will be described in the last paragraph of this chapter [41,42].

The study involved in my thesis is related to CD169^{+} macrophages in the LN. Therefore, after describing the different macrophages population in lymphoid tissues, I will now focus on the function of CD169^{+} macrophages, that is LN SSM and MSM as well as MMM in the spleen.

4.2. Functions of CD169^{+} macrophages in LNs and spleen

4.2.1 Pathogen elimination and innate immunity

As described before, SIGN-R1 and MARCO are pattern-recognition receptors (PRR) expressed by macrophages from the spleen and the LN. CD169^{+} macrophages also express Toll-like receptors (TLR) leading to cell activation and initiation of immune response. Therefore, the first function of these macrophages is to recognize pathogens and to induce an innate immune response. It was shown that MMM are essential for the trapping of particulate antigen from *Listeria monocytogenes* and limit spreading of this bacteria [43]. MMM also limit *plasmodium berghei* infection [44]. Moreover, CD169^{+} macrophages are the first line in antiviral defense. It was observed that MMM have a crucial role in eliminating lymphocytic choriomeningitis virus (LCMV) and preventing spreading of the virus to other organs [45]. On the other hand, SSM reduce the spread of murine cytomegalovirus (MCMV)

[46]. The main pathway involved in prevention of virus replication is IFN-I secretion and activation of IFNAR receptors. IFN-I production by SSM but also plasmacytoid DCs is needed to prevent central nervous system infection via intranodal nerves [47]. It was also shown that MMM produce IFN-I after herpes simplex virus infection [32]. Moreover, it was observed that lymphotoxin (LT) expressed by B cells plays a critical role in viral protection induced by SSMs [48]. Indeed no production of IFN-I was observed in absence of LT expression. Production of IFN-I by SSM also recruits natural-killer (NK) cells in the subcapsular sinus in a mechanism dependent on CXCR3 [49].

Additionally, SSM and MSM are closely located to innate lymphocytes (NK cells, NKT cells, γδT cells, innate-like CD8 T cells) in the LN and are able to induce their activation [33,50,51]. It was observed that pathogen recognition by SSM activates their inflammasome leading to IL-18 and IL-1β secretion [52]. IL-18 induces IFNγ production by innate lymphocytes in a loop further activating macrophages. IL-1β enables fast recruitment of neutrophils and efficient pathogen clearance. SSM also play an important role in mediating the effect of vaccine adjuvants [53,54].

4.2.2   Antigen presentation and adaptive immunity

In addition to pathogen recognition and induction of innate immunity, CD169^{+} macrophages are able to capture and present antigens and thus act as antigen presenting cells (APC) initiating adaptive immune responses. Indeed, many studies brought evidence that CD169^{+} LN and splenic macrophages are able to capture viral particles as well as particulate antigens and immune complexes [18,20–22,55]. To achieve this function, SSM have a projection in the lymph sinus called the "head" and a "tail" that extends in the B cell follicle (**figure 4.3**). Interestingly, it has been shown by imaging that this shape is stable in contrast to dendrites of DCs [18,20,21,55]. The development of confocal microscopy techniques also allowed to observe that SSM are able to transfer intact immune complexes to B cells [18]. B cells can acquire immune complexes through the complement receptor and transport them to the follicle were immune complexes can be transferred to follicular dendritic cells (FDCs) [56]. However, spleen is less accessible than LNs and this was not shown for MMM. MCH-II expressing CD169^{+} macrophages have been identified in the LN floor subcapsular sinus confirming that SSM are gatekeepers able to transfer antigens to B cells and induce a humoral response [20]. Whether MMM express MHC-II remains unclear. Antigen in complex with MR can be acquired by both MMM and SSM [19]. Furthermore, MR-L targeting allowed to visualize SSM and MMM migrating to B cell follicle after antigen uptake [19,57]. This is probably to increase presentation to B cells thus enabling a longer presentation of antigens. However, this migration leads to loss of LN integrity which causes problems in secondary infections [58]. Overall, antigen uptake and presentation to B cells by CD169^{+} macrophages is important for initiation of an immune

response. However, since the B cell response occurs even after depletion of CD169^{+} macrophages it is thought that macrophages only play an accessory role in inducing B cell activation [28].
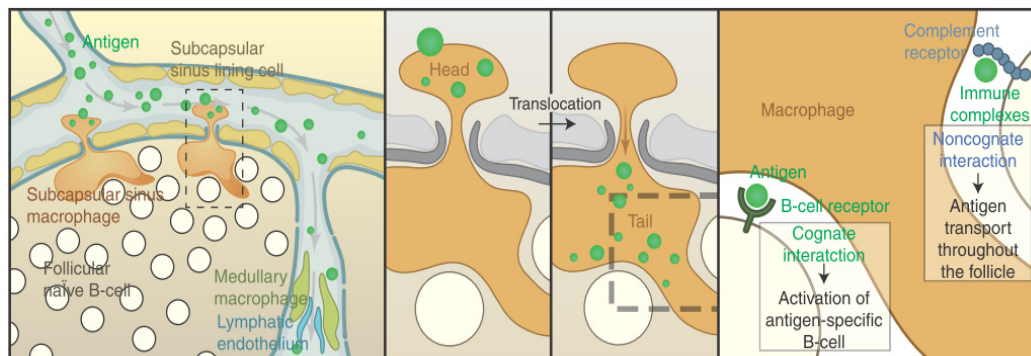

Figure 4.3: Antigen presentation by subcapsular sinus macrophages. Scheme representing the characteristic shape of subcapsular sinus macrophages inserted in the lymphatic endothelium. The "head" is responsible for capture of lymph borne antigen and the "tail" for transfer of antigens to B cells. Antigen can be directly recognized by B cell in a cognate interaction leading to direct activation of B cells. Immune complexes can also be recognized by complement receptors and transported by B cells into the follicle. After reference [56].

Another role of CD169^{+} macrophages is cross-presentation of antigens. Indeed, SSM would also play a role in central memory CD8^{+} T cells and DCs activation [22]. It is of great interest to understand the effects on cytotoxic CD8^{+} T cells to set up new vaccination strategies. It was shown that SSM and MMM are able to internalize, process and present antigens trough MHC-I molecule, thus replacing CD8α^{+} DCs and directly priming CD8^{+} T cells [18,59,60]. It was also demonstrated that MMM present antigens to CD8^{+} DCs and induce CD8^{+} T cells response [61]. Bernhard and colleagues recently showed that cross-presentation by CD169^{+} macrophages is restricted to peptides strongly binding MHC-I [60]. This cross-presentation mechanism seems to be independent of B cell activation as depletion of B cells do not impair CD8^{+} T cells activation [62]. Furthermore, LCMV infection leads to production of CXCR3 ligands by MMM guiding CD8^{+} T cells and inducing a short term effector cells response [63].

Moreover, investigation of *T. Gondii* infection showed that SSM invaded with this parasite cluster with CD8^{+} T cells leading to release of the pathogens from macrophages and infection of T cells [59,64]. Additionally, spleen infection with *P. chabaudi* induces deletion of MMM by CD8^{+} T cells via CD95/CD95L and perforin [65]. These mechanisms are used by pathogens to promote their dissemination.

4.2.3   Permissivity to infection

Beside secretion of interferon type I in response to viral infection, it has also been shown that viruses can infect and replicate in CD169^{+} macrophages [26]. Vaccinia virus (VV) was shown to replicate in SSM [66], LCMV in MMM [63] and MCMV and Vesicular stomatitis virus (VSV) in both SSM and MMM [20,67,68]. A study of VSV infection in the spleen demonstrated that permissivity to virus infection in MMM is due to negative regulation of IFNAR pathway in these cells. Indeed, it has been shown that MMM express Usp18, a negative regulator of IFN-I signaling cascade. Thus, CD169^{+} macrophages responsiveness to IFN-I is decreased which allows locally restricted replication of the virus [68]. We can assume that this mechanism extends to SSM. Moreover, viral replication in CD169^{+} macrophages generates intact viral particles that are more effective to activate B cells than free antigens. This mechanism would induce antibody response as Usp18-/- mice and CD169-DTR mice present reduced antibody response to infection [68]. However, the link between CD169^{+} macrophages and antibody response remains unclear. Additionally, production and release of live viruses leads to T cell priming via DCs [69]. The mechanism controlling live viruses release remains to be investigated. Therefore, Usp-18 inhibition of IFNAR signaling cascade is required to allow local replication of viruses and induce a protective adaptive immune response. This involves activation of antiviral T cells and neutralizing antibodies production. These observations could explain why attenuated live vaccines are more effective than inactivated or subunit vaccines in inducing protective immunity [69]. Permissivity to infection is not restricted to viruses as *Toxoplasma gondii* also infects and replicates in SSM [70].
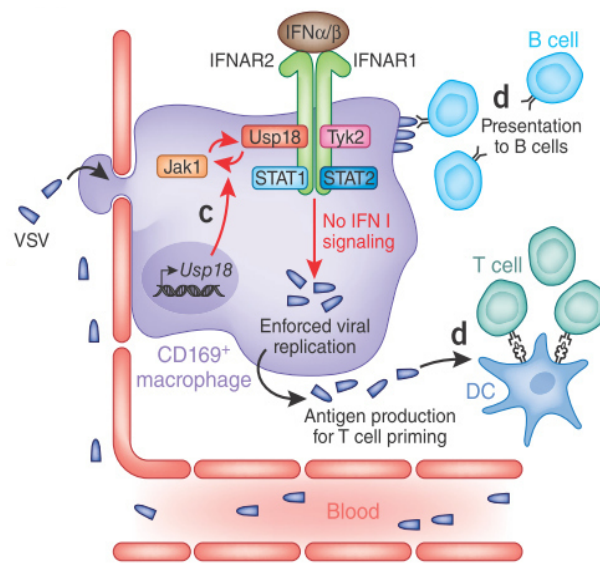
Figure 4.4: Mechanism allowing marginal metallophilic macrophages permissivity to infection. Vesicular stomatitis virus (VSV) arrives in the spleen via blood circulation. Virus recognition leads to type I interferon secretion and activation of IFNAR receptor. In CD169^{+} marginal metallophilic macrophages Usp18 prevents binding of Jak1 to IFNAR2 and inhibits downstream IFN-I signaling allowing replication of the virus. Intact virus particles are presented to induce B cell response. Live viruses release allows T cells priming via dendritic cells (DC). Modified after reference [69].

Finally, LNs medullary and subcapsular sinus macrophages probably do not play the same role in host defense. Indeed, MSMs do not allow virus replication [47,48]. These cells are more phagocytic and express more TLR4 and TLR13 than SSMs. Thus, they are able to recognize and destroy extracellular viruses and rather play a role in innate immune response through IFN-I [26].

4.2.4   Tolerance and anti-tumor immunity

In addition to preventing systemic infection, it has also been observed that CD169^{+} macrophages play an important role in tolerance and anti-tumor immunity. MMM and MSM are able to clear apoptotic cells thus preventing autoimmune responses. MSM express Tim-4 and MMM express Tim-4 and Trem14 receptors for apoptotic cells. Uptake of cell debris leads to secretion of immunosuppressive factors [71,72]. MSM uptake of apoptotic cells was indeed shown to induce tolerance in lung draining LNs [73]. Additionally, apoptotic cell uptake by MMM leads to CCL22 secretion and activation of Foxp3^{+} Treg cells and DCs hence inducing tolerance [74].

Dead tumor cells are a source of tumor antigens. It was shown that immunization with irradiated tumor cells induced protection against syngeneic tumors in mice [75]. In this study, Asano and colleagues showed that SSM present tumor antigens to CD8^{+} T cells without involving DCs. Depletion of CD169^{+} macrophages in CD169-DTR mice suppressed the antitumor effect of immunization with

tumor dead cells and CD8^{+} T cells were not activated. A mechanism for the uptake of dead cells could be recognition of phosphatidylserine by SSM [76]. Thus, it would be interesting to take advantage of this mechanism for antitumoral vaccination strategies. Moreover, Pucci et al studied Tumor-derived extracellular vesicles (tEVs) in the context of melanoma. They showed that tEVs are drained from the tumor in lymphatics and bind SSM in tumor draining LNs then preventing cancer progression [77]. However, they also show that the SSM barrier can be disrupted by chemotherapy agents or CSF1-R inhibitor immunotherapy. In the spleen, tumor antigen targeting to MMM also induce antitumor immunity in a CD8^{+} T cells dependent mechanism [61]. CD169^{+} macrophages were also shown to be important in humans. CD169^{+} macrophage numbers in regional LN (RLN) correlated with longer survival in colorectal cancer and endometrial carcinoma patients. In these patients, SSM were closely associated with CD8^{+} T cells [78,79]. CD169^{+} macrophage numbers in RLN also correlated with clinical stages of breast cancer. Decrease in the CD169^{+} macrophage population was associated with cancer progression [80].

4.3. Development of CD169^{+} macrophages in LNs and spleen

Different factors required for CD169^{+} macrophages development have been identified. SSM and MMM development is sensitive to CSF-1. Op/op mice missing CSF-1 expression lack these macrophage populations [81,82]. Interestingly, treatment of op/op mice with CSF-1 from 3 days of age to 3-4 months of age rescues the presence of MMMs [82]. Moreover, increased levels of CSF-1 were observed in macrophage-enriched zones in spleen and LNs [83]. SSM and MMM have been shown to depend also on LTα1β2 secreted by B cells. In fact, SSM population was greatly reduced in B cell-deficient mice and after treatment with LTBR-Fc both in LN sections and by flow cytometry [18]. Impaired spleen architecture and lack of MMM was also observed in these mice [84,85]. NF-κB signaling induction by LTβR seems to be essential as NF-κB p52 deficient mice lack MMM [86]. It is not known whether NF-κB signaling is also involved in SSM development. However, CSF-1 does not affect LNs MSM presence and LTα1β2 blockage had a moderate effect on MSM population [18,81,82]. Moreover, TNF appears to be important for spleen macrophages but not for LN macrophages [87,88]. The nuclear factor LXRα was also suggested to be required for splenic macrophage development as LXRα deficient mice lack MMM [89].

Beside the identification of these factors regulating the presence of CD169^{+} macrophages, the origin and precise developmental mechanism of those cells remains unclear. It has been observed in many tissues that tissue-resident macrophages renewal is based on local proliferation in adult steady-state rather than recruitment from peripheral monocytes [5]. However, it was recently proposed that spleen macrophages derive from CX3CR1[int]LY6C^{hi} monocytes [89]. Moreover, intravital imaging

allowed to observe monocytes accumulation in the spleen and mobilization of monocytes in inflammatory conditions [90]. Whether this phenomenon contributes to renewal of spleen macrophages remains unclear. On the other hand, early studies showed that splenic macrophages renewal is due, at least in part, to local proliferation [91,92]. Overall, further fate mapping experiments are required to better understand splenic CD169^{+} macrophage ontogeny.

To study the development of SSM, Delemarre et al studied in 1990 the repopulation of these macrophages after dichloromethylene diphosphonate (Cl_2MDP)-liposomes injection. After 5 days of treatment, all LN macrophages disappeared. Macrophages populations were again present in the LNs of all animals after 5 months. There was no difference in the repopulation kinetic of SSM and MSM meaning that the two populations probably have the same precursors [27]. Conversely, splenic macrophages did not have the same repopulation kinetic after Cl_2MDP-liposomes injection. MMM complete reappearance was observed 2 weeks after injection while it took 1 month for MZM to be back in normal numbers [93]. Following selective depletion of CD169^{+} macrophages by a single injection of diphtheria toxin (DT) in CD169-DTR mice, recovery of LN and splenic macrophages was observed after 7-10 days [75,94]. The effect seen in liposomes treated mice might be due to long lasting effect of the toxin.

Delemarre's group also investigated whether LN macrophages precursor are coming from the blood compartment. They transplanted Cl_2MDP-liposomes treated LNs into control animals. In this case, the macrophages repopulated the LNs after 5 weeks only [95]. Moreover, after lymphatics occlusion, disappearance of SSM was observed showing that macrophages in LN might come from new immigration from interstitial tissues through the lymph rather than local proliferation [92,95]. In this study, they also excluded that precursors come from monocytes influx via high endothelial venules. On the other hand, irradiation chimeras experiments suggest that LN CD169^{+} macrophages have a bone marrow origin [3]. Overall, the origin of LNs and splenic CD169^{+} macrophages remains unclear and whether they have the same precursors or not remains to be investigated. They might show different terminal differentiation due to distinct tissue of residence. Lineage tracing experiments would be required to further understand CD169^{+} macrophages origin and development. Finally, the stromal environment might play a role in macrophages differentiation and would require further investigation.

4.4. CD169^{+} macrophages in other tissues

CD169^{+} macrophages were recently identified in intestinal tissues by two independent groups [41,42]. Hiemstra and colleagues identified the presence of CD169^{+} macrophages in lamina propria of the colon. They show that development of this population does not rely on LTα as in the spleen but rather relies on vitamin A. Mice deficient for vitamin A present a reduced number of colonic CD169^{+} macrophages [41]. These findings show the different requirements for CD169^{+} macrophage differentiation depending on the tissue of residence. Moreover, Asano and colleagues observed CD169^{+} macrophages in the bottom of the lamina propria, distant from the intestinal lumen. Hence this macrophage population is not directly exposed to commensal bacteria. In a mouse model, colitis epithelial-mucosal injury leads to production of CCL8 by CD169^{+} macrophages and recruitment of inflammatory monocytes. Depletion of this macrophage population ameliorates the colitis symptoms [42].

CD169^{+} macrophages were also identified in bone marrow (BM). Erythropoiesis is a process leading to development of red blood cells from erythroid precursors and occurs in BM. It was shown that CD169^{+} macrophages play a role in erythropoiesis. Depletion of CD169^{+} macrophages in BM leads to impaired erythropoiesis and reduced number of erythroblasts [96,97]. Therefore, CD169^{+} macrophages would play a role in anemia-associated diseases. CD169^{+} macrophages are also able to retain hematopoietic stem cells (HSC) in bone marrow [98,99] thus regulating the number of HSC leaving bone marrow to the peripheral blood.

Additionally, CD169^{+} macrophages are involved in kidney diseases however contrary roles have been described depending on the study. Ikezumi and colleagues found accumulation of CD169^{+} macrophages in glomerulonephritis patients and the number of this macrophage population correlated with proteinuria and histological damage [100]. On the other hand, Karazawa and colleagues recently demonstrated the presence of kidney resident CD169^{+} macrophages in renal ischemia-reperfusion injury (IRI) mouse model. They show that CD169^{+} macrophages depletion worsen renal IRI symptoms. Hence this population would play a role in suppression and resolution of IRI. Interestingly, this study also showed that CD169^{+} macrophages would play a role in vascular homeostasis by regulating the expression of adhesion molecules such as ICAM-1 on endothelial cells [101].

Moreover, in arthritis accumulation of CD169^{+} macrophages was observed in the synovium. But whether macrophages play a role in this autoimmune disease or their accumulation is a result of inflammatory conditions remains unclear [102].

CD169^{+} macrophages were also found in models of cerebral vasculature injury [103] and atherosclerosis [104].

Finally, CD169^{+} macrophages are located in hepatocellular carcinoma tissues were they activate CD8^{+} T cells and are therefore associated with favorable prognosis [105].

4.5. Conclusions

CD169^{+} macrophages play an important role in inducing both innate and adaptive immunity in LNs and spleen. SSMs are able to present antigen to B cells and cross-present antigens to cytotoxic CD8^{+} T cells. Moreover, they have a characteristic permissivity to infection enabling local proliferation of viruses in order to enhance adaptive immune response. Recent studies also demonstrated the importance of CD169^{+} macrophages in other non-lymphoid tissues. However, the mechanisms leading to their differentiation are still poorly understood and might be tissue dependent. Due to the importance of CD169^{+} macrophages in protecting against infections and tumors development, it appears crucial to understand the key mechanisms leading to their differentiation. Many studies have been investigating the splenic CD169^{+} macrophages counterpart of SSM, but whether the mechanisms involved in the spleen are the same in the LNs remain to be better understood. The role of the tissue microenvironment would also require further investigations.

CD169^{+} macrophages were also identified in human spleen but functional studies are lacking [106]. Moreover, macrophages with the same phenotype as mouse LN macrophages were identified in human LNs [107]. However, there is still a limited knowledge about the similarities of LN macrophages and more generally CD169^{+} macrophages between mouse and human [22].

4.6. References

1. Tauber AI. Metchnikoff and the phagocytosis theory. Nat Rev Mol Cell Biol. 2003;4: 897–901. doi:10.1038/nrm1244

2. van Furth R, Cohn ZA, Hirsch JG, Humphrey JH, Spector WG, Langevoort HL. The mononuclear phagocyte system: a new classification of macrophages, monocytes, and their precursor cells. Bull World Health Organ. 1972;46: 845–852.

3. Gray EE, Cyster JG. Lymph node macrophages. J Innate Immun. 2012;4: 424–436. doi:10.1159/000337007

4. Gordon S. The macrophage: Past, present and future. Eur J Immunol. 2007;37: S9–S17. doi:10.1002/eji.200737638

5. Gordon S, Taylor PR. Monocyte and macrophage heterogeneity. Nat Rev Immunol. 2005;5: 953–964. doi:10.1038/nri1733

6. Pollard JW. Trophic macrophages in development and disease. Nat Rev Immunol. 2009;9: 259–270. doi:10.1038/nri2528

7. O'Neill ASG, van den Berg TK, Mullen GED. Sialoadhesin – a macrophage-restricted marker of immunoregulation and inflammation. Immunology. 2013;138: 198–207. doi:10.1111/imm.12042

8. Delputte PL, Gorp HV, Favoreel HW, Hoebeke I, Delrue I, Dewerchin H, et al. Porcine Sialoadhesin (CD169/Siglec-1) Is an Endocytic Receptor that Allows Targeted Delivery of Toxins and Antigens to Macrophages. PLOS ONE. 2011;6: e16827. doi:10.1371/journal.pone.0016827

9. Chen WC, Kawasaki N, Nycholat CM, Han S, Pilotte J, Crocker PR, et al. Antigen Delivery to Macrophages Using Liposomal Nanoparticles Targeting Sialoadhesin/CD169. PLOS ONE. 2012;7: e39039. doi:10.1371/journal.pone.0039039

10. Gordon S, Hamann J, Lin H-H, Stacey M. F4/80 and the related adhesion-GPCRs. Eur J Immunol. 2011;41: 2472–2476. doi:10.1002/eji.201141715

11. Geijtenbeek TBH, Groot PC, Nolte MA, Vliet SJ van, Gangaram-Panday ST, Duijnhoven GCF van, et al. Marginal zone macrophages express a murine homologue of DC-SIGN that captures blood-borne antigens in vivo. Blood. 2002;100: 2908–2916. doi:10.1182/blood-2002-04-1044

12. Chen Y, Pikkarainen T, Elomaa O, Soininen R, Kodama T, Kraal G, et al. Defective Microarchitecture of the Spleen Marginal Zone and Impaired Response to a Thymus-Independent Type 2 Antigen in Mice Lacking Scavenger Receptors MARCO and SR-A. J Immunol. 2005;175: 8173–8180. doi:10.4049/jimmunol.175.12.8173

13. Mukhopadhyay S, Chen Y, Sankala M, Peiser L, Pikkarainen T, Kraal G, et al. MARCO, an innate activation marker of macrophages, is a class A scavenger receptor for Neisseria meningitidis. Eur J Immunol. 2006;36: 940–949. doi:10.1002/eji.200535389

14. Karlsson MCI, Guinamard R, Bolland S, Sankala M, Steinman RM, Ravetch JV. Macrophages Control the Retention and Trafficking of B Lymphocytes in the Splenic Marginal Zone. J Exp Med. 2003;198: 333–340. doi:10.1084/jem.20030684

15. Gordon S, Plüddemann A, Mukhopadhyay S. Sinusoidal Immunity: Macrophages at the Lymphohematopoietic Interface. Cold Spring Harb Perspect Biol. 2015;7: a016378. doi:10.1101/cshperspect.a016378

16. Clark SL. The reticulum of lymph nodes in mice studied with the electron microscope. Am J Anat. 1962;110: 217–257. doi:10.1002/aja.1001100303

17. Fossum S. The architecture of rat lymph nodes. IV. Distribution of ferritin and colloidal carbon in the draining lymph nodes after foot-pad injection. Scand J Immunol. 1980;12: 433–441.

18. Phan TG, Green JA, Gray EE, Xu Y, Cyster JG. Immune complex relay by subcapsular sinus macrophages and noncognate B cells drives antibody affinity maturation. Nat Immunol. 2009;10: 786–793. doi:10.1038/ni.1745

19. Martínez-Pomares L, Kosco-Vilbois M, Darley E, Tree P, Herren S, Bonnefoy JY, et al. Fc chimeric protein containing the cysteine-rich domain of the murine mannose receptor binds to macrophages from splenic marginal zone and lymph node subcapsular sinus and to germinal centers. J Exp Med. 1996;184: 1927–1937. doi:10.1084/jem.184.5.1927

20. Junt T, Moseman EA, Iannacone M, Massberg S, Lang PA, Boes M, et al. Subcapsular sinus macrophages in lymph nodes clear lymph-borne viruses and present them to antiviral B cells. Nature. 2007;450: 110–114. doi:10.1038/nature06287

21. Carrasco YR, Batista FD. B Cells Acquire Particulate Antigen in a Macrophage-Rich Area at the Boundary between the Follicle and the Subcapsular Sinus of the Lymph Node. Immunity. 2007;27: 160–171. doi:10.1016/j.immuni.2007.06.007

22. Martinez-Pomares L, Gordon S. CD169+ macrophages at the crossroads of antigen presentation. Trends Immunol. 2012;33: 66–70. doi:10.1016/j.it.2011.11.001

23. Carrasco YR, Fleire SJ, Cameron T, Dustin ML, Batista FD. LFA-1/ICAM-1 Interaction Lowers the Threshold of B Cell Activation by Facilitating B Cell Adhesion and Synapse Formation. Immunity. 2004;20: 589–599. doi:10.1016/S1074-7613(04)00105-0

24. Nossal GJV, Ada GL, Austin CM, Pye J. Antigens in immunity. Immunology. 1965;9: 349–357.

25. Steer HW, Foot RA. Changes in the medulla of the parathymic lymph nodes of the rat during acute gastro-intestinal inflammation. J Anat. 1987;152: 23–36.

26. Kuka M, Iannacone M. The role of lymph node sinus macrophages in host defense. Ann N Y Acad Sci. 2014;1319: 38–46. doi:10.1111/nyas.12387

27. Delemarre FG, Kors N, Kraal G, van Rooijen N. Repopulation of macrophages in popliteal lymph nodes of mice after liposome-mediated depletion. J Leukoc Biol. 1990;47: 251–257.

28. Haan JMM den, Martinez-Pomares L. Macrophage heterogeneity in lymphoid tissues. Semin Immunopathol. 2013;35: 541–552. doi:10.1007/s00281-013-0378-4

29. Mebius RE, Kraal G. Structure and function of the spleen. Nat Rev Immunol. 2005;5: 606–616. doi:10.1038/nri1669

30. Borges da Silva H, Fonseca R, Pereira RM, Cassado A dos A, Álvarez JM, Lima D, et al. Splenic Macrophage Subsets and Their Function during Blood-Borne Infections. Front Immunol. 2015;6. doi:10.3389/fimmu.2015.00480

31. Davies LC, Jenkins SJ, Allen JE, Taylor PR. Tissue-resident macrophages. Nat Immunol. 2013;14: 986–995. doi:10.1038/ni.2705

32. Eloranta, Alm. Splenic Marginal Metallophilic Macrophages and Marginal Zone Macrophages are the Major Interferon-α/β Producers in Mice upon Intravenous Challenge with Herpes Simplex Virus. Scand J Immunol. 1999;49: 391–394. doi:10.1046/j.1365-3083.1999.00514.x

33. Kawasaki N, Vela JL, Nycholat CM, Rademacher C, Khurana A, Rooijen N van, et al. Targeted delivery of lipid antigen to macrophages via the CD169/sialoadhesin endocytic pathway induces robust invariant natural killer T cell activation. Proc Natl Acad Sci. 2013;110: 7826–7831. doi:10.1073/pnas.1219888110

34. Kraal G, Janse M. Marginal metallophilic cells of the mouse spleen identified by a monoclonal antibody. Immunology. 1986;58: 665–669.

35. den Haan JMM, Kraal G. Innate Immune Functions of Macrophage Subpopulations in the Spleen. J Innate Immun. 2012;4: 437–445. doi:10.1159/000335216

36. Kang Y-S, Yamazaki S, Iyoda T, Pack M, Bruening SA, Kim JY, et al. SIGN-R1, a novel C-type lectin expressed by marginal zone macrophages in spleen, mediates uptake of the polysaccharide dextran. Int Immunol. 2003;15: 177–186. doi:10.1093/intimm/dxg019

37. Elomaa O, Kangas M, Sahlberg C, Tuukkanen J, Sormunen R, Liakka A, et al. Cloning of a novel bacteria-binding receptor structurally related to scavenger receptors and expressed in a subset of macrophages. Cell. 1995;80: 603–609. doi:10.1016/0092-8674(95)90514-6

38. Gordon S, Plüddemann A, Martinez Estrada F. Macrophage heterogeneity in tissues: phenotypic diversity and functions. Immunol Rev. 2014;262: 36–55. doi:10.1111/imr.12223

39. Kohyama M, Ise W, Edelson BT, Wilker PR, Hildner K, Mejia C, et al. Role for Spi-C in the development of red pulp macrophages and splenic iron homeostasis. Nature. 2009;457: 318–321. doi:10.1038/nature07472

40. Hume DA, Robinson AP, MacPherson GG, Gordon S. The mononuclear phagocyte system of the mouse defined by immunohistochemical localization of antigen F4/80. Relationship between macrophages, Langerhans cells, reticular cells, and dendritic cells in lymphoid and hematopoietic organs. J Exp Med. 1983;158: 1522–1536. doi:10.1084/jem.158.5.1522

41. Hiemstra IH, Beijer MR, Veninga H, Vrijland K, Borg EGF, Olivier BJ, et al. The identification and developmental requirements of colonic CD169+ macrophages. Immunology. 2014;142: 269–278. doi:10.1111/imm.12251

42. Asano K, Takahashi N, Ushiki M, Monya M, Aihara F, Kuboki E, et al. Intestinal CD169+ macrophages initiate mucosal inflammation by secreting CCL8 that recruits inflammatory monocytes. Nat Commun. 2015;6: 7802. doi:10.1038/ncomms8802

43. Aichele P, Zinke J, Grode L, Schwendener RA, Kaufmann SHE, Seiler P. Macrophages of the Splenic Marginal Zone Are Essential for Trapping of Blood-Borne Particulate Antigen but Dispensable for Induction of Specific T Cell Responses. J Immunol. 2003;171: 1148–1155. doi:10.4049/jimmunol.171.3.1148

44. Gupta P, Lai SM, Sheng J, Tetlak P, Balachander A, Claser C, et al. Tissue-Resident CD169+ Macrophages Form a Crucial Front Line against Plasmodium Infection. Cell Rep. 2016;16: 1749–1761. doi:10.1016/j.celrep.2016.07.010

45. Seiler P, Aichele P, Odermatt B, Hengartner H, Zinkernagel RM, Schwendener RA. Crucial role of marginal zone macrophages and marginal zone metallophils in the clearance of lymphocytic choriomeningitis virus infection. Eur J Immunol. 1997;27: 2626–2633. doi:10.1002/eji.1830271023

46. Farrell HE, Davis-Poynter N, Bruce K, Lawler C, Dolken L, Mach M, et al. Lymph Node Macrophages Restrict Murine Cytomegalovirus Dissemination. J Virol. 2015;89: 7147–7158. doi:10.1128/JVI.00480-15

47. Iannacone M, Moseman EA, Tonti E, Bosurgi L, Junt T, Henrickson SE, et al. Subcapsular sinus macrophages prevent CNS invasion on peripheral infection with a neurotropic virus. Nature. 2010;465: 1079–1083. doi:10.1038/nature09118

48. Moseman EA, Iannacone M, Bosurgi L, Tonti E, Chevrier N, Tumanov A, et al. B Cell Maintenance of Subcapsular Sinus Macrophages Protects against a Fatal Viral Infection Independent of Adaptive Immunity. Immunity. 2012;36: 415–426. doi:10.1016/j.immuni.2012.01.013

49. Garcia Z, Lemaître F, Rooijen N van, Albert ML, Levy Y, Schwartz O, et al. Subcapsular sinus macrophages promote NK cell accumulation and activation in response to lymph-borne viral particles. Blood. 2012;120: 4744–4750. doi:10.1182/blood-2012-02-408179

50. Barral P, Polzella P, Bruckbauer A, van Rooijen N, Besra GS, Cerundolo V, et al. CD169+ macrophages present lipid antigens to mediate early activation of iNKT cells in lymph nodes. Nat Immunol. 2010;11: 303–312. doi:10.1038/ni.1853

51. Coombes JL, Han S-J, van Rooijen N, Raulet DH, Robey EA. Infection-Induced Regulation of Natural Killer Cells by Macrophages and Collagen at the Lymph Node Subcapsular Sinus. Cell Rep. 2012;2: 124–135. doi:10.1016/j.celrep.2012.06.001

52. Kastenmüller W, Torabi-Parizi P, Subramanian N, Lämmermann T, Germain RN. A Spatially-Organized Multicellular Innate Immune Response in Lymph Nodes Limits Systemic Pathogen Spread. Cell. 2012;150: 1235–1248. doi:10.1016/j.cell.2012.07.021

53. Desbien AL, Cauwelaert ND, Reed SJ, Bailor HR, Liang H, Carter D, et al. IL-18 and Subcapsular Lymph Node Macrophages are Essential for Enhanced B Cell Responses with TLR4 Agonist Adjuvants. J Immunol. 2016;197: 4351–4359. doi:10.4049/jimmunol.1600993

54. Detienne S, Welsby I, Collignon C, Wouters S, Coccia M, Delhaye S, et al. Central Role of CD169+ Lymph Node Resident Macrophages in the Adjuvanticity of the QS-21 Component of AS01. Sci Rep. 2016;6: 39475. doi:10.1038/srep39475

55. Phan TG, Grigorova I, Okada T, Cyster JG. Subcapsular encounter and complement-dependent transport of immune complexes by lymph node B cells. Nat Immunol. 2007;8: 992–1000. doi:10.1038/ni1494

56. Martinez-Pomares L, Gordon S. Antigen Presentation the Macrophage Way. Cell. 2007;131: 641–643. doi:10.1016/j.cell.2007.10.046

57. Berney C, Herren S, Power CA, Gordon S, Martinez-Pomares L, Kosco-Vilbois MH. A Member of the Dendritic Cell Family That Enters B Cell Follicles and Stimulates Primary Antibody Responses Identified by a Mannose Receptor Fusion Protein. J Exp Med. 1999;190: 851–860.

58. Gaya M, Castello A, Montaner B, Rogers N, Sousa CR e, Bruckbauer A, et al. Inflammation-induced disruption of SCS macrophages impairs B cell responses to secondary infection. Science. 2015;347: 667–672. doi:10.1126/science.aaa1300

59. Chtanova T, Han S-J, Schaeffer M, van Dooren GG, Herzmark P, Striepen B, et al. Dynamics of T cell, antigen presenting cell, and pathogen interactions during recall responses in the lymph node. Immunity. 2009;31: 342–355. doi:10.1016/j.immuni.2009.06.023

60. Bernhard CA, Ried C, Kochanek S, Brocker T. CD169+ macrophages are sufficient for priming of CTLs with specificities left out by cross-priming dendritic cells. Proc Natl Acad Sci. 2015;112: 5461–5466. doi:10.1073/pnas.1423356112

61. Backer R, Schwandt T, Greuter M, Oosting M, Jüngerkes F, Tüting T, et al. Effective collaboration between marginal metallophilic macrophages and CD8+ dendritic cells in the generation of cytotoxic T cells. Proc Natl Acad Sci. 2010;107: 216–221. doi:10.1073/pnas.0909541107

62. Bouaziz J-D, Yanaba K, Venturi GM, Wang Y, Tisch RM, Poe JC, et al. Therapeutic B cell depletion impairs adaptive and autoreactive CD4+ T cell activation in mice. Proc Natl Acad Sci. 2007;104: 20878–20883. doi:10.1073/pnas.0709205105

63. Hu JK, Kagari T, Clingan JM, Matloubian M. Expression of chemokine receptor CXCR3 on T cells affects the balance between effector and memory CD8 T-cell generation. Proc Natl Acad Sci. 2011;108: E118–E127. doi:10.1073/pnas.1101881108

64. Persson EK, Agnarson AM, Lambert H, Hitziger N, Yagita H, Chambers BJ, et al. Death Receptor Ligation or Exposure to Perforin Trigger Rapid Egress of the Intracellular Parasite Toxoplasma gondii. J Immunol. 2007;179: 8357–8365. doi:10.4049/jimmunol.179.12.8357

65. Beattie L, Engwerda CR, Wykes M, Good MF. CD8+ T Lymphocyte-Mediated Loss of Marginal Metallophilic Macrophages following Infection with Plasmodium chabaudi chabaudi AS. J Immunol. 2006;177: 2518–2526. doi:10.4049/jimmunol.177.4.2518

66. Hickman HD, Takeda K, Skon CN, Murray FR, Hensley SE, Loomis J, et al. Direct priming of antiviral CD8+ T cells in the peripheral interfollicular region of lymph nodes. Nat Immunol. 2008;9: 155–165. doi:10.1038/ni1557

67. Hsu KM, Pratt JR, Akers WJ, Achilefu SI, Yokoyama WM. Murine cytomegalovirus displays selective infection of cells within hours after systemic administration. J Gen Virol. 2009;90: 33–43. doi:10.1099/vir.0.006668-0

68. Honke N, Shaabani N, Cadeddu G, Sorg UR, Zhang D-E, Trilling M, et al. Enforced viral replication activates adaptive immunity and is essential for the control of a cytopathic virus. Nat Immunol. 2012;13: 51–57. doi:10.1038/ni.2169

69. Ludewig B, Cervantes-Barragan L. CD169+ macrophages take the bullet. Nat Immunol. 2012;13: 13–14. doi:10.1038/ni.2189

70. Chtanova T, Schaeffer M, Han S-J, van Dooren GG, Nollmann M, Herzmark P, et al. Dynamics of Neutrophil Migration in Lymph Nodes during Infection. Immunity. 2008;29: 487–496. doi:10.1016/j.immuni.2008.07.012

71. Hemmi H, Idoyaga J, Suda K, Suda N, Kennedy K, Noda M, et al. A New Triggering Receptor Expressed on Myeloid Cells (Trem) Family Member, Trem-Like 4, Binds to Dead Cells and Is a DNAX Activation Protein 12-Linked Marker for Subsets of Mouse Macrophages and Dendritic Cells. J Immunol. 2009;182: 1278–1286. doi:10.4049/jimmunol.182.3.1278

72. Freeman GJ, Casasnovas JM, Umetsu DT, DeKruyff RH. TIM genes: a family of cell surface phosphatidylserine receptors that regulate innate and adaptive immunity. Immunol Rev. 2010;235: 172–189. doi:10.1111/j.0105-2896.2010.00903.x

73. Albacker LA, Yu S, Bedoret D, Lee W-L, Umetsu SE, Monahan S, et al. TIM-4, expressed by medullary macrophages, regulates respiratory tolerance by mediating phagocytosis of antigen-specific T cells. Mucosal Immunol. 2013;6: 580–590. doi:10.1038/mi.2012.100

74. Ravishankar B, Shinde R, Liu H, Chaudhary K, Bradley J, Lemos HP, et al. Marginal zone CD169+ macrophages coordinate apoptotic cell-driven cellular recruitment and tolerance. Proc Natl Acad Sci. 2014;111: 4215–4220. doi:10.1073/pnas.1320924111

75. Asano K, Nabeyama A, Miyake Y, Qiu C-H, Kurita A, Tomura M, et al. CD169-Positive Macrophages Dominate Antitumor Immunity by Crosspresenting Dead Cell-Associated Antigens. Immunity. 2011;34: 85–95. doi:10.1016/j.immuni.2010.12.011

76. Bratton DL, Henson PM. Apoptotic Cell Recognition: Will the Real Phosphatidylserine Receptor(s) Please Stand up? Curr Biol. 2008;18: R76–R79. doi:10.1016/j.cub.2007.11.024

77. Pucci F, Garris C, Lai CP, Newton A, Pfirschke C, Englblom C, et al. SCS macrophages suppress melanoma by restricting tumor-derived vesicle–B cell interactions. Science. 2016; aaf1328. doi:10.1126/science.aaf1328

78. Ohnishi K, Komohara Y, Saito Y, Miyamoto Y, Watanabe M, Baba H, et al. CD169-positive macrophages in regional lymph nodes are associated with a favorable prognosis in patients with colorectal carcinoma. Cancer Sci. 2013;104: 1237–1244. doi:10.1111/cas.12212

79. Ohnishi K, Yamaguchi M, Erdenebaatar C, Saito F, Tashiro H, Katabuchi H, et al. Prognostic significance of CD169-positive lymph node sinus macrophages in patients with endometrial carcinoma. Cancer Sci. 2016; n/a-n/a. doi:10.1111/cas.12929

80. Shiota T, Miyasato Y, Ohnishi K, Yamamoto-Ibusuki M, Yamamoto Y, Iwase H, et al. The Clinical Significance of CD169-Positive Lymph Node Macrophage in Patients with Breast Cancer. PLOS ONE. 2016;11: e0166680. doi:10.1371/journal.pone.0166680

81. Witmer-Pack MD, Hughes DA, Schuler G, Lawson L, McWilliam A, Inaba K, et al. Identification of macrophages and dendritic cells in the osteopetrotic (op/op) mouse. J Cell Sci. 1993;104: 1021–1029.

82. Cecchini MG, Dominguez MG, Mocci S, Wetterwald A, Felix R, Fleisch H, et al. Role of colony stimulating factor-1 in the establishment and regulation of tissue macrophages during postnatal development of the mouse. Development. 1994;120: 1357–1372.

83. Ryan GR, Dai X-M, Dominguez MG, Tong W, Chuan F, Chisholm O, et al. Rescue of the colony-stimulating factor 1 (CSF-1)–nullizygous mouse (Csf1 op /Csf1 op) phenotype with a CSF-1 transgene and identification of sites of local CSF-1 synthesis. Blood. 2001;98: 74–84. doi:10.1182/blood.V98.1.74

84. Rennert PD, Browning JL, Mebius R, Mackay F, Hochman PS. Surface lymphotoxin alpha/beta complex is required for the development of peripheral lymphoid organs. J Exp Med. 1996;184: 1999–2006. doi:10.1084/jem.184.5.1999

85. Tumanov AV, Grivennikov SI, Shakhov AN, Rybtsov SA, Koroleva EP, Takeda J, et al. Dissecting the role of lymphotoxin in lymphoid organs by conditional targeting. Immunol Rev. 2003;195: 106–116. doi:10.1034/j.1600-065X.2003.00071.x

86. Poljak L, Carlson L, Cunningham K, Kosco-Vilbois MH, Siebenlist U. Distinct Activities of p52/NF-κB Required for Proper Secondary Lymphoid Organ Microarchitecture: Functions Enhanced by Bcl-3. J Immunol. 1999;163: 6581–6588.

87. Ettinger R, Mebius R, Browning JL, Michie SA, Tuijl S van, Kraal G, et al. Effects of tumor necrosis factor and lymphotoxin on peripheral lymphoid tissue development. Int Immunol. 1998;10: 727–741. doi:10.1093/intimm/10.6.727

88. Pasparakis M, Kousteni S, Peschon J, Kollias G. Tumor Necrosis Factor and the p55TNF Receptor Are Required for Optimal Development of the Marginal Sinus and for Migration of Follicular Dendritic Cell Precursors into Splenic Follicles. Cell Immunol. 2000;201: 33–41. doi:10.1006/cimm.2000.1636

89. A-Gonzalez N, Guillen JA, Gallardo G, Diaz M, de la Rosa JV, Hernandez IH, et al. The nuclear receptor LXRα controls the functional specialization of splenic macrophages. Nat Immunol. 2013;14: 831–839. doi:10.1038/ni.2622

90. Pittet MJ, Weissleder R. Intravital Imaging. Cell. 2011;147: 983–991. doi:10.1016/j.cell.2011.11.004

91. Furth R van, Dulk MMD. Dual origin of mouse spleen macrophages. J Exp Med. 1984;160: 1273–1283. doi:10.1084/jem.160.5.1273

92. Westermann J, Ronneberg S, Fritz FJ, Pabst R. Proliferation of macrophage subpopulations in the adult rat: comparison of various lymphoid organs. J Leukoc Biol. 1989;46: 263–269.

93. van Rooijen N, Kors N, Kraal G. Macrophage subset repopulation in the spleen: differential kinetics after liposome-mediated elimination. J Leukoc Biol. 1989;45: 97–104.

94. Miyake Y, Asano K, Kaise H, Uemura M, Nakayama M, Tanaka M. Critical role of macrophages in the marginal zone in the suppression of immune responses to apoptotic cell–associated antigens. J Clin Invest. 2007;117: 2268–2278. doi:10.1172/JCI31990

95. Mebius RE, Martens G, Brevé J, Delemarre FGA, Kraal G. Is early repopulation of macrophage-depleted lymph node independent of blood monocyte immigration? Eur J Immunol. 1991;21: 3041–3044. doi:10.1002/eji.1830211221

96. Chow A, Huggins M, Ahmed J, Hashimoto D, Lucas D, Kunisaki Y, et al. CD169+ macrophages provide a niche promoting erythropoiesis under homeostasis and stress. Nat Med. 2013;19: 429–436. doi:10.1038/nm.3057

97. Jacobsen RN, Forristal CE, Raggatt LJ, Nowlan B, Barbier V, Kaur S, et al. Mobilization with granulocyte colony-stimulating factor blocks medullary erythropoiesis by depleting F4/80+VCAM1+CD169+ER-HR3+Ly6G+ erythroid island macrophages in the mouse. Exp Hematol. 2014;42: 547–561.e4. doi:10.1016/j.exphem.2014.03.009

98. Albiero M, Poncina N, Ciciliot S, Cappellari R, Menegazzo L, Ferraro F, et al. Bone Marrow Macrophages Contribute to Diabetic Stem Cell Mobilopathy by Producing Oncostatin M. Diabetes. 2015;64: 2957–2968. doi:10.2337/db14-1473

99. Chow A, Lucas D, Hidalgo A, Méndez-Ferrer S, Hashimoto D, Scheiermann C, et al. Bone marrow CD169+ macrophages promote the retention of hematopoietic stem and progenitor cells in the mesenchymal stem cell niche. J Exp Med. 2011;208: 261–271. doi:10.1084/jem.20101688

100. Ikezumi Y, Suzuki T, Hayafuji S, Okubo S, Nikolic-Paterson DJ, Kawachi H, et al. The sialoadhesin (CD169) expressing a macrophage subset in human proliferative glomerulonephritis. Nephrol Dial Transplant. 2005;20: 2704–2713. doi:10.1093/ndt/gfi105

101. Karasawa K, Asano K, Moriyama S, Ushiki M, Monya M, Iida M, et al. Vascular-Resident CD169-Positive Monocytes and Macrophages Control Neutrophil Accumulation in the Kidney with Ischemia-Reperfusion Injury. J Am Soc Nephrol JASN. 2015;26: 896–906. doi:10.1681/ASN.2014020195

102. Hartnell A, Steel J, Turley H, Jones M, Jackson DG, Crocker PR. Characterization of human sialoadhesin, a sialic acid binding receptor expressed by resident and inflammatory macrophage populations. Blood. 2001;97: 288–296. doi:10.1182/blood.V97.1.288

103. Graeber MB, Streit WJ, Kiefer R, Schoen SW, Kreutzberg GW. New expression of myelomonocytic antigens by microglia and perivascular cells following lethal motor neuron injury. J Neuroimmunol. 1990;27: 121–132. doi:10.1016/0165-5728(90)90061-Q

104. Gijbels MJJ, van der Cammen M, van der Laan LJW, Emeis JJ, Havekes LM, Hofker MH, et al. Progression and regression of atherosclerosis in APOE3-Leiden transgenic mice: an immunohistochemical study. Atherosclerosis. 1999;143: 15–25. doi:10.1016/S0021-9150(98)00263-9

105. Zhang Y, Li J-Q, Jiang Z-Z, Li L, Wu Y, Zheng L. CD169 identifies an anti-tumour macrophage subpopulation in human hepatocellular carcinoma. J Pathol. 2016;239: 231–241. doi:10.1002/path.4720

106. Steiniger BS. Human spleen microanatomy: why mice do not suffice. Immunology. 2015;145: 334–346. doi:10.1111/imm.12469

107. Martens J-H, Kzhyshkowska J, Falkowski-Hansen M, Schledzewski K, Gratchev A, Mansmann U, et al. Differential expression of a gene signature for scavenger/lectin receptors by endothelial cells and macrophages in human lymph node sinuses, the primary sites of regional metastasis. J Pathol. 2006;208: 574–589. doi:10.1002/path.1921

Thesis objectives

The RANK/RANKL/OPG triad is involved in many biological processes and unknown mechanisms probably remain to be discovered. Many molecules targeting RANKL have been developed and evaluated. However antibodies targeting the receptor RANK were poorly characterized and would be useful to identify and study RANK expressing cells. Moreover, while a monoclonal antibody targeting RANKL is used for treatment of osteoporosis and bone metastases, no small molecule inhibiting RANK/RANKL interaction was reported. Therefore, the objective of a first part of my thesis was to develop and characterize new molecular tools to study RANK/RANKL. Firstly, I characterized two anti-RANK antibodies for their binding and affinity to RANK as well as their biological activity. Secondly, I performed the screening of a small molecule library to identify compounds inhibiting RANK/RANKL interaction.

It is known that RANKL is required for lymph node development but whether RANKL is required for lymph node homeostasis in adults is not known. Moreover, RANKL plays a role in osteoclast differentiation but whether it also contributes to the differentiation of other macrophages subsets is currently unclear. RANKL is expressed by a stromal cell subset (MRC) in the adult lymph node. Therefore, the objective of a second part of my thesis was to study the effect of RANKL on lymph node homeostasis, more precisely its impact on lymphatic endothelial cells and macrophages. In this work, we identified a new marker of LECs under the control of RANKL. Moreover, we investigated the effect of RANKL deficiency in MRCs on lymph node macrophages and studied the underlying cellular mechanism. The lymph node contains several cell types which could express many signal inducing factors. Thus, a goal of this thesis was to identify RANK expressing cells and try to understand the signals they provide to maintain lymph node macrophage homeostasis.

RESULTS

1. Development of new molecular tools to target RANK-RANKL

1.1. Introduction :

The TNF family member Receptor activator of NF-kB (RANK) was first discovered for its role in osteoclastogenesis caused by increased RANKL levels in response to hormonal changes. In spite of its recognized role in osteoporosis, RANK also plays an important role in the immune system, in the activation of epithelial cells and pathological conditions such as cancer. Therefore, high affinity tools that target the RANK-RANKL axis are important both in investigative research and in therapy. Denosumab is a human monoclonal antibody targeting RANKL and is used for treatment of osteoporosis and bone metastases. Other reagents are also used to manipulate the RANK-RANKL pathway such as OPG-Fc, RANK-Fc or the anti-mouse RANKL antibody IK22-5. To target mouse RANK, an anti-mRANK monoclonal antibody was generated (R12-31) by immunizing rats. Also, screening of a phage display library led to the discovery of a single-chain fraction variable (scFv) binding human and mouse RANK. However, these tools are often insufficiently characterized.

Moreover, two main strategies were used to target RANK activation. Firstly, peptides binding RANK intracellular domain and small molecules interacting with downstream signaling were identified. On the other hand, blocking the interaction between RANK and RANKL is another strategy. Peptidomimetics such as peptides base on the loop 3 of RANK or the binding motif of OPG were described. However, to our knowledge, a small molecule inhibiting the interaction between RANK and RANKL was not reported. Such a molecule could have advantages regarding cost of treatment and route of administration compared to therapeutic antibodies.

During my thesis, we aimed to find new tools to target RANK/RANKL. First we developed a monoclonal antibody targeting RANK based on the sequence of the scFv described by Newa and colleagues. We characterized this antibody together with the already published R12-31 antibody with regard to binding capacity, biological activity, distinct or shared epitope and binding of primary cells (Article 1, *Immunology letters* 2016). We also investigated the effect of these antibodies *in vivo*.

In order to identify a small molecule inhibiting the interaction between RANK and RANKL, I performed the screening of the Prestwick Chemical Library (PCL) using a competitive ELISA assay. We identified a hit and validated it by testing 10 close analogues. We completed the study by testing the compounds *in vitro* in a cellular assay using Jurkat JOM2 cells as well as in an osteoclast differentiation assay (Article 2, in preparation).

1.2. Article 1

Characterization and application of two RANK-specific antibodies with different biological activities

M. Chypre, J. Seaman, O.G. Cordeiro, L. Willen, K.A. Knoop, A. Buchanan, R.C.A. Sainson, I.R. Williams, H. Yagita, P. Schneider, C.G. Mueller

Characterization and application of two RANK-specific antibodies with different biological activities

Mélanie Chypre [a,b], Jonathan Seaman [c], Olga G. Cordeiro [a], Laure Willen [d], Kathryn A. Knoop [e], Andrew Buchanan [c], Richard C.A. Sainson [c], Ifor R. Williams [e], Hideo Yagita [f], Pascal Schneider [d], Christopher G. Mueller [a,*]

[a] CNRS UPR 3572, Laboratory of Immunopathology and Therapeutic Chemistry, University of Strasbourg, Strasbourg 67000, France
[b] Prestwick Chemical, Blvd Gonthier d'Andernach, Parc d'innovation, 67400 Illkirch, France
[c] MedImmune, Granta Park, Cambridge CB21 6GH, UK
[d] Department of Biochemistry, University of Lausanne, Epalinges, Switzerland
[e] Department of Pathology and Laboratory Medicine, Emory University School of Medicine, Atlanta, GA 30322, USA
[f] Department of Immunology, Juntendo University School of Medicine, Tokyo 113-8421, Japan

ARTICLE INFO

ABSTRACT

Antibodies play an important role in therapy and investigative biomedical research. The TNF-family member Receptor Activator of NF-κB (RANK) is known for its role in bone homeostasis and is increasingly recognized as a central player in immune regulation and epithelial cell activation. However, the study of RANK biology has been hampered by missing or insufficient characterization of high affinity tools that recognize RANK. Here, we present a careful description and comparison of two antibodies, RANK-02 obtained by phage display (Newa, 2014 [1]) and R12-31 generated by immunization (Kamijo, 2006 [2]). We found that both antibodies recognized mouse RANK with high affinity, while RANK-02 and R12-31 recognized human RANK with high and lower affinities, respectively. Using a cell apoptosis assay based on stimulation of a RANK:Fas fusion protein, and a cellular NF-κB signaling assay, we showed that R12-31 was agonist for both species. R12-31 interfered little or not at all with the binding of RANKL to RANK, in contrast to RANK-02 that efficiently prevented this interaction. Depending on the assay and species, RANK-02 was either a weak agonist or a partial antagonist of RANK. Both antibodies recognized human Langerhans cells, previously shown to express RANK, while dermal dendritic cells were poorly labeled. In vivo R12-31 agonist activity was demonstrated by its ability to induce the formation of intestinal villous microfold cells in mice. This characterization of two monoclonal antibodies should now allow better evaluation of their application as therapeutic reagents and investigative tools.

© 2016 Elsevier B.V. All rights reserved.

1. Introduction

RANK (Receptor activator of NF-κB) is a signaling receptor [3] engaged by its ligand RANKL [4] but blocked by OPG (osteoprotegerin) that binds RANKL and prevents it from recognizing RANK [5] (for review see Ref. [6]). The RANK–RANKL–OPG triad was originally identified as a regulator of bone mass based on expression of the signaling receptor by pre-osteoclasts and their differentiation into mature osteoclasts by RANKL [5,7,8]. Thus, mice deficient for or overexpressing any of the three proteins display alterations in bone density. The triad is under the regulatory control by different factors, among which sex hormones that link osteoporosis with menopausal hormonal changes or hormone ablation therapy [9]. Hence, a treatment of osteoporosis consists of the administration of Denosumab, a human monoclonal RANKL-neutralizing antibody [10]. Similar reagents are used in animal models, such as anti-RANKL monoclonal antibody IK22-5 [2,11], RANK-Fc fusion protein [12,13] or recombinant OPG [14]. A murine RANK-specific monoclonal antibody (R12-31) has been generated, which was reported as unable to block the binding of RANK-Fc to RANKL [2]. Recently, an antagonist RANK single-chain variable fragment (scFv) reactive against human and mouse RANK has been identified with a capacity to inhibit osteoclastogenesis [1].

The role of RANK is not limited to bone. Macrophages and dendritic cells are of the same lineage as osteoclasts and express this receptor. RANK activation of these cells enhances the immune response by increased cell survival and cytokine production

[3,4,8,15–20]. Also epithelial cells are responsive to RANKL. Thymic medullary epithelial cells require RANK activation signals for maturation [21–23] (for review see Ref. [24]), the development of intestinal microfold epithelial cells is dependent on RANK signals [25,26], and RANK activation is required for the development of lactating mammary gland epithelial cells during pregnancy [27–29] (for review see Ref. [9]). However, although studies employ RANK-specific antibodies [13,25,30,31], these antibodies remain insufficiently characterized.

Therefore, in addition to potential therapeutic applications, specific antibodies are important investigative tools to study the distribution and function of RANK, RANKL and OPG. The RANKL monoclonal antibody IK22-5 [2] was used to demonstrate the production of RANKL by osteocytes [32], T cells [32–34], innate lymphoid cells [35] or lymph node stromal cells [36]. The monoclonal antibody R12-31 has shown RANK expression in synovial tissue and the myeloid cell lineage [37–39]. Although reported as non-antagonist [2] a rigorous analysis of its affinity and its biological activity against mouse and human RANK had not been published. Recently, a scFv reactive against RANK has been generated by phage display [1]. It was shown to recognize human RANK by ELISA, by immunoblot and by immunofluorescence on human osteoclasts and to inhibit osteoclastogenesis of the murine RAW cell line. A detailed affinity and functional analysis of the scFv to evaluate its utility in preclinical studies and investigative research was not performed.

In the present study, we generated an antibody (RANK-02) from the amino acid sequence of RANK-binding scFv and compared it with the anti-RANK monoclonal antibody R12-31 with regard to biological activity, interference with RANKL–RANK interaction, distinct or shared epitopes and recognition of primary RANK-expressing cells. We find that both mAbs recognize human and mouse RANK with high affinity but differ in their biological activity. Both mAbs were used to identify RANK-expressing primary cells and R12-31 was administered to mice to induce the differentiation of intestinal microfold cells.

2. Material and methods

2.1. Production of RANK-02 antibody

The variable domains from the anti-RANK scFv [1] were cloned into human IgG1 heavy chain and light chain expression vectors. These were co-transfected into Chinese hamster ovary cells, and the IgG1, named RANK-01, was purified using MabSelect SuRE (GE Healthcare). RANK-01 demonstrated severe aggregation on production, correlating with the aggregation pattern seen originally with the anti-RANK scFv (see Lam M., Master's thesis, University of Alberta, 2011; https://era.library.ualberta.ca/public/view/item/uuid:0036405c-4d76-49a0-b2c7-21c148af44f4). Analysis of the variable domain sequence identified the absence of a canonical heavy chain framework methionine residue at Kabat position 82. Site directed mutagenesis was therefore employed to insert the missing codon, generating a new human IgG heavy chain vector. This vector was co-transfected with the existing light chain vector to generate an improved anti-RANK IgG1, named RANK-02, which did not aggregate on production.

2.2. ELISA

For ELISA with RANK-02, recombinant human and mouse RANK-Fc were coated overnight at 20 μg/ml in PBS in 96 well plates (Nunc). Plates were washed with PBS, blocked for 1 h at room temperature with PBS containing 3% (w/v) milk powder and washed again. RANK-02 and an isotype control IgG1 were added, the

plates incubated for one hour at room temperature and washed three times with PBS/0.1% Tween 20. Peroxidase-coupled goat anti-human kappa light chain antibody (Sigma, A7164) was diluted 1:5000, 50 μl was added to each well and the plates were incubated for 1 h. After three washes with PBS/0.1% Tween 20, 50 μl of tetramethylbenzidine (TMB, Sigma–Aldrich) was added to each well and incubated for five minutes before neutralization with 50 μl 0.5 M H_2SO_4. Plates were read on a PerkinElmer Envision 2100 plate reader measuring absorbance at 450 nm and analyzed in Graph-Pad PRISM. For ELISA with R12-31, hRANK and mRANK-Fc were coated at 1 μg/ml in PBS for 3 h at 37 °C. Plates were blocked with PBS containing 4% (w/v) milk powder and 0.05% Tween 20 for 1 h 37 °C. Titrated amounts of R12-31 were added, the plates incubated for 1 h at 37 °C and washed 3 times with PBS/0.05% Tween 20. Peroxidase-coupled goat anti-rat IgG, light chain specific (Jackson Immunoreasearch) was diluted 1:5000, 100 μl was added to the plates and the plates were incubated for 1 h at 37 °C. After three washes with PBS/0.05% Tween 20, 75 μl of tetramethylbenzidine (TMB) was added to each wells and then neutralized with 25 μl HCL 1 N. Plates were read at 450 nm on Multiskan Ex (MTX Labsystems Inc.).

For the competitive ELISA assay, hRANK-Fc was coated at 5 μg/ml. After blocking, wells were incubated for 1 h at 37 °C with titrated amounts of the four antibodies (RANK-02 hIgG1 anti-RANK, NIP288 hIgG1 control; R12.31 rat IgG2a anti-mRANK, rat IgG2a control). Without washing, a constant volume of conditioned supernatant of 293T cells transfected with Flag-ACRP-hRANKL (5 μl) or Flag-mRANKL (20 μl) was added to wells. Volumes were chosen for their abilities to generate a close to maximal but non-saturating signal. Binding of Flag-ACRP-hRANKL was revealed with biotin-conjugated M2-antibody (0.5 μg/ml) (Sigma) and streptavidin-HRP (Jackson immunoresearch) (1/4000).

2.3. Affinity measurements by surface plasmon resonance

Real-time binding kinetics to mRANK-Fc (Sigma–Aldrich) and hRANK-Fc (purified from transfected HEK 293 cells) were measured on a BIAcore 3000. The proteins were immobilized by injecting 6 μg of RANK-Fc on a CM5 chip activated with N-ethyl-N'-dimethylaminopropyl carbodiimide/N-hydroxysuccinimide (GE-Healthcare, Uppsala, Sweden) in formate buffer, pH 4.3, which gave a signal of approximately 2000 RU. Free active sites were quenched with ethanolamine hydrochloride, pH 8.5. Binding was performed in 10 mM HEPES-buffered saline containing 0.005% v/v surfactant P20 at 25 °C with a constant flow rate of 30 μl/min. The antibodies were injected at 0.1–4 nM (RANK-02) and 2–70 nM for R12-31. The sensor chip was regenerated after each experiment by injecting 10 μl of EDTA 0.5 M, pH 8. The kinetic parameters were calculated using the BIAeval 4.1 software, and the analysis used the simple Langmuir binding model k_{on}/k_{off}. Specific binding profiles were obtained by subtracting the response signal from the control channel (activated/deactivated) and from blank-buffer injection. The fitting of each model was judged by the χ^2 value and randomness of residue distribution compared to the theoretical model (Langmuir binding 1:1).

2.4. Flow cytometry

All labeling were performed at 4 °C in PBS, 2% fetal calf serum (FCS), 2.5 mM EDTA with the following antibodies: anti-RANK R12-31, anti-RANK RANK-02, rat IgG2a isotype control (BectonDickinson [BD]-Pharmingen, San Jose, CA, USA), NIP228 human IgG1 isotype control (MedImmune Inc.), donkey anti-rat Ig-PE (Jackson Immunoresearch), donkey anti-human Ig-PE (Jackson Immunoresearch). For flow cytometric analysis of human skin the following antibodies were used: anti-HLA DR (L203, R&D Systems),

7

anti-DC-SIGN (DCN46, BD-Pharmingen), anti-Langerin (929F3.01, Dendritics, Lyon, France), anti-CD14 (M5E2, BD-Pharmingen). Fixable Viability Dye eFluor® 780 (ebioscience) was used to exclude the dead cells. Flow cytometry was performed on a FACS-Calibur (BD) or Gallios (Beckman-Coulter, Fullerton, CA, USA) and the flow cytometry data were analyzed using the FlowJo software (Treestar, Ashland, OR, USA). Langerhans and dermal dendritic cells were isolated from human skin as described [40].

To determine recognition of different epitopes, Jurkat JOM2 mRANK:Fas and Jurkat JOM2 hRANK:Fas were incubated on ice for 15 min with increasing amounts of unlabeled competitor antibody, followed without washing by a fixed concentration of biotinylated test mAb for 20 min on ice. Cells were then washed and binding of test mAb revealed with PE-conjugated streptavidin.

2.5. Cell culture

All cells were maintained in a humidified incubator with 5% CO_2 at 37 °C. Jurkat JOM2, Jurkat JOM2 mRANK:Fas and Jurkat JOM2 hRANK:Fas, were grown in RPMI 1640 medium supplemented with 10% FCS. Jurkat JOM2 mRANK:Fas and Jurkat JOM2 hRANK:Fas were generated according to a described protocol [41,42]. HEK 293 cells stably transfected with mRANK [31] or with hRANK (a kind gift of Dr. D. Heymann, University of Nantes, France) were grown in DMEM supplemented with 10% FCS, gentamicin (10 μg/ml) and penicillin/streptomycin (100 U/ml). G418 selection (500 μg/ml) was used to maintain HEK 293-mRANK cell line.

2.5.1. Cell viability assay

Jurkat JOM2, Jurkat JOM2 mRANK:Fas and Jurkat JOM2 hRANK:Fas (50×10^3 cells/100 μl) were incubated for 16 h with ligands or antibodies as indicated. For RANK-02 blocking assay, 75×10^3 cells/100 μl were incubated for 1 h with 50 μg/ml RANK-02 antibody before treatment with GST-mRANKL for 6 h. Cell viability was then assessed using the CellTiter 96 Aqueous One Solution (Promega) according to manufacturer's instructions. Absorbance was measured at 490 nm using a Mithras LB940 reader (Berthold technologies). All assays were performed in duplicates and repeated at least three times. Untreated cells were set at 100% control level of cell viability.

2.5.2. NF-κB reporter gene assay

HEK 293-mRANK and HEK 293-hRANK were transiently transfected with NF-κB1 luciferase reporter vector (Panomics) and an internal control EF1-β-galactosidase plasmid (a kind gift from Sylvie Mémet, Institut Pasteur, Paris, France) using lipofectamine 2000 (Life Technologies). 24 h after transfection, cells were treated in duplicates with ligands or antibodies as indicated. After 16 h of treatment, cells were lysed using reporter lysis buffer (Promega). Luciferase activity was measured by luminescence on a Mithras LB940 reader (Berthold Technologies) using luciferase assay system (Promega). Beta-galactosidase activity was used to normalize the luminescence values for transfection efficiency. It was measured by reading absorbance at 450 nm on Multiskan Ex (MTX Labsystems Inc.) using β-galactosidase enzyme assay system (Promega). To assay RANK-02 antagonist activity, transfected HEK 293-mRANK were pretreated for 1 h with RANK-02 at 50 μg/ml before adding GST-mRANKL at 0.1 μg/ml for 6 h. IK22-5 anti-RANKL antibody was used at 10 μg/ml as a positive control for inhibition of RANK–RANKL interaction.

2.6. Villous microfold cell induction by R12-31 and GST-mRANKL administration

C57BL/6 mice were treated i.p. with 100 μg of anti-RANK R12-31 antibody on days 0, 2, and 4 or with 50 μg i.p. of GST-mRANKL

on day 0 plus 100 μg GST-mRANKL s.c. on days 0–4. On day 5, the proximal ileum was removed for tissue analysis. The tissue was stained with rhodamine-UEA-I as previously described [25].

2.7. Serum TRACP 5b detection after RANK-02 and GST-mRANKL administration

Adult C57BL/6 mice were treated i.p with RANK-02 antibody 1 h before administration of GST-mRANKL (25 μg/mouse) i.p. Fifteen hours afterwards, serum was taken for the measure of TRACP 5b by ELISA according to the manufacturer's instructions (Immunodiagnostic systems).

2.8. Statistical analysis

Statistical significance was calculated by one or two way ANOVA/Bonferroni using the PRISM software. *<0.05, **<0.01, ***<0.001, ****<0.0001, ns = not statistically significant.

3. Results

3.1. Specificity and affinity of R12-31 and RANK-02 for mouse RANK

The nucleic acid sequence obtained from a human RANK-Fc-selected scFv [1] was modified to generate a recombinant human antibody, termed RANK-02 (see Section 2). We first investigated its affinity and specificity for mouse (m) RANK and could expect recognition of mRANK because the scFv inhibited osteoclast formation of a murine cell line. However, no further analyses were reported [1]. To first evaluate binding to mRANK we performed an ELISA in comparison with the known RANK-specific mAb R12-31 [2]. Both antibodies recognized the fusion protein in a dose dependent manner (Fig. 1A). Affinities of both mAbs were determined by surface plasmon resonance, and they bound mRANK-Fc with high affinity (~0.2 nM) (Table 1). To further confirm their specificity, we performed flow cytometry analysis on two different cell lines both expressing the extracellular domain of mRANK and compared the signal intensity with that obtained with the parental cell lines. We used the Jurkat human T cell line, deficient for Fas (Jurkat JOM2) and stably expressing the mRANK extracellular domain fused to the transmembrane and intracellular domains of human Fas (Jurkat JOM2 mRANK:Fas) [41], and the human embryonic kidney cells HEK 293 cells, stably transfected with full-length mRANK (HEK 293-mRANK). The antibodies failed to recognize parental cell lines but bound the mRANK-expressing cells (Fig. 1B). The analysis of the mean fluorescence intensity showed that R12-31 generated a slightly stronger signal than RANK-02 (Supplementary Fig. 1A, B). Therefore, RANK-02 and R12-31 specifically recognize the extracellular domain of mRANK with high affinity.
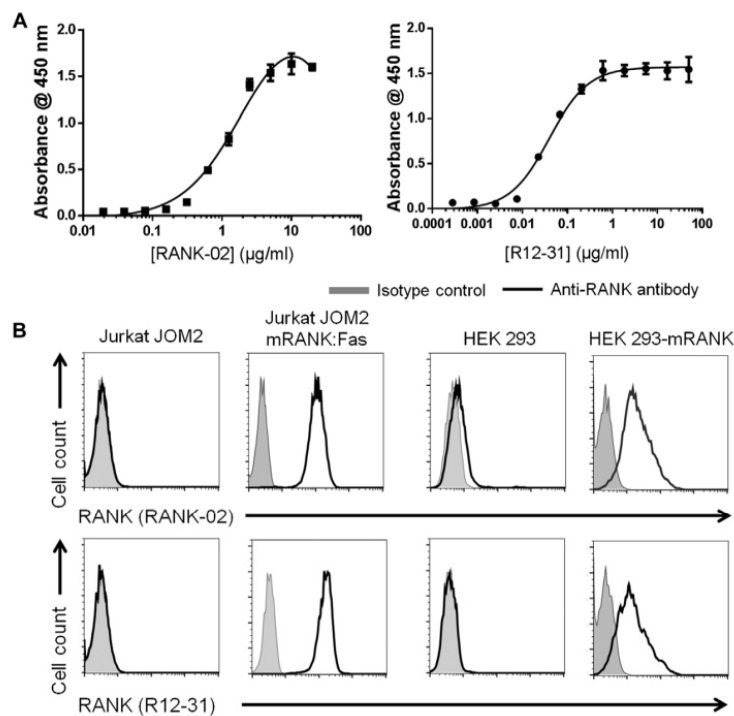
Table 1
Association rates (K_{on}), dissociation rates (K_{off}) and binding affinities (KD) of anti-RANK antibodies on murine and human RANK-Fc were measured by surface plasmon resonance.

	K_{on} ($M^{-1}\,s^{-1}$)	K_{off} (s^{-1})	KD (M)
	Mouse RANK-Fc		
RANK-02	7.08×10^5	1.44×10^{-4}	2.03×10^{-10}
R12-31	5.14×10^4	8.99×10^{-6}	1.75×10^{-10}
	Human RANK-Fc		
RANK-02	3.32×10^5	4.12×10^{-5}	1.24×10^{-10}
R12-31	2.32×10^3	5.97×10^{-5}	2.57×10^{-8}

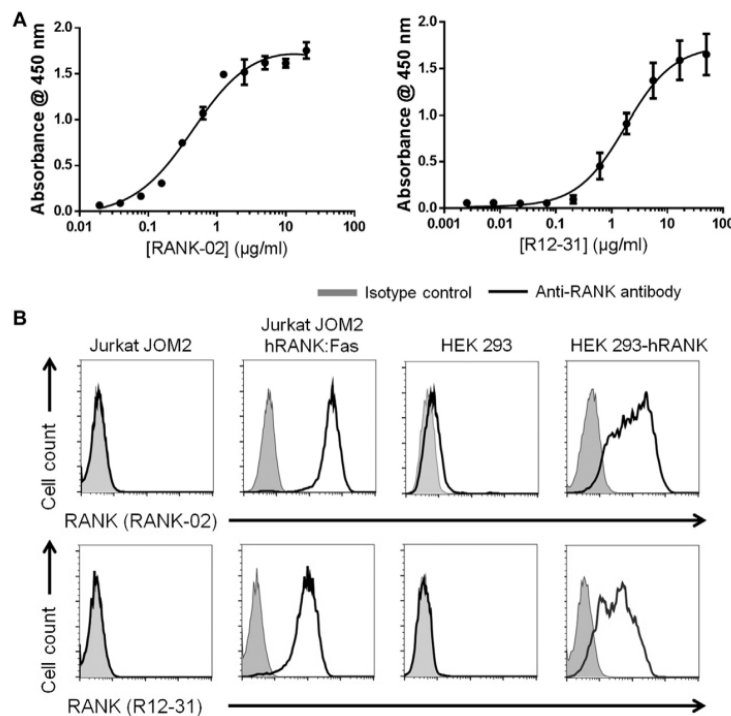8   *M. Chypre et al. / Immunology Letters 171 (2016) 5–14*

Fig. 1. RANK-directed antibodies RANK-02 and R12-31 bind to the mouse RANK extracellular domain. (A) Recognition of mouse RANK-Fc fusion protein by ELISA. Data is expressed as color production (absorbance at 450 nm) by enzyme-coupled secondary antibody recognizing increasing concentrations of RANK-02 and R12-31 bound to fixed concentration of surface-attached mRANK-Fc. (B) Detection by flow cytometry of mouse RANK stably expressed either by Jurkat JOM2 cells (as fusion protein between the RANK extracellular domain and the intracellular domain of human Fas) or by HEK 293 cells (as full-length RANK). Primary antibodies were either RANK-02 or R12-31 and secondary antibodies were donkey anti-human immunoglobulin or donkey anti-rat immunoglobulin, respectively, conjugated to phycoerythrin. Controls were untransfected cells and primary antibody isotypes. Data is representative of 5 independent experiments.

3.2. Biological activity of R12-31 and RANK-02 on mouse RANK

Like any TNF receptor superfamily member, RANK signaling requires multimerization to recruit downstream signaling adaptors. The biological activity of antibodies was first characterized using the JOM2 mRANK:Fas cell line. A comparison between JOM2 mRANK:Fas cells and the parental cell line showed that GST-mRANKL specifically killed JOM2 mRANK:Fas cells by engaging the surrogate Fas apoptotic signaling pathway (Supplementary Fig. 2A). Apoptosis was not observed in response to GST alone (Supplementary Fig. 2B). Incubation of JOM2 mRANK:Fas cells with R12-31 led to cell death (Fig. 2A), while its isotype control (data not shown) and the RANK-02 antibody had no observed effect even at high concentrations (Fig. 2B). These results suggest that R12-31 and RANK-02 antibodies have distinct biological properties. These findings were validated using a canonical NF-κB activation assay in HEK293 cells transfected with full-length mRANK. Stimulation of these cells with GST-mRANKL as a positive control or with R12-31 both induced NF-κB activation, while RANK-02 did not (Fig. 2C, D). R12-31 and RANK-02 were used at 25 μg/ml and 50 μg/ml, respectively, to be in line with the concentrations of 100 nM of scFV used in Newa et al. and the expected low biological activity of the latter (Fig. 2B) [1]. Because the RANK-02 equivalent scFv could inhibit osteoclastogenesis [1], we next assayed the antagonist activity of RANK-02. Indeed, when Jurkat JOM2 mRANK:Fas cells were pre-incubated with 50 μg/ml RANK-02 prior to addition of recombinant mRANKL, cell death was almost completely inhibited (Fig. 2E). Similarly, the anti-RANK-02 antibody diminished NF-κB activation by recombinant RANKL (Fig. 2F), but again less efficiently than the anti-RANKL antibody IK22-5 (Fig. 2E, F). Altogether, the above data demonstrate

that R12-31 and RANK-02 bind mRANK with similar affinities, but differ in their biological effects.

3.3. Specificity and affinity of R12-31 and RANK-02 for human RANK

We extended these analyses to human (h) RANK and observed that RANK-02 and R12-31 also recognized hRANK-Fc in ELISA (Fig. 3A). We next compared the affinity of both antibodies to hRANK-Fc by surface plasmon resonance and obtained an affinity of RANK-02 for hRANK in the subnanomolar range (0.12 nM) while R12-31 recognized hRANK with a 200-fold lower affinity (25 nM) (Table 1). To test if the antibodies recognized hRANK-transfected cell lines, we used JOM2 hRANK:Fas cells and HEK 293 cells transfected with full length hRANK. Both antibodies bound Jurkat JOM2 hRANK:Fas and HEK 293-hRANK, but not their parent cell lines (Fig. 3B). Although R12-31 labeled hRANK-expressing cells by flow cytometry, it did so less efficiently than RANK-02, as its MFI values were lower compared to those obtained with RANK-02 (Supplementary Fig. 1C, D). This may be attributable to the lower affinity of R12-31 for hRANK. This confirms that the specificity of these antibodies extends to hRANK.

3.4. Biological effects of R12-31 and RANK-02 on human RANK

We used cell lines expressing hRANK or hRANK:Fas fusion protein to investigate the biological effects of the antibodies on hRANK. R12-31 again displayed agonist activity (Fig. 4A) with an EC50 of 5.7 ng/ml, comparable to that observed with mRANK:Fas cells (EC50 of 2.4 ng/ml). However, as hRANK:Fas reporter cells are about 6 times more sensitive than mRANK:Fas reporter cells (Supplemen-

115
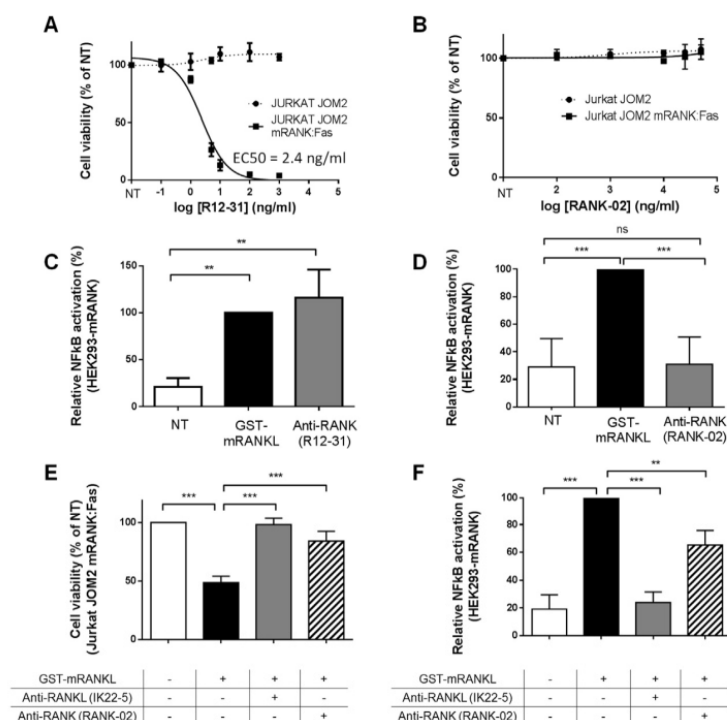
Fig. 2. The anti-RANK antibodies have different biological activities on mouse RANK. (A) Dose–response curve of R12-31 antibody on Jurkat JOM2 cells expressing or not mRANK:Fas. The graph displays % cell viability relative to Jurkat JOM2 cells grown in the absence of antibody (non-treated, NT) as a function of increasing concentrations of R12-31. Data points are the mean ($\pm$SD, $n = 3$ with duplicate wells). Curve fitting was performed using the PRISM software. (B) As for panel A, but using the antibody RANK-02. (C) NF-κB activation by R12-31 of HEK 293 cells stably expressing full-length murine RANK and transfected with an NF-κB responsive luciferase reporter gene and a β-galactosidase expressing transfection control plasmid. Data are the mean % relative to RANKL-activated cells ($\pm$SD, $n = 3$ with duplicate wells). Data are for 0.1 μg/ml RANKL and 25 μg/ml R12-31 antibody. NT = non-treated cells. (D) As for panel B, but using RANK-02 antibody (50 μg/ml). (E) The antagonist activity of RANK-02 was tested by its capacity to block mRANK:Fas-mediated cell apoptosis triggered by recombinant GST-mRANKL. The graph presents JOM2 mRANK:Fas cell viability in the absence or presence of recombinant RANKL, the RANKL-blocking antibody IK22-5 and RANK-02, relative to non-treated cells (NT). RANKL was used at 1 ng/ml, IK22-5 at 10 μg/ml and RANK-02 at 50 μg/ml. (F) The antagonist effect of RANK-02 was tested by its capacity to block NF-κB activation elicited by recombinant RANKL. Data are expressed as the mean% ($\pm$SD, $n = 3$ with duplicate wells) relative to RANKL-induced NF-κB activation. RANKL was used at 0.1 μg/ml, IK22-5 at 10 μg/ml and RANK-02 at 50 μg/ml. For data panels (C–F), statistical significance was calculated by one way ANOVA/Bonferroni using the PRISM software.

tary Fig. 2C, D), the agonist activity of R12-31 is altogether roughly more than 10-fold less efficient on hRANK:Fas cells compared to mRANK:Fas cells, in line with its lower affinity for hRANK. RANK-02 exhibited weak agonist activity on hRANK:Fas cells at high concentrations (EC50 of 470 ng/ml) that however never induced complete apoptosis (Fig. 4B). This apparent discrepancy with results obtained on mRANK:Fas cells might be explained by the intrinsic higher sensitivity of hRANK:Fas cells to apoptosis. Isotype controls had no effect at the highest dose tested for R12-31 and RANK-02 (Fig. 4C). We next performed the NF-κB reporter assay in HEK 293-hRANK cells and observed agonist effects for both mAbs with RANK-02 displaying again weaker activity (Fig. 4D). These findings confirm that R12-31 is an agonist for RANK, across the species, and revealed a weak agonist effect of RANK-02 on hRANK.

3.5. RANK-02 efficiently interfered with RANK–RANKL interaction and recognized an epitope distinct from R12-31

In order to understand the molecular mechanism by which RANK-02 antagonized the action of RANKL on RANK-expressing cells, we measured its ability to interfere with the binding of Flag-RANKL to Fc-RANK in an ELISA-based assay. Pre-incubation of coated hRANK-Fc with RANK-02 efficiently prevented further binding of human or mouse RANKL, strongly suggesting that the binding sites of RANK-02 and RANKL on hRANK overlap (Fig. 5A).

In contrast, pre-incubation of coated hRANK-Fc with the mAb R12-31 did not prevent the binding of hRANKL, and only marginally interfered with the binding of mRANKL, indicating that its binding site is distinct, or only very partially common with that of hRANKL and mRANKL, respectively (Fig. 5A). Control antibodies did not interfere with RANKL–RANK interactions. To further address the question of overlapping or distinct epitopes between the mAbs, we performed a competition assay for their binding to hRANK-, or to mRANK-expressing cells by FACS. To this end, h/mRANK:Fas cells were incubated with increasing concentrations of unlabeled RANK-02, R12-31, or their isotype controls, followed by biotinylated RANK-02 and phycoerythrin-conjugated streptavidin. Cell labeling was determined by FACS and the MFI calculated. This was also performed for R12-31. As depicted in Supplementary Fig. 3 and summarized in Fig. 5B, RANK-02 competes only with biotinylated RANK-02 on h/mRANK, and R12-31 competes only with biotinylated R12-31 on h/mRANK, showing that RANK-02 and R12-31 recognize distinct epitopes.

3.6. Labeling of RANK on primary human Langerhans cells with RANK-02 and R12-31

To investigate whether the antibodies are suitable for the detection of endogenous RANK, we incubated them with primary human skin dermal dendritic cells and Langerhans cells. Langerhans cells

10   *M. Chypre et al. / Immunology Letters 171 (2016) 5–14*

Fig. 3. RANK-directed antibodies RANK-02 and R12-31 bind to the human RANK extracellular domain. (A) Recognition of human RANK-Fc fusion protein by ELISA. Data is expressed as color production (absorbance at 450 nm) by enzyme-coupled secondary antibody recognizing increasing concentrations of RANK-02 and R12-31 bound to fixed concentration of surface-attached RANK-Fc. (B) Detection by flow cytometry of human RANK stably expressed either by Jurkat JOM2 cells (as a fusion protein between the RANK extracellular domain and the intracellular domain of human Fas) or by HEK 293 cells (as full-length RANK). Detection was performed as described in Fig. 1B. Data is representative of 5 independent experiments.

have previously been shown to express RANK using the mAb683 (R&D Systems) [18,19]. Whether the related dermal dendritic cells also express RANK is not known. After allowing cells to migrate from human skin into culture medium, they were harvested and labeled for different markers to identify three subsets (Fig. 6A). The Langerhans cells (subset I) was clearly recognized by both RANK-02 and R12-31 mAbs (Fig. 6B), the CD14− dermal dendritic cells (subset II) expressed low levels of RANK, and the CD14+ population (subset III) was devoid of RANK (Fig. 6C, D). Both mAbs are valid tools to detect RANK expression on primary cells, as the values of % positive Langerhans cells (Fig. 6E) and the MFI (Fig. 6F) were not significantly different. The data show that migrated human Langerhans cells express the highest levels of RANK among human skin dendritic cells.

3.7. Assessment of antibody activity in vivo

To assess mAb activities *in vivo*, we determined the capacity of RANK-02 to inhibit recombinant RANKL to activate the release of the tartrate-resistant acid phosphatase isoform b (TRACP 5b) by osteoclasts [43,44]. Mice received increasing doses of RANK-02 1 h before administration of 25 μg GST-RANKL (1 mg/kg), and TRACP 5b was measured in the serum by ELISA 15 h later. RANKL resulted in a 30% increase of TRACP 5b, however RANK-02 did not significantly alter this level (Fig. 7A). We had previously shown that the administration of GST-mRANKL induced the ectopic differentiation of cells of the villous small intestinal epithelium into microfold (M) cells [25]. We therefore tested whether R12-31 could induce the formation of villous M cells. To this end, mice were left untreated

or received either R12-31 or GST-mRANKL for 5 days. Thin strips of intestinal tissue were then prepared for staining with rhodamine UEA-I that labels M cells. Small intestinal UEA-I+ villous M cells were readily observed in mice treated with R12-31 or with recombinant RANKL, in contrast to untreated mice that showed only few UEA-I+ cells (Fig. 7B and C). This shows that R12-31 exerts agonist activity *in vivo*.

4. Discussion

We estimated that a detailed characterization of two RANK-specific mAbs, one derived from a scFv selected against hRANK and one generated in the rat against mRANK [1,2], would be beneficial to their evaluation as therapeutic reagents and investigative tools. We found that both mAbs bound to mouse and human RANK-Fc in ELISA and surface plasmon resonance and recognized RANK-expressing cell lines or primary cells in flow cytometry. The mAbs recognized distinct epitopes on RANK and displayed differences in their biological activities and in their capacity to inhibit RANKL–RANK interaction. We showed that the agonist mAb R12-31 is functional *in vivo*.

RANK-02 and R12-31 recognized human and mouse RANK in ELISA, plasmon resonance and in flow cytometry. Cross-reactivity between RANK from both species can be expected because mouse and human RANK share 73% sequence identity [3]. R12-31, which was generated by immunization of rats with mRANK-transfected cells, had a high affinity for mRANK but a lower affinity for hRANK. Although R12-31 comparatively stained mRANK-transfected cells better than hRANK-transfected ones, it was good enough to label
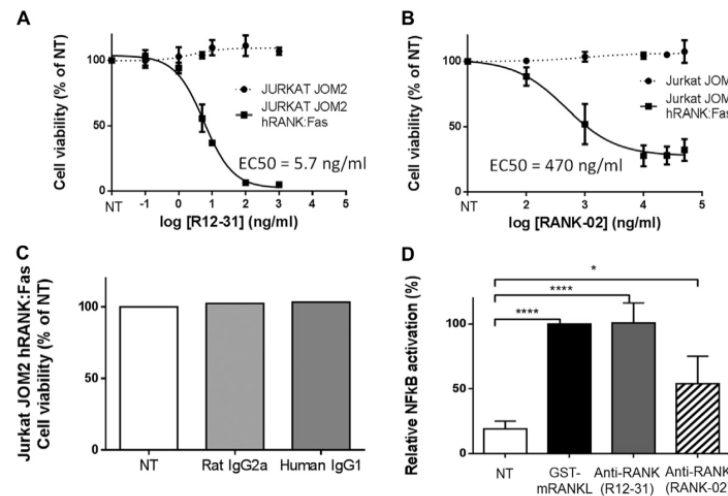
Fig. 4. Both antibodies are agonists on human RANK. (A) Dose–response curve of the R12-31 antibody on Jurkat JOM2 cells expressing or not hRANK:Fas. The graph displays cell viability relative to the percentage of Jurkat JOM2 cells grown in the absence of antibody as a function of increasing concentrations of anti-RANK antibody R12-31. Data points are the mean ($\pm$SD, $n = 3$ with duplicate wells). Curve fitting was performed using the PRISM software. NT = non-treated cells. (B) As for panel A, but using the RANK-02 antibody. (C) The JOM2 hRANK:Fas cell viability assay shows that isotype controls for R12-31 (rat IgG2a, 1 μg/ml) and for RANK-02 (human IgG1, 50 μg/ml) have no human RANK-stimulating effect. (D) NF-κB activation by R12-31 and RANK-02 antibodies in HEK 293 cells stably expressing full-length human RANK and transfected with an NF-κB-responsive luciferase reporter gene. Data are the mean % relative to RANKL-activated cells ($\pm$SD, $n = 3$ with duplicate wells). Data is shown for 0.1 μg/ml RANKL, 25 μg/ml R12-31 and 50 μg/ml RANK-02. NT = non-treated cells. Statistical significance was calculated by one way ANOVA/Bonferroni using the PRISM software.

human Langerhans cells. RANK-02 was obtained using a phage display selection with the hRANK extracellular domain and had a high affinity for both human and mouse RANK. Thus, this mAb may be the reagent of choice to detect human cells expressing low levels of RANK, such as CD14$^-$ dermal dendritic cells.

Biological activities of these antibodies were determined using cell lines stably expressing either RANK:Fas fusion proteins or full-length RANKs. Data showed that R12-31 was agonist on both human and mouse RANK, however, in line with its higher affinity, the activity was stronger on mRANK. A competitive ELISA further revealed that R12-31 most probably recognized a site distinct from that occupied by RANKL. This is compatible with a scenario upon which engagement of RANK by R12-31 induces conformational changes and/or aggregation of RANK that all in all mimic the action of the ligand. The biological activity of R12-31 was demonstrated *in vivo* by its ability to trigger the conversion of intestinal cells into M cells. The biological assays for RANK-02 yielded species-specific results: an antagonist activity was observed for mRANK and an agonist effect was seen for the human orthologue. However, its antagonist effect was weaker than that seen with anti-RANKL IK22-5 antibody, and the agonist activity may only have been detectable because of the high sensitivity of the cellular assays. *In vivo*, RANK-02 proved unable to inhibit recombinant RANKL-stimulated osteoclast activity. The competitive ELISA assay showed that RANK-02 competed at low concentrations with mouse and human RANKL for binding to hRANK. Thus, the capacity of RANK-02 to interfere with receptor–ligand interaction can explain its *in vitro* antagonist activity, while its agonist activity is likely triggered by its direct binding to RANK. EDAR is like RANK a TNF family member, and in a previous study characterizing a panel of anti-EDAR antibodies, it was found, using EDAR:Fas reporter cells, that several antibodies were agonist in this system while others were not. What correlated with agonist activity in this experimental system was not the affinities of antibodies, but their ability to detach slowly once bound (small k_{off}) [42]. Interestingly, RANK-02 and R12-31 have the same affinity for mRANK but R12-31 has a lower k_{off} rate. Differences in agonist activities between RANK-02 and R12-31 might also reflect binding epitopes that may be more or less

favorable for generating an active conformation of the receptor. Indeed, we found that the mAbs recognized distinct epitopes on RANK. RANK-02 proved to be an excellent reagent for the detection of endogenous RANK on primary human skin Langerhans cells by FACS. A staining protocol with both antibodies would provide a strong guarantee of specificity because they recognize distinct epitopes, implying that if these antibodies cross-react with other antigens, these are unlikely to be shared. We confirm using primary human skin cells that Langerhans cells express high levels of RANK, whereas CD14$^-$ dendritic cells express RANK weakly and CD14$^+$ dendritic cells none. It has been shown that RANK expression by dendritic cells, inclusive Langerhans cells, prolongs cell survival [4,18], which may also endow Langerhans cells exiting the skin to prolong interaction with T cells. Indeed, human Langerhans cells have been shown to be more potent T cell activators than dermal dendritic cells [45]. Interestingly, RANK has also been implicated in the formation of regulatory T cells [12], suggesting an implication of RANK in the regulation of immunity by Langerhans cells [46–48]. Hair follicles in their growth phase are a natural source of RANKL [31], and this phase of the hair cycle is characterized by a reduced delayed-type hypersensitivity response [49], a cutaneous reaction implicating Langerhans cells. Intestinal M cells are specialized epithelial cells implicated in the transport of antigen from the lumen to underlying cells. Peyer's patches and isolated lymphoid follicles comprise numerous M cells to help generate immune responses against intestinal microflora. M cells are absent in RANKL or Spi-B knock-out mice entailing the failure of the immune system to respond to intestinal pathogens. Administration of recombinant RANKL has been shown to restore M cells in RANKL−/− mice and leads to an increase in M cells on small intestinal villi [25,26]. Here we show that RANK agonist R12-31 likewise leads to ectopic M cell differentiation of villous epithelial cells, demonstrating its agonist activity *in vivo* and that RANK signaling is responsible for M cell formation.

In conclusion, we have performed a detailed characterization of two anti-RANK mAbs with respect to affinity, specificity, activity and applications. These findings should help advance our under-
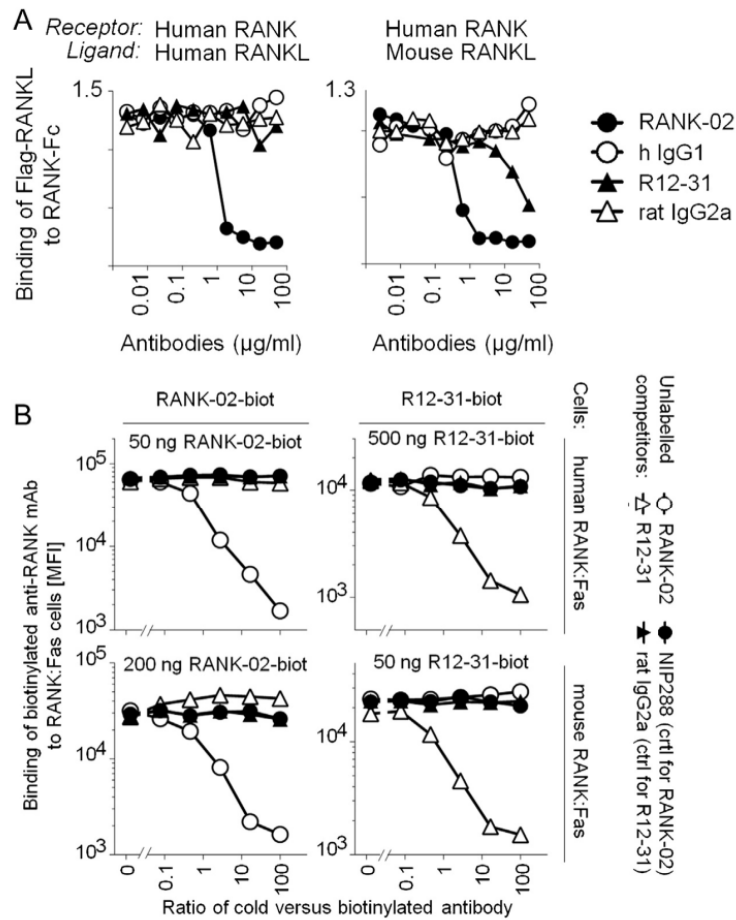
Fig. 5. Analysis of shared or distinct epitopes. (A) RANKL blocking by the mAbs. ELISA plates were coated with human RANK-Fc, incubated first with the mAbs and then with human (left) or mouse (right) RANKL. The amount of bound RANKL was measured. The data show that the binding sites of RANK-02 and RANKL overlap, but that they are distinct for R12-31 and RANKL. (B) Competitive FACS to determine RANK-02/R12-31 distinct or shared epitopes. Jurkat JOM2 mRANK:Fas and Jurkat JOM2 hRANK:Fas were incubated on ice for 15 min with increasing amounts of unlabeled competitor antibody, followed without washing by a fixed concentration of biotinylated test mAb for 20 min on ice. Cells were then washed and the binding of test mAb revealed with PE-conjugated streptavidin. Graphs show that RANK-02 and R12-31 do not cross-compete for binding to RANK-expressing cells.
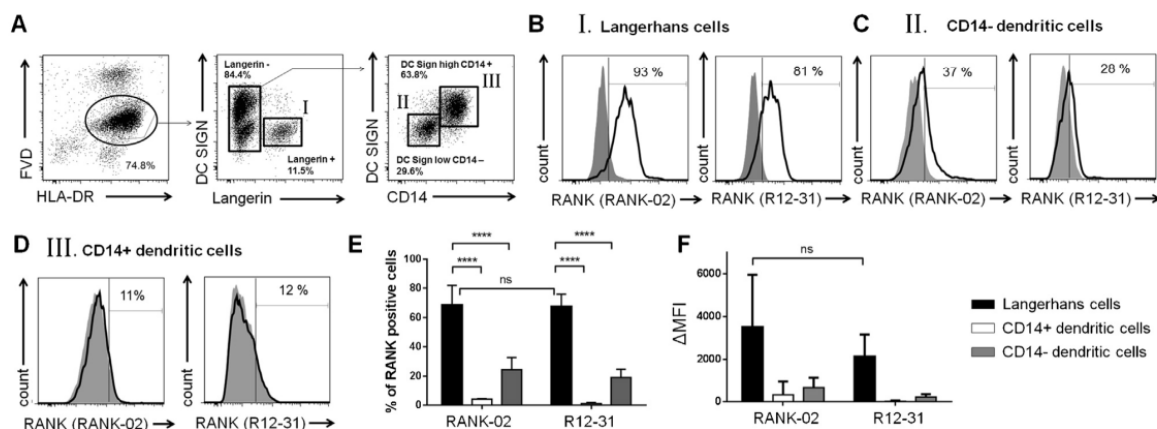
Fig. 6. The anti-RANK mAbs recognize RANK on primary human Langerhans cells. (A) Flow cytometry gating strategy to obtain three cell populations: Langerin+ cells (population I), and CD14− and CD14+ dermal dendritic cells (populations II and III, respectively). Dead cells are excluded using the FVD stain. Human RANK expression by Langerhans cells (B), CD14− dendritic cells (C) and CD14+ dendritic cells (D) using both anti-RANK mAbs and their isotype controls (in gray). The percentage of positive cells is indicated. (E) Mean percentage of RANK-positive cells ± SD measured with RANK-02 or R12-31 staining in three different populations of dendritic cells isolated from three donors ($n = 3$ donors). (F) mean of ΔMFI ± SD measured with RANK-02 or R12-31 staining in the three different populations of dendritic cells isolated from three donors ($n = 3$). ΔMFI = MFI RANK antibody − MFI isotype control. Statistical significance was calculated by two way ANOVA/Bonferroni using the PRISM software.
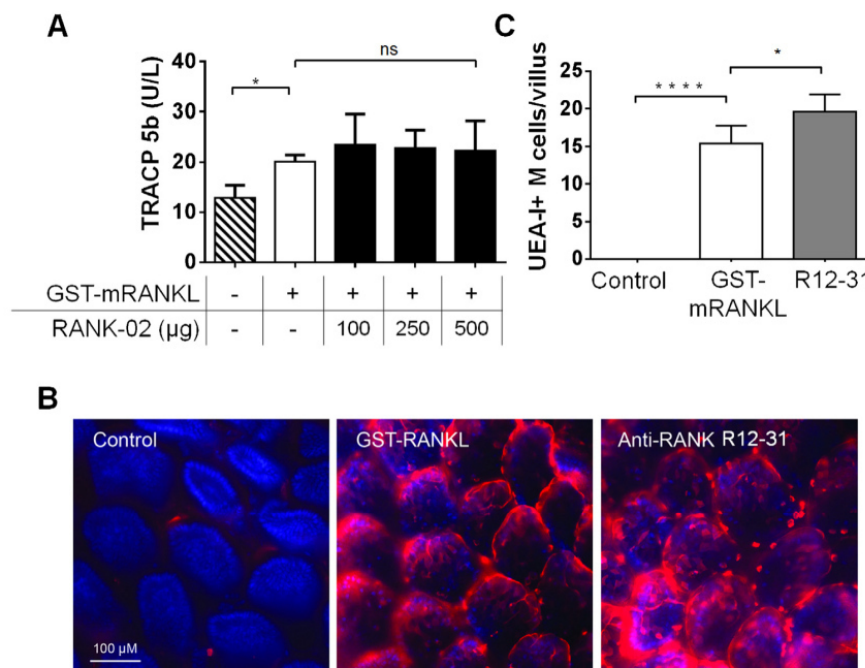
Fig. 7. Assessment of biological activities *in vivo*. (A) RANK-02 antagonist activity was measured as inhibition of osteoclast-dependent release of TRACP 5b into serum. The data is the mean (SEM, $n = 4$) of TRACP 5b in mice mock treated (PBS), or injected with 25 μg GST-mRANKL alone or in the presence of increasing amounts of RANK-02. (B, C) R12-31 agonist activity was determined as the capacity to induce M cells in the proximal ileum of C57BL/6 mice. (B) Whole mount staining for UEA-I$^+$ M cells in the proximal ileum, untreated or treated with GST-mRANKL or R12-31 mAb for 5 days. Nuclear counterstain was with DAPI. In untreated mice no villous M cells are found, whilst anti-RANK R12-31 mAb and recombinant-mRANKL induce a large number of polygonal UEA-I$^+$ villous M cells. Scale bar is 100 μm. (C) The graph presents the cell counts of UEA-I$^+$ M cells per villus of 5 representable villous tips on the whole mount images in the three different conditions. Data is the mean ± SD of five representative villous tips for each group. Statistical significance was calculated by two way ANOVA/Bonferroni using the PRISM software.

standing of RANK–RANKL–OPG biology and pave the way for their use *in vitro* and *in vivo*.

Acknowledgements

Appendix A. Supplementary data

Supplementary data associated with this article can be found, in the online version, at http://dx.doi.org/10.1016/j.imlet.2016.01.003.

References

[1] M. Newa, M. Lam, K.H. Bhandari, B. Xu, M.R. Doschak, Expression, characterization, and evaluation of a RANK-binding single chain fraction variable: an osteoclast targeting drug delivery strategy, Mol. Pharm. 11 (2014) 81–89.

[2] S. Kamijo, A. Nakajima, K. Ikeda, K. Aoki, K. Ohya, H. Akiba, et al., Amelioration of bone loss in collagen-induced arthritis by neutralizing anti-RANKL monoclonal antibody, Biochem. Biophys. Res. Commun. 347 (2006) 124–132.

[3] D.M. Anderson, E. Maraskovsky, W.L. Billingsley, W.C. Dougall, M.E. Tometsko, E.R. Roux, et al., A homologue of the TNF receptor and its ligand enhance T-cell growth and dendritic-cell function, Nature 390 (1997) 175–179.

[4] B.R. Wong, R. Josien, S.Y. Lee, B. Sauter, H.L. Li, R.M. Steinman, et al., TRANCE (tumor necrosis factor [TNF]-related activation-induced cytokine), a new TNF family member predominantly expressed in T cells, is a dendritic cell-specific survival factor, J. Exp. Med. 186 (1997) 2075–2080.

[5] W.S. Simonet, D.L. Lacey, C.R. Dunstan, M. Kelley, M.S. Chang, R. Luthy, et al., Osteoprotegerin: a novel secreted protein involved in the regulation of bone density, Cell 89 (1997) 309–319.

[6] M.C. Walsh, Y. Choi, Biology of the RANKL–RANK–OPG system in immunity, bone, and beyond, Front. Immunol. 5 (2014) 511.

[7] D.L. Lacey, E. Timms, H.L. Tan, M.J. Kelley, C.R. Dunstan, T. Burgess, et al., Osteoprotegerin ligand is a cytokine that regulates osteoclast differentiation and activation, Cell 93 (1998) 165–176.

[8] H. Yasuda, N. Shima, N. Nakagawa, K. Yamaguchi, M. Kinosaki, S. Mochizuki, et al., Osteoclast differentiation factor is a ligand for osteoprotegerin/osteoclastogenesis-inhibitory factor and is identical to TRANCE/RANKL, Proc. Natl. Acad. Sci. U. S. A. 95 (1998) 3597–3602.

[9] D. Schramek, V. Sigl, J.M. Penninger, RANKL and RANK in sex hormone-induced breast cancer and breast cancer metastasis, Trends Endocrinol. Metab. 22 (2011) 188–194.

[10] M.B. Bridgeman, R. Pathak, Denosumab for the reduction of bone loss in postmenopausal osteoporosis: a review, Clin. Ther. 33 (2011) 1547–1559.

[11] F. Lezot, J. Chesneau, B. Navet, B. Gobin, J. Amiaud, Y. Choi, et al., Skeletal consequences of RANKL-blocking antibody (IK22-5) injections during growth: mouse strain disparities and synergic effect with zoledronic acid, Bone 20 (2014) 463.

[12] E.A. Green, Y. Choi, R.A. Flavell, Pancreatic lymph node-derived CD4(+)CD25(+) Treg cells: highly potent regulators of diabetes that require TRANCE-RANK signals, Immunity 16 (2002) 183–191.

[13] E. Gonzalez-Suarez, A.P. Jacob, J. Jones, R. Miller, M.P. Roudier-Meyer, R. Erwert, et al., RANK ligand mediates progestin-induced mammary epithelial proliferation and carcinogenesis, Nature 468 (2010) 103–107.

[14] G. Schett, K. Redlich, S. Hayer, J. Zwerina, B. Bolon, C. Dunstan, et al., Osteoprotegerin protects against generalized bone loss in tumor necrosis factor-transgenic mice, Arthritis Rheum. 48 (2003) 2042–2051.

[15] K. Fuller, B. Wong, S. Fox, Y. Choi, T.J. Chambers, TRANCE is necessary and sufficient for osteoblast-mediated activation of bone resorption in osteoclasts, J. Exp. Med. 188 (1998) 997–1001.

[16] W.C. Dougall, M. Glaccum, K. Charrier, K. Rohrbach, K. Brasel, T. De Smedt, et al., RANK is essential for osteoclast and lymph node development, Genes Dev. 13 (1999) 2412–2424.

[17] I. Cremer, M.C. Dieu-Nosjean, S. Marechal, C. Dezutter-Dambuyant, S. Goddard, D. Adams, et al., Long-lived immature dendritic cells mediated by TRANCE–RANK interaction, Blood 100 (2002) 3646–3655.

[18] J.B. Barbaroux, M. Beleut, C. Brisken, C.G. Mueller, R. Groves, Epidermal receptor activator of NF-kB ligand controls Langerhans cell numbers and proliferation, J. Immunol. 181 (2008) 1103–1108.

[19] A. Schöppl, A. Botta, M. Prior, J. Akgun, C. Schuster, A. Elbe-Burger, Langerhans cell precursors acquire RANK/CD265 in prenatal human skin, Acta Histochem. 117 (2015) 425–530.

[20] R. Josien, B.R. Wong, H.L. Li, R.M. Steinman, Y. Choi, TRANCE, a TNF family member, is differentially expressed on T cell subsets and induces cytokine production in dendritic cells, J. Immunol. 162 (1999) 2562–2568.

[21] S.W. Rossi, M.Y. Kim, A. Leibbrandt, S.M. Parnell, W.E. Jenkinson, S.H. Glanville, et al., RANK signals from CD4+3– inducer cells regulate development of Aire-expressing epithelial cells in the thymic medulla, J. Exp. Med. 204 (2007) 1267–1272.

[22] T. Akiyama, Y. Shimo, H. Yanai, J. Qin, D. Ohshima, Y. Maruyama, et al., The tumor necrosis factor family receptors RANK and CD40 cooperatively establish the thymic medullary microenvironment and self-tolerance, Immunity 29 (2008) 423–437.

[23] Y. Hikosaka, T. Nitta, I. Ohigashi, K. Yano, N. Ishimaru, Y. Hayashi, et al., The cytokine RANKL produced by positively selected thymocytes fosters medullary thymic epithelial cells that express autoimmune regulator, Immunity 29 (2008) 438–450.

[24] T. Akiyama, M. Shinzawa, N. Akiyama, TNF receptor family signaling in the development and functions of medullary thymic epithelial cells, Front. Immunol. 3 (2012) 278.

[25] K.A. Knoop, N. Kumar, B.R. Butler, S.K. Sakthivel, R.T. Taylor, T. Nochi, et al., RANKL is necessary and sufficient to initiate development of antigen-sampling M cells in the intestinal epithelium, J. Immunol. 183 (2009) 5738–5747.

[26] T. Kanaya, K. Hase, D. Takahashi, S. Fukuda, K. Hoshino, I. Sasaki, et al., The Ets transcription factor Spi-B is essential for the differentiation of intestinal microfold cells, Nat. Immunol. 13 (2012) 729–736.

[27] S. Srivastava, M. Matsuda, Z. Hou, J.P. Bailey, R. Kitazawa, M.P. Herbst, et al., Receptor activator of NF-kappaB ligand induction via Jak2 and Stat5a in mammary epithelial cells, J. Biol. Chem. 278 (2003) 46171–46178.

[28] J.E. Fata, Y.Y. Kong, J. Li, T. Sasaki, J. Irie-Sasaki, R.A. Moorehead, et al., The osteoclast differentiation factor osteoprotegerin-ligand is essential for mammary gland development, Cell 103 (2000) 41–50.

[29] N.S. Kim, H.T. Kim, M.C. Kwon, S.W. Choi, Y.Y. Kim, K.J. Yoon, et al., Survival and differentiation of mammary epithelial cells in mammary gland development require nuclear retention of Id2 due to RANK signaling, Mol. Cell. Biol. 31 (2011) 4775–4788.

[30] E. Gonzalez-Suarez, D. Branstetter, A. Armstrong, H. Dinh, H. Blumberg, W.C. Dougall, RANK overexpression in transgenic mice with mouse mammary tumor virus promoter-controlled RANK increases proliferation and impairs alveolar differentiation in the mammary epithelia and disrupts lumen formation in cultured epithelial acini, Mol. Cell. Biol. 27 (2007) 1442–1454.

[31] V. Duheron, E. Hess, M. Duval, M. Decossas, B. Castaneda, J.E. Klöpper, et al., Receptor activator of NF-kB (RANK) stimulates the proliferation of epithelial cells of the epidermo-pilosebaceous unit, Proc. Natl. Acad. Sci. U. S. A. 108 (2011) 5342–5347.

[32] T. Nakashima, M. Hayashi, T. Fukunaga, K. Kurata, M. Oh-Hora, J.Q. Feng, et al., Evidence for osteocyte regulation of bone homeostasis through RANKL expression, Nat. Med. 17 (2011) 1231–1234.

[33] C. Fionda, F. Nappi, M. Piccoli, L. Frati, A. Santoni, M. Cippitelli, 15-deoxy-Delta12,14-prostaglandin J2 negatively regulates rankl gene expression in activated T lymphocytes: role of NF-kappaB and early growth response transcription factors, J. Immunol. 178 (2007) 4039–4050.

[34] T. Totsuka, T. Kanai, Y. Nemoto, T. Tomita, R. Okamoto, K. Tsuchiya, et al., RANK-RANKL signaling pathway is critically involved in the function of CD4+CD25+ regulatory T cells in chronic colitis, J. Immunol. 182 (2009) 6079–6087.

[35] S. Schmutz, N. Bosco, S. Chappaz, O. Boyman, H. Acha-Orbea, R. Ceredig, et al., Cutting edge: IL-7 regulates the peripheral pool of adult ROR gamma+ lymphoid tissue inducer cells, J. Immunol. 183 (2009) 2217–2221.

[36] T. Cupedo, M.F. Vondenhoff, E.J. Heeregrave, A.E. De Weerd, W. Jansen, D.G. Jackson, et al., Presumptive lymph node organizers are differentially represented in developing mesenteric and peripheral nodes, J. Immunol. 173 (2004) 2968–2975.

[37] A. Hoshino, T. Iimura, S. Ueha, S. Hanada, Y. Maruoka, M. Mayahara, et al., Deficiency of chemokine receptor CCR1 causes osteopenia due to impaired functions of osteoclasts and osteoblasts, J. Biol. Chem. 285 (2010) 28826–28837.

[38] M. Arizon, I. Nudel, H. Segev, G. Mizraji, M. Elnekave, K. Furmanov, et al., Langerhans cells down-regulate inflammation-driven alveolar bone loss, Proc. Natl. Acad. Sci. U. S. A. 109 (2012) 7043–7048.

[39] A. Hakozaki, M. Yoda, T. Tohmonda, M. Furukawa, T. Hikata, S. Uchikawa, et al., Receptor activator of NF-kappaB (RANK) ligand induces ectodomain shedding of RANK in murine RAW264.7 macrophages, J. Immunol. 184 (2010) 2442–2448.

[40] E. Schaeffer, V. Flacher, V. Papageorgiou, M. Decossas, J. Fauny, M. Krämer, et al., Dermal CD14+ dendritic cell and macrophage infection by dengue virus is stimulated by interleukin-4, J. Invest. Dermatol. 135 (2015) 1743–1751.

[41] P. Schneider, L. Willen, C.R. Smulski, Tools and techniques to study ligand–receptor interactions and receptor activation by TNF superfamily members, Methods Enzymol. 545 (2014) 103–125.

[42] C. Kowalczyk-Quintas, L. Willen, A.T. Dang, H. Sarrasin, A. Tardivel, K. Hermes, et al., Generation and characterization of function-blocking anti-ectodysplasin A (EDA) monoclonal antibodies that induce ectodermal dysplasia, J. Biol. Chem. 289 (2014) 4273–4285.

[43] A.J. Janckila, K. Takahashi, S.Z. Sun, L.T. Yam, Tartrate-resistant acid phosphatase isoform 5b as serum marker for osteoclastic activity, Clin. Chem. 47 (2001) 74–80.

[44] Y. Tomimori, K. Mori, M. Koide, Y. Nakamichi, T. Ninomiya, N. Udagawa, et al., Evaluation of pharmaceuticals with a novel 50-hour animal model of bone loss, J. Bone Miner. Res. 24 (2009) 1194–1205.

[45] L. Furio, I. Briotet, A. Journeaux, H. Billard, J. Peguet-Navarro, Human langerhans cells are more efficient than CD14(−)CD1c(+) dermal dendritic cells at priming naive CD4(+) T cells, J. Invest. Dermatol. 130 (2010) 1345–1354.

[46] K. Loser, A. Mehling, S. Loeser, J. Apelt, A. Kuhn, S. Grabbe, et al., Epidermal RANKL controls regulatory T-cell numbers via activation of dendritic cells, Nat. Med. 12 (2006) 1372–1379.

[47] M. Gomez de Aguero, M. Vocanson, F. Hacini-Rachinel, M. Taillardet, T. Sparwasser, A. Kissenpfennig, et al., Langerhans cells protect from allergic contact dermatitis in mice by tolerizing CD8(+) T cells and activating Foxp3(+) regulatory T cells, J. Clin. Invest. 122 (2012) 1700–1711.

[48] V. Flacher, C.H. Tripp, D.G. Mairhofer, R.M. Steinman, P. Stoitzner, J. Idoyaga, et al., Murine Langerin+ dermal dendritic cells prime CD8+ T cells while Langerhans cells induce cross-tolerance, EMBO Mol. Med. 6 (2014) 1191–1204.

[49] U. Hofmann, Y. Tokura, R. Ruckert, R. Paus, The anagen hair cycle induces systemic immunosuppression of contact hypersensitivity in mice, Cell. Immunol. 184 (1998) 65–73.

121
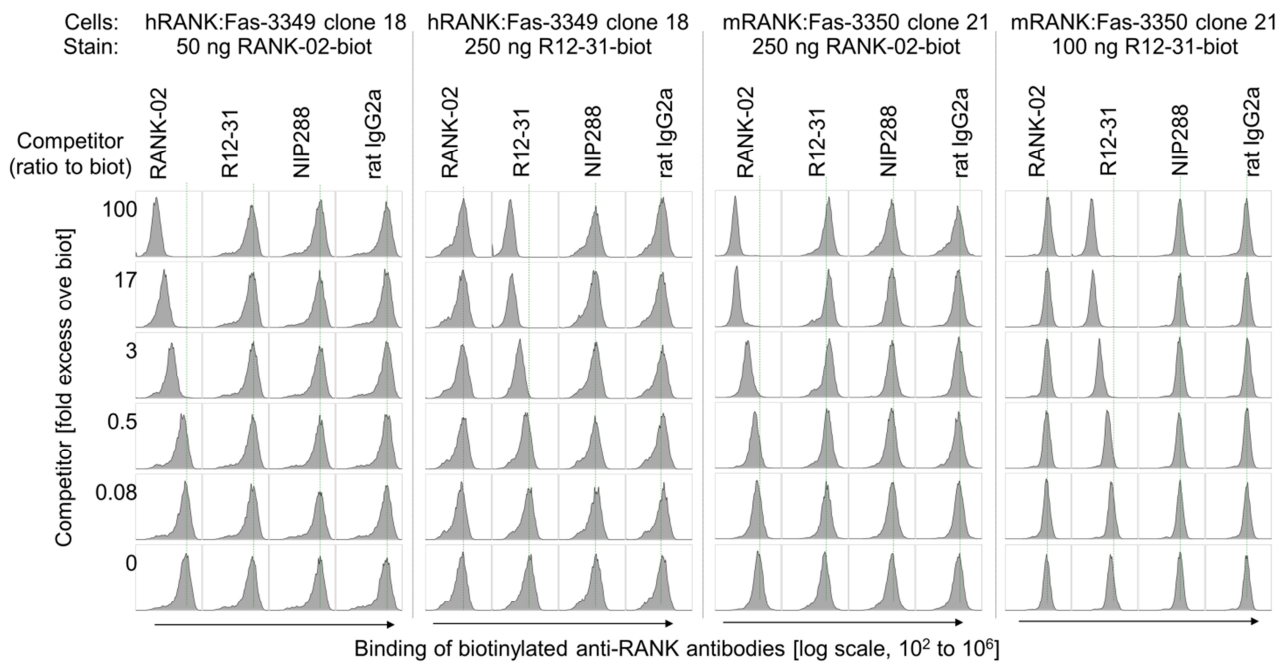
Supplementary Figure 1:
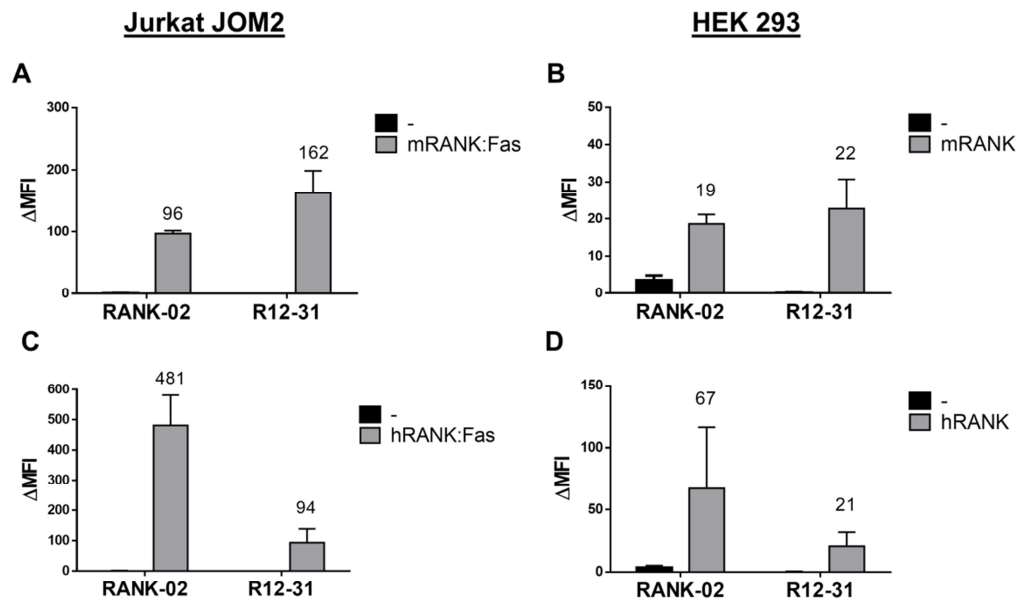
Supplementary Figure 1. The figure presents the ΔMFI of the flow cytometry RANK staining with the two mAbs (RANK-02 and R12-31) for the six different cell lines. The data was derived from Figure 1 and 3 and the ΔMFI= MFI RANK antibody – MFI isotype control was calculated. (A) ΔMFI for the Jurkat JOM2 mRANK:Fas cell line and its parental cell line Jurkat JOM2. (B) ΔMFI for the HEK 293 mRANK cell line and its parental cell line. (C) Same as (A) but for Jurkat JOM2 hRANK:Fas cell line. (D) same as (B) but for HEK 293 hRANK cell line, n=3.

Supplementary Figure 2:
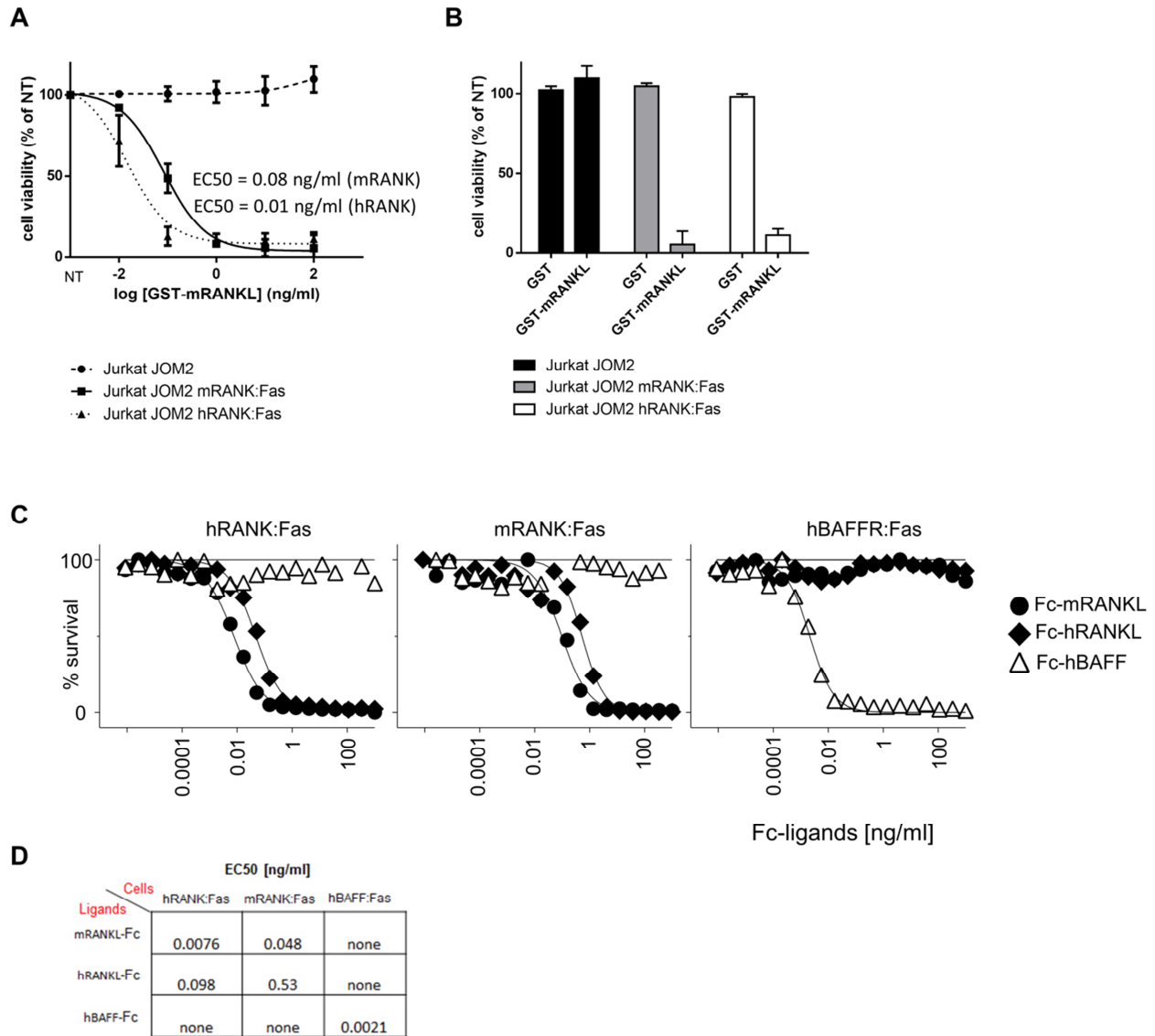
Supplementary Figure 2. (**A**) Dose response curve for recombinant mRANKL fused to GST on Jurkat JOM2 cells expressing or not mouse or human RANK:Fas. The graph displays the percentage cell viability relative to Jurkat JOM2 cells grown in the absence of mRANKL (non-treated, NT) as a function of increasing concentrations of GST-mRANKL. Data points are the mean (± SD, n=3 with duplicate wells). Curve fitting was performed using the PRISM software. (**B**) Cell viability of Jurkat JOM2 cells expressing or not mouse or human RANK:Fas fusion protein treated with 0.1 µg/ml GST only or 0.1 µg/ml GST-mRANKL. Data is the mean (± SD, n=3 with duplicate wells) relative to JOM2 cells exposed to GST. (**C**) Same as panel A but with Fc-mRANKL and Fc-hRANKL. The hBAFFR:Fas cell line and Fc-hBAFF were used as a negative controls. (**D**) EC50 values from results of panel C.

Supplementary Figure 3:

Supplementary Figure 3. Competitive FACS to determine RANK-02 / R12-31 distinct or shared epitopes. Cells in 50 µl FACS buffer were coated for 15 min on ice with 100, 200 or 500 µg/ml of RANK-02 (human anti-RANK), or R12-31 (rat IgG2a anti-RANK), or NIP288 (ctrl for RANK-02) or rat IgG2a (ctrl for R12-31) in 6-fold dilutions (10 µl passed in 50 µl). Without washing, biotinylated RANK-02 at 10 or 50 µg/ml (50 or 250 ng/staining) or biotinylated R12-31 at 20 or 50 µg/ml (100 or 250 ng/staining) was added. After 20 min on ice, the cells were washed and biotinylated mAb revealed with PE-conjugated streptavidin. The histograms for each condition are shown. The dashed green line indicated the signal of uncompleted antibody binding.

125

1.3.   Article 2

Porphyrin derivatives inhibit the interaction between Receptor activator of NF-κB and its ligand

M.Chypre, M-B Madel, C. Blin-Wakkach, C. Morice, C.G. Mueller

In preparation

Porphyrin derivatives inhibit the interaction between receptor activator of NF-κB and its ligand

Mélanie Chypre[a,b], Maria-Bernadette Madel[c,d], Claudine Blin-Wakkach[c,d], Christophe Morice [a], Christopher G. Mueller [b]

[a] Prestwick Chemical, PC SAS, 67400 Illkirch-Graffenstaden, France

[b] Université de Strasbourg, CNRS, Immunopathology and therapeutic chemistry, UPR 3572, 67000 Strasbourg, France

[c] CNRS, LP2M, UMR7370, Faculté de Médecine, Nice, France.

[d] Université Nice Sophia Antipolis, Nice, France.

Abstract

Receptor Activator of NF-κB (RANK) is a member of the TNF-receptor superfamily essential for osteoclastogenesis and bone resorption. Many efforts have been made to identify molecules inhibiting RANK activation to prevent pathological bone loss. Denosumab, a human monoclonal antibody blocking RANKL, is already approved for treatment of osteoporosis and bone metastasis. However, a small molecule inhibiting RANK activation is still needed to reduce the cost of treatment and facilitate the administration with orally available therapeutic agents. Here, we report the discovery of the first non-peptidic inhibitors of RANK-RANKL interaction. We screened the Prestwick Chemical Library® using a competitive ELISA assay. Verteporfin was identified as a hit, presenting a dose dependent activity with an IC50 of 0.4µM and inhibiting osteoclast differentiation *in vitro*. By testing 10 analogues, we confirmed the activity of porphyrin derivatives and the structural benefit of this specific chemical series. This discovery of a family of small molecules inhibiting RANK-RANKL interaction represents a useful tool for further characterization of novel therapeutic agents targeting bone destruction.

Keywords

porphyrinoids, inhibitors, Receptor activator of NF-κB, drug discovery, biological activity

The TNF superfamily member Receptor Activator of NF-κB (RANK) and its ligand RANKL were discovered in the late 1990's for their function in bone homeostasis and immune regulation.[1,2] Osteoprotegerin (OPG), member of the tumor necrosis factor (TNF) receptor superfamily was shown to act as a decoy receptor of RANKL, thus preventing RANK activation.[3] The RANK/RANKL/OPG triad was identified for its role in bone homeostasis through the activity of RANKL to induce osteoclastogenesis of RANK-expressing precursor cells.[4] Uncontrolled RANK activation can lead to decreased bone mass and higher risk of fractures in osteoporosis or inflammatory arthritis.[4,5] Furthermore, the triad is involved in several immunological processes and plays an important role in cancer development and metastasis.[4,6] Two main strategies have been developed to target the RANK/RANKL/OPG axis to counteract increased bone resorption in pathological conditions. Firstly, jolkinolide B and aliin phytopharmaceuticals, chloroquine and 5-(2',4'-difluorophenyl)-salicylanilide derivatives are example of molecules inhibiting RANK induced signaling.[7–10] Peptides interacting with the cytoplasmic part of RANK where also developed to inhibit downstream signaling.[11,12] Another strategy consists in blocking the interaction between RANK and RANKL. For this purpose peptidomimetics of RANK or OPG such as peptides based on the RANK loop3 sequence or on the OPG binding site of RANKL have been described.[13,14] Fusion proteins of the RANK and OPG binding domains with immunoglobulin Fc were also generated.[15] Amgen Inc. developed the human monoclonal antibody Denosumab that neutralizes RANKL. This antibody is more potent and has a longer half-life than the OPG-Fc constructs, and, importantly, no safety risks were reported so far in clinical trials.[15] Denosumab is a first-in-class, first-in-pathway monoclonal antibody approved for post-menopausal osteoporosis and prevention of skeletal related events (SRE) in patients with bone metastasis from solid tumors.[15] However, small synthetic molecules inhibiting the RANKL interaction with its receptor RANK have so far not been reported but might represent cost and pharmacological advantages over proteins.

The Prestwick Chemical Library (PCL) is a collection of 1280 small molecules; all are approved drugs (FDA, EMA and other agencies) selected by a team of medicinal chemists and pharmacists for their high chemical and pharmacological diversity as well as for their known bioavailability and safety in humans.[16,17] We used a competitive ELISA assay to screen the Prestwick Chemical Library for small molecules that inhibit the interaction between human RANK and its ligand human RANKL. Herein, we report the identification of porphyrin derivatives as inhibitors of this interaction in ELISA as well as in a viability cellular assay using Jurkat JOM2 cell lines and an osteoclast differentiation assay using the RAW 264.7 macrophagic cell line.

We screened the 1280 compounds at a concentration of 100µM with a cutoff inhibitory effect ≥ 40%. Surprisingly, only one hit was identified (Verteporfin; compound **14G06**, **Fig.1**) despite the high concentration used. In a dose response the IC50 of 0.4µM was determined **(Fig. 1)**. Verteporfin is a benzoporphyrin derivative currently used for neovascular macular degeneration in ocular photodynamic therapy. Considering the large chemical diversity of the Prestwick Chemical Library and the fact that verteporfin is a unique representative of porphyrin macrocycles, this chemical structure seems to have a specific behavior with regard to the interaction between RANK and its ligand RANKL.
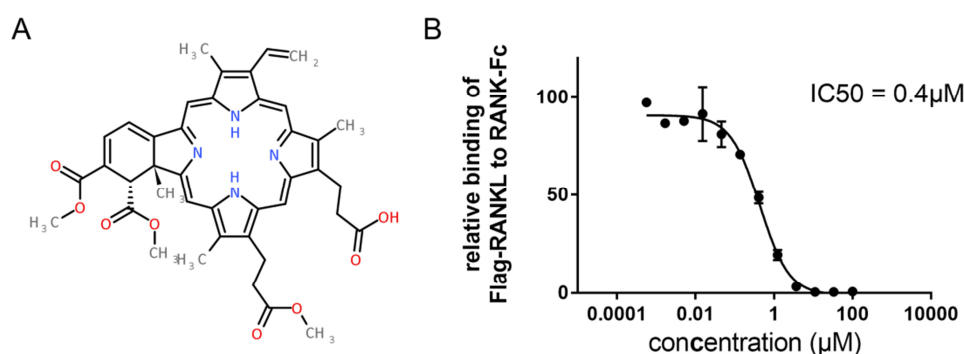
Figure 1: Verteporfin inhibits the interaction between RANK and RANKL. (A) Verteporfin structure and **(B)** dose response curve of verteporfin in a competitive ELISA of RANKL binding to RANK. The ELISA plate was coated with hRANK-Fc followed by incubation of hRANKL together with increasing doses of verteporfin. The amount of bound hRANKL was measured. Values are the mean %, relative to hRANKL binding positive control (± SD) in the absence of the inhibitor. These data reveal that verteporfin inhibits hRANKL binding to hRANK in a dose dependent manner with an IC50 of 0.4µM.

In order to validate the activity of this class of molecules, a hit follow-up process was performed by testing 10 close analogues, 5 phorphyrin and 5 chlorine macrocycles **(Fig. 2 and table 1)**. Chlorines are closely related to porphyrin as they have the same macrocycle with a mono saturation at one of the four pyrrole site. Hematoporphyrin IX dimethyl ester (**3**) and Pyropheophorbide-a (**9**) had a similar activity to verteporfin with an IC50 of 0.3µM and 0.5µM, respectively. Pheophorbide a (**8**) and Purpurin 18 (**10**) had also a low micromolar activity with an IC50 of 1.2µM and 1.5µM, respectively. Pyropheophorbide-a methyl ester (**5**) and Chlorin e6 (**2**) were likewise active with an IC50 of 2.4 µM and 8.4 µM, respectively. Isohematoporphyrin IX (**4**) and Protoporphyrin IX dimethyl ester (**7**) presented weak activity with an IC50 > 20µM and some solubility issues led to only approximate IC50 determination. Finally, Coproporphyrin I dihydrochloride (**1**) and Protoporphyrin IX (**6**) did not reveal any inhibitory activity. The variability of the results obtained for this small set of 10 structurally close analogues from potent to inactive in ELISA experiment validated the original hit, verteporfin (14G06). These results show a first promising Structure-Activity Relationship (SAR) for this chemical series in

regard to RANK-RANKL binding inhibition. Porphyrin macrocycles (**1**,**6**,**4**,**7**) are poorly to not inhibiting the interaction. On the other hand, benzoporphyrin (**14G06**) and chlorines (**5, 8, 9 and 10**) seem more efficient in inhibiting the interaction. The number of Hydrogen Bond Donor (HBD) functionalities (alcohol, carboxylic acid) and the presence of neutral Hydrogen Bond Acceptor (HBA) seem to be detrimental for activity. The more potent compounds bear preferentially one carboxylic acid group (**8, 9 and 10)** or hydroxyl groups in replacement (**3**). With more than two hydroxy or acid groups (**1**, **2** or **4**), activity drops progressively until inactive tetraacid coproporphyrin I (**1**). Neutral oxygenated HBA groups such as ketone (**5, 8, 9**), ester (**14G06**) or anhydride (**10**) are suspected to participate in the binding. The close association of one HBD and one HBA enhances the inhibitory effect (**9** vs **5, 6** and **7**). Some results remained ambiguous, especially in the Porphyrin subseries (**3** vs **6** and **7**) and further analogues would need to be tested to better understand the first SAR observed. Moreover, it would be interesting to test fragments of those macrocycles in order to determine how the aromatic macrocycle is detrimental for the inhibition.
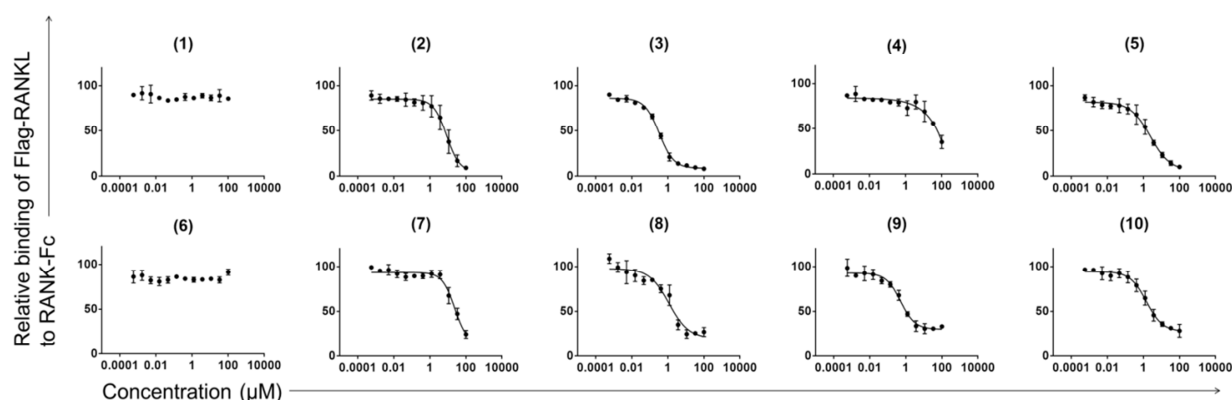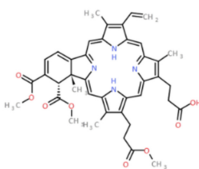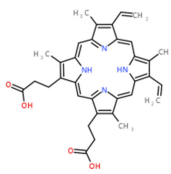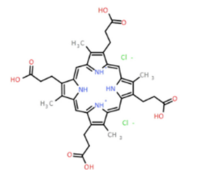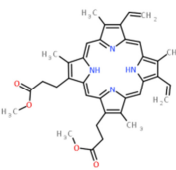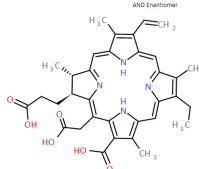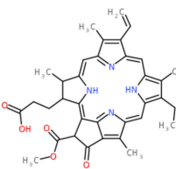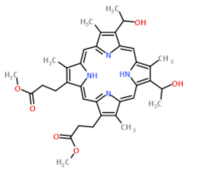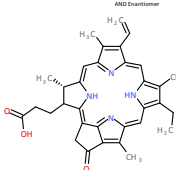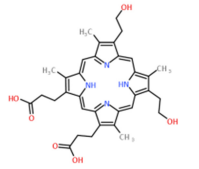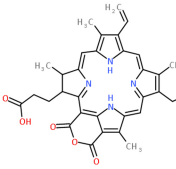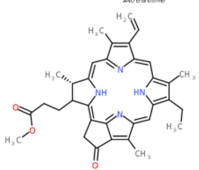
Figure 2: Activity evaluation of verteporfin analogues. Dose response curves of verteporfin analogues in a competitive ELISA of RANKL binding to RANK. The ELISA plate was coated with hRANK-Fc followed by incubation of hRANKL together with increasing doses of compounds. The amount of bound hRANKL was measured. Values are the mean % relative to RANKL binding positive control (± SD). The numbers refer to compounds **1-10** described in table 1.

Table 1: **Name, structure and IC50 of the compounds tested in competitive ELISA.**

n°	Name	Structure	IC50 (µM)	n°	Name	Structure	IC50 (µM)
14G06	Verteporfin		0.43	6	Protoporphyrin IX		-
1	Coproporphyrin I dihydrochloride		-	7	Protoporphyrin IX dimethyl ester		23.82
2	Chlorin e6		8.37	8	Pheophorbide a (mixture of diastereomers)		1.15
3	Hematoporphyrin IX dimethyl ester		0.32	9	Pyropheophorbide-a		0.51
4	Isohematoporphyrin IX		Ambi-guous	10	Purpurin 18		1.45
5	Pyropheophorbide-a methyl ester		2.37				

We next tested Verteporfin and its analogs in an *in vitro* cellular assay using Jurkat JOM2 cells expressing a chimeric receptor of the extracellular domain of hRANK fused to the intracellular domain of hFas. Activation of hRANK-hFas by RANKL leads to apoptosis, which is measured by propidium iodide (PI) incorporation into dead cells by flow cytometry.[18] However, a receptor-ligand inhibition would rescue from cell death. First, we tested the efficacy of the assay by incubating the

cells with recombinant mRANKL in 0.05% DMSO alone or with the IK22-5 anti-RANKL antibody.[18] Recombinant RANKL triggered cell death while the antibody IK22-5 rescued the cells from apoptosis. The cell death values induced by RANKL were arbitrarily set to 100% **(Fig 3A)**. Next, we verified the activity of the compounds that showed inhibitory activity in the ELISA assay at 10µM in the absence of RANKL. None-to-little cell death was observed, demonstrating their low cytotoxicity and their low RANK agonist effect **(Fig 3A)**. We then tested their inhibitory activity by incubating the cells with RANKL together with 10µM of the compounds. The cellular inhibition is in accordance with the binding experiment **(Fig. 3B)**, the most effective inhibitors in ELISA showing the highest inhibitory effects in cells (compounds **14G06**, **2, 3**, **8**, **9** and **10**). Inversely, **4** and **7**, two poor RANK/RANKL binding inhibitors (IC50 > 20µM), were inactive in the cell assay at 10 µM. The three most potent inhibitors (**8**, **9** and **10**) in cells were the chlorines bearing only one carboxylic acid group. Compound **2** was less potent at the same concentration of 10µM. One possible explanation could be the free fraction of the inhibitor available at the cell surface in the experimental conditions. This local concentration could be modulated by the solubility of the compound and its global negative charge. Therefore, too many carboxylate functions (three in compound **2**) may have a repulsive effect to access the membrane surface.
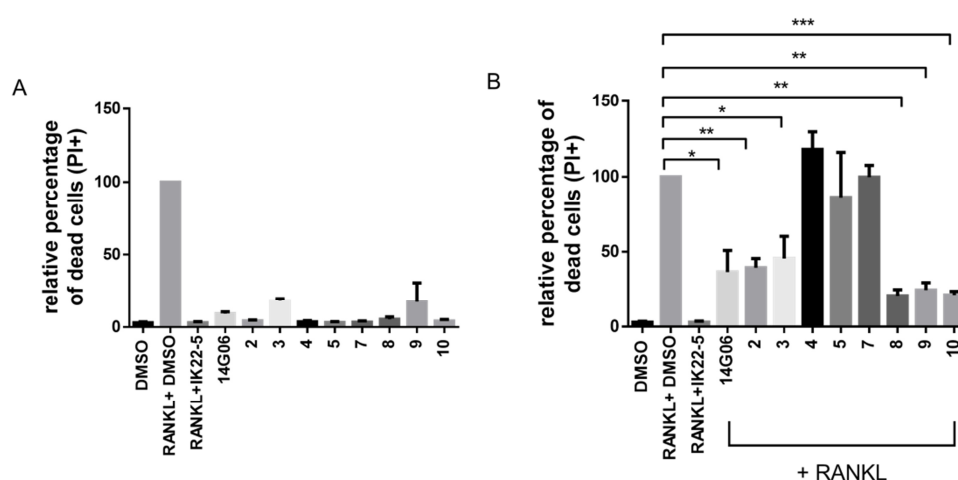
Figure 3: **Verteporfin and analogues have low cytotoxicity and inhibit RANK activation in Jurkat JOM2 hRANK:Fas cells.** Graph represent the Mean Fluorescence Intensity (MFI) of propidium iodide (PI) staining normalized to cells treated with RANKL + 0.05% DMSO. **(A)** Cells were treated for 16h with 10µM of the respective compounds. **(B)** Cells were treated with 10µM of the compounds together with RANKL at 1ng/ml. IK22-5 anti-RANKL antibody was used at 10µg/ml as a positive control for RANKL inhibition. Mean ± SD, t-test was used to calculate statistical significance. * p<0.05 ** p<0.001 ***p<0.001

Finally, we tested **14G06** in an osteoclast differentiation assay with the murine RAW-264.7 macrophage cell line (**Fig. 4**). Their culture with mM-CSF and mRANKL is known to induce the formation of large multinucleated osteoclasts positive for Tartrate-resistant acid phosphatase (TRAcP).[19] We observed a dose dependent inhibition of osteoclast formation with micromolar concentrations confirming the efficiency of verteporfin to inhibit RANK-RANKL interaction.
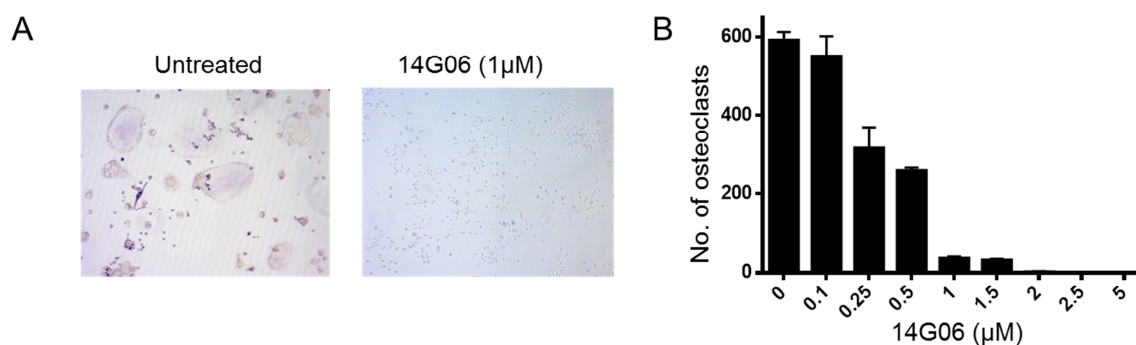
Figure 4: Verteporfin inhibits osteoclastogenesis. **(A)** Microscopy images showing the effect of verteporfin on RAW-264.7 differentiation. RAW-264.7 cells were cultured with M-CSF (25 ng/ml) and RANKL (30 ng/ml) for differentiation into osteoclasts for 4 days in the presence or absence of 14G06 (verteporfin, 1μM). The cells were stained for TRAcP assay and photographed (x10). **(B)** Graph represents the number of multinucleated (≥ 3 nuclei) TRAcP positive osteoclasts (mean ± SD in triplicates) after the treatment with different doses of verteporfin.

Here, we report the first non-peptidic inhibitors of RANK-RANKL interaction. Detailed SAR remains to be investigated but these first results show that porphyrin derivatives and, more specifically, chlorines are validated core structures that effectively inhibit RANK-RANKL binding. This inhibition is influenced by modifications of the central aromatic macrocycle. The number of carboxylic acid groups affected the inhibitory activity. We based our initial screen on an ELISA assay to identify rapidly and cell-independently molecules that show inhibitory activity of RANK-RANKL interaction. We then confirmed the inhibitory activity in a cellular assay with the readout of rescuing cell death of Jurkat JOM2 hRANK:Fas cells by RANKL. Finally we showed that verteporfin inhibits osteoclastogenesis in a dose-dependent manner. This procedure is therefore different from those aiming to identify inhibitors of osteoclast formation or activity using osteoclasts or their precursor cells. The here identified compounds had a micromolar IC50 in ELISA and in cellular assays. This concentration range is comparable with peptides and small molecules inhibiting RANK signaling but it is higher than Denosumab or OPG-Fc with an IC50 in the nanomolar range in osteoclastogenesis assays.[7,8,13,14,20] To our knowledge, no small molecule has been identified that blocks RANKL-RANKL interaction. Thus, this study provides for the first time the identification of chemical compounds

inhibiting RANK binding to its ligand RANKL. Furthermore, the porphyrin derivatives can serve as chemical backbone for refinement and activity enhancement. Similarly to OPG-Fc and Denosumab, the here described molecules or their derivatives could be applicable in diseases such as osteoporosis, cancer and inflammation caused by an increased RANKL expression.[4,6,21] Verteporfin is currently used as a photosensitizer in photodynamic therapy of the eyes.[22] Activation of verteporfin with a 689nm laser leads to production of singlet oxygen and free radicals inducing cell damage. Therefore, it can be activated with normal light and leads to skin photosensitivity for at least 48h after injection. Verteporfin extravasation out of blood vessels could also lead to pain, inflammation, swelling or discoloration.[23] Thus, the use of these compounds *in vivo* could lead to potential side effects. We therefore propose porphyrin derivatives as useful tools to investigate the RANK/RANKL interaction blockade and to further develop more efficient and specific molecules that could be suitable for therapy. Though, at present, only anti-RANK and anti-RANKL antibodies could be used as a positive control for inhibition of RANK/RANKL interaction.

Experimental Section:

ELISA: Competitive ELISA to study RANK-RANKL interaction was already described.[18] Goat-anti-human antibody (5µg/ml) was coated in carbonate buffer overnight in 96-well plates. Plates were washed with PBS/0.05% Tween (PBS-T), blocked for 1h at 37°C with PBS containing 4% (w/v) milk powder and washed again. Conditioned supernatant of 293T cells transfected with hRANK-Fc (5µl/well) was then incubated 2h at 37°C. Plates were washed with PBS-T, titrated amounts of compounds together with supernatant containing Flag-hRANKL (2µl/well) were added and incubated for 1h at 37°C. Supernatant volumes were chosen for their ability to generate a close to maximal but non-saturating signal. Binding of Flag-hRANKL was revealed with biotin-conjugated M2-antibody (0.5µg/ml) (Sigma) and streptavidin-HRP (Jackson immunoresearch) (1/4000). Tetramethylbenzidine (TMB, 75µl) was added to each well and then neutralized with HCL 1 N (25µl). Plates were read at 450 nm on Multiskan Ex (MTX Labsystems Inc.). Plasmids were a kind gift from Dr. Pascal Schneider, University of Lausanne.

Cell culture: Jurkat JOM2 hRANK:Fas (a kind gift from Dr. Pascal Schneider, University of Lausanne) were maintained in a humidified incubator with 5% CO_2 at 37°C and grown in RPMI 1640 medium supplemented with 10% FCS. Jurkat JOM2 hRANK:Fas were generated according to a described protocol.[18,24,25] RAW-264.7 cells were cultured in αMEM containing 5% FCS, 1% penicillin-streptomycin as well as 50 µM β-mercaptoethanol.

Cell viability assay: Jurkat JOM2 hRANK:Fas (1×10^5 cells/100 µl) were incubated for 16h with compounds and/or recombinant RANKL or anti-RANKL antibody IK22-5 as indicated. Cells were then washed with PBS and incubated with 1µg/ml propidium iodide (PI) for 15min at room temperature. Cell viability was assessed by measurement of PI mean fluorescence by flow cytometry using FACS Calibur (BD) and Flowjo software (Treestar) for analysis.

Osteoclastogenesis assay: 5×10^3 RAW-264.7 cells/well were seeded in a 48-well plate. Cells were incubated with 30 ng/ml murine RANKL and 25 ng/ml murine M-CSF (R&D Systems) and without or with different concentrations of verteporfin. After 4 days of culture, cells were fixed and stained for TRAcP activity according to manufacturer's instructions (Sigma-Aldrich). TRAcP positive cells with 3 and more nuclei were counted as osteoclasts. Cells were photographed (magnification 10x) using the Zeiss Primo Vert phase-contrast microscope and the Axiocam ERc 5s microscope camera (Zeiss) utilizing the AxioVision Rel 4.8 (Zeiss) imaging software. The number of osteoclasts were visually scored.

References:

[1] D. M. Anderson, E. Maraskovsky, W. L. Billingsley, W. C. Dougall, M. E. Tometsko, E. R. Roux, M. C. Teepe, R. F. DuBose, D. Cosman, L. Galibert, *Nature* **1997**, *390*, 175–179.

[2] B. R. Wong, R. Josien, S. Y. Lee, B. Sauter, H.-L. Li, R. M. Steinman, Y. Choi, *J. Exp. Med.* **1997**, *186*, 2075–2080.

[3] W. S. Simonet, D. L. Lacey, C. R. Dunstan, M. Kelley, M.-S. Chang, R. Lüthy, H. Q. Nguyen, S. Wooden, L. Bennett, T. Boone, et al., *Cell* **1997**, *89*, 309–319.

[4] M. C. Walsh, Y. Choi, *Inflammation* **2014**, *5*, 511.

[5] K. Okamoto, H. Takayanagi, *Arthritis Res. Ther.* **2011**, *13*, 219.

[6] E. González-Suárez, A. Sanz-Moreno, *FEBS J.* **2016**, *283*, 2018–2033.

[7] X. Ma, Y. Liu, Y. Zhang, X. Yu, W. Wang, D. Zhao, *Biochem. Biophys. Res. Commun.* **2014**, *445*, 282–288.

[8] Y. Chen, J. Sun, C. Dou, N. Li, F. Kang, Y. Wang, Z. Cao, X. Yang, S. Dong, *Int. J. Mol. Sci.* **2016**, *17*, DOI 10.3390/ijms17091516.

[9] Y. Xiu, H. Xu, C. Zhao, J. Li, Y. Morita, Z. Yao, L. Xing, B. F. Boyce, *J. Clin. Invest.* **2014**, *124*, 297–310.

[10] C.-C. Lee, F.-L. Liu, C.-L. Chen, T.-C. Chen, D.-M. Chang, H.-S. Huang, *Eur. J. Med. Chem.* **2015**, *98*, 115–126.

[11] B. Aggarwal, B. Darnay, S. Singh, *Inhibitors of Receptor Activator of NF-kappaB and Uses Thereof*, **2004**, US20040167072 A1.

[12] H. Kim, H. K. Choi, J. H. Shin, K. H. Kim, J. Y. Huh, S. A. Lee, C.-Y. Ko, H.-S. Kim, H.-I. Shin, H. J. Lee, et al., *J. Clin. Invest.* **2009**, *119*, 813–825.

[13] G. Kato, Y. Shimizu, Y. Arai, N. Suzuki, Y. Sugamori, M. Maeda, M. Takahashi, Y. Tamura, N. Wakabayashi, R. Murali, et al., *Arthritis Res. Ther.* **2015**, *17*, 251.

[14] J. Hur, A. Ghosh, K. Kim, H. M. Ta, H. Kim, N. Kim, H.-Y. Hwang, K. K. Kim, *Mol. Cells* **2016**, *39*, 316–321.

[15] D. L. Lacey, W. J. Boyle, W. S. Simonet, P. J. Kostenuik, W. C. Dougall, J. K. Sullivan, J. S. Martin, R. Dansey, *Nat. Rev. Drug Discov.* **2012**, *11*, 401–419.

[16] G. Porcu, E. Serone, V. D. Nardis, D. D. Giandomenico, G. Lucisano, M. Scardapane, A. Poma, A. Ragnini-Wilson, *PLOS ONE* **2015**, *10*, e0144550.

[17] C. Corbel, B. Zhang, A. Le Parc, B. Baratte, P. Colas, C. Couturier, K. S. Kosik, I. Landrieu, V. Le Tilly, S. Bach, *Chem. Biol.* **2015**, *22*, 472–482.

[18] M. Chypre, J. Seaman, O. G. Cordeiro, L. Willen, K. A. Knoop, A. Buchanan, R. C. A. Sainson, I. R. Williams, H. Yagita, P. Schneider, et al., *Immunol. Lett.* **2016**, *171*, 5–14.

[19] T. Ciucci, L. Ibáñez, A. Boucoiran, E. Birgy-Barelli, J. Pène, G. Abou-Ezzi, N. Arab, M. Rouleau, X. Hébuterne, H. Yssel, et al., *Gut* **2015**, *64*, 1072–1081.

[20] P. J. Kostenuik, H. Q. Nguyen, J. McCabe, K. S. Warmington, C. Kurahara, N. Sun, C. Chen, L. Li, R. C. Cattley, G. Van, et al., *J. Bone Miner. Res.* **2009**, *24*, 182–195.

[21] F. Toberer, J. Sykora, D. Göttel, V. Ruland, W. Hartschuh, A. Enk, T. A. Luger, S. Beissert, K. Loser, S. Joos, et al., *Exp. Dermatol.* **2011**, *20*, 600–602.

[22] V. I. P. T. S. Group, *Am. J. Ophthalmol.* **2001**, *131*, 541–560.

[23] U. Schmidt-Erfurth, T. Hasan, *Surv. Ophthalmol.* **2000**, *45*, 195–214.

[24] P. Schneider, L. Willen, C. R. Smulski, in *Methods Enzymol.* (Ed.: J.A.W. and J.Y. Avi Ashkenazi), Academic Press, **2014**, pp. 103–125.

[25] L. K. Swee, K. Ingold-Salamin, A. Tardivel, L. Willen, O. Gaide, M. Favre, S. Demotz, M. Mikkola, P. Schneider, *J. Biol. Chem.* **2009**, *284*, 27567–27576.

1.4. Conclusions

Investigation of RANK-RANKL axis and discovery of new therapeutic applications requires well characterized high affinity tools. In these studies, we developed and characterized new tools to target RANK-RANKL axis. To do so, I set up different and complementary assays to study binding to RANK and activation of downstream signaling. In the first study, we carefully characterized two monoclonal antibodies (mAbs) targeting RANK. We observed that they bind both mRANK and hRANK by ELISA, plasmon resonance and in flow cytometry. The mAbs showed different biological activity probably due to the binding of different epitopes. R12-31 presented an agonist activity against both mRANK and hRANK. RANK-02 showed partial antagonist activity on mRANK and weak agonist activity on hRANK. Both mAbs recognized RANK at the surface of migrating primary Langerhans cells. R12-31 was active *in vivo* and induced the differentiation of M cells of the intestinal villi.

In a second study, I used the tests set up in the previous part to identify small molecules inhibiting the interaction between RANK and RANKL. I screened the Prestwick Chemical Library of small molecules using the competitive ELISA. One hit with a micromolar IC50 was identified (Verteporfin). To validate the hit we tested 10 analogues, only two of them did not show inhibitory activity. These results allowed the evaluation of the first keys for structure-activity relationship. Some analogues were also tested for their effect in the cellular assay using Jurkat JOM2 hRANK:Fas cells. The structure-activity relationship found in ELISA was confirmed and showed that these compounds can efficiently inhibit RANKL interaction with the RANK extracellular domain. Finally verteporfin was tested in an osteoclastogenesis assay *in vitro*. It potently inhibited murine osteoclasts differentiation at micromolar concentrations.

In this part of my thesis work, I set up several *in vitro* methods to characterize tools targeting RANK-RANKL. The competitive ELISA and the cellular assay using Jurkat JOM2 hRANK:Fas were validated with the antibody study and enabled the identification of a family of small molecules inhibiting RANK-RANKL interaction. Together, these findings pave the way for the use of these mAbs and small molecules to better understand RANK-RANKL-OPG triad biology and discover new therapeutic agents.

2. RANKL in adult lymph node homeostasis: effect on lymphatic endothelial cells and macrophages

2.1. Introduction

Lymph nodes (LNs) are well organized organs comprising both hematopoietic and non-hematopoietic cells playing an important role in the initiation of an immune response. Lymph containing antigen presenting cells as well as particulate antigens arrives in the LN subcapsular sinus via the afferent lymphatics. The subcapsular sinus is formed by lymphatic endothelial cells (LECs) creating two layers called the ceiling and the floor. The $CD169^+$ subcapsular sinus macrophages (SSMs) are inserted into the floor LEC layer. Marginal reticular cells (MRCs) are found between the floor of the sinus and the B cell follicles. Lymph flows through LN via medullary and cortical sinuses which are also formed by LECs. The $CD169^+$ medullary sinus macrophages (MSM) are found in the medullary sinuses.

RANKL together with LTαβ are known to play a role in LN organogenesis. Mice deficient for RANK or RANKL do not develop LNs. Moreover, MRCs are known to constitutively express RANKL in the adult LN. Nonetheless, the role of RANKL in the adult LN remains unclear.

During my thesis, we addressed the question of the heterogeneity of LECs by investigating a new marker of these cells, ITGA2b, sensitive to RANKL (Article 3, *Plos One* 2016). ITGA2b was known to be expressed by platelets and megakaryocytes. We show that LECs also express this integrin in the floor of the subcapsular sinus and heterogeneously in medullary and cortical regions of the LN. The expression of ITGA2b by LECs was sensitive to stromal RANKL and to LTαβ blockage.

In a second study, we investigated whether stromal RANKL also impacts LN macrophages (Article 4, in preparation). We observed that stromal RANKL deficiency reduced $CD169^+$ SSM numbers. This did not involve a direct mechanism activating RANK on macrophages or an autocrine effect on MRCs. Expression of ITGA2b and MAdCAM-1 on LECs could be restored to WT levels with recombinant RANKL.

2.2.　　Article 3

Integrin-Alpha IIb Identifies Murine Lymph Node Lymphatic Endothelial Cells Responsive to RANKL

O.G. Cordeiro, <u>M. Chypre</u>, N. Brouard, S. Rauber, F. Alloush, M. Romera-Hernandez, C. Bénézech, Z. Li, A. Eckly, M.C. Coles, A. Rot, H. Yagita, C. Léon, B. Ludewig, T. Cupedo, F. Lanza, C.G. Mueller

PLOS ONE 11, e0151848, 2016

PLOS ONE

RESEARCH ARTICLE

Integrin-Alpha IIb Identifies Murine Lymph Node Lymphatic Endothelial Cells Responsive to RANKL

Olga G. Cordeiro[1], Mélanie Chypre[1,2], Nathalie Brouard[3], Simon Rauber[1], Farouk Alloush[1], Monica Romera-Hernandez[4], Cécile Bénézech[5], Zhi Li[6], Anita Eckly[3], Mark C. Coles[6], Antal Rot[6], Hideo Yagita[7], Catherine Léon[3], Burkhard Ludewig[8], Tom Cupedo[4], François Lanza[3], Christopher G. Mueller[1]*

1 CNRS UPR 3572, University of Strasbourg, Laboratory of Immunopathology and Therapeutic Chemistry/MEDALIS, Institut de Biologie Moléculaire et Cellulaire, Strasbourg, France, 2 Prestwick Chemical, Blvd Gonthier d'Andernach, Parc d'innovation, 67400, Illkirch, France, 3 INSERM, UMR_S949, Etablissement Français du Sang-Alsace, Faculté de Médecine, Fédération de Médecine Translationnelle, Université de Strasbourg, Strasbourg, France, 4 Department of Hematology, Erasmus University Medical Center, Rotterdam, The Netherlands, 5 BHF Centre for Cardiovascular Science, Queens Medical Research Institute, University of Edinburgh, Edinburgh, United Kingdom, 6 Center for Immunology and Infection, Department of Biology, University of York, York, United Kingdom, 7 Department of Immunology, Juntendo University School of Medicine, Tokyo, 113–8421, Japan, 8 Institute of Immunobiology, Kantonspital St. Gallen, 9007, St. Gallen, Switzerland

* c.mueller@cnrs-ibmc.unistra.fr

Abstract

Microenvironment and activation signals likely imprint heterogeneity in the lymphatic endothelial cell (LEC) population. Particularly LECs of secondary lymphoid organs are exposed to different cell types and immune stimuli. However, our understanding of the nature of LEC activation signals and their cell source within the secondary lymphoid organ in the steady state remains incomplete. Here we show that integrin alpha 2b (ITGA2b), known to be carried by platelets, megakaryocytes and hematopoietic progenitors, is expressed by a lymph node subset of LECs, residing in medullary, cortical and subcapsular sinuses. In the subcapsular sinus, the floor but not the ceiling layer expresses the integrin, being excluded from ACKR4+ LECs but overlapping with MAdCAM-1 expression. ITGA2b expression increases in response to immunization, raising the possibility that heterogeneous ITGA2b levels reflect variation in exposure to activation signals. We show that alterations of the level of receptor activator of NF-κB ligand (RANKL), by overexpression, neutralization or deletion from stromal marginal reticular cells, affected the proportion of ITGA2b+ LECs. Lymph node LECs but not peripheral LECs express RANK. In addition, we found that lymphotoxin-β receptor signaling likewise regulated the proportion of ITGA2b+ LECs. These findings demonstrate that stromal reticular cells activate LECs via RANKL and support the action of hematopoietic cell-derived lymphotoxin.

142

Introduction

Molecules, cells and pathogens carried by the lymph flow are filtered by lymph nodes (LNs). In these specialized organs, resident immune cells recognize, eliminate and mount an immune response against pathogens. The LECs provide an important structural and functional support to this process by mediating lymph drainage, organizing cellular compartments, regulating the immune response and controlling lymph exit [1]. Lymph first drains into the subcapsular sinus, which comprises an outermost (ceiling-lining) and an inner (floor-lining) lymphatic endothelial layer. Differential expression of the chemokine ACKR4 (also called CCRL1) has recently highlighted structural and functional specialization of these layers [2]. LECs also form the cortical and medullary sinuses that allow distribution of cells and large molecules within different LN compartments and exit into the efferent lymph [3]. Platelet adhesion to lymphatic endothelium mediates blood and lymphatic vessel separation during embryonic development [4].

Integrins play an important role in a variety of biological processes ranging from development, cancer, and inflammation [5]. The large family of transmembrane receptors, composed of α and β subunits, provides structural and functional integrity to connective tissues and organs, mediates cell extravasation from blood and contributes to cell activation. The integrin α2b (ITGA2b, CD41 or glycoprotein IIb) pairs exclusively with integrin β3 (ITGB3, CD61 or glycoprotein IIIa), while the latter can also form a heterodimer with integrin αV (ITGAV, CD51). ITGA2B/ITGB3 is well known for its role in blood clotting through its expression by megakaryocytes and platelets [6]. Upon platelet stimulation, the surface integrin heterodimer becomes activated, binds fibrinogen and von Willebrand factor resulting in platelet aggregation. ITGA2b and ITGB3 are also expressed by embryonic erythroid and hematopoietic progenitor cells arising from the hemogenic endothelium of the conceptus and embryo [7–9]. Although hemogenic endothelium generates ITGA2b$^+$ hematopoietic progenitor cells, these special endothelial cells themselves lack the integrin [7]. Otherwise, blood endothelial cells express a number of integrins, both in the abluminal space to adhere to the basement membrane and in the lumen to recruit leucocytes [5].

The TNF family member RANKL (TNFSF11), alike other member of the protein family such as lymphotoxin-α and β, plays an important role in LN development [10]. It is expressed in the embryo by the hematopoietic lymphoid tissue inducing cells and triggers lymphotoxin production [11]. In a second phase RANKL is expressed by the lymphoid organizer cells of mesenchymal origin [12], which are thought to persist as marginal reticular cells (MRCs) in the adult [13]. The role of RANKL produced by MRCs remains unknown. In a model of skin overexpression RANKL was shown to activate LN lymphatic and blood endothelial cells as well as fibroblastic reticular cells raising the possibility that RANKL of MRCs functions as internal activator of these cells [14].

In this study, we show that a subset of LECs of mouse and human LNs express ITGA2b. In the murine LN the ITGA2b$^+$ LECs are heterogeneously distributed in the medullary and cortical areas as well as in the subcapsular sinus, where only the floor-lining cells carry the integrin. ITGA2b could potentially heterodimerize with ITGB3 to bind ligands, such as fibronectin, but the alternative α-chain, ITGAV, is also present to pair with ITGB3 to anchor the cells to matrix components. In mice overexpressing RANKL the level of ITGA2b increases, while its neutralization or its genetic deletion from MRCs reduce the integrin expression. Similarly, inhibition of lymphotoxin-β receptor signaling negatively affects the proportion of ITGA2b$^+$ LECs. Therefore, ITGA2b is a novel marker for LN LECs constitutively activated by TNF-family members RANKL and lymphotoxin-αβ.

Material and Methods

Mice

C57BL/6, *Itga2b*^{-/-} [15], ACKR4-eGFP transgenic mice (otherwise known as CCRL-1-eGFP) [2], RANK-transgenic [14], and RANKL[ΔCcl19] mice were bred and kept in specific pathogen-free conditions, and all experiments were carried out in conformity to the animal bioethics legislation approved by and according to national guidelines of the CREMEAS (Comité Régional d'Ethique en Matière d'Expérimentation Animale de Strasbourg), permit number AL/02/22/11/11 and AL/03/12/05/12. All efforts were made to minimize suffering. To generate mice with conditional RANKL deficiency in marginal reticular cells (*RANKL[ΔCcl19]*), mice containing a single copy of the *Ccl19-cre* BAC transgene [16] were crossed with RANKL[f/f] (B6.129-Tnfsf11tm1.1Caob/J) mice [17]. For adoptive bone marrow transfer, 6-wk-old mice were lethally irradiated with 9 Gy (Caesium source), and 3 h later they received 5x10^{6} bone marrow cells i.v. harvested from *Itga2b*^{-/-} mice. Chimerism was complete by the absence of ITGA2b on platelets.

Preparation of LN Stromal Cells

Stromal cells were prepared from murine peripheral (inguinal, axial and brachial) or mesenteric LNs as previously described [18]. CD45^{+} and TER119^{+} cells were depleted using anti-TER119 and anti-CD45 coupled magnetic beads (Miltenyi Biotec). Use of all human tissues was approved by the Medical Ethical Commission of the Erasmus University Medical Center Rotterdam and was contingent on written informed consent from the donor. Stromal cells from human LNs were obtained as described [19].

Flow Cytometry and Cell Sorting

All reactions were performed at 4°C for 20 min in PBS supplemented with 2% FCS and 2.5 mM EDTA. The following antibodies were used for flow cytometry: CD45-APC/CY7 (30-F11, Biolegend), Ter119-APC/CY7 (Ter119, Biolegend), gp38/podoplanin-A488 (8.1.1, Biolegend), CD31-PcPeF710 (390, eBioscience), ITGA2b (APC-conjugated MWReg30, Biolegend, A647-conjugated RAM-2), ITGB3-PE (2C9.G2, Biolegend), glycoprotein subunit IBβ-A647 (RAM-1 [20]), ITGAV-PE (RMV-7, eBioscience), CD3-FITC (145-2C11, BD), CD19-APC (1D3, BD), CD103-PerCP-Cy5.5 (M290, BD), CD11c-PerCP-Cy5.5 (N418, BD), RANK-02 [21] or their isotype controls. Integrin αIIbβ3-PE (JON/A, EMFRET analytics GmbH, Eibelstadt, Germany) was used to stain for the active integrin conformation in tyrode-albumin buffer pH 7.3 (137 mM NaCl, 2,7mM KCl, 12mM NaHCO3, 0.36 mM NaH2PO4, 1mM MgCl2, 2mM CaCl2, 5mM Hepes, 0,35% albumin, 5.55 mM Glucose). Flow cytometry was performed on a Gallios (Beckman-Coulter, Fullerton, CA, USA) or a Fortessa X-20 SORP (BD) and analyzed with FlowJo software (Treestar, Ashland, OR, USA). For flow cytometric analysis of human fetal LNs the following antibodies were used: gp38/podoplanin A488 (NC-08, Biolegend), CD31 Pacific-blue (WM59, Biolegend), CD45 PE-Cy7 (HI30, Biolegend), and mouse anti-Donkey A647 (Life technologies). Primary antibodies were added to the cells for 30 min at 4°C. Then, cells were stained with secondary antibodies for 20 min at 4°C.

Lymphatic Endothelial Cell Culture

LECs were cell-sorted based on gp38 and CD31 expression and cultured in a single drop of endothelial cell growth medium (Lonza) in culture slides (Corning) pre-coated with 5 μg/cm^{2} of fibronectin and collagen (Sigma-Aldrich) over-night at 37°C 5% CO_2. The next day, 300 μl of endothelial cell growth medium were added. Cells were fixed in 4% formaldehyde and then

144

stained for ITGA2b and mCLCA1 with DAPI nuclear counterstain. Images were acquired on a Microscope Zeiss Axio Observer Z1 Confocal LSM780 (Carl Zeiss) with the Carl Zeiss proprietary software Zen and on a spinning disk inverted microscope (Carl Zeiss) with a confocal head Yokogawa CSU and a Metamorph software (Metamorph). Analysis of all microscopic images was done using the open source imageJ-based Fiji distribution.

Immunofluorescence

Organs were embedded in Tissue-Tek O.C.T Compound (Electron Microscopy Science) and frozen in liquid nitrogen. Six to 8 μm sections were cut, fixed in cold acetone and then blocked with 2% BSA. The following antibodies were used: mCLCA1 (hamster mAb 10.1.1), Lyve-1-A488 (ALY7, eBioscience), ITGA2b-APC (MWReg30, Biolegend), Prox-1 (polyclonal goat, R&D Systems), GPIbß (RAM1-A645), MAdCAM-1 (MECA-367, BD-Pharmingen), fibronectin (Rabbit polyclonal, Patricia Simon-Assmann, UMR-S 1109 INSERM, Strasbourg), RANKL (IK22.5, Rat IgG2a, [22]), goat anti-rabbit-A488 (Molecular Probes), goat anti-hamster-A488/A546 (Molecular Probes), donkey anti-rat-Cy3 (Jackson) or streptavidin A546 or A647 (Molecular Probes). Sections were mounted using DAKO mounting medium (Dako, Hamburg, Germany). Images were acquired and treated as noted above.

Transmission Electron Microscopy

ITGA2b$^+$ sorted LECs were fixed in 2.5% glutaraldehyde for 1 h and 200 μl blue AccuDrops^R beads (BD Biosciences) were added to facilitate cell pellet visualization during the subsequence sample preparation as described [23]. Cells were visualized on a CM120 microscope with biotwin lens configuration operating at 120 kV (FEI, Eindhoven, The Netherlands)

Quantitative Reverse Transcription Coupled Polymerase Chain Reaction (qRT-PCR)

RNA from total LNs and from sorted LECs were extracted with RNeasy kits (Qiagen) and cDNA was synthesized with Maxima First Strand cDNA Synthesis Kit (Thermo Scientific) and Improm-II (Promega) using oligo(dT)15 primers. RT-PCR was performed using Luminaris color HiGreen qPCR Master Mix (Thermo Scientific) using the following primers to amplify ITGA2b: Forward 5'-ATTCCTGTTTAGGACGTTTGGG and Reverse: 5'-TCTTGACTT GCGTTTAGGGC [24] with the housekeeping gene coding for GAPDH (Forward 5'-T GACGTGCCGCCTGGAGAAA and Reverse 5'-AGTGTAGCCCAAGATGCCCTTCAG). Quantitative RT-PCR was run on a Bio-Rad CFX96 thermal cycler, and threshold values (Ct) of the target gene were normalized to GAPDH (ΔCt = CtITGA2b –CtGAPDH). The relative expression was calculated for each sample versus the mean of total 5 day LN ΔCt: ΔΔCt = ΔCtsample– ΔCttotal LN at 5 days; and relative quantification was performed as 2-ΔΔCt.

Immunization

Six-week-old mice were injected in both posterior limbs with 70 μg of chicken ovalbumin, 600 μg aluminium hydroxide (Sigma-Aldrich) and $6x10^8$ heat inactivated *B. pertussis* ml^{-1}. A boost was administrated 2 weeks later. Inguinal and popliteal LN were sampled 4 days later.

Imiquimod Treatment

Adult mice were anesthetized by intraperitoneal injection of ketamine and xylazine (100 μg/g body weight and 10 μg/g body weight, respectively). Back skin or ear skin received 12.5 μg/g (0.1mg/kg body weight) of Toll-like receptor (TLR)-7 agonist imiquimod (Aldara), diluted in

145

neutral cream (Diprobase) [25]. Back skin hair was trimmed before hair removal with cold wax (Klorane, France). The animals were sacrificed 12h after.

RANKL and Lymphotoxin β Receptor Blockage

The neutralizing anti-RANKL mAb IK22-5 [22] or the rat IgG2a isotype control (BioXell) were administrated s.c. into 6-week old C57BL/6 mice every 3 days (50 μg/ mouse in sterile saline) for two weeks and for 3 consecutive days for the third week. The lymphotoxin β receptor -Ig fusion protein or mIgG1 isotype control (20μg/mouse in sterile saline) were administrated s.c. into 6-week old mice every 3 days for four weeks.

Statistical Analysis

An unpaired two-tailed Student t-test and ANOVA with the Bonferroni method were used to determine statistically significant differences. The p values <0.05 were considered statistically significant. GraphPad Prism version 5 for Windows (GraphPad software) was used for the analysis.

Results

LN LECs Express ITGA2b

Microarray gene expression analysis of murine LN stromal cells had revealed transcription of *Itga2b* by LECs but by no other stromal or hematopoietic cells [26]. To study ITGA2b expression by LECs, we prepared stromal cells from peripheral LNs following the same procedure as used in the microarray study. LECs (gp38$^+$CD31$^+$), fibroblastic reticular cells (FRCs, gp38$^+$CD31$^-$), blood endothelial cells (BECs, gp38$^-$CD31$^+$), and pericyte-containing double-negative cells (DNCs, gp38$^-$CD31$^-$) were identified in the cell suspension (**panel A in S1 Fig**). ITGA2b-specific mAbs (MWReg30 and RAM-2), validated on platelets (**panel B in S1 Fig**), recognized a major subset of LECs and a minor subset of BECs (**Fig 1A** **and panel A in S1 Fig**). To verify whether the labelling was due to platelets bound to the cells, we exposed them to an antibody specific for glycoprotein subunit GPIbβ (CD42c) that is exclusively carried by megakaryocytes and platelets [20] (**panel B in S1 Fig**). The antibody recognized the minor fraction of BECs but did not interact with LECs (**Fig 1B**). To further assure that LECs were platelet-free, ITGA2b$^+$ LECs were FACS sorted and examined for the adherence of platelets by electron microscopy, however none were found (**panel C in S1 Fig**). To confirm ITGA2b expression, LECs were prepared from mice deficient for ITGA2b [15]. As shown in **Fig 1C**, LECs from heterozygous mice expressed reduced levels of the integrin and LECs from mice with the homozygous deletion fully lacked ITGA2b. We next irradiated WT C57BL/6 mice and adoptively transferred bone marrow from *Itga2b$^{-/-}$* mice. Six weeks later, circulating platelets were devoid of ITGA2b but LECs still expressed the integrin (**Fig 1D** and **panel A in S2 Fig**). Also the staining for platelets on LN cross-sections did not reveal any presence, whereas platelets were found in the spleen red pulp (**panel B in S2 Fig**). We tested whether the integrin could be detected on FACS-sorted LECs grown in culture. The cells were labelled for ITGA2b and the pan-LEC marker mCLCA1 (recognized by mAb 10.1.1, [27,28]). LECs expressing ITGA2b could be seen, which was found distributed throughout the cell and occasionally concentrated at cell-cell junctions (see arrows) (**Fig 1E**). Finally, to extend this finding to man, human embryonic mesenteric LNs were processed in a similar fashion to obtain the four stromal subsets (**panel C in S2 Fig**). An ITGA2b-reactive mAb that recognized platelets from healthy donors but not from an ITGA2b-deficient Glanzmann donor (**panel D in S2 Fig**)

146

RANKL Activates Lymphatic Integrin-αIIb Expression
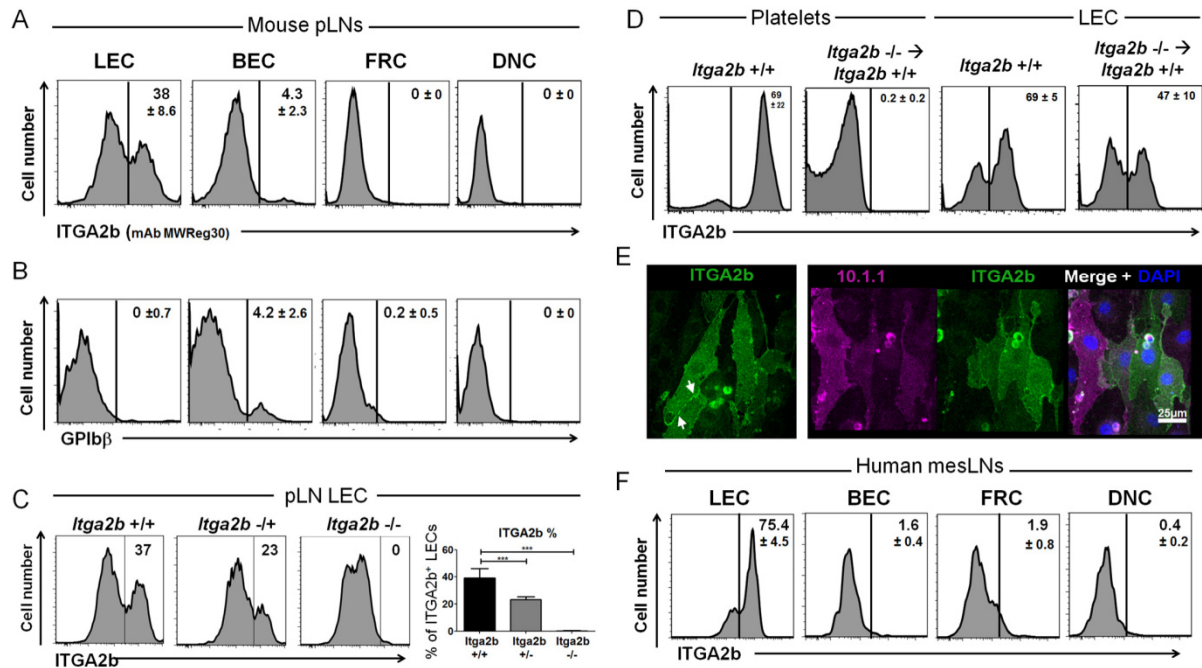
Fig 1. LN LECs express ITGA2b. (A) Flow cytometry histograms display ITGA2b expression by peripheral (p)LN stromal subsets, lymphatic endothelial cells (LEC), blood endothelial cells (BEC), fibroblastic reticular cells (FRC) and the pericyte-containing gp38⁻CD31⁻ double negative cells (DNC). Peripheral LNs are inguinal, brachial and axial LNs. The percentage ±SD (n = 13) of cells labelled by the mAb is indicated. (B) Histograms of the four stromal cell types incubated with a mAb specific for platelet-restricted GPIBβ. The percentage ±SD (n = 8) of cells labelled by the antibody is indicated. (C) Histograms show ITGA2b expression by LECs of WT mice, but reduced and no expression by LECs isolated from mice heterozygous or homozygous for *Itga2b* genetic deletion. The graph depicts the mean ± SD (n = 9) percentage of ITGA2b⁺ LECs in WT controls and in mice heterozygous or homozygous for the *Itga2b* genetic deletion. (D) Histograms of ITGA2b expression by platelets and LECs in control mice and in mice after adoptive transfer of *Itga2b⁻ᐟ⁻* bone marrow (n = 8 for adoptive bone marrow transfer, n = 4 for WT mice). The percentage ±SD of ITGA2b⁺ cells is indicted. (E) Confocal fluorescence microscopy images of cell-sorted LECs in culture showing mCLCA1 (mAb 10.1.1) (magenta) and ITGA2b (green) expression. (F) Flow cytometry histograms ±SD (n = 2) display ITGA2b expression within the four stromal subsets of human embryonic mesenteric LN. ***p<0.001.

labelled LECs but not the other stromal subsets (**Fig 1F**). Taken together, these finding demonstrated that LN LECs, but not other stromal cells, express the ITGA2b integrin.

ITGA2B Is Restricted to LN LEC Subsets

Because only a proportion of LN LECs expressed ITGA2b, we next wished to localize the ITGA2b⁺ LECs in the mouse LN. ITGA2b immunofluorescence on cross-sections together with LEC marker mCLCA1 (10.1.1 mAb) revealed that LECs of the medullary and the cortical area expressed ITGA2b in a heterogenous manner (**Fig 2A**). Remarkably, the subcapsular sinus ceiling LECs were totally devoid of ITGA2, while its floor counterpart uniformly expressed the integrin. We repeated the immunofluorescence with the lymphatic vessel endothelial hyaluronan receptor (Lyve)-1 and observed again a restricted expression of ITGA2b to a subset of LECs (**panel A in S3 Fig**). Colabelling for Prox-1, the most specific LEC marker, confirmed LEC-restricted ITGA2b staining (**panel B in S3 Fig**). At E18.5, the subcapsular sinus of the embryonic inguinal LNs were not yet formed and was constituted of a single layer of Lyve-1⁺ LECs expressing the integrin to different extents (**Fig 2B**). To verify its exclusion from the subcapsular sinus ceiling-lining cells, LECs of adult mice that express GFP exclusively in this

147
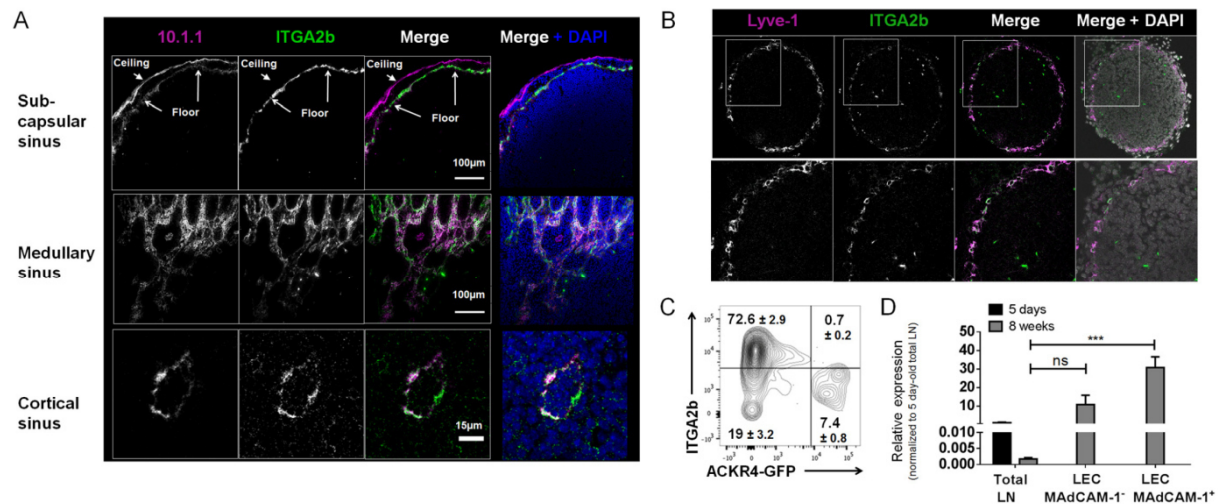
Fig 2. ITGA2b is heterogeneously expressed in the adult and embryonic LN. (A) Confocal microscopy images of an adult inguinal LN probed for ITGA2b together with LEC marker mCLCA1 (mAb 10.1.1) in the subcapsular, the medullary and the cortical sinus. Scale bars are indicated. (B) Confocal microscopy images of an embryonic (E18.5) inguinal LN of ITGA2b and LEC marker Lyve-1. Higher magnification of boxed area is shown below. (C) Flow cytometry counterplot of ITGA2b versus ACKR4 expression by LN LECs of ACKR4-GFP transgenic mice. The percentage ±SD (n = 3) of positive cells is indicated. (D) Mean ± SEM *Itga2b* mRNA expression of total LN from mice aged 5 days and 8 weeks, and of MAdCAM-1+ and MAdCAM-1- cell-sorted LECs from mice aged 8 weeks. Statistical analysis: ***p<0.001, ns = non significant by one way Anova with the Bonferroni method.

doi:10.1371/journal.pone.0151848.g002

subset [2] were labelled for ITGA2b. Indeed, the ACKR4-GFP+ LECs lacked the integrin (**Fig 2C**). To verify ITGA2b expression in the floor-lining cells, we sorted LECs based on gp38/CD31 and MAdCAM-1 expression for qRT-PCR analysis. MAdCAM-1 is uniformly carried by the floor-lining subcapsular sinus LECs but not the ceiling counterpart (**panel A in S4 Fig**) and colabelling showed that all MAdCAM-1+ cells express ITGA2b (**panel B in S4 Fig**). MRCs identified by RANKL expression localize close to the LECs but do not carry the integrin (**panel C in S4 Fig**). In whole adult LN, *Itga2b* mRNA was barely detectable, however sorted MAd-CAM-1+ and MAdCAM-1- cells clearly expressed the message (**Fig 2D**). Sorted LN BECs were devoid of the mRNA (data not shown). This supports its restricted expression in LECs, and in particular the floor-lining MAdCAM-1+ LECs. To determine whether ITGA2b is expressed by non-LN LECs, skin was processed into a cell suspension and LECs were identified as CD45-F4/80-gp38+CD31+ cells. However, we saw no ITGA2b expression by FACS or qRT-PCR, neither in LECs from resting skin, after activation with imiquimod [25] or from RANK-transgenic mice overexpressing RANKL from hair follicles [14,29] (**panel D in S4 Fig** and data not shown). Taken together, the data show that ITGA2b is restricted to subsets of LN LECs.

LEC ITGA2b Is Not Required for Residence in Fibronectin-Rich Environments

To explore the function of ITGA2b for LECs, we first asked whether ITGA2b could heterodi-merize with ITGB3 to interact with ligands, such as fibronectin. Indeed, ITGB3 was uniformly expressed by LECs and BECs, while there was little of the β-chain found on FRCs and DNCs (**Fig 3A**). We next assessed whether there was a correlation between ITGA2b expression and

148

RANKL Activates Lymphatic Integrin-αIIb Expression
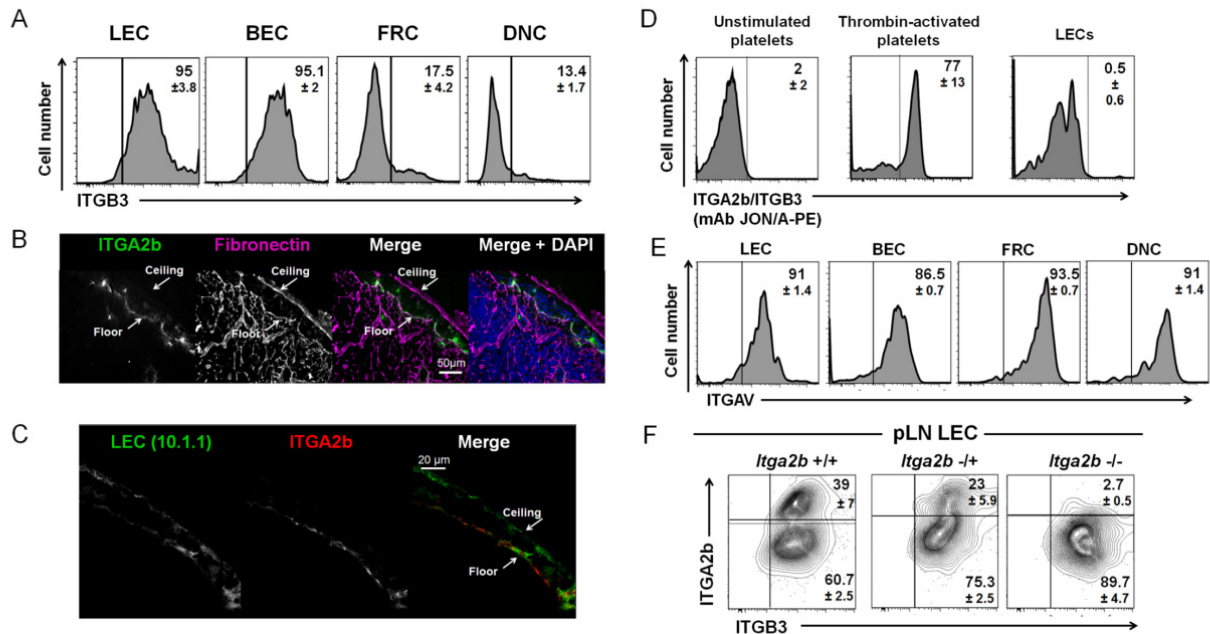
Fig 3. LEC ITGA2b is not required for residence in fibronectin-rich environments. (A) Flow cytometry histograms show the percentage ±SD (n = 4) of LECs expressing ITGB3 by the four stromal subsets. (B) Confocal microscopic images of a LN subcapsular area labelled for fibronectin (magenta) and ITGA2b (green). Nuclear coloration was with DAPI. (C) Confocal high resolution microscopy of the subcapsular area labelled for ITGA2b and mCLCA1 (mAb 10.1.1). (D) Histograms show recognition of the active conformation of the ITGA2b/ITGB3 complex on activated platelets but not on LECs or unstimulated platelets by the PE-conjugated JON/A mAb. (E) Histograms show ITGAV expression ±SD (n = 3) on the stromal subsets. (F) Flow cytometry counterplots of LECs probed for expression of ITGA2b and ITGB3 in *Itga2b$^{+/+}$*, *Itga2b$^{+/-}$* and *Itga2b$^{-/-}$* mice (n = 3).

doi:10.1371/journal.pone.0151848.g003

residence in a fibronectin-containing environment. To this end, we stained the LN subcapsular area that contained the ITGA2b$^+$ floor-lining and the ITGA2b$^-$ ceiling-lining LECs for fibronectin. It was apparent that this extracellular matrix component was present in both sites, demonstrating that the absence of ITGA2b does not prevent LECs to take up position in the fibronectin-containing ceiling (**Fig 3B**). Further, the positioning of the integrin relative to the sinus luminal or abluminal side was investigated and no preferential location was found (**Fig 3C**). To explore whether a functional ITGA2b/ITGB3 complex was indeed formed, LECs and, as controls unstimulated and thrombin-activated platelets, were incubated with the phycoerythrin (PE)-conjugated JON/A mAb, which recognizes only the ITGA2b/ITGB3 complex in its activated state, as found on platelets [30,31]. While agonist stimulated platelets were labelled with this mAb, LECs were not recognized (**Fig 3D**). This suggests that if an ITGA2B/ITGB3 heterodimer is formed on LECs, it is not in a configuration recognized by PE-JON/A and may present a low affinity for its ligands. We therefore asked whether ITGA2b could be substituted by ITGAV to pair with ITGB3. LECs, alike all other stromal cells, expressed ITGAV, suggesting that they could anchor to matrix proteins through ITGAV/ITGB3 (**Fig 3E**). In platelets (**panel B in S1 Fig**) but not in embryonic hematopoietic stem cells or mast cells [24,32], ITGA2b is required to translocate ITGB3 to the cell surface [15,33], raising the question of whether, in the absence of ITGA2b, ITGB3 would be available to heterodimerize with ITGAV on the cell surface. To assess this issue, we labelled LECs from mice deficient for ITGA2 and observed that

149

cell surface expression of the ITGB3 was maintained in *Itga2b*^{-/-} mice (**Fig 3F**). Taken together, ITGA2b is not required for residence of the ceiling LECs in its fibronectin-containing environment, most probably by the formation of an ITGAV/ITGB3 complex that binds with high affinity to this matrix protein.

The ITGA2b⁺ Subset Is Sensitive to Activation by RANKL and Lymphotoxin

We noted that in comparison to peripheral LNs, the proportion of ITGA2b⁺ LECs was higher in mesenteric LNs (**Fig 4A**). Because mesenteric LNs are stimulated by the intestinal microflora, this evoked the possibility that the heterogenous LN ITGA2b expression reflects differences in cell activation. To test this hypothesis, we administered heat-inactivated *Bordetella pertussis* subcutaneously, and after a secondary immunization, compared ITGA2b expression in draining and non-draining LNs. The proportion of ITGA2b⁺ LECs was markedly increased in response to immunization (**Fig 4B**), while the other stromal cells remained devoid of the integrin (**Fig 4C**). The upregulation was not due to platelet adherence to LECs because there was no recognition of LECs by the GPIbβ-specific mAb (**Fig 4D**). We also tested whether the innate immune stimulus imiquimod (TLR7 ligand) resulted in a similar upregulation. LECs from auricular LNs draining imiquimod or mock-treated ears were analyzed, however, the proportion of ITGA2b⁺ LECs did not rise after application of the TLR-7 ligand (**panel A in S5 Fig**). We have previously observed that RANKL activates LN LECs in a transgenic model of cutaneous RANKL overproduction [14]. Therefore, we determined in these mice whether RANKL affected ITGA2b levels and indeed found that ITGA2b expression was positively regulated by this TNF-family member (**Fig 4E**). We addressed the question of whether integrin upregulation was due to its externalization to the cell surface. In WT controls, immunolabelling of permeabilized cells revealed a stronger signal compared with the cell surface, however, the signal was identical in the LECs isolated from the transgenic mice (**panel B in S5 Fig**). This suggests that the increased expression of ITGA2b by RANKL stimulation likely involves its translocation from the cytoplasm to the cell membrane. We tested whether the upregulation was accompanied by a rise in transcriptional activity. In comparison with WT controls, there was no major increase in mRNA synthesis in the LEC subsets isolated from the mutant mice (**panel C in S5 Fig**). However, because the proportion of MAdCAM-1⁺ LECs greatly augmented in the transgenic mice (**panel C in S5 Fig**), the increase in ITGA2b expression in these mice is principally the result of an expansion of the MAdCAM-1⁺ subset that naturally expresses more ITGA2b. We next determined if neutralizing RANKL in WT mice led to a downregulation of ITGA2b. Administration of RANKL-blocking mAb caused a significant decrease in ITG2b expression by LECs in comparison to isotype injected controls (**Fig 4F**). Immunofluorescence on sections confirmed the strong decline of ITGA2b in subcapsular and medullary sinuses (**Fig 4G**). Because in the LN, RANKL is principally produced by the marginal reticular cells (MRCs) [13], this raised the possibility that MRC RANKL activates LECs resulting in ITGA2b expression. To address this question, we generated mice conditionally deficient for RANKL in MRCs by crossing *Ccl19-cre* mice [16] with *Rankl*^{f/f} mice [17]. These mice were devoid of RANKL expression by MRCs (**panel D in S5 Fig**). Analysis of RANKL^{ΔCCL19} mice showed that the disappearance of MRC RANKL significantly compromised ITGA2b expression (**Fig 4H**), supporting a role of RANKL in LEC activation. However, because there was not a complete loss of ITGA2b other factors could contribute to LEC activation. Indeed, approximately 15% of LECs were double positive for RANK and ITGA2b, suggesting that a proportion of LECs reacts to other stimulatory factors (**panel E in S5 Fig**). On the other hand, cutaneous LECs that do not respond to RANKL do not carry any RANK

150

RANKL Activates Lymphatic Integrin-αIIb Expression
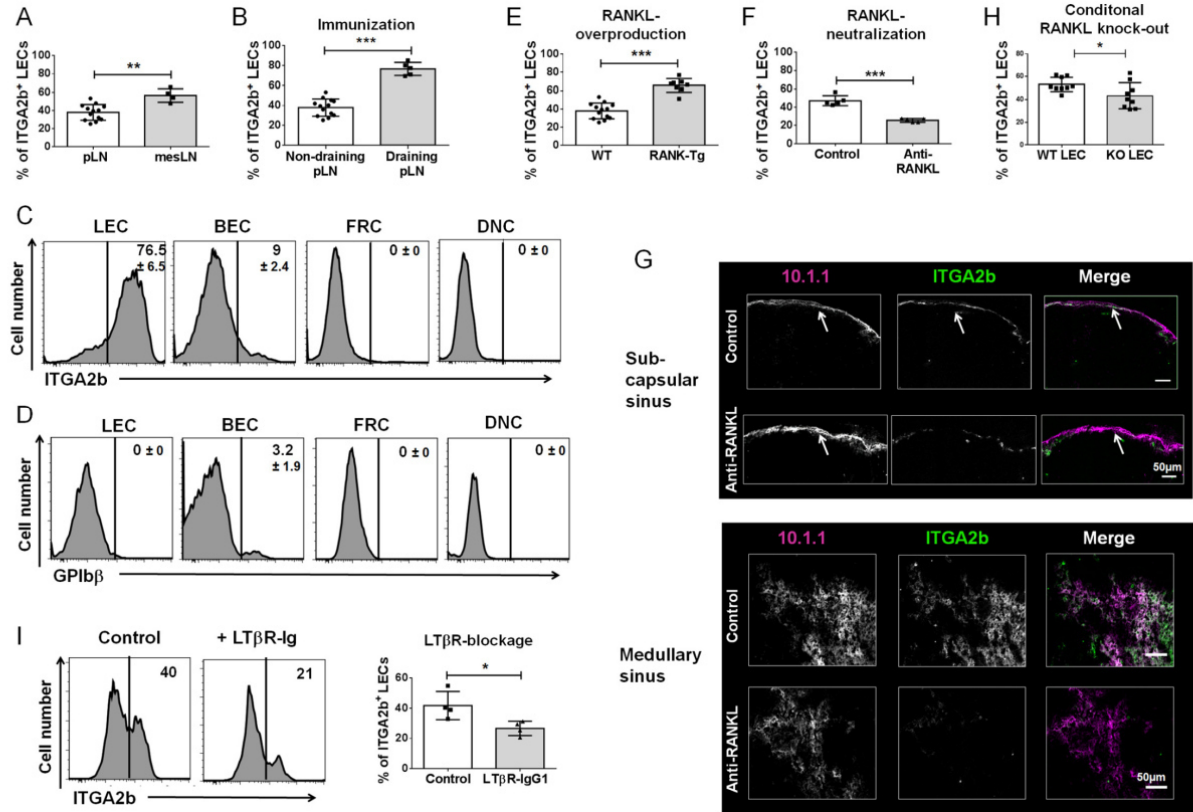
Fig 4. ITGA2b+ LECs are responsive to RANKL and lymphotoxin activation. (A) Mean ± SD (n = 6) percentage of ITGA2b+ LECs of peripheral (p)LNs (inguinal, axial and brachial) versus mesenteric (mes) LNs. (B) Mice were immunized with heat-inactivated *B. pertussis* and LEC ITGA2b expression of draining and non-draining LNs was compared. The graph shows the mean ± SD (n = 6) percentage of ITGA2b+ LECs, revealing increased ITGA2b proportions in response to immunization. (C) Flow cytometry histograms display representative ITGA2b expression ±SD (n = 6) by stromal subsets of inguinal and popliteal LNs draining the immunization site. (D) Histograms show reactivity to anti-GPIBβ labelling of stromal subsets of inguinal and popliteal LNs draining the immunization site. The percentage ±SD (n = 6) of cells labelled by the antibody is indicated. (E) The increase in the proportion of ITGA2b+ pLN LECs from RANK-Tg mice (overproducing soluble RANKL in the skin) compared with LECs of WT controls is shown as mean ± SD (n = 8). (F) Graph shows reduction in the percentage of ITGA2b+ LECs upon RANKL neutralization (mean ± SD, n = 5). (G) Confocal microscopy imaging in inguinal LN subcapsular and medullary sinuses of ITGA2b expression (green) by LECs (10.1.1, magenta) after RANKL-neutralization or after administration of isotype-control antibody. (H) Mean ± SD (n = 9) percentage of ITGA2b+ LECs from mice with conditional deficiency of RANKL in marginal reticular cells (KO) versus WT littermate controls. (I) Histograms of ITGA2b expression of LECs from mice treated with LTβR-Ig or IgG1 control. The graph depicts the mean ± SD (n = 3) percentage of ITGA2b+ LECs. *p<0.5, **p < 0.01, ***p < 0.001.

(**panel F in S5 Fig**). In light of similar activities of RANKL and lymphotoxin αβ (LT) [10,34] and the expression of the LTβ receptor (R) by LECs [35], we asked whether also LT regulated ITGA2b expression. Therefore, mice were treated with soluble LTβR-Ig to inhibit LTβR signaling [36]. We found that this treatment likewise reduced ITGA2b (**Fig 4I**). Taken together, ITGA2b is a novel marker for subsets of LN LECs that respond to activation by TNF-family members RANKL and LT.

151

Discussion

In this study we show that ITGA2b is expressed by a subset of LN LECs in the subcapsular, cortical and medullary sinus. This subset is also marked by MAdCAM-1. The ITGA2b$^+$ population is sensitive to stimulation by the TNFSF members RANKL and LT.

ITGA2b is known to be carried by megakaryocytes and platelets as well as by hematopoietic stem and progenitor cells in the embryo and the adult [7–9,37]. Here we show for the first time that LN LECs also carry this integrin. A number of studies had analyzed ITGA2b expression using different experimental approaches, including a genetic reporter system to mark ITGA2b-expressing cells by β-galactosidase [7–9]. However, these reports, which investigated whole embryos, the embryonic aorta-gonad-mesonephros region, spleen, thymus and bone marrow, did not analyze LNs. Although platelets interact with endothelial cells in the embryo during separation of blood and lymphatic systems [4], the following observations exclude the possibility that ITGA2b expression by LEC is the result of platelet contamination: (i) the platelet glycoprotein subunit Iβ was not detected on LECs, (ii) electron microscopy did not reveal platelets adhering to the cells, (iii) ITGA2b-deficient platelets lacked surface ITGB3, yet the β-chain was expressed by LECs of *Itga2b$^{-/-}$* mice, (iv) after adoptive transfer of *Itga2b$^{-/-}$* bone marrow resulting in the repopulation of ITGA2b$^-$ platelets, the integrin was still expressed by LECs and (vi) *Itga2b* mRNA was amplified from sorted LECs. The related BECs were devoid of the integrin, irrespective of the site of residence or the presence of stimulatory signals. This is supported by an early report noting the absence of ITGA2b in the blood endothelial cell line bEnd3 [38].

LN LECs and BECs uniformly expressed ITGB3 and ITGAV, while only a subset of LECs also carried ITGA2b. Both α-chains pair with ITGB3 and recognize similar matrix proteins, such as fibronectin, fibrinogen, von Willebrand factor and vitronectin, which raises the question of the necessity of the ITGA2b chain. This is in contrast to platelets that predominantly express ITGA2b to ensure platelet aggregation. Indeed, although ITGA2b was expressed by LECs in embryonic LNs, its absence had no discernible impact on LN development. In addition, those LECs that naturally lack ITGA2b are still capable of taking up residence in the fibronectin-rich subcapsular sinus. Further, the absence of polarization towards the luminal or the abluminal side does not point to a predominant function in cell-cell interaction or cell-extracellular matrix contact. It is likely that LECs rendered genetically deficient for ITGA2b function normally, since the migration of tissue-derived dendritic cells to the LN cortex of ITGA2b-deficient mice was unperturbed (data not shown). Although we observed a reduction in the number of B cells, it cannot be excluded that this defect was the result of a loss of ITGA2b from platelets (data not shown). Indeed, a minor defect in LN structuring during development was seen in mice lacking platelet CLEC-2 [39]. Further investigation into the specific role of ITGA2b for LEC function will await the generation of mice with conditional deletion of ITGA2b in these cells. Inside-out signaling of platelets results in a conformation change of ITGA2b/ITGB3 to increase affinity for its ligands. This conformation is detected by the PE-conjugated JON/A mAb. LECs were not recognized by the antibody indicating either that ITGA2b does not pair with ITGB3 or that the complex is not in the same configuration as that found on platelets. On the other hand, to our knowledge, this mAb has only been used successfully on activated platelets and may not be a suitable reagent to probe for the ITAG2b/ITGB3 heterodimer on other cells. It is also noteworthy that although bone marrow-derived mast cells express ITGA2b and ITGB3, no binding to fibrinogen was seen, and, paradoxically, cell adhesion to fibronectin increased in ITGA2b-deficient cells [24]. It should also be noted that the densities of the α and β chains are at least 10-fold higher on platelets owing to their approximately 10-fold smaller size with roughly equal mean fluorescence intensities, resulting in greatly increasing the avidity.

ITGA2b was carried by the subcapsular floor-lining LECs but absent from its ceiling equivalent. Interestingly, this expression pattern was shared with MAdCAM-1. Hence, MAdCAM-1$^+$ LECs displayed the highest *Itga2b* transcriptional activity. In addition, there was a heterogenous expression of ITGA2b in the medullary and the cortical sinuses. Skin LECs were devoid of the integrin on protein and mRNA levels in all conditions tested. Difference in tissue versus secondary lymphoid organ LECs is supported by other examples, such as Sphingosine-1-phosphate [3], found expressed by LN LECs, or ITGA9 [40] that is carried exclusively by vessel LECs. In view of its uniform expression by the subcapsular floor-lining LECs, their juxtaposition to the RANKL-expressing MRCs, and the finding that RANKL upregulates MAdCAM-1 expression [14], we reasoned that RANKL may control ITGA2b synthesis. Using overexpression and neutralization / genetic deletion, we showed that RANKL positively regulates the proportion of ITGA2b$^+$ LECs. The finding that conditional deficiency of RANKL from MRCs lowers ITGA2b expression to the same extent as RANKL neutralization concords with the idea that MRC RANKL is the main LN RANKL source and identifies a cellular target for the stromal cell-produced RANKL. However, in the absence of definite proof that RANKL activates ITGA2b transcription we cannot completely rule out the possibility that RANKL stimulates the expansion of the ITGA2b$^+$ subset. Two elements suggested that RANKL is not the exclusive ITGA2b regulatory factor: (i) RANKL neutralization or genetic deletion do not eliminate its expression and (ii) only a proportion of ITGA2b$^+$ LECs express RANK. Lymphotoxin and RANKL share not only biological functions (requirement for secondary lymphoid organ formation), signaling (canonical and non-canonical NF-κB pathways) but also receptor expression by LECs, so that it appeared rational to investigate the impact of LTβR blockage. Indeed, administration of LTβR-Ig also led to reduced ITGA2b expression. It is therefore likely that both RANKL and LT contribute to the expression of this integrin by LECs and that its upregulation in response to immunization is the consequence of stimulatory factors including RANKL produced by primed T cells and LT expressed by activated B and T cells. The finding that imiquimod had no effect on ITGA2b may therefore reflect a failure to stimulate RANKL and LT synthesis. Further work is necessary to determine whether other stimuli such as TNF-α or T and B cell-released cytokines also impact on ITGA2b expression by LN LECs. Beyond the question of its function for LN LECs, the ITGA2b integrin sheds a new light on the heterogeneity of LECs and their response to activation signals.

Supporting Information

S1 Fig. (A) Left: Flow cytometry dot plot profiles displaying the gating strategy for stromal cell identification in CD45/Ter119-depleted LN cell suspensions. Right: Flow cytometry histograms show ITGA2b expression by the four stromal subsets using the RAM-2 mAb. The percentage ±SD (n = 6) of cells labelled by the antibody is indicated. (B) Validation of MWReg30 and RAM.2 (anti-ITGA2b antibodies), RAM.1 (anti-GPIbβ antibody) and 2C9.G2 (anti-ITGB3 antibody) in WT and knock-out animals. Expression of ITGA2b and ITGB3 was seen on platelets from *Itgab2*$^{+/+}$ mice but not on platelets from *Itgab2*$^{-/-}$ mice. GPIbβ was present on platelets of both mice. (C) FACS sorting of Itga2b$^+$ LECs. Plots for sorting and post-sort analyses are represented. Sorted cells were then viewed by transmission electron microscopy. Eight representative images of LECs are shown together with an image of platelets with the same magnification.
(TIF)

S2 Fig. (A) Microscopy images of a LN of mouse that was lethally irradiated and had received *Itgab2*$^{-/-}$ bone marrow, labelled for ITGA2b (clone MWReg30) and the LEC marker mCLCA1 (mAb 10.1.1). (B) Staining of spleen and LN sections for platelets using the platelet-specific

glycoprotein GPIbβ (mAb RAM.1) together with LEC marker mCLCA1 (mAb 10.1.1).
RP = red pulp. (C) Flow cytometry dot plot profiles displaying the gating strategy for stromal
cell identification from human embryonic mesenteric LN. (D) The histogram displays ITGA2b
expression (SDF.2 mAb) on human healthy donor platelets but not on platelets from a patient
with Glanzmann's thrombasthenia. Representative image of over 10 donors.
(TIF)

S3 Fig. (A) Confocal microscopy images of an inguinal LN, showing the medullary and the
subcapsular sinus LECs labelled with anti-Lyve-1 and anti-ITGA2b mAbs. Images are repre-
sentative of 2 different experiments. (B) Upper: Images of the medullary region stained for
ITGA2b and nuclear Prox-1. Lower: Images of the subcapsular sinus from a LN of a mouse
expressing GFP under the control of the Prox-1 promoter.
(TIF)

S4 Fig. (A) Confocal microscopy images of a LN subcapsular sinus showing MAdCAM-1
expression by the floor-lining but not the ceiling-lining LECs marked with the 10.1.1 mAb. (B)
Images show overlapping staining of subcapsular sinus LECs for mCLCA1 (mAb 10.1.1),
MAdCAM-1 (MECA-367) and ITGA2b (MWReg30). The flow cytometry profile shows dou-
ble labelling of LECs with ITGA2b and MAdCAM-1. (C) Confocal microscopy images of a LN
subcapsular sinus labelled for MAdCAM-1 and RANKL. (D) Flow cytometry of mouse skin:
upper dot plot panels depict the gating strategy for skin LECs; lower panels show the histo-
grams for ITGA2b expression ± SD (n = 3) of skin LECs from control mice, imiquimod-treated
skin and from RANK-transgenic skin (overexpressing RANKL in the hair follicles).
(TIF)

S5 Fig. (A) Histograms show ITGA2b expression of auricular LN LECs from mice non-treated
or after 2 or 4 day topical application of imiquimod on ears. Graph depicts the levels (geomet-
ric mean of fluorescence) of ITGA2b expression (mean ±SD, n = 3–4). (B) Histograms show
LEC ITGA2b expression on the cell surface or on the cell surface and in the cytoplasm for WT
and RANK-Tg mice. The graphs show the expression levels of the integrin in LECs after cell
surface or intracellular/cell surface labelling. The data for WT mice are of 8 mice and for Tg
mice are of 4 mice. (C) Graphs show mean ± SEM (n = 6) *Itga2b* mRNA expression of total
LN, MAdCAM-1^{+} and MAdCAM-1^{-} LECs from WT and RANK-Tg mice (left) normalized
with respect to WT 5 day LNs. Right: Graph shows the mean ± SD (n = 10) percentage of
MAdCAM-1[+] LECs in WT and RANK-Tg mice measured by flow cytometry. (D) Confocal
microscopy images of WT and RANKL[ΔCcl19] inguinal LNs, showing the subcapsular sinus area
labelled for mCLCA1 (red) and RANKL (green). The RANKL[ΔCcl19] LN is devoid of RANKL
expression. Representative of 4 mice. (E) Counterplot of LN LECs double stained for ITGA2b
and RANK expression. Graph bar (n = 6) shows the percentage of LECs expressing both
ITGA2b and RANK. (F) Histograms show RANK expression by LECs and BECs from skin and
LNs. The percentage of ITGA2b^{+} cells is indicated. Graph shows their mean ± SD (n = 6) per-
centages. ns = not significant, *p<0.5, **p < 0.01, ***p < 0.001.
(TIF)

Acknowledgments

Author Contributions

Conceived and designed the experiments: CGM FL CL OGC MC NB. Performed the experiments: OGC MC NB SR FA MRH CB ZL AE. Analyzed the data: OGC MC NB SR FA MRH CB ZL CGM MCC TC AE. Contributed reagents/materials/analysis tools: MCC AR HY BL FL TC. Wrote the paper: CGM FL OGC MC.

References

1. Tewalt EF, Cohen JN, Rouhani SJ, Engelhard VH (2012) Lymphatic endothelial cells—key players in regulation of tolerance and immunity. Front Immunol 3:305.: 1–6.

2. Ulvmar MH, Werth K, Braun A, Kelay P, Hub E, Eller K, et al. (2014) The atypical chemokine receptor CCRL1 shapes functional CCL21 gradients in lymph nodes. Nat Immunol 15: 623–630. doi: 10.1038/ni.2889 PMID: 24813163

3. Schwab SR, Cyster JG (2007) Finding a way out: lymphocyte egress from lymphoid organs. Nat Immunol 8: 1295–1301. PMID: 18026082

4. Bertozzi CC, Schmaier AA, Mericko P, Hess PR, Zou Z, Chen M, et al. (2010) Platelets regulate lymphatic vascular development through CLEC-2-SLP-76 signaling. Blood 116: 661–670. doi: 10.1182/blood-2010-02-270876 PMID: 20363774

5. Lowell CA, Mayadas TN (2012) Overview: studying integrins in vivo. Methods Mol Biol 757: 369–397. doi: 10.1007/978-1-61779-166-6_22 PMID: 21909923

6. Lefkovits J, Plow EF, Topol EJ (1995) Platelet glycoprotein IIb/IIIa receptors in cardiovascular medicine. N Engl J Med 332: 1553–1559. PMID: 7739710

7. Mitjavila-Garcia MT, Cailleret M, Godin I, Nogueira MM, Cohen-Solal K, Schiavon V, et al. (2002) Expression of CD41 on hematopoietic progenitors derived from embryonic hematopoietic cells. Development 129: 2003–2013. PMID: 11934866

8. Emambokus NR, Frampton J (2003) The glycoprotein IIb molecule is expressed on early murine hematopoietic progenitors and regulates their numbers in sites of hematopoiesis. Immunity 19: 33–45. PMID: 12871637

9. Ferkowicz MJ, Starr M, Xie X, Li W, Johnson SA, Shelley WC, et al. (2003) CD41 expression defines the onset of primitive and definitive hematopoiesis in the murine embryo. Development 130: 4393–4403. PMID: 12900455

10. Mueller CG, Hess E (2012) Emerging Functions of RANKL in Lymphoid Tissues. Frontiers in Immunology 3: 261–267. doi: 10.3389/fimmu.2012.00261 PMID: 22969763

11. Yoshida H, Naito A, Inoue J, Satoh M, Santee-Cooper SM, Ware CF, et al. (2002) Different cytokines induce surface lymphotoxin-alphabeta on IL-7 receptor-alpha cells that differentially engender lymph nodes and Peyer's patches. Immunity 17: 823–833. PMID: 12479827

12. Sugiyama M, Nakato G, Jinnohara T, Akiba H, Okumura K, Ohno H, et al. (2012) Expression pattern changes and function of RANKL during mouse lymph node microarchitecture development. Int Immunol 24: 369–378. doi: 10.1093/intimm/dxs002 PMID: 22354913

13. Katakai T, Suto H, Sugai M, Gonda H, Togawa A, Suematsu S, et al. (2008) Organizer-like reticular stromal cell layer common to adult secondary lymphoid organs. J Immunol 181: 6189–6200. PMID: 18941209

14. Hess E, Duheron V, Decossas M, Lézot F, Berdal A, Chea S, et al. (2012) RANKL induces organized lymph node growth by stromal cell proliferation. J Immunol 188: 1245–1254. doi: 10.4049/jimmunol.1101513 PMID: 22210913

15. Zhang J, Varas F, Stadtfeld M, Heck S, Faust N, Graf T (2007) CD41-YFP mice allow in vivo labeling of megakaryocytic cells and reveal a subset of platelets hyperreactive to thrombin stimulation. Exp Hematol 35: 490–499. PMID: 17309829

155

16. Chai Q, Onder L, Scandella E, Gil-Cruz C, Perez-Shibayama C, Cupovic J, et al. (2013) Maturation of lymph node fibroblastic reticular cells from myofibroblastic precursors is critical for antiviral immunity. Immunity 38: 1013–1024. doi: 10.1016/j.immuni.2013.03.012 PMID: 23623380

17. Xiong J, Onal M, Jilka RL, Weinstein RS, Manolagas SC, O'Brien CA (2011) Matrix-embedded cells control osteoclast formation. Nat Med 17: 1235–1241. doi: 10.1038/nm.2448 PMID: 21909103

18. Link A, Vogt TK, Favre S, Britschgi MR, Acha-Orbea H, Hinz B, et al. (2007) Fibroblastic reticular cells in lymph nodes regulate the homeostasis of naive T cells. Nat Immunol 8: 1255–1265. PMID: 17893676

19. Onder L, Narang P, Scandella E, Chai Q, Iolyeva M, Hoorweg K, et al. (2012) IL-7-producing stromal cells are critical for lymph node remodeling. Blood 120: 4675–4683. doi: 10.1182/blood-2012-03-416859 PMID: 22955921

20. Perrault C, Moog S, Rubinstein E, Santer M, Baas MJ, de la Salle C, et al. (2001) A novel monoclonal antibody against the extracellular domain of GPIbbeta modulates vWF mediated platelet adhesion. Thromb Haemost 86: 1238–1248. PMID: 11816713

21. Chypre M, Seaman J, Cordeiro OG, Willen L, Knoop KA, Buchanan A, et al. (2016) Characterization and application of two RANK-specific antibodies with different biological activities. Immunol Lett 171:5–14. doi: 10.1016/j.imlet.2016.01.003 PMID: 26773232

22. Kamijo S, Nakajima A, Ikeda K, Aoki K, Ohya K, Akiba H, et al. (2006) Amelioration of bone loss in collagen-induced arthritis by neutralizing anti-RANKL monoclonal antibody. Biochem Biophys Res Commun 347: 124–132. PMID: 16815304

23. Eckly A, Strassel C, Cazenave JP, Lanza F, Leon C, Gachet C (2012) Characterization of megakaryocyte development in the native bone marrow environment. Methods Mol Biol 788:175–92. doi: 10.1007/978-1-61779-307-3_13 PMID: 22130708

24. Berlanga O, Emambokus N, Frampton J (2005) GPIIb (CD41) integrin is expressed on mast cells and influences their adhesion properties. Exp Hematol 33: 403–412. PMID: 15781330

25. Voisin B, Mairhofer DG, Chen S, Stoitzner P, Mueller CG, Flacher V (2014) Anatomical distribution analysis reveals lack of Langerin+ dermal dendritic cells in footpads and tail of C57BL/6 mice. Exp Dermatol 23: 354–356. doi: 10.1111/exd.12373 PMID: 24629018

26. Malhotra D, Fletcher AL, Astarita J, Lukacs-Kornek V, Tayalia P, Gonzalez SF, et al. (2012) Transcriptional profiling of stroma from inflamed and resting lymph nodes defines immunological hallmarks. Nat Immunol 13: 499–510. doi: 10.1038/ni.2262 PMID: 22466668

27. Ruddell A, Mezquita P, Brandvold KA, Farr A, Iritani BM (2003) B lymphocyte-specific c-Myc expression stimulates early and functional expansion of the vasculature and lymphatics during lymphomagenesis. Am J Pathol 163: 2233–2245. PMID: 14633598

28. Furuya M, Kirschbaum SB, Paulovich A, Pauli BU, Zhang H, Alexander JS, et al. (2010) Lymphatic endothelial murine chloride channel calcium-activated 1 is a ligand for leukocyte LFA-1 and Mac-1. J Immunol 185: 5769–5777. doi: 10.4049/jimmunol.1002226 PMID: 20937843

29. Duheron V, Hess E, Duval M, Decossas M, Castaneda B, Klöpper JE, et al. (2011) Receptor Activator of NF-kB (RANK) stimulates the proliferation of epithelial cells of the epidermo-pilosebaceous unit. Proc Natl Acad Sci USA 108: 5342–5347. doi: 10.1073/pnas.1013054108 PMID: 21402940

30. Bergmeier W, Schulte V, Brockhoff G, Bier U, Zirngibl H, Nieswandt B (2002) Flow cytometric detection of activated mouse integrin alphaIIbbeta3 with a novel monoclonal antibody. Cytometry 48: 80–86. PMID: 12116368

31. Wang Y, Jobe SM, Ding X, Choo H, Archer DR, Mi R, et al. (2012) Platelet biogenesis and functions require correct protein O-glycosylation. Proc Natl Acad Sci U S A 109: 16143–16148. doi: 10.1073/pnas.1208253109 PMID: 22988088

32. Boisset JC, Clapes T, Van Der Linden R, Dzierzak E, Robin C (2013) Integrin alphaIIb (CD41) plays a role in the maintenance of hematopoietic stem cell activity in the mouse embryonic aorta. Biol Open 2: 525–532. doi: 10.1242/bio.20133715 PMID: 23789102

33. Hodivala-Dilke KM, McHugh KP, Tsakiris DA, Rayburn H, Crowley D, Ullman-Cullere M, et al. (1999) Beta3-integrin-deficient mice are a model for Glanzmann thrombasthenia showing placental defects and reduced survival. J Clin Invest 103: 229–238. PMID: 9916135

34. Kong YY, Yoshida H, Sarosi I, Tan HL, Timms E, Capparelli C, et al. (1999) OPGL is a key regulator of osteoclastogenesis, lymphocyte development and lymph-node organogenesis. Nature 397: 315–323. PMID: 9950424

35. Cohen JN, Tewalt EF, Rouhani SJ, Buonomo EL, Bruce AN, Xu X, et al. (2014) Tolerogenic properties of lymphatic endothelial cells are controlled by the lymph node microenvironment. PLoS ONE 9: e87740. doi: 10.1371/journal.pone.0087740 PMID: 24503860

156

36. Ettinger R, Browning JL, Michie SA, van Ewijk W, McDevitt HO (1996) Disrupted splenic architecture, but normal lymph node development in mice expressing a soluble lymphotoxin-beta receptor-IgG1 fusion protein. Proc Natl Acad Sci USA 93: 13102–13107. PMID: 8917551

37. Gekas C, Graf T (2013) CD41 expression marks myeloid-biased adult hematopoietic stem cells and increases with age. Blood 121: 4463–4472. doi: 10.1182/blood-2012-09-457929 PMID: 23564910

38. Nieswandt B, Echtenacher B, Wachs FP, Schroder J, Gessner JE, Schmidt RE, et al. (1999) Acute systemic reaction and lung alterations induced by an antiplatelet integrin gpIIb/IIIa antibody in mice. Blood 94: 684–693. PMID: 10397735

39. Benezech C, Nayar S, Finney BA, Withers DR, Lowe K, Desanti GE, et al. (2014) CLEC-2 is required for development and maintenance of lymph nodes. Blood 123: 3200–3207. doi: 10.1182/blood-2013-03-489286 PMID: 24532804

40. Bazigou E, Xie S, Chen C, Weston A, Miura N, Sorokin L, et al. (2009) Integrin-alpha9 is required for fibronectin matrix assembly during lymphatic valve morphogenesis. Dev Cell 17: 175–186. doi: 10.1016/j.devcel.2009.06.017 PMID: 19686679

157

Supplemental Figure 1 (related to Figure 1)
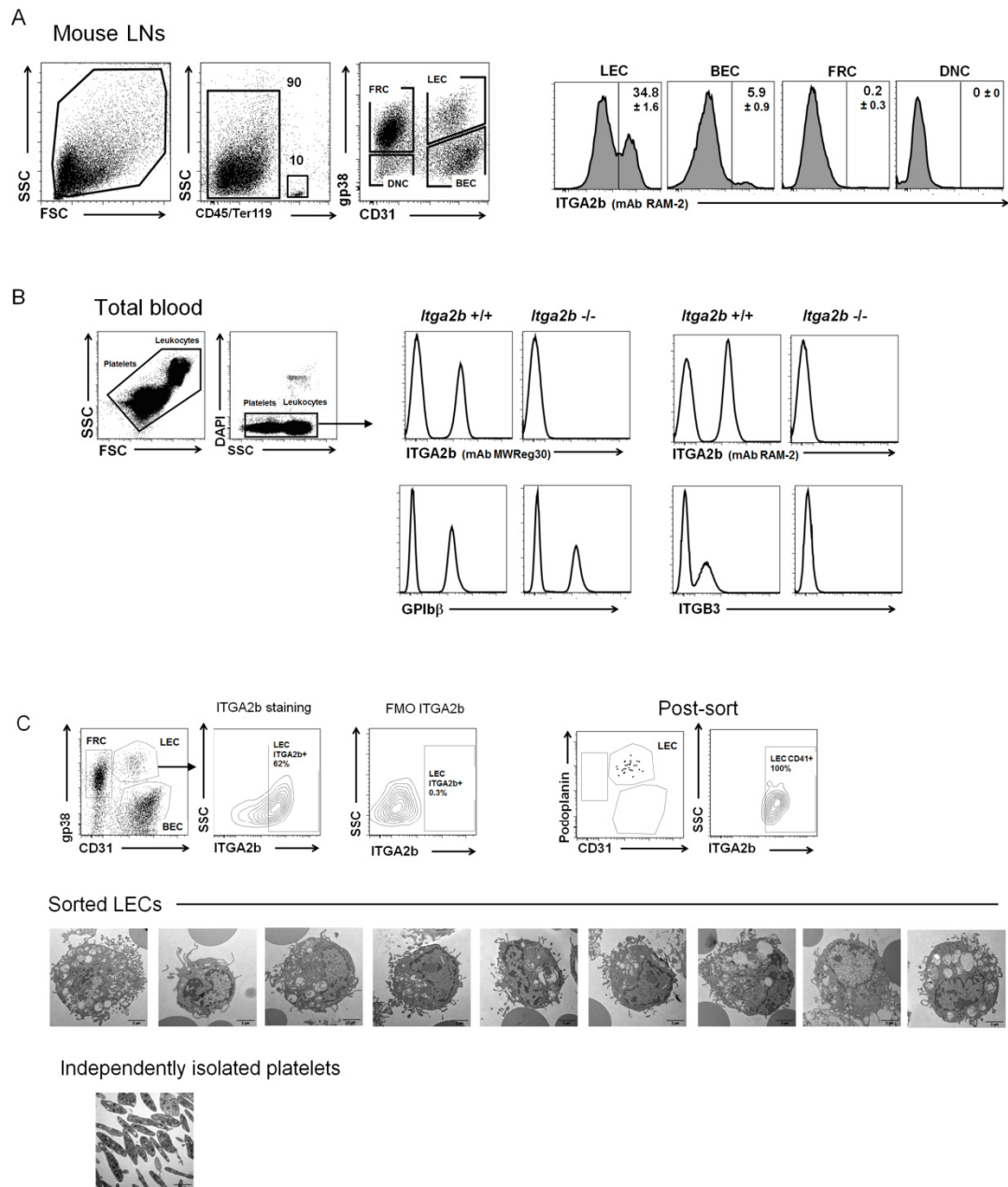
Supplemental Figure 2 (related to Figure 1)

A

Itga2b -/- ➔ Itga2b +/+

10.1.1 (LECs)   ITGA2b   Merge

Medullary sinus

B

Spleen   **Lymph node**

GPIbß (RAM1)   GPIbß + DAPI   GPIbß (RAM1)   10.1.1 (LECs)   GPIbß + 10.1.1 + DAPI

C   Human LNs

SSC   FSC   7AAD   CD45   gp38   CD31
                                      FRC   LEC
                                      DNC   BEC

D

Human Platelets

Healthy donor
Glanzmann patient
Healthy MOPC
Glanzmann MOPC

ITGA2b
(SDF-2)
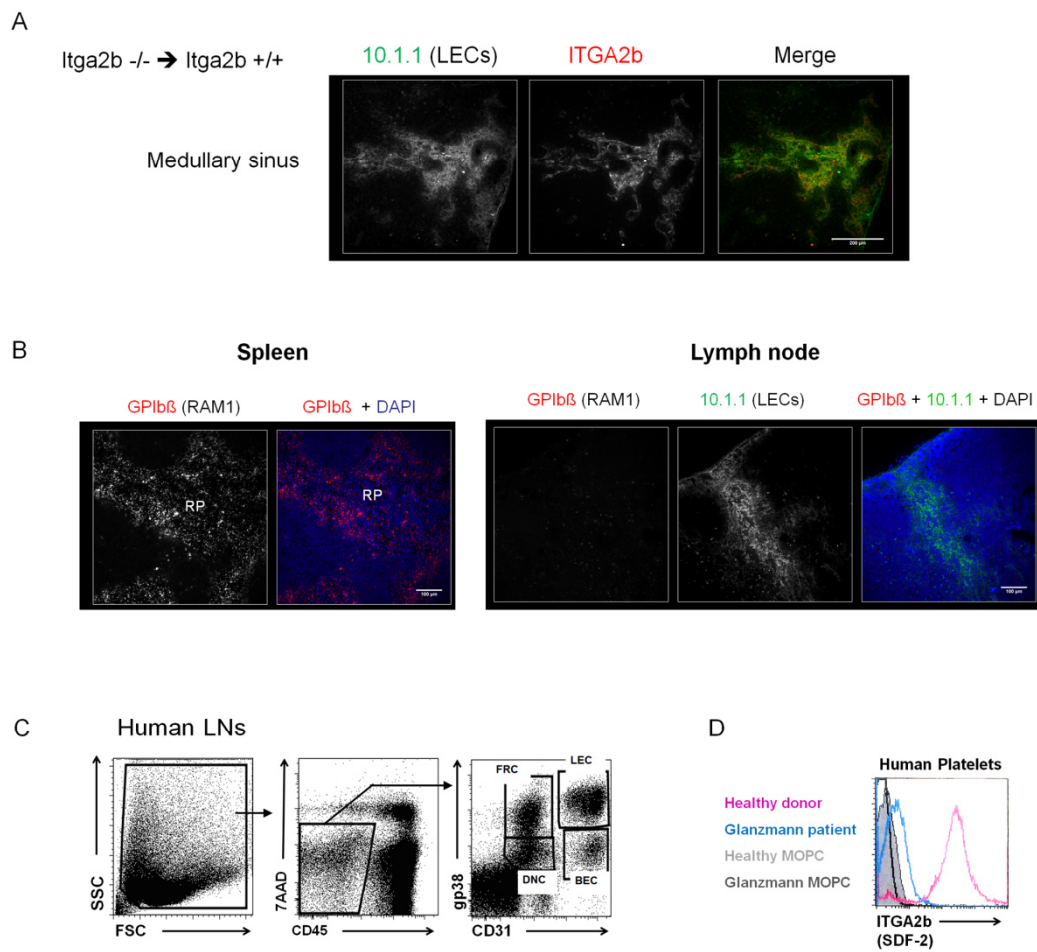
Supplemental Figure 3 (related to Figure 2)

A

B

160
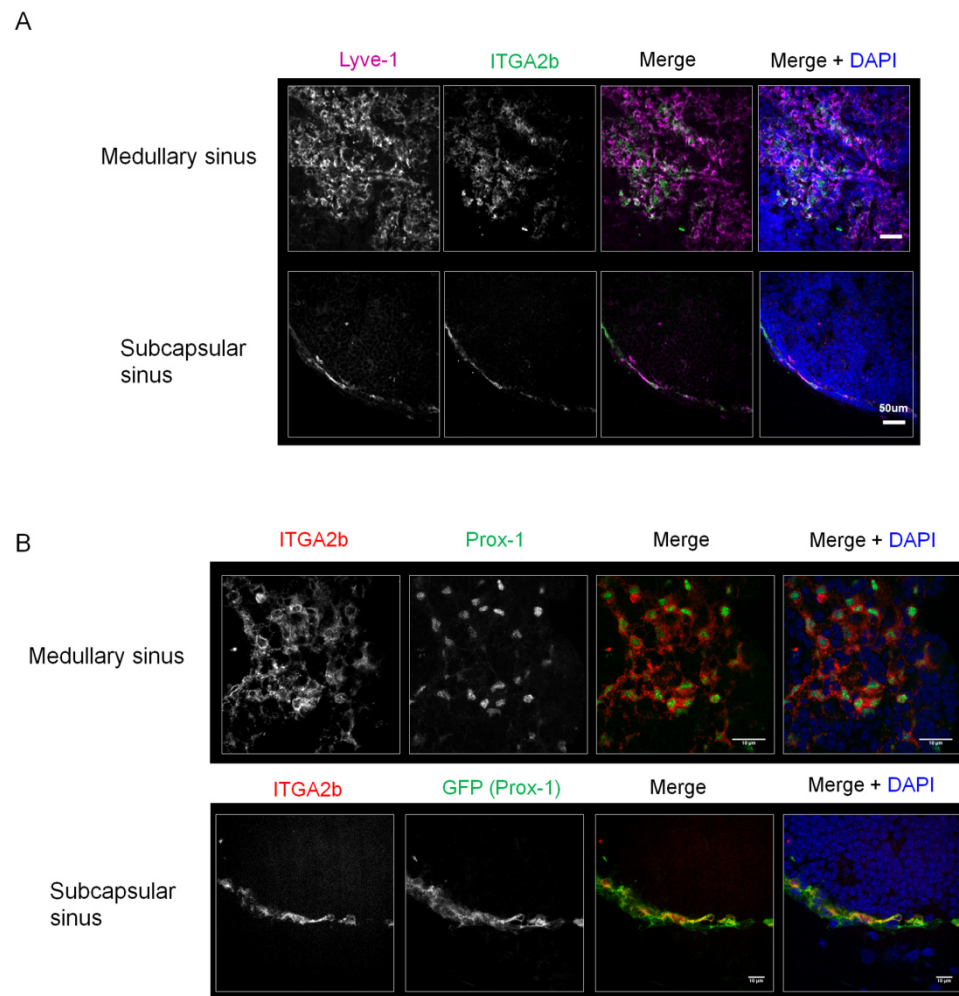
Supplemental Figure 4 (related to Figure 2)

A

Subcapsular sinus

10.1.1   MAdCAM-1   Merge

B

Subcapsular sinus

10.1.1   MAdCAM-1   ITGA2b   Merge

LEC

MAdCAM

ITGA2b

C

Subcapsular sinus

ITGA2b   RANKL (MRC)   Merge   Merge + DAPI

D

Mouse Skin

SSC / FSC

CD45 + F4/80 / Fvd 780 — 84

gp38 / CD31 — LEC 0.9 — BEC 0.4

WT Skin LECs   Imiquimod-treated skin LECs   RANK-Tg Skin LECs

Cell number / ITGA2b

0 ± 0   1.1 ± 0.6   0 ± 0
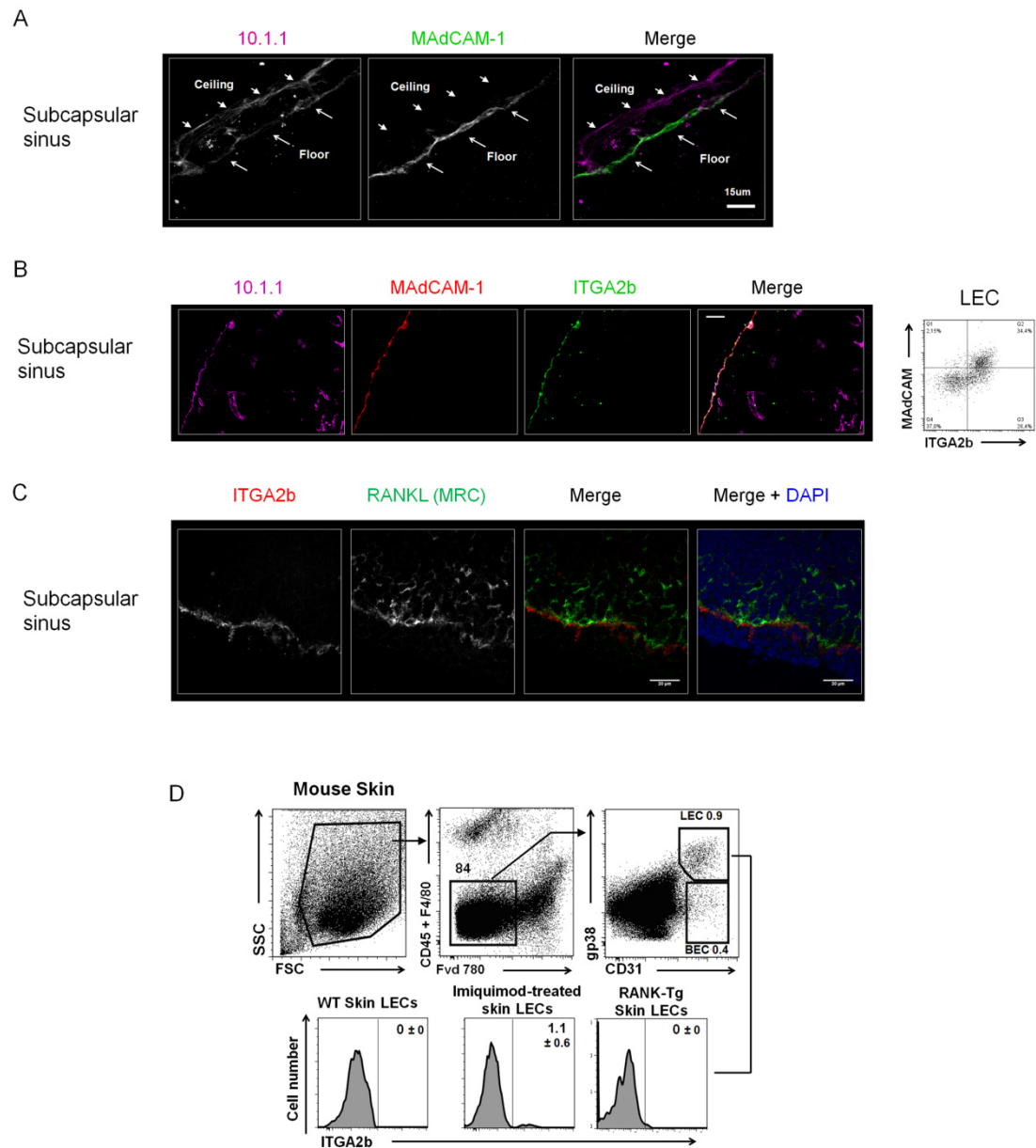
Supplemental Figure 5 (related to Figure 4)

163
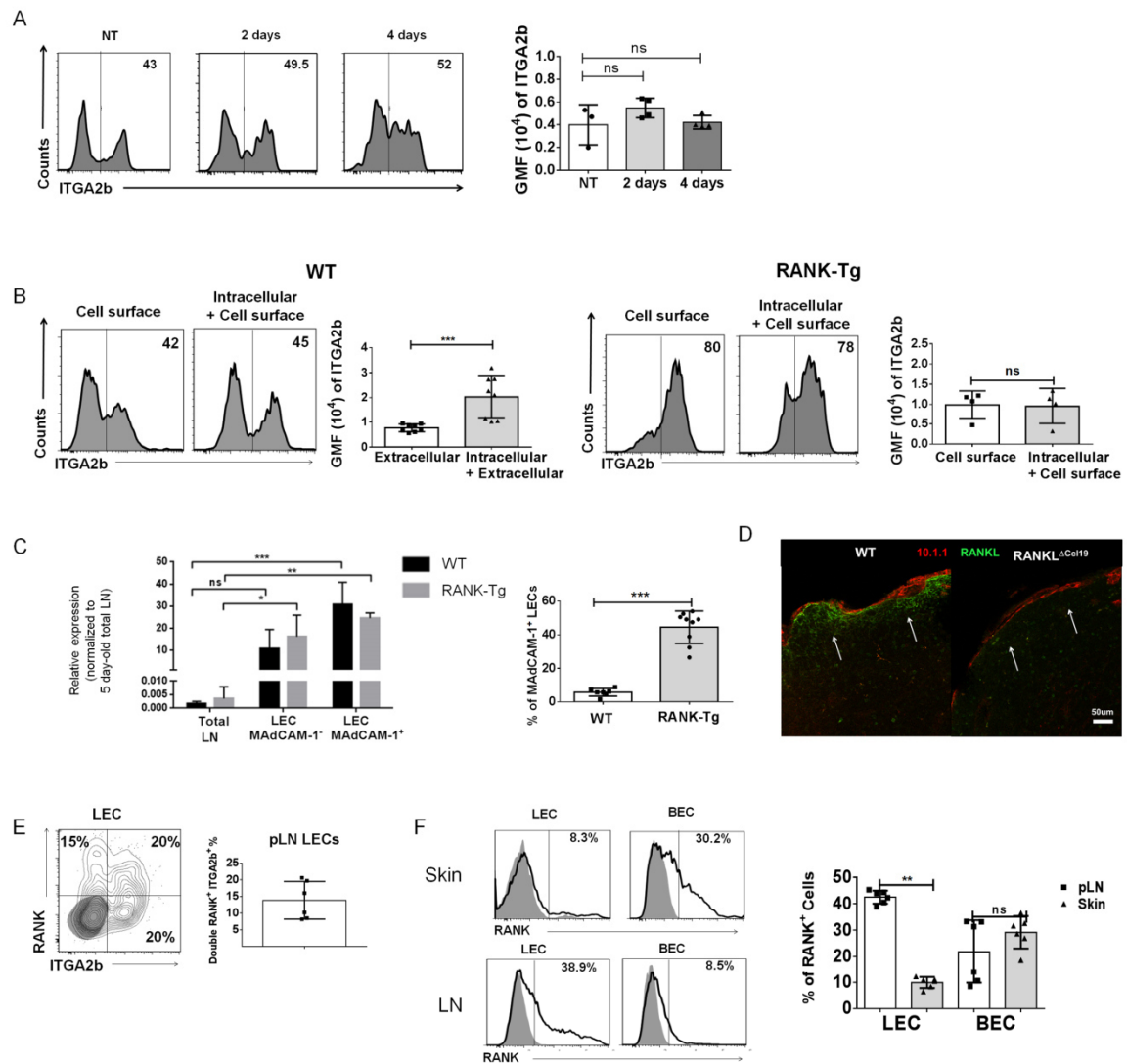
2.3.   Article 4

Stromal RANKL regulates LN subcapsular sinus macrophages differentiation

<u>M. Chypre</u>, O.G. Cordeiro, J. Sponsel, G. Anderson, B. Ludewig, H. Yagita, T. Lawrence, C.G. Mueller

In preparation

Stromal RANKL regulates LN subcapsular sinus macrophages differentiation

Mélanie Chypre[1,2], Olga Cordeiro[1], Janina Sponsel[1], Graham Anderson[3], Burkhard Ludewig[4], Hideo Yagita[5], Toby Lawrence[6], Christopher G. Mueller[1].

[1] Université de Strasbourg, CNRS, Immunopathology and therapeutic chemistry, UPR 3572, Strasbourg, France

[2] Prestwick Chemical PC SAS, Illkirch, France

[3] Medical research council centre for immune regulation, Institute for biomedical research, University of Birmingham, United Kingdom

[4] Institute of immunobiology, Kantonspital St. Gallen, Switzerland

[5] Department of Immunology, Juntendo University School of Medicine, Tokyo 113-8421, Japan

[6] CNRS-INSERM, CIML, Aix-Marseille University, France

Abstract

BACKGROUND: The TNF superfamily member RANKL functions in osteoclastogenesis by activating RANK signaling in myeloid osteoclast precursors, such as monocytes, macrophages or dendritic cells. However, whether it also plays a role in the differentiation of other cells of the myeloid lineage is not known. LN macrophages are tissue-resident macrophages important for both innate and adaptive immunity but their differentiation process is still not well understood.

AIM: The aim of this study is to investigate whether RANKL is involved in the differentiation of LN macrophages.

METHODS: To answer this question, we used the cre/lox system to generate mice lacking either RANKL or its receptor. We then analyzed LNs for different macrophage populations by flow cytometry and fluorescence microscopy.

RESULTS: After conditional deletion of RANKL in marginal reticular stromal cells (MRCs), we observed impaired differentiation of the subcapsular sinus macrophages (SSMs) leading to dysfunctional antigen transport to B cells. To understand the mechanisms behind SSMs regulation by RANKL, we generated mice with conditional deficiency of RANK in macrophages. We also adoptively transferred RANK$^-$ and RANK$^+$ fetal liver hematopoietic progenitors into irradiated mice to competitively reconstitute the myeloid compartment. However, in all cases the SSM population was normal, excluding a direct effect of RANKL. Moreover, we generated mice with conditional deficiency of RANK in MRCs and did not observe impaired differentiation of SSMs. We have recently shown that RANKL activated RANK$^+$ lymphatic endothelial cells (LECs) to express ITGA2b [1]. We were able to recover ITGA2b expression on LECs after recombinant RANKL administration to mice deficient in stromal RANKL.

CONCLUSIONS: We conditionally deleted RANKL in MRCs and were able to show that stromal RANKL alters SSM differentiation. We show that this is not due to a direct effect on RANK on macrophages or to an autocrine effect of RANKL on MRCs. Therefore, we are now investigating whether there is a cross-talk between RANKL-activated LECs and SSMs.

Introduction

Sinuses of lymph nodes (LNs) and the splenic marginal zone in mouse and human are lined by macrophages that play an important role in initiation and regulation of innate and adaptive immunity. In the LN, the CD169$^+$ subcapsular sinus macrophages (SSMs) are localized between the B cell follicles and the floor lymphatic endothelial cells (LECs) and constitute an early target cell for pathogen replication and a key player for a rapid innate immune defense [2–5]. SSMs also capture non-infectious antigen, otherwise too large to penetrate into the LN [6,7]. Their position together with their lower lysosomal enzymatic activity, favors antigen relay to activate B cells and the humoral response. The CD169$^+$ medullary sinus macrophages (MSMs) are associated with the medullary lymphatics that collect lymph before its exit through efferent lymphatics. MSMs also capture viral pathogens [4,8] but are more mature macrophages as indicated by expression of F4/80 and SIGN-R1 and by their active proteolytic machinery [9]. Thus, MSMs are equipped to recognize and probably eliminate pathogens.

The TNFSF member RANKL (TNFSF11) is required for the formation of osteoclasts, specialized bone-resorbing macrophages, by activating the signaling receptor RANK (Receptor activator of NF-κB, TNFRSF11a) [10–12]. In the periphery, the Langerhans cells are under RANKL regulatory control, as their number decreases in mice lacking RANKL [13]. However, although mature dendritic cells of the secondary lymphoid organs carry the receptor, so far no function for RANKL for these dendritic cells was found *in vivo* [10,11]. This is in spite of the essential role of RANKL for LN formation during embryogenesis [12,14].

In adult secondary lymphoid organs RANKL is constitutively expressed by the marginal zone reticular cells (MRCs) [15]. Using RANKL as marker for MRCs, suggestive evidence was provided that MRCs are precursors for follicular dendritic cells (FDC) [16]; however, other than this the role of MRC RANKL in LN integrity and its function remains unclear.

In the light of the dual role of RANKL in osteoclastogenesis and lymphoid organogenesis, we asked whether these two elements are united in the regulation of LN macrophages. Using a conditional knock-out of RANKL in MRCs, we showed that RANKL regulates CD169$^+$ SSMs differentiation. Antigen transfer to B cells was compromised. We investigated the possible mechanistic insights linking stromal RANKL and SSMs differentiation. We generated mice with conditional deletion of RANK in macrophages and performed adoptive transfer of RANK- and RANK+ fetal liver hematopoietic

progenitors to irradiated mice to competitively reconstitute the myeloid compartment. In both cases SSMs differentiation was not impaired, excluding a direct effect of stromal RANKL on macrophages. We also excluded an autocrine mechanism involving MRCs as mice deficient for RANK under the control of CCL19 promoter did not show impaired differentiation of SSM. We observed that LECs are sensitive to stromal RANKL which leads to the hypothesis of an indirect mechanism involving LECs.

Material and methods

Mice

C57BL/6 (Charles River Laboratories France), RANKL-/- [17], Ly5.1 (CD45.1) and RANKL$^{\Delta Ccl19}$, RANK$^{\Delta CD11c}$ and RANK$^{\Delta LysM}$ mice were bred and kept in specific pathogen-free conditions. All experiments were carried out in conformity with the animal bioethics legislation and institutional guidelines. To generate mice with conditional RANKL deficiency in marginal reticular cells (RANKL$^{\Delta Ccl19}$), mice containing a single copy of the Ccl19-cre BAC transgene [18] were crossed with RANKLf/f (B6.129-Tnfsf11tm1.1Caob/J) mice [19]. CD11c Cre;RANK flox/flox (RANK$^{\Delta CD11c}$) mice and LysM Cre;RANK flox/flox (RANK$^{\Delta LysM}$) mice were kindly provided by Toby Lawrence, CIML, Marseille, France. Unless otherwise indicated all mice were 8 weeks old. To inhibit lymphotoxin, RANKL and TNF pathway, mice received 20 µg of LTβR-muIgG1 (LTβR-Fc , kindly provided by Biogen, Cambridge, MA, USA), anti-RANKL antibody IK22-5 [20] or TNFR2-Fc (Etanercept) i.p. 3 times per week for 3 weeks. To rescue lymphatic endothelial cell activation in RANKL$^{\Delta Ccl19}$ mice, mice were treated with 100µg GST-mRANKL i.p. on day 0 and 100µg GST-mRANKL s.c. on day 0-3. On day 4, mice were sacrificed and LNs were collected.

In vivo generation of immune complexes was performed as described [9]. In brief, mice were injected i.p. with 2 mg rabbit IgG anti-PE (Rocklands) 12-16 h before s.c. administration of 10 µg PE (Invitrogen Molecular Probes) into hind legs to drain into the inguinal and popliteal LNs. Mice were sacrificed 8 h later.

Ly5.1 x C57BL/6 F1 mice (CD45.1+;CD45.2+) were lethally irradiated and 2x10^6 fetal liver hematopoietic stem cells from C57BL/6 RANK$^{\Delta b-actin}$ (CD45.2+) and from Ly5.1 (RANK$^{+/+}$;CD45.1+) mice were adoptively transferred in equal proportions. Eight weeks later the origin of the SSMs was determined using the congenic CD45.1/2 markers.

Isolation and analysis of LN cells

Stromal cells from peripheral LNs were prepared as published [21,22]. Briefly, lymph nodes were digested in RPMI + 2% FCS + Dispase II (Roche, 1mg/ml), Collagenase D (Roche,1mg/ml), DNase I (Roche, 0.1mg/ml) under agitation at 37°C for 1h. The cell suspension was then filtered at 100µm.

ACK buffer was used to remove red blood cells. CD45^{+} and TER119^{+} cells were depleted using anti-TER119 and anti-CD45 coupled magnetic beads (Miltenyi Biotec). LN macrophages were isolated following the same protocol as for stromal cells omitting the CD45+ cell depletion step.

Flow cytometry and immunofluorescence

Primary and secondary antibodies used are listed in Supplemental Table. Flow cytometry was performed on a Gallios (Beckman-Coulter) and analyzed with FlowJo software (Treestar). Cells were sorted on a FACS Aria II (BD bioscience).

Eight μm LN and spleen sections were cut on a cryostat (Leica), fixed in cold acetone and blocked with 2% BSA. After immunolabelling, sections were mounted in Fluomount (Dako) and images acquired on a spinning disk inverted microscope (Carl Zeiss) and the appropriate software (Metamorph). Images were analyzed using the open source imageJ software.

Quantitative reverse transcription coupled polymerase chain reaction (qRT-PCR)

RNA from sorted LN lymphatic endothelial cells (LECs), blood endothelial cells (BEC) and fibroblastic reticular cells (FRC) was extracted using the RNeasy kit (Qiagen) and cDNA was synthesized with Maxima First Strand cDNA Synthesis Kit (Thermo Scientific) and Improm-II (Promega) using oligo(dT)15 primers. RT-PCR was performed using Luminaris color HiGreen qPCR Master Mix (Thermo Scientific) using the following primers to amplify RANK: forward 5'- tgcgtgctgctcgttcca, reverse 5'-accgtccgagatgctcataat with the housekeeping gene coding for GAPDH (Forward 5'-TGACGTGCCGCCTGGAGAAA and Reverse 5'-AGTGTAGCCCAAGATGCCCTTCAG). Quantitative RT-PCR was run on a Bio-Rad CFX96 thermal cycler, and threshold values (Ct) of the target gene were normalized to GAPDH ($\Delta Ct = Ct_{RANK} - Ct_{GAPDH}$). RANK expression was finally expressed relatively to expression in BEC.

Statistical analysis

Mann-Whitney test and one or two way ANOVA with bonferroni correction were used on GraphPad Prism (GraphPad software) to calculate statistical significance. ns = not statistically significant, *p<0.05 **p<0.01 ***p<0.001 ****p<0.0001

Results

RANKL regulates the differentiation of splenic CD169+ macrophages and LN SSM but not MSM.

It has previously been reported that the spleen of RANK-deficient mice displays reduced expression of CD169, recognized by the Moma-1 monoclonal antibody [10]. We therefore examined the spleen of *Rankl*$^{-/-}$ mice by microscopy for the expression of CD169 and also observed a reduction in CD169 expression (**Fig. 1A**). This suggests a requirement for RANKL-RANK for the formation of the CD169+ marginal metallophilic macrophages (MMMs). Because *Rank*$^{-/-}$ or *Rankl*$^{-/-}$ mice lack LNs, these organs cannot be studied in these mice. Therefore, to extend this finding to LNs we injected the antagonistic anti-RANKL (IK22-5) antibody in C57BL/6 mice. Because it has previously been shown that LTβR-Fc decreases CD169+ SSM numbers [9], we used LTβR-Fc as a positive control. On the other hand, administration of TNFR2-Fc served a negative control as the inhibition of TNFα has no effect on LN CD169+ macrophages [23,24]. We saw that RANKL and LTαβ blockage decreased CD169 staining both in spleen and LNs in comparison with TNFR2-Fc treatment (**Fig1. B**). Medullary sinus macrophages (MSMs) that also express CD169 in the LNs were not affected by the treatments (**Fig1. B**). We further assessed the presence of the CD169+ macrophages in LNs by flow cytometry using a previously established cell gating strategy [9] (**Fig.1 C**). We confirmed that RANKL neutralization and LTαβ inhibition decreased CD169+ SSM numbers. As for the MSMs, although there was a tendency for reduction after anti-RANKL administration, the difference with TNFR2-Fc was not significant (**Fig.1 C**). As expected, MSMs were not affected by LTβR-Fc [4,9]. These findings demonstrate the role of RANKL in CD169+ SSM differentiation in LN and spleen.

Stromal RANKL deficiency decreases CD169+ SSM numbers and impairs SSM functionality

To confirm the role of RANKL in mediating MMM and SSM differentiation genetically, we generated mice with a conditional *Rankl* knock-out under control of the CCL19 promoter [18]. CCL19 is active in Lymphoid tissue organizer cells (LTos) in embryos that give rise to the lymphoid stromal compartment including marginal reticular cells (MRCs), the main constitutive source of RANKL in the adult [15,25]. RANKL^{ΔCCL19} mice developed LNs but immunolabelling of the embryonic inguinal LNs revealed a strong reduction in RANKL expression by the LTos (**Fig. 2A**). In the adult LN, RANKL expression by MRCs was no longer detected (**Fig. 2B**). We therefore analysed the LNs for CD169 expression and found an almost complete absence of CD169 in the subcapsular sinus (**Fig. 3A**). Because, it was previously shown that LTαβ inhibition lead to the aberrant expression of SIGN-R1 by SSM [4], we also labelled the LNs sections for this marker. Indeed, SIGN-R1 largely replaced CD169 in

the subcapsular sinus. We then assessed LN macrophages numbers by flow cytometry. There was a 5-fold reduction in the SSM population (**Fig. 3B**). However, despite a tendency of reduction, MSM numbers were not significantly different between RANKL$^{\Delta CCL19}$ mice and control littermates.

We next probed for the functional consequences by determining the relay of immune complexes to B cells. Passive immunization with phycoerythrin (PE)-specific antibodies followed by subcutaneous administration of PE led to the capture of PE-labeled immune complexes by B cells via SSMs [7]. Fewer B cells captured the fluorochrome in RANKL$^{\Delta CCL19}$ mice showing a decreased functionality of SSM (**Fig. 3C**).

As for the spleen, although the CCL19 Cre transgene shows activity in the splenic stroma, we found no change in CD169$^+$ expression in RANKL$^{\Delta CCL19}$ in comparison to Cre-negative littermate controls (data not shown).

Therefore, the generation of mice deficient for LN stromal RANKL allowed us to show that stromal RANKL is required for CD169 expression by subcapsular sinus macrophages which is important for functional immune complexes transfer to B cells.

Stromal RANKL does not act directly on macrophages or in an autocrine manner

In order to understand the mechanistic insights of SSM differentiation we investigated whether stromal RANKL acts directly on macrophages. We used RANK$^{\Delta CD11c}$ and RANK$^{\Delta LysM}$ mice in which RANK is deleted from cells expressing CD11c or LysM respectively, including LN macrophages. We assessed the proportion of SSMs among the CD11b$^+$ CD11c$^{lo/-}$ cells by flow cytometry and observed no difference between knockout mice and control littermates (**Fig. 4A**). To address the requirement of RANK for SSMs differently, we adoptively co-transferred fetal liver hematopoietic progenitors from RANK$^{-/-}$ CD45.2 C57BL/6 and from WT CD45.1 mice to irradiated CD45.1 x CD45.2 F1 mice. After reconstitution of the immune system, the proportion of CD45.1 (RANK$^{+/+}$ donor origin) versus CD45.2 (RANK$^{-/-}$ donor origin) and CD45.1/2 (recipient origin) was assessed for SSMs and other myeloid cell populations. We observed that SSMs, as well as MSMs or other myeloid cells (DCs and CD11b$^+$CD11c^{lo} macrophages) derived from both the RANK$^{+/+}$ and the RANK$^{-/-}$ donor origin (**Fig. 4B**). Residual recipient myeloid cells remained owing to radiation resistance. This confirmed that RANK expression was not required for SSM formation.

Next, we addressed the question of an autocrine effect of RANKL on MRCs by generating mice with conditional RANK deficiency in CCL19 expressing cells. We assessed SSMs in these mice and did not observe a difference in SSM percentage between RANK$^{\Delta CCL19}$ mice and control littermates (**Fig. 4D**).

Therefore, the involvement of an autocrine mechanism through MRCs for CD169^{+} SSM differentiation can also be excluded (**Fig. 4E**).

LECs are sensitive to stromal RANKL and can be rescued by recombinant RANKL injections

We have previously shown that stromal RANKL activates LECs resulting in ITGA2b and MAdCAM-1 expression [1,26]. We therefore envisioned the possibility that RANKL controls SSM differentiation indirectly through lymphatic endothelial cells. First, we explored the expression of RANK by qRT-PCR in LECs, BECs and FRCs and found highest transcription in LECs, none in FRCs and low levels in BECs (**Fig. 5A**). Indeed, the level of ITGA2b and MAdCAM-1 expression was greatly reduced in RANKL[ΔCcl19] mice (**Fig. 5B**). Then, we investigated whether the administration of recombinant RANKL fused to GST could restore ITGA2b and MAdCAM-1 expression. RANKL injection increased ITGA2b and MAdCAM-1 expression on LECs from RANKL[ΔCcl19] mice to a level comparable to control littermates (**Fig. 5B**). Knowing that these cells are in close contact with SSM in LNs, we hypothesize an indirect mechanism involving LECs leading to CD169^{+} SSM differentiation (**Fig. 5C**).

Discussion

Here we have shown that stromal RANKL is required for LN CD169^{+} subcapsular sinus macrophages (SSM) and splenic CD169^{+} marginal metallophilic macrophage differentiation. We found that this is not due to a direct effect on macrophages or precursor cells and that there is not an autocrine effect on MRCs. We confirm that LECs are sensitive to stromal RANKL and hypothesize an indirect mechanism implicating LECs as intermediate cells between RANKL-expressing MRCs and SSMs.

RANKL is constitutively expressed by MRCs in adults [15]. We conditionally deleted RANKL using the CCL19 promoter [18,25] and RANKL was efficiently deleted from MRCs in adult LNs. Unlike a total RANKL knock-out, the RANKL[ΔCCL19] mice developed LNs enabling us to investigate the effect of MRC RANKL in immune cell homeostasis. Strikingly, we observed a reduction in CD169^{+} SSMs. This finding supports initial observations made in the spleen of total RANK-deficient mice [10] and confirmed in this study with RANKL^{-/-} animals and injections of anti-RANKL antibody. The LN CD169^{+} macrophages comprise two populations, the SSMs and the MSMs, phenotypically distinct by F4/80 and SIGN-R1 expression. RANKL[ΔCCL19] mice showed impaired formation of SSMs but not MSMs. SSM capture particulate antigen, virus or dead cells and present them to the underlying B cells [6,7,27]. Thus, mice with stromal RANKL deficiency display lower B cell uptake of immune complexes. This impaired function of SSMs shows that complete differentiation into CD169 expressing cells is required for SSMs function. Moreover, upregulation of SIGN-R1 by cells in the subcapsular sinus was observed in

RANKL$^{\Delta CCL19}$ mice. This supports a defective macrophage differentiation pathway in the absence of RANKL.

We further addressed the mechanistic insights linking RANKL to SSM differentiation. Macrophages, dendritic cells and monocytes are known to express RANK, respond to RANKL and differentiate into osteoclasts [12,28]. We therefore investigated whether RANKL acts directly on macrophages in LNs. We obtained mice deficient for RANK under the control of the CD11c or the LysM promoter. CD11c cre targets dendritic cells but would be expressed in macrophages including SSM that express low levels of CD11c. LysM cre targets all macrophage populations, but also monocytic precursor cells [29,30]. Moreover, in the case that these Cre promotors should not be adequately expressed in SSMs, we performed adoptive transfer of RANK$^-$ and RANK$^+$ fetal liver hematopoietic progenitors to irradiated mice to competitively reconstitute the myeloid compartment. Under all conditions, the SSM population was normal, excluding a direct effect of stromal RANKL. We additionally investigated whether stromal RANKL could act in an autocrine manner directly on MRCs which could subsequently express other factors triggering macrophages differentiation. We generated mice deficient for RANK under the control of CCL19 promoter. The SSM population was not affected in these mice excluding an autocrine mechanism involving MRCs.

We previously described a new marker of activated LECs, ITGA2b [1]. This integrin is overexpressed by LECs in RANKL overexpressing mice but almost absent from LECs in RANKL$^{\Delta CCL19}$ mice. This result was confirmed in this study. Moreover, we also showed previously that MAdCAM-1 is expressed by LECs and overexpressed in RANKL overexpressing mice [1,26]. Here we demonstrated that MAdCAM-1 expression on LECs is also dependent on stromal RANKL as MAdCAM-1$^+$ LECs population is decreased in RANKL$^{\Delta CCL19}$ mice. We next showed that decreased expression of ITGA2b and MAdCAM-1 by LECs can be rescued to WT levels by injecting recombinant RANKL for 4 days. SSMs lie in the layer formed by LECs in the subcapsular sinus and by RANKL expressing MRCs, thus these three cell populations are in close contact. We therefore hypothesize that an indirect mechanism involving LECs could trigger SSM differentiation. RANK expressing LECs activated by MRC RANKL could further participate in SSM differentiation. The reason why MSM differentiation is not affected although these cells also reside close to LECs may be related to the increased distance between the medulla and MRCs, together with the likelihood that RANKL is expressed in its cell-anchored version. To confirm that RANK on LECs plays a role in SSM differentiation, generation of mice deficient for RANK in LECs and analysis of their phenotype is required. Moreover, detailed investigation of the LEC transcriptome after RANKL activation may identify potential factors regulating SSM differentiation.

Altogether, this study points out the complexity of immune cell homeostasis in LNs and more precisely that of CD169^{+} macrophage differentiation. Few things are known to date about SSM development. Here we provided the first evidence that RANKL is involved in this process but further investigations are required to fully understand this complex mechanism. We found SIGN-R1 expression in the subcapsular sinus of RANKL[ΔCcl19] mice. Therefore SSM are probably present in a more advanced differentiation state. Indeed, MSM expressing SIGN-R1 were found to have a more mature signature than SSM shown by higher levels of lysosomal enzymes [9]. New insights in CD169^{+} macrophage biology are of interest for basic and applied research. LN CD169^{+} macrophages play a role in cancer development [31,32]. Moreover, CD169^{+} macrophages are present in other tissues such as colon and bone marrow [33–35]. Understanding their differentiation process might consequently also be helpful in certain pathological conditions such as cancers, colitis and anemia.

Acknowledgement

References

1. Cordeiro OG, Chypre M, Brouard N, Rauber S, Alloush F, Romera-Hernandez M, et al. Integrin-Alpha IIb Identifies Murine Lymph Node Lymphatic Endothelial Cells Responsive to RANKL. PLOS ONE. 2016;11: e0151848. doi:10.1371/journal.pone.0151848

2. Garcia Z, Lemaître F, Rooijen N van, Albert ML, Levy Y, Schwartz O, et al. Subcapsular sinus macrophages promote NK cell accumulation and activation in response to lymph-borne viral particles. Blood. 2012;120: 4744–4750. doi:10.1182/blood-2012-02-408179

3. Iannacone M, Moseman EA, Tonti E, Bosurgi L, Junt T, Henrickson SE, et al. Subcapsular sinus macrophages prevent CNS invasion on peripheral infection with a neurotropic virus. Nature. 2010;465: 1079–1083. doi:10.1038/nature09118

4. Moseman EA, Iannacone M, Bosurgi L, Tonti E, Chevrier N, Tumanov A, et al. B Cell Maintenance of Subcapsular Sinus Macrophages Protects against a Fatal Viral Infection Independent of Adaptive Immunity. Immunity. 2012;36: 415–426. doi:10.1016/j.immuni.2012.01.013

5. Coombes JL, Han S-J, van Rooijen N, Raulet DH, Robey EA. Infection-Induced Regulation of Natural Killer Cells by Macrophages and Collagen at the Lymph Node Subcapsular Sinus. Cell Rep. 2012;2: 124–135. doi:10.1016/j.celrep.2012.06.001

6. Carrasco YR, Batista FD. B Cells Acquire Particulate Antigen in a Macrophage-Rich Area at the Boundary between the Follicle and the Subcapsular Sinus of the Lymph Node. Immunity. 2007;27: 160–171. doi:10.1016/j.immuni.2007.06.007

7. Phan TG, Grigorova I, Okada T, Cyster JG. Subcapsular encounter and complement-dependent transport of immune complexes by lymph node B cells. Nat Immunol. 2007;8: 992–1000. doi:10.1038/ni1494

8. Gonzalez SF, Lukacs-Kornek V, Kuligowski MP, Pitcher LA, Degn SE, Kim Y-A, et al. Capture of influenza by medullary dendritic cells via SIGN-R1 is essential for humoral immunity in draining lymph nodes. Nat Immunol. 2010;11: 427–434. doi:10.1038/ni.1856

9. Phan TG, Green JA, Gray EE, Xu Y, Cyster JG. Immune complex relay by subcapsular sinus macrophages and noncognate B cells drives antibody affinity maturation. Nat Immunol. 2009;10: 786–793. doi:10.1038/ni.1745

10. Dougall WC, Glaccum M, Charrier K, Rohrbach K, Brasel K, Smedt TD, et al. RANK is essential for osteoclast and lymph node development. Genes Dev. 1999;13: 2412–2424.

11. Kong Y-Y, Yoshida H, Sarosi I, Tan H-L, Timms E, Capparelli C, et al. OPGL is a key regulator of osteoclastogenesis, lymphocyte development and lymph-node organogenesis. Nature. 1999;397: 315–323. doi:10.1038/16852

12. Walsh MC, Choi Y. Biology of the RANKL–RANK–OPG system in immunity, bone, and beyond. Inflammation. 2014;5: 511. doi:10.3389/fimmu.2014.00511

13. Barbaroux J-BO, Beleut M, Brisken C, Mueller CG, Groves RW. Epidermal Receptor Activator of NF-κB Ligand Controls Langerhans Cells Numbers and Proliferation. J Immunol. 2008;181: 1103–1108.

14. Mueller CG, Hess E. Emerging Functions of RANKL in Lymphoid Tissues. Front Immunol. 2012;3. doi:10.3389/fimmu.2012.00261

15. Katakai T, Suto H, Sugai M, Gonda H, Togawa A, Suematsu S, et al. Organizer-Like Reticular Stromal Cell Layer Common to Adult Secondary Lymphoid Organs. J Immunol. 2008;181: 6189–6200. doi:10.4049/jimmunol.181.9.6189

16. Jarjour M, Jorquera A, Mondor I, Wienert S, Narang P, Coles MC, et al. Fate mapping reveals origin and dynamics of lymph node follicular dendritic cells. J Exp Med. 2014;211: 1109–1122. doi:10.1084/jem.20132409

17. Kim N, Odgren PR, Kim D-K, Marks SC, Choi Y. Diverse roles of the tumor necrosis factor family member TRANCE in skeletal physiology revealed by TRANCE deficiency and partial rescue by a lymphocyte-expressed TRANCE transgene. Proc Natl Acad Sci U S A. 2000;97: 10905–10910.

18. Chai Q, Onder L, Scandella E, Gil-Cruz C, Perez-Shibayama C, Cupovic J, et al. Maturation of Lymph Node Fibroblastic Reticular Cells from Myofibroblastic Precursors Is Critical for Antiviral Immunity. Immunity. 2013;38: 1013–1024. doi:10.1016/j.immuni.2013.03.012

19. Xiong J, Onal M, Jilka RL, Weinstein RS, Manolagas SC, O'Brien CA. Matrix-embedded cells control osteoclast formation. Nat Med. 2011;17: 1235–1241. doi:10.1038/nm.2448

20. Kamijo S, Nakajima A, Ikeda K, Aoki K, Ohya K, Akiba H, et al. Amelioration of bone loss in collagen-induced arthritis by neutralizing anti-RANKL monoclonal antibody. Biochem Biophys Res Commun. 2006;347: 124–132. doi:10.1016/j.bbrc.2006.06.098

21. Fletcher AL, Malhotra D, Acton SE, Lukacs-Kornek V, Bellemare-Pelletier A, Curry M, et al. Reproducible Isolation of Lymph Node Stromal Cells Reveals Site-Dependent Differences in Fibroblastic Reticular Cells. Front Immunol. 2011;2. doi:10.3389/fimmu.2011.00035

22. Link A, Vogt TK, Favre S, Britschgi MR, Acha-Orbea H, Hinz B, et al. Fibroblastic reticular cells in lymph nodes regulate the homeostasis of naive T cells. Nat Immunol. 2007;8: 1255–1265. doi:10.1038/ni1513

23. Ettinger R, Mebius R, Browning JL, Michie SA, Tuijl S van, Kraal G, et al. Effects of tumor necrosis factor and lymphotoxin on peripheral lymphoid tissue development. Int Immunol. 1998;10: 727–741. doi:10.1093/intimm/10.6.727

24. Pasparakis M, Kousteni S, Peschon J, Kollias G. Tumor Necrosis Factor and the p55TNF Receptor Are Required for Optimal Development of the Marginal Sinus and for Migration of Follicular Dendritic Cell Precursors into Splenic Follicles. Cell Immunol. 2000;201: 33–41. doi:10.1006/cimm.2000.1636

25. Bénézech C, White A, Mader E, Serre K, Parnell S, Pfeffer K, et al. Ontogeny of Stromal Organizer Cells during Lymph Node Development. J Immunol. 2010;184: 4521–4530. doi:10.4049/jimmunol.0903113

26. Hess E, Duheron V, Decossas M, Lézot F, Berdal A, Chea S, et al. RANKL Induces Organized Lymph Node Growth by Stromal Cell Proliferation. J Immunol. 2012;188: 1245–1254. doi:10.4049/jimmunol.1101513

27. Moalli F, Proulx ST, Schwendener R, Detmar M, Schlapbach C, Stein JV. Intravital and Whole-Organ Imaging Reveals Capture of Melanoma-Derived Antigen by Lymph Node Subcapsular Macrophages Leading to Widespread Deposition on Follicular Dendritic Cells. Front Immunol. 2015;6. doi:10.3389/fimmu.2015.00114

28. Theill LE, Boyle WJ, Penninger JM. RANK-L AND RANK: T Cells, Bone Loss, and Mammalian Evolution. Annu Rev Immunol. 2002;20: 795–823. doi:10.1146/annurev.immunol.20.100301.064753

29. Abram CL, Roberge GL, Hu Y, Lowell CA. Comparative analysis of the efficiency and specificity of myeloid-Cre deleting strains using ROSA-EYFP reporter mice. J Immunol Methods. 2014;408: 89–100. doi:10.1016/j.jim.2014.05.009

30. Jakubzick C, Bogunovic M, Bonito AJ, Kuan EL, Merad M, Randolph GJ. Lymph-migrating, tissue-derived dendritic cells are minor constituents within steady-state lymph nodes. J Exp Med. 2008;205: 2839–2850. doi:10.1084/jem.20081430

31. Asano K, Nabeyama A, Miyake Y, Qiu C-H, Kurita A, Tomura M, et al. CD169-Positive Macrophages Dominate Antitumor Immunity by Crosspresenting Dead Cell-Associated Antigens. Immunity. 2011;34: 85–95. doi:10.1016/j.immuni.2010.12.011

32. Pucci F, Garris C, Lai CP, Newton A, Pfirschke C, Engblom C, et al. SCS macrophages suppress melanoma by restricting tumor-derived vesicle–B cell interactions. Science. 2016; aaf1328. doi:10.1126/science.aaf1328

33. Hiemstra IH, Beijer MR, Veninga H, Vrijland K, Borg EGF, Olivier BJ, et al. The identification and developmental requirements of colonic CD169+ macrophages. Immunology. 2014;142: 269–278. doi:10.1111/imm.12251

34. Chow A, Lucas D, Hidalgo A, Méndez-Ferrer S, Hashimoto D, Scheiermann C, et al. Bone marrow CD169+ macrophages promote the retention of hematopoietic stem and progenitor cells in the mesenchymal stem cell niche. J Exp Med. 2011;208: 261–271. doi:10.1084/jem.20101688

35. Chow A, Huggins M, Ahmed J, Hashimoto D, Lucas D, Kunisaki Y, et al. CD169+ macrophages provide a niche promoting erythropoiesis under homeostasis and stress. Nat Med. 2013;19: 429–436. doi:10.1038/nm.3057

Figures
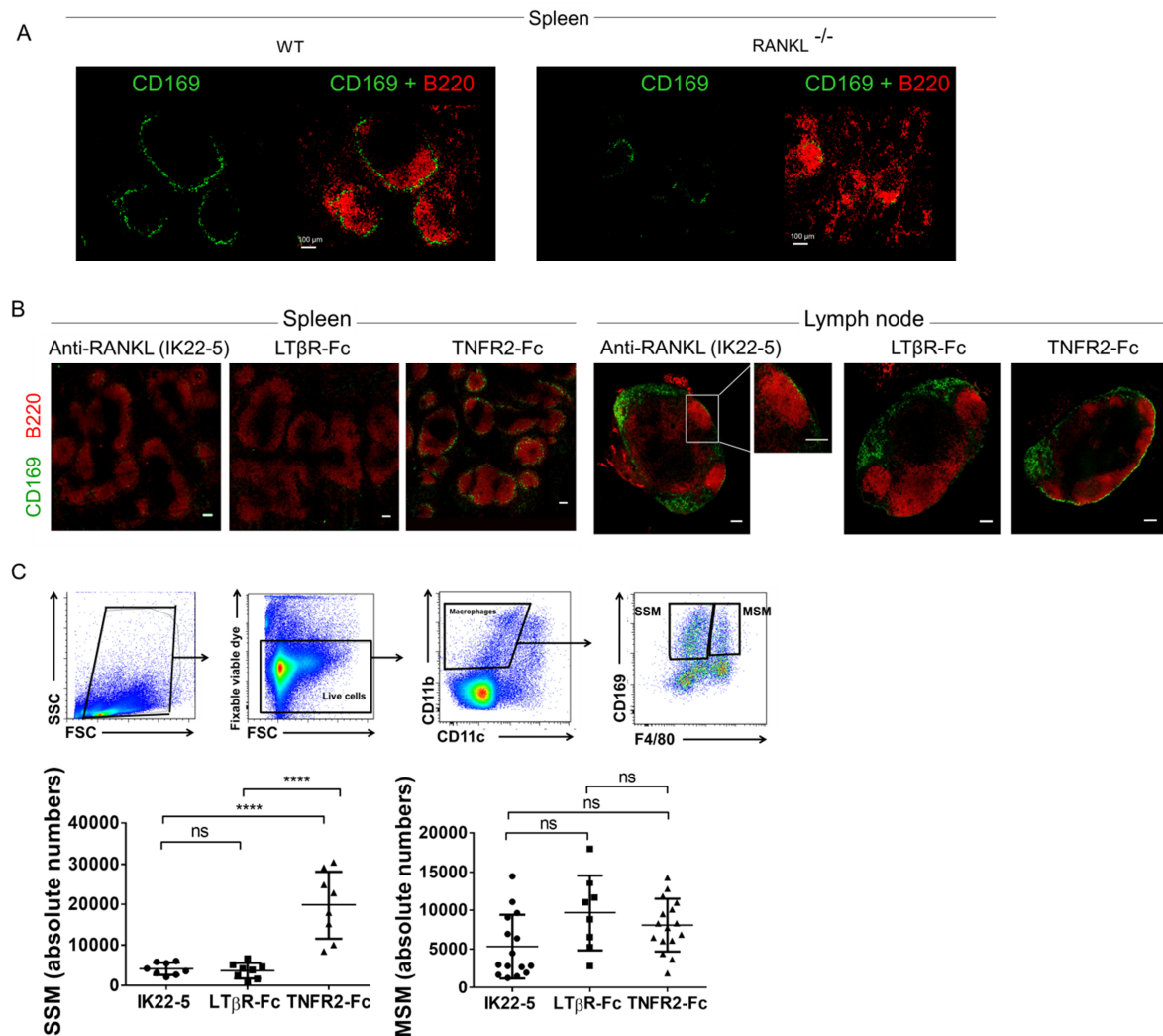
Figure 1: Impact of loss of RANKL on CD169-expressing macrophages in spleen and LNs. **(A)** Wide-field microscopy imaging of spleen sections from WT and RANKL$^{-/-}$ mice stained for CD169 (green) and B220 (red). Scale bar = 100μm. **(B)** Imaging of spleen and LN sections stained for CD169 (green) and B220 (red) after treatment with 20μg of anti-RANKL-IK22-5, LTβR-Fc or TNFR2-Fc 3 times per week for 3 weeks. Scale bar = 100μm **(C)** Gating strategy to study LN macrophages by flow cytometry. Graphs show the absolute numbers (mean ± SD) of subcapsular sinus macrophages (SSM) or medullary sinus macrophages (MSM) as indicated after treatment with anti-RANKL-IK22-5, LTβR-Fc or TNFR2-Fc. Datas from inguinal and brachial lymph nodes analysed separately were pooled. Statistical significance was calculated using one way ANOVA with bonferroni correction. **** p< 0.0001

E18.5 iLN
Scale 50 µm
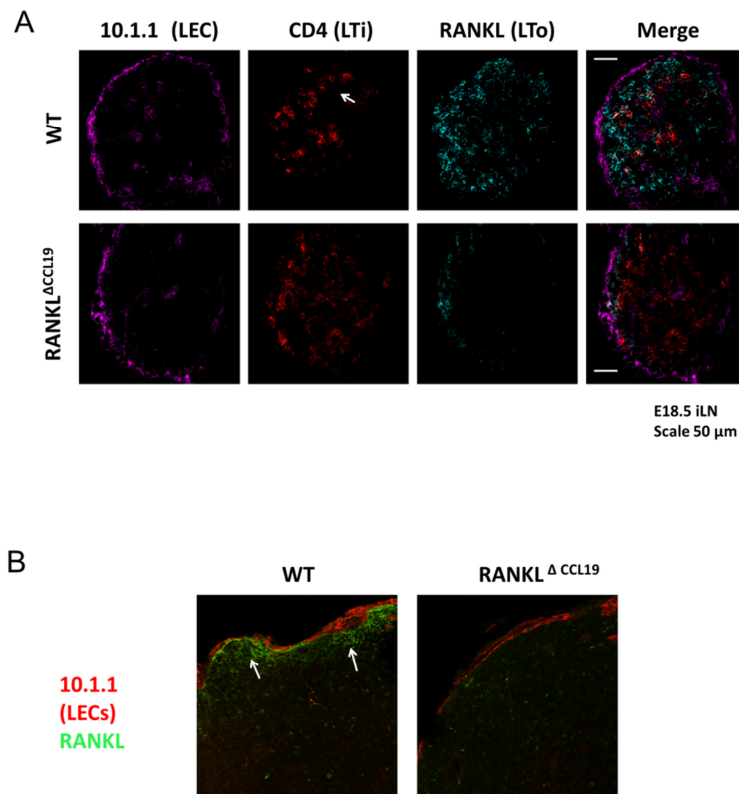
Figure 2: RANKL deficiency in RANKL^{ΔCcl19} mice. **(A)** Confocal microscopy images of inguinal LN anlagen of RANKL^{ΔCcl19} mice and Cre - littermate controls at E18.5, labelled for lymphatic endothelial cells (LECs) (using monoclonal antibody 10.1.1), for LTi cells (CD4) and RANKL (expressed by LTOs). Scale bar = 50µm. **(B)** Confocal microscopy images of inguinal LNs of RANKL^{ΔCcl19} mice and Cre - littermates at 8 weeks of age, labelled for RANKL and LECs (using monoclonal antibody 10.1.1). Scale bar = 50µm.
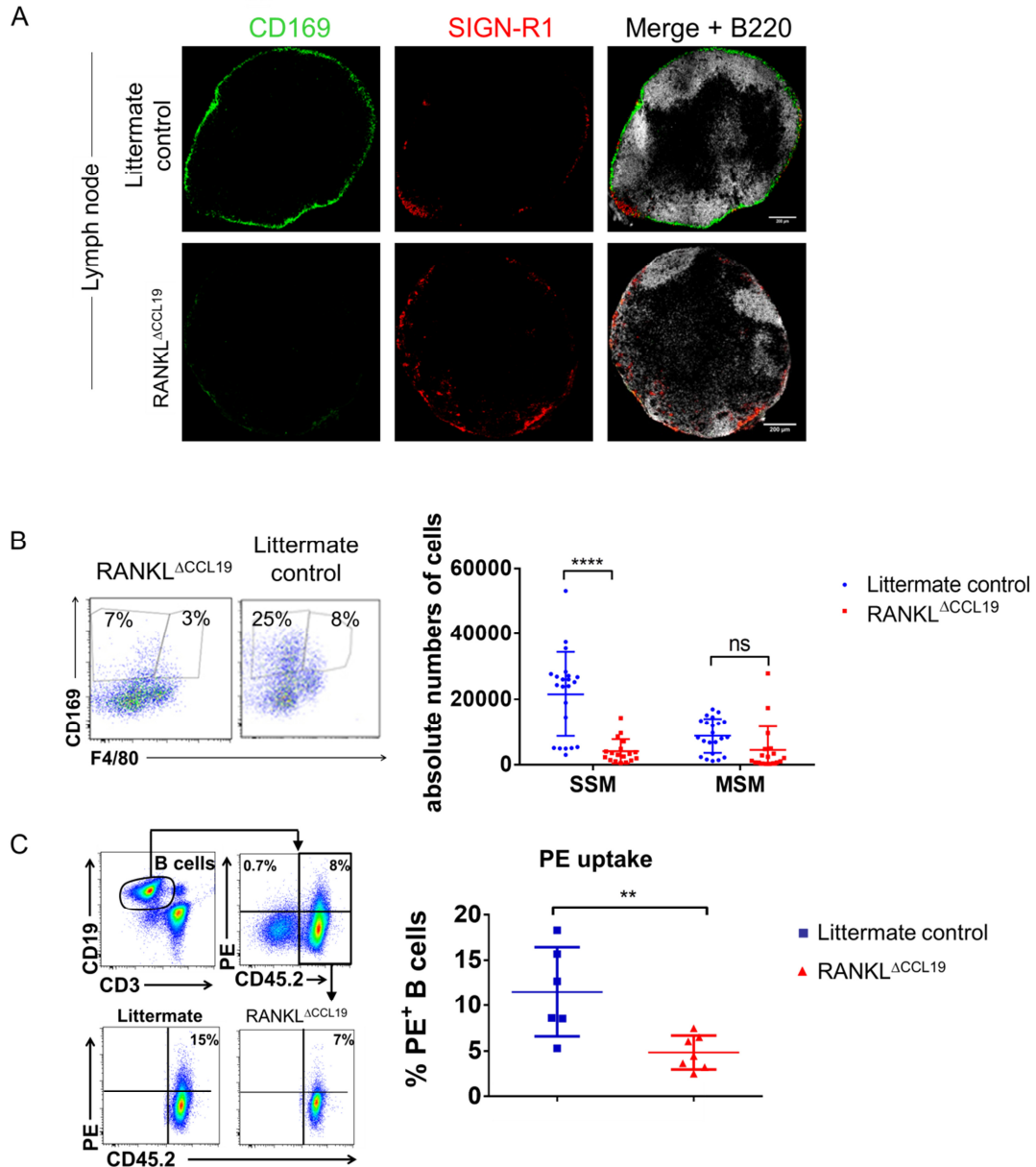
Figure 3: Stromal RANKL knockout impairs CD169$^+$ subcapsular sinus macrophage differentiation and function. **(A)** Wide field microscopy imaging of LN sections from RANKL$^{\Delta CCL19}$ mice and control littermates stained for CD169 (green), SIGN-R1 (red) and B220 (grey). Scale bar = 200µm. **(B)** Plots depict LN macrophage populations in RANKL$^{\Delta CCL19}$ mice and control littermates. Graph shows the absolute numbers (mean ± SD) of subcapsular sinus macrophages (SSM) and medullary sinus macrophages (MSM) in RANKL$^{\Delta CCL19}$ mice and cre- control littermates. Statistical significance was calculated using two way ANOVA with bonferroni correction ***p<0.001. (C) Plots depict the gating strategy to investigate PE-IC complexes uptake by B cells. Graph shows the percentage (mean ± SD) of PE$^+$ B cells in RANKL$^{\Delta CCL19}$ mice and cre- control littermates. Statistical significance was calculated using Mann-Whitney test. **p<0.01.
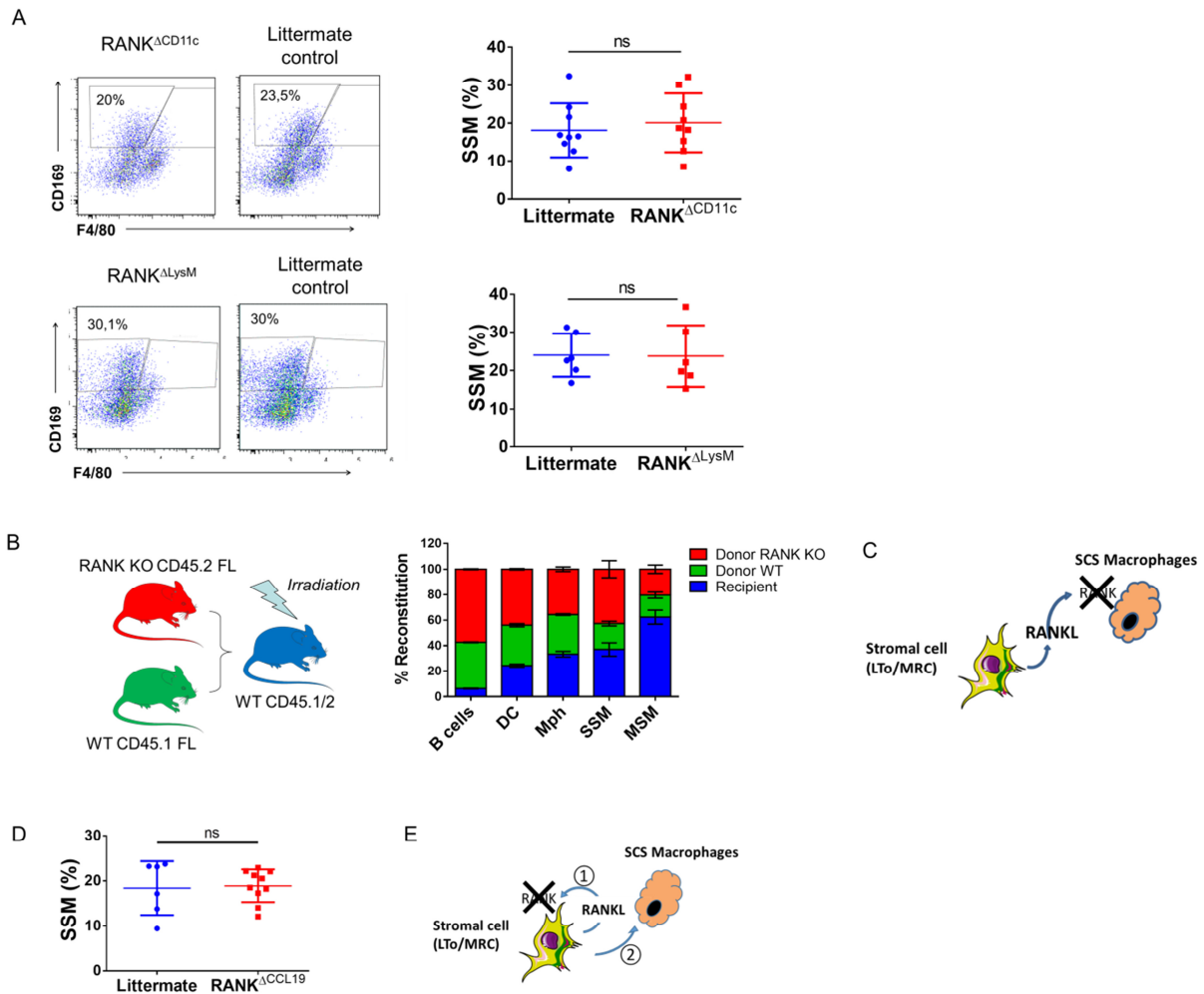
Figure 4: Stromal RANKL does not act directly on macrophages or stromal cells **(A)** Graphs represent the mean (± SD) percentage of subcapsular sinus macrophages (SSM) in RANK$^{\Delta CD11c}$ and RANK$^{\Delta LysM}$ mice and cre- control littermates. **(B)** Scheme representing the protocol for RANK-KO versus WT fetal liver transfer in irradiated WT mice. Graph shows the reconstitution percentage (mean ± SD) of different cell populations according to their origin as indicated. FL= fetal liver, Mph= total macrophages. **(C)** Schematic representation summarizing our results that stromal RANKL does not act directly on macrophages. **(D)** Graph shows the percentage (mean ± SD) of SSM in RANK$^{\Delta CCL19}$ mice and cre- control littermates. **(E)** Schematic representation showing that stromal RANKL does not act in an autocrine manner on RANK expressing stromal cells, nor does it directly stimulate SSM differentiation. Statistical significance was calculated using Mann-Whitney test.
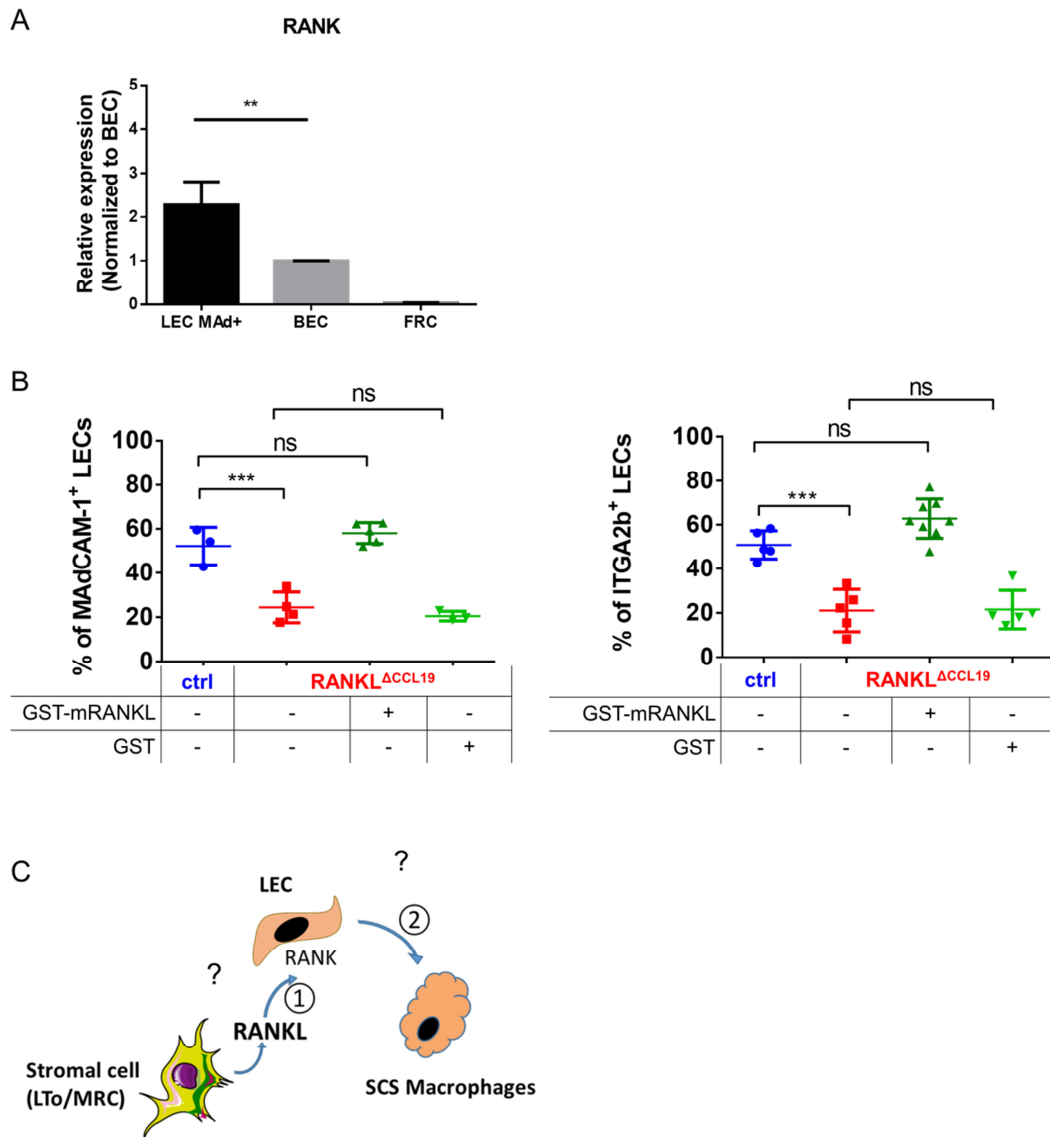
Figure 5: LECs are sensitive to stromal RANKL and can be rescued. **(A)** Relative expression (mean ± SEM) of RANK mRNA in LN lymphatic endothelial cells (LEC), blood endothelial cells (BEC) and fibroblastic reticular cells (FRC). Statistical significance was calculated using Mann-Whitney test. **p<0.01 **(B)** Graph represents the percentage (mean ± SD) of MAdCAM-1+ and ITGA2b+ LECs in RANKL$^{\Delta CCL19}$ injected or not with 100μg GST-mRANKL or GST for 4 days compared to cre- control littermates. Statistical significance was calculated using one way ANOVA with bonferroni correction. ***p<0.001 **(C)** Schematic representation of a possible indirect mechanism involving LECs.

Supplemental Table.

Antibodies used in the study.

Target	Species	Clone	Conjugation	Supplier
CD45	Rat IgG2a	30-F11	APC-CY7	Biolegend
Ter-119	Rat IgG2b	TER-119	APC-CY7	Biolegend
CD31	Rat IgG2a	390	A488	Biolegend
Gp38	Syrian Hamster IgG	8.1.1	PE/CY7	Biolegend
MAdCAM-1	Rat IgG2a	MECA-367	biotin	eBioscience
CD41	Rat IgG1	MWReg30	APC	Biolegend
B220	Rat IgG2a	RA3-6B2	Biotine	eBioscience
RANKL	Rat IgG2a	IK22.5	Purified	Hideo Yagita
CD16/32	Rat IgG2b	2.4G2	Purified	BD Pharmingen
CD11c	Armenian hamster	N418	PE/Cy7	eBioscience
CD11b	Rat IgG2b	M1/70	PerCP CY5.5	BD
CD169	Rat IgG2a	3D6.112	FITC	Biolegend
F4/80	Rat IgG2a	BM8	APC	eBioscience
CD45.1	Mouse IgG2a	A20	APC	eBioscience
CD45.2	mouse IgG2a	104	APC	eBioscience
CD3	Armenian hamster IgG1, k	145-2C11	FITC; PE	BD
CD4	Rat IgG2a	RM4-5	PerCPCy5.5; APC	BD
CD19	Rat IgG2a	RA3-6B2	PE, PerCPCy5.5; APC	BD
LTβR-muIgG1	Mouse IgG1			Biogen
SIGN-R1	Armenian Hamster IgG	22D1	Purified	BioXcell
mCLCA1	Syrian Hamster IgG	10.1.1	Purified	Andy Farr
Hamster IgG	Goat	Polyclonal	A488; A546	Molecular probes
Streptavidin			PE; APC	BD

2.4. Conclusions

LECs represent heterogeneous populations in LNs and in peripheral lymphatic vasculature. In a first study we described a new marker of LECs, ITGA2b, expressed by a subset of LN LECs from the subcapsular, cortical and medullary sinuses. The ITGA2b$^+$ LECs also expressed MAdCAM-1. ITGA2b is known to be expressed by megakaryocytes and platelets; we excluded platelet contamination in our experiments. We demonstrated that ITGA2b expression by LECs is sensitive to RANKL and LT. Functional relevance of ITGA2b expression requires further investigations but this study illustrates LEC heterogeneity and shows that RANKL is an important activation factor of these cells.

CD169$^+$ macrophages are present in the subcapsular and medullary sinus of the LNs. RANKL is known to regulate osteoclast differentiation but whether it has an impact on the differentiation of other macrophage subsets was not known. RANKL is constitutively expressed by MRCs in the LN subcapsular area, therefore we generated mice with conditional deletion of RANKL in MRCs (RANKL$^{\Delta CCL19}$). We observed a reduced number of CD169$^+$ SSM in these mice while the MSM population was not significantly decreased. We investigated the possible underlying mechanism and showed that RANKL does not act directly on RANK on macrophages or myeloid precursors. We also observed that RANKL is not acting in an autocrine manner on MRCs. As we have previously shown that LECs are sensitive to RANKL, we injected RANKL$^{\Delta CCL19}$ mice with GST-mRANKL. We observed a restored expression of ITGA2b and MAdCAM-1 to WT levels on LECs. Therefore, we hypothesize an indirect mechanism of SSM differentiation to occur via LECs. Further studies are required to confirm that RANK expression on LECs is important for SSM differentiation and to identify the potential factors involved in this process.

DISCUSSION

&

PERSPECTIVES

Discussion and perspectives

Development of new molecular tools to target RANK/RANKL

The RANK/RANKL/OPG triad is involved in many biological processes. Therefore, targeting RANK/RANKL interaction could be of interest in several pathological conditions such as osteoporosis, autoimmunity, lymphangiogenesis and epithelial cell proliferation in cancers. Anti-RANKL antibody denosumab is currently approved for treatment of osteoporosis and tumor bone metastases [1]. Several molecules, peptides, fusion-proteins or antibodies were studied to target RANKL, RANK or the signaling pathway of RANK [1–5]. However, a small molecule inhibiting the interaction between RANK and its ligand was not reported. Such a molecule could have advantages regarding cost and route of administration compared to therapeutic antibodies. Moreover, there was a lack of well characterized anti-RANK antibodies that remain important tools to study RANK biology. In this thesis, the development of a new anti-RANK antibody (RANK-02) and its characterization together with an existing antibody (R12-31) brought better understanding of their binding to human and murine RANK. Additionally, we characterized their biological activity *in vitro* and *in vivo* and they constitute new tools to further address mechanisms implicating RANK. This study also allowed setting up the *in vitro* tests for the screening of a library of small molecules we performed in a second step. Moreover, we showed that RANK-02 interferes with RANKL binding on RANK therefore we were able to use this antibody as a positive control for inhibition of RANK-RANKL interaction. We screened the Prestwick Chemical Library® containing 1280 already approved drugs using a competitive ELISA assay. Surprisingly, beside the large chemical diversity of the library, only one hit was validated. This compound is verteporfin, a benzoporphyrin derivative used as a treatment in photodynamic therapy of neovascular age-related macular degeneration (AMD). We confirmed the activity of this compound by testing 10 close analogues, only two of them did not show inhibitory activity. The compounds inhibited RANK activation *in vitro* in a cellular assay using Jurkat JOM2 hRANK:Fas cells as well as in an osteoclasts differentiation assay. This study provides the proof of concept that it is possible to inhibit RANK/RANKL interaction with a small molecule. Benzoporphyrin derivatives have a specific porphyrin macrocycle structure that may provide the molecular base for interference with RANK-RANKL interaction. Verteporfin is commercialized since 2000 by Novartis under the name Visudyne®. It is approved to treat "wet" AMD in photodynamic therapy of the eye. In this form of AMD, choroidal neovascularization by leaking vessels impairs vision and can lead to blindness. Intravenous injection of verteporfin followed by laser irradiation at 689nm on the site of neovascularization leads to generation of singlet oxygen and other free radicals. This results in intravascular damage of endothelial cells, thrombus formation and platelet activation leading to

vascular occlusion and vision improvement. The liposomal formulation of Visudyne® aims to target lipoproteins expressed by proliferating endothelial cells and increase selectivity of the drug [6]. In recent studies, other properties of verteporfin were demonstrated in absence of light activation. Verteporfin inhibits autophagosome accumulation and increases antitumor activity of Gemcitabine in pancreatic ductal adenocarcinoma [7,8]. Verteporfin also inhibited YAP transcriptional co-activator of the Hippo pathway in ovarian cancer cells and suppressed their invasive/migratory capacity [9]. Moreover this compound was able to kill tumor cells in a colorectal cancer model in a YAP independent mechanism involving impaired clearance of p62/STAT3 [10]. However, due to its ability to generate free radicals when exposed to light, verteporfin is a photosensitizing agent. Extravasation of verteporfin outside of blood vessels and exposure to light could cause severe pain, inflammation, swelling or discoloration [6]. With a half-life of 2-5h, verteporfin is cleared rapidly compared to other photosensitizers. Nonetheless, patients injected with Visudyne® present skin photosensitivity for at least 48h. Overall, verteporfin presents several potential side effects due to its photosensitizer properties. Moreover, the recent studies showing inhibition of autophagy and tumor cell proliferation describe potential off-target effects if it were used to target RANK/RANKL. Specificity for RANK or RANKL would have to be investigated in more details as structures of the TNF/TNFR family members are well conserved within the family. Therefore, further investigations would be required to evaluate verteporfin as a therapeutic molecule targeting RANK/RANKL axis. Verteporfin and porphyrin derivatives could be used as new tools to identify other molecules inhibiting RANK/RANKL interaction. This could improve the discovery of small molecules in a way we used antibodies targeting RANK and RANKL as positive controls.

Stromal RANKL implication in lymph node homeostasis

RANKL is constitutively expressed by marginal reticular cells (MRCs) in the subcapsular area of LNs. RANKL was shown to play a role in osteoclast differentiation but whether it also plays a role in the differentiation of other macrophages was not known. We generated mice deficient for stromal RANKL (RANKL$^{\Delta CCL19}$) and observed a decreased number of CD169$^+$ subcapsular sinus macrophages (SSMs). SSMs play an important role in the transfer of antigens from the lymph to B cells [11–14]. Consequently, antigen uptake by B cells was impaired in RANKL$^{\Delta CCL19}$ mice. SSM are also important in virus infection as they are permissible to infection, enabling viral replication and enhancing antiviral response through IFN-I production [13,15]. Therefore, to further confirm the functional relevance of CD169 loss in the subcapsular sinus of RANKL$^{\Delta CCL19}$ mice, we will perform Vesicular stomatitis virus (VSV) infection and study mouse mortality.

In the absence of stromal RANKL, we observed that a subset of cells from the subcapsular sinus express the C-type lectin SIGN-R1. This suggests that macrophages are still present in the LN subcapsular sinus but in a different differentiation state. MSM express SIGN-R1 and are described as more phagocytic thus more mature cells [11,16–18]. Therefore, the absence of RANKL would lead to advanced differentiation and expression of SIGN-R1 by SSMs. Injection of recombinant RANKL for 4 or 8 days did not rescue CD169 expression in the subcapsular sinus. This inefficacy of RANKL is in line with the idea that CD169 is a marker of immature macrophages requiring the replacement of – probably longlived- mature macrophages by precursor cells in order to recover bona fide SSMs. A key signal might be needed in the embryo or during early life to inhibit complete differentiation into phagocytic, SIGN-R1 expressing cells. GST-mRANKL construct is likely immunogenic and its prolonged used *in vivo* could promote immune reaction against GST and thus its neutralization. Irradiation and reconstitution with WT bone marrow in the presence of recombinant RANKL could be tested to investigate whether the formation of new SSM is accelerated.

Lymphotoxin (LT) is also part of the TNF superfamily. It was shown that LTβR-Fc injections reduced SSM numbers [11]. We confirmed these results and showed that anti-RANKL antibody injection reduced SSM numbers in the same extent as LTβR-Fc. Both RANKL and LT blockage had more effect on the SSM population than on MSMs. However, Phan and colleagues showed that MSMs express more LTβR than SSMs but SSMs are more sensitive to LT blockage. This apparent discrepancy was not studied in detail and would require further attention. Moreover, the phenotype of mice deficient for LTbR was opposite to LTβR-Fc injections with decreased MSM population and less effect on SSMs [11]. The transfer of *Ltbr-/-* bone marrow into irradiated mice showed that LTβR expression on macrophages or precursors seems to be required for SSM development. In this study, we showed that RANK expression by macrophages or myeloid precursors is not required for the presence of SSMs. Therefore, the mechanisms involving LT and RANKL affecting SSM differentiation are probably different. Moseman and colleagues showed that LT expressed by B cells is important for CD169 expression by SSM [19]. B cells deficient mice showed decreased expression of CD169 and increased SIGN-R1 expression in the subcapsular sinus. This shows that lack of LT stimulation leads to a phenotype of SSM that we observed in stromal RANKL deficient mice. Therefore, RANKL and LT could be linked in a mechanism leading to triggering CD169 expression and SSM differentiation. However, we observed normal levels of LTα and LTβ as well as absolute B cell numbers in RANKL[ΔCCL19] mice (data not shown). Further investigations are required to understand whether LT and RANKL are linked in order to maintain LN macrophages homeostasis. We also confirmed in this study that TNF do not play a role in CD169^{+} macrophages differentiation. Knowing the existing redundancy between

different members of the TNF/TNFR superfamily, further investigations would be required to understand the roles of RANKL, LT and TNF in LN homeostasis.

We decided to focus our work on identifying which cell type expressing RANK is important for CD169^{+} SSM differentiation and understanding the underlying cellular mechanisms. As already mentioned, we excluded a direct action of RANK on macrophages. The expression of RANK by MRCs was also not required, excluding an autocrine effect of RANKL. Lymphatic endothelial cells (LECs) are forming the floor subcapsular sinus which is in close contact with MRCs and SSMs. Hence, we investigated the effect of RANKL on LECs. It was previously shown in our group that LECs overexpress markers such as MAdCAM-1 in a mouse model overexpressing RANKL [20]. During this thesis, we found a new marker expressed by LECs, ITGA2b. Expression of this integrin by LECs is sensitive to RANKL as mice treated with anti-RANKL antibody and RANKL[ΔCCL19] mice have a lower percentage of ITGA2b^{+} LECs. Moreover, this study further highlights the heterogeneity of LECs in the LN. Expression of ITGA2b and MAdCAM-1 is different depending on the localization of LECs, showing different activation state. A factor responsible for LEC activation is RANKL. We confirmed this by injecting GST-mRANKL to RANKL[ΔCCL19] mice and observed a rescue of ITGA2b and MAdCAM-1 to WT levels on LECs. In the subcapsular sinus, floor LECs are more activated probably because they are in close contact with RANKL expressing MRCs. We used RANK-02 anti-RANK antibody and observed that only a part of LECs population express RANK on the cell surface. This might be explained by internalization of the receptor upon stimulation. This could also show that other factors are responsible for LECs activation. We observed that LT blockage decreased the proportion of ITGA2b^{+} LECs in the LN. LT was also shown to affect MAdCAM-1 expression as LTβR-Fc injection decreased MAdCAM-1 expression in the subcapsular sinus [21]. However, in this study Cohen and colleagues also showed that LTβR deletion in LECs under the control of Prox-1 promoter did not reduce MAdCAM-1 expression by LECs. These results show that the subcapsular sinus area is a complicated region with different cell types and factors influencing their activation state. Observed phenotypes probably result from several indirect mechanisms. We showed that LECs express RANK by qRT-PCR. Therefore, we generated mice deficient for RANK under Prox-1 promoter by crossing Prox-1 cre ERT2 mice with RANK flox/flox mice (RANK[ΔProx-1]). We have set the conditions of tamoxifen injection to efficiently delete RANK from LECs (**fig. 1**). We now need to investigate whether these mice present the same phenotype as RANKL[ΔCCL19] mice regarding ITGA2b/MAdCAM-1 expression by LECs and CD169 expression by SSMs. If RANK[ΔProx-1] mice show a decreased CD169^{+} SSM number similar to RANKL[ΔCCL19] mice, we will be able to conclude that RANKL expressed by MRCs is acting on floor LECs and LECs further provide a signal enabling

CD169 expression by SSM. This signal would contribute to maintenance of a differentiation state characterized by absence of SIGN-R1 and low phagocytic activity (**Fig. 2**).

F. Alloush
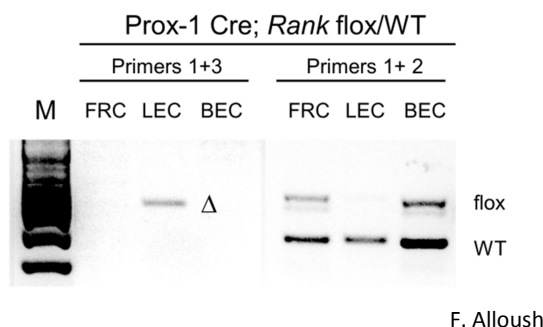
Figure 1: Deletion of exon 2 and 3 of the *tnfrsf11a* gene in DNA of LECs from RANK$^{\Delta Prox-1}$ mice after tamoxifen injections. LECs were sorted from Prox-1 RANK flox/WT mice aged of 8 weeks. Before taking the LNs, mice were injected for 4 consecutive days with 3mg tamoxifen every day. To confirm Prox-1 cre recombinase-mediated deletion of exon 2 and 3 of the *tnfrsf11a* gene, two PCR were performed on LECs DNA using 3 different primers. Primer 1 (5'-TGTCCCACTGACACAGGAGA-3') and primer 2 (5'-AGCTCACAACGCACAAAACA-3') amplify a 469 bp fragment from the floxed locus and a 290 bp fragment from WT locus. Primer 1 and primer 3 (5'-GAGTTCAAGGCCAACCTGAG-3') amplify a 392 bp fragment resulting from excision of the floxed region by Prox-1-cre recombinase [22].

Identification of the potential factors expressed by RANKL stimulated LECs that could trigger macrophages differentiation or precursor recruitment will then be required. It was shown that LECs can produce CSF1 [23] and GM-CSF [24]. Moreover, CSF-1 is required for SSMs development but not MSMs [25] which could explain the differences we observe in RANKL$^{\Delta CCL19}$ mice. Another factor that was shown to induce CD169 expression is type I interferon (IFN). Studies using human monocytes show that CD169 expression can be induced *in vitro* by TLR ligands and IFNα and that CD169 is increased on circulating monocytes in patients with pathological type I IFN increase [26,27]. In rodents, only a study in rats showed that CD169 expression can be induced on macrophages by IFNβ [28]. Conversely, SSMs were still present in IFNAR deficient mice [15]. Therefore elucidating a potential link between RANKL and type I IFN in inducing CD169 macrophages differentiation could be of interest. RANKL was also shown to induce CCL20 expression. CCL20 is responsible for migration of lymphocytes in the follicular associated epithelium (FAE) of the intestine. Lympho-epithelial cells interactions is necessary for M cell maturation [29]. Moreover, RANKL expressing T cells induce CCL20 production by astrocytes thus recruiting lymphocytes in the CNS. Mice deficient for RANKL in T cells are resistant to autoimmune encephalomyelitis [30]. Therefore, another hypothesis could be that stromal RANKL induces CCL20 expression by LECs which could play a role in recruitment of myeloid precursors of SSMs. In order to investigate the potential factors linking LECs with CD169 expression by macrophages, we sorted LECs from RANKL$^{\Delta CCL19}$ mice treated or not with GST-mRANKL and performed RNA sequencing. The results are currently being analysed.
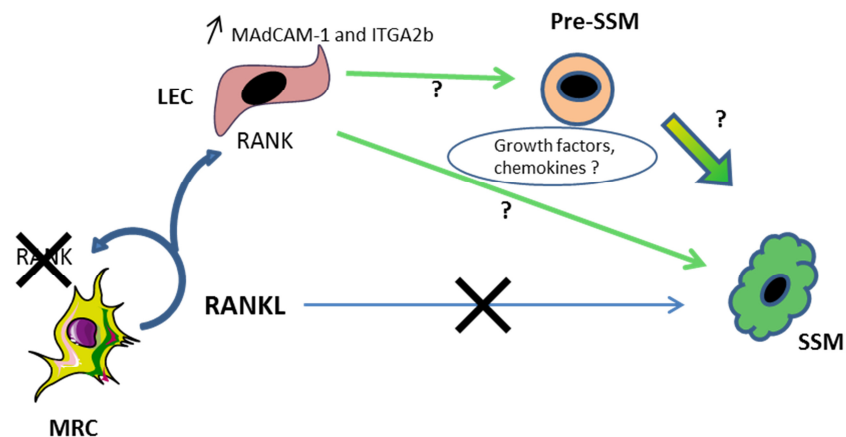
Figure 2: Schematic representation of the mechanism linking stromal RANKL and subcapsular sinus macrophages (SSM) differentiation. RANKL is expressed by MRCs in the LN. We showed that RANKL does not act directly on macrophages or myeloid precursors. We also excluded an autocrine loop with RANKL acting on MRCs. We observed that LECs are sensitive to RANKL therefore we hypothesized an indirect mechanism with RANKL acting on LECs. The factors expressed by LECs upon RANKL stimulation and responsible for the differentiation of SSM remain to be identified.

Co-culture of LECs and macrophages or monocytes could also enable the validation of important factors. However, culturing LECs was challenging and we did not succeed in culturing enough cells to perform these experiments. Recently, a new protocol consisting in culturing total stromal cells before sorting LECs showed promising results. This experiment requires further set up.

These findings showing the importance of RANKL in CD169^{+} SSM differentiation could also be of great interest in other tissues. Indeed, CD169^{+} macrophages are also present in tissues such as intestines [31,32] where stromal cells also produce RANKL. Moreover, depletion of CD169^{+} macrophages in intestines ameliorates colitis symptoms [32]. Therefore, identifying the factors responsible for their development could be of interest in this pathological condition. On the other hand, it was also shown that SSMs can induce anti-tumor immunity by presenting tumor antigens to CD8+ T cells [33]. Hence, depending on the pathology, it would be of interest to locally modulate the presence or absence of the SSM population.

In this study, we confirmed that LECs express RANK. It was previously shown in our group that RANKL overexpression in mouse induces LEC proliferation [20]. We confirmed that RANKL is involved in LEC activation. Moreover, RANKL is known to induce angiogenesis of blood endothelial cells [34]. Lymphangiogenesis is increased in cancers and promotes tumor spread [35]. Therefore it could be interesting to study in more details the role of RANKL in lymphangiogenesis to evaluate it as a therapeutic target. Moreover, we observed that RANKL-activated LECs upregulate MAdCAM-1

expression. MAdCAM-1$^+$ LECs were mainly located in the floor of the subcapsular sinus. MAdCAM-1 is a ligand for Integrin α4β7 and L-selectin on leukocytes [36,37] thus RANKL activation of LECs might also play a role in leukocyte adherence to subcapsular sinus and entry in the LN.

Overall, this work further shows the complexity of the mechanisms orchestrating LN organisation and homeostasis. The detailed characterization of the cells and factors leading to the presence of CD169 expressing macrophages in the LN subcapsular sinus remain to be identified. This work also shows a novel role of RANKL beyond bone homeostasis and could help understanding the potential side effects of anti-RANKL therapy. On the other hand, activation of LECs by RANKL could play a role in immune pathologies and cancers. This paves the way to further investigate RANKL as a therapeutic target in cancers and autoimmune disorders.

References

1. Lacey DL, Boyle WJ, Simonet WS, Kostenuik PJ, Dougall WC, Sullivan JK, et al. Bench to bedside: elucidation of the OPG–RANK–RANKL pathway and the development of denosumab. Nat Rev Drug Discov. 2012;11: 401–419. doi:10.1038/nrd3705

2. Coste E, Greig IR, Mollat P, Rose L, Gray M, Ralston SH, et al. Identification of small molecule inhibitors of RANKL and TNF signalling as anti-inflammatory and antiresorptive agents in mice. Ann Rheum Dis. 2015;74: 220–226. doi:10.1136/annrheumdis-2013-203700

3. Aggarwal B, Darnay B, Singh S. Inhibitors of receptor activator of NF-kappaB and uses thereof [Internet]. US20040167072 A1, 2004. Available: http://www.google.tl/patents/US20040167072

4. Naidu VGM, Dinesh Babu KR, Thwin MM, Satish RL, Kumar PV, Gopalakrishnakone P. RANKL targeted peptides inhibit osteoclastogenesis and attenuate adjuvant induced arthritis by inhibiting NF-κB activation and down regulating inflammatory cytokines. Chem Biol Interact. 2013;203: 467–479. doi:10.1016/j.cbi.2012.12.016

5. Cheng X, Kinosaki M, Takami M, Choi Y, Zhang H, Murali R. Disabling of Receptor Activator of Nuclear Factor-κB (RANK) Receptor Complex by Novel Osteoprotegerin-like Peptidomimetics Restores Bone Loss in Vivo. J Biol Chem. 2004;279: 8269–8277. doi:10.1074/jbc.M309690200

6. Schmidt-Erfurth U, Hasan T. Mechanisms of Action of Photodynamic Therapy with Verteporfin for the Treatment of Age-Related Macular Degeneration. Surv Ophthalmol. 2000;45: 195–214. doi:10.1016/S0039-6257(00)00158-2

7. Donohue E, Tovey A, Vogl AW, Arns S, Sternberg E, Young RN, et al. Inhibition of Autophagosome Formation by the Benzoporphyrin Derivative Verteporfin. J Biol Chem. 2011;286: 7290–7300. doi:10.1074/jbc.M110.139915

8. Donohue E, Thomas A, Maurer N, Manisali I, Zeisser-Labouebe M, Zisman N, et al. The Autophagy Inhibitor Verteporfin Moderately Enhances the Antitumor Activity of Gemcitabine in a Pancreatic Ductal Adenocarcinoma Model. J Cancer. 2013;4: 585–596. doi:10.7150/jca.7030

9. Feng J, Gou J, Jia J, Yi T, Cui T, Li Z. Verteporfin, a suppressor of YAP–TEAD complex, presents promising antitumor properties on ovarian cancer. OncoTargets Ther. 2016;9: 5371–5381. doi:10.2147/OTT.S109979

10. Zhang H, Ramakrishnan SK, Triner D, Centofanti B, Maitra D, Győrffy B, et al. Tumor-selective proteotoxicity of verteporfin inhibits colon cancer progression independently of YAP1. Sci Signal. 2015;8: ra98-ra98. doi:10.1126/scisignal.aac5418

11. Phan TG, Green JA, Gray EE, Xu Y, Cyster JG. Immune complex relay by subcapsular sinus macrophages and noncognate B cells drives antibody affinity maturation. Nat Immunol. 2009;10: 786–793. doi:10.1038/ni.1745

12. Phan TG, Grigorova I, Okada T, Cyster JG. Subcapsular encounter and complement-dependent transport of immune complexes by lymph node B cells. Nat Immunol. 2007;8: 992–1000. doi:10.1038/ni1494

13. Junt T, Moseman EA, Iannacone M, Massberg S, Lang PA, Boes M, et al. Subcapsular sinus macrophages in lymph nodes clear lymph-borne viruses and present them to antiviral B cells. Nature. 2007;450: 110–114. doi:10.1038/nature06287

14. Carrasco YR, Batista FD. B Cells Acquire Particulate Antigen in a Macrophage-Rich Area at the Boundary between the Follicle and the Subcapsular Sinus of the Lymph Node. Immunity. 2007;27: 160–171. doi:10.1016/j.immuni.2007.06.007

15. Iannacone M, Moseman EA, Tonti E, Bosurgi L, Junt T, Henrickson SE, et al. Subcapsular sinus macrophages prevent CNS invasion on peripheral infection with a neurotropic virus. Nature. 2010;465: 1079–1083. doi:10.1038/nature09118

16. Nossal GJV, Ada GL, Austin CM, Pye J. Antigens in immunity. Immunology. 1965;9: 349–357.

17. Fossum S. The architecture of rat lymph nodes. IV. Distribution of ferritin and colloidal carbon in the draining lymph nodes after foot-pad injection. Scand J Immunol. 1980;12: 433–441.

18. Steer HW, Foot RA. Changes in the medulla of the parathymic lymph nodes of the rat during acute gastro-intestinal inflammation. J Anat. 1987;152: 23–36.

19. Moseman EA, Iannacone M, Bosurgi L, Tonti E, Chevrier N, Tumanov A, et al. B Cell Maintenance of Subcapsular Sinus Macrophages Protects against a Fatal Viral Infection Independent of Adaptive Immunity. Immunity. 2012;36: 415–426. doi:10.1016/j.immuni.2012.01.013

20. Hess E, Duheron V, Decossas M, Lézot F, Berdal A, Chea S, et al. RANKL Induces Organized Lymph Node Growth by Stromal Cell Proliferation. J Immunol. 2012;188: 1245–1254. doi:10.4049/jimmunol.1101513

21. Cohen JN, Tewalt EF, Rouhani SJ, Buonomo EL, Bruce AN, Xu X, et al. Tolerogenic Properties of Lymphatic Endothelial Cells Are Controlled by the Lymph Node Microenvironment. PLoS ONE. 2014;9: e87740. doi:10.1371/journal.pone.0087740

22. Rios D, Wood MB, Li J, Chassaing B, Gewirtz AT, Williams IR. Antigen sampling by intestinal M cells is the principal pathway initiating mucosal IgA production to commensal enteric bacteria. Mucosal Immunol. 2016;9: 907–916. doi:10.1038/mi.2015.121

23. Malhotra D, Fletcher AL, Astarita J, Lukacs-Kornek V, Tayalia P, Gonzalez SF, et al. Transcriptional profiling of stroma from inflamed and resting lymph nodes defines immunological hallmarks. Nat Immunol. 2012;13: 499–510. doi:10.1038/ni.2262

24. Fiorentini S, Luganini A, Dell'Oste V, Lorusso B, Cervi E, Caccuri F, et al. Human cytomegalovirus productively infects lymphatic endothelial cells and induces a secretome that promotes angiogenesis and lymphangiogenesis through interleukin-6 and granulocyte–macrophage colony-stimulating factor. J Gen Virol. 2011;92: 650–660. doi:10.1099/vir.0.025395-0

25. Cecchini MG, Dominguez MG, Mocci S, Wetterwald A, Felix R, Fleisch H, et al. Role of colony stimulating factor-1 in the establishment and regulation of tissue macrophages during postnatal development of the mouse. Development. 1994;120: 1357–1372.

26. Rempel H, Calosing C, Sun B, Pulliam L. Sialoadhesin Expressed on IFN-Induced Monocytes Binds HIV-1 and Enhances Infectivity. PLOS ONE. 2008;3: e1967. doi:10.1371/journal.pone.0001967

27. York MR, Nagai T, Mangini AJ, Lemaire R, van Seventer JM, Lafyatis R. A macrophage marker, siglec-1, is increased on circulating monocytes in patients with systemic sclerosis and induced by type i interferons and toll-like receptor agonists. Arthritis Rheum. 2007;56: 1010–1020. doi:10.1002/art.22382

28. Berg TK van den, Die I van, Lavalette CR de, Döpp EA, Smit LD, Meide PH van der, et al. Regulation of sialoadhesin expression on rat macrophages. Induction by glucocorticoids and enhancement by IFN-beta, IFN-gamma, IL-4, and lipopolysaccharide. J Immunol. 1996;157: 3130–3138.

29. Mabbott NA, Donaldson DS, Ohno H, Williams IR, Mahajan A. Microfold (M) cells: important immunosurveillance posts in the intestinal epithelium. Mucosal Immunol. 2013;6: 666–677. doi:10.1038/mi.2013.30

30. Guerrini MM, Okamoto K, Komatsu N, Sawa S, Danks L, Penninger JM, et al. Inhibition of the TNF Family Cytokine RANKL Prevents Autoimmune Inflammation in the Central Nervous System. Immunity. 2015;43: 1174–1185. doi:10.1016/j.immuni.2015.10.017

31. Hiemstra IH, Beijer MR, Veninga H, Vrijland K, Borg EGF, Olivier BJ, et al. The identification and developmental requirements of colonic CD169+ macrophages. Immunology. 2014;142: 269–278. doi:10.1111/imm.12251

32. Asano K, Takahashi N, Ushiki M, Monya M, Aihara F, Kuboki E, et al. Intestinal CD169+ macrophages initiate mucosal inflammation by secreting CCL8 that recruits inflammatory monocytes. Nat Commun. 2015;6: 7802. doi:10.1038/ncomms8802

33. Asano K, Nabeyama A, Miyake Y, Qiu C-H, Kurita A, Tomura M, et al. CD169-Positive Macrophages Dominate Antitumor Immunity by Crosspresenting Dead Cell-Associated Antigens. Immunity. 2011;34: 85–95. doi:10.1016/j.immuni.2010.12.011

34. Kim Y-M, Kim Y-M, Lee YM, Kim H-S, Kim JD, Choi Y, et al. TNF-related Activation-induced Cytokine (TRANCE) Induces Angiogenesis through the Activation of Src and Phospholipase C (PLC) in Human Endothelial Cells. J Biol Chem. 2002;277: 6799–6805. doi:10.1074/jbc.M109434200

35. Stacker SA, Williams SP, Karnezis T, Shayan R, Fox SB, Achen MG. Lymphangiogenesis and lymphatic vessel remodelling in cancer. Nat Rev Cancer. 2014;14: 159–172. doi:10.1038/nrc3677

36. Berg EL, McEvoy LM, Berlin C, Bargatze RF, Butcher EC. L-selectin-mediated lymphocyte rolling on MAdCAM-1. Nature. 1993;366: 695–698. doi:10.1038/366695a0

37. Berlin C, Berg EL, Briskin MJ, Andrew DP, Kilshaw PJ, Holzmann B, et al. α4β7 integrin mediates lymphocyte binding to the mucosal vascular addressin MAdCAM-1. Cell. 1993;74: 185–195. doi:10.1016/0092-8674(93)90305-A

APPENDIX

CD41 (Itga2b) identifies lymph node lymphatic endothelial cells activated by RANKL

O. Cordeiro[1], M. Chypre[1], S. Rauber[1], N. Brouard[2], C. Leon[2], F. Lanza[2], C. G. Mueller[1]

[1]CNRS, Laboratory of Immunopathology and Chemistry, UPR3572, IBMC, University of Strasbourg, France;
[2] UMRS 949 INSERM, University of Strasbourg, EFS, France;

Introduction

CD41 (integrin αIIb) forms a complex with CD61 (integrin βIIIa), known as glycoprotein (GP) complex IIb/IIIa. GPIIb/IIIa is a receptor for fibronectin, fibrinogen, von Willebrand factor, vitronectin and thrombospondin[1,2] and plays a well known function in platelet aggregation[3]. CD41 is also a marker of pre-hematopoietic stem cells[3]. Surprisingly, a transcriptional study of mice lymph node (LN) non hematopoietic cells (stromal cells) identified CD41 (Itga2b) gene expression by lymphatic endothelial cells (LECs) **(Figure 1)**[4]. CD61 (Itgb3) is also expressed by LECs **(Figure 1)**. We therefore investigated the function of CD41/CD61 LEC in the immune system using different experimental approaches.
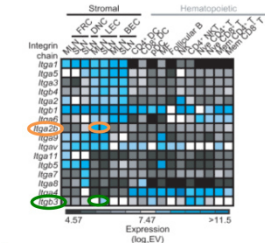
Figure 1: Image adapted from Malhotra et al., showing CD41 and CD61 expression on LECs. (Malhotra, D. et al., 2012 Nat Immunol)

Methods
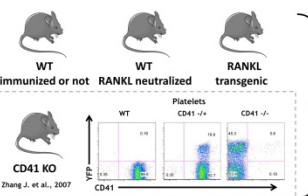
FRC: Fibroblastic reticular cells
LEC: Lymphatic endothelial cells
BEC: Blood endothelial cells
DNC: Double negative cells
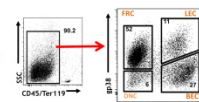
Results

1. LECs express the CD41/61 active complex
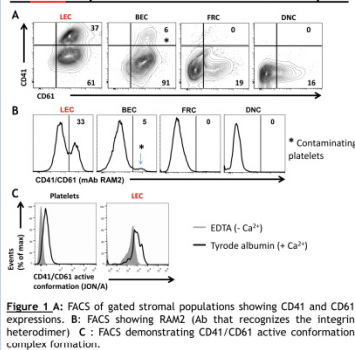
Figure 1 A: FACS of gated stromal populations showing CD41 and CD61 expressions. **B:** FACS showing RAM2 (Ab that recognizes the integrin heterodimer) **C :** FACS demonstrating CD41/CD61 active conformation complex formation.

2. Localization of CD41+ LEC subsets
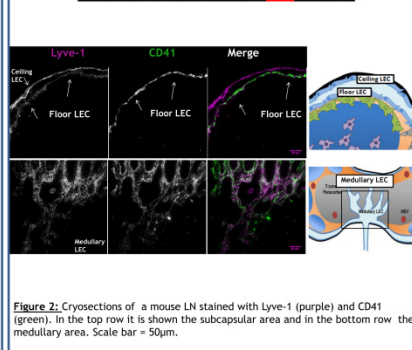
Figure 2: Cryosections of a mouse LN stained with Lyve-1 (purple) and CD41 (green). In the top row it is shown the subcapsular area and in the bottom row the medullary area. Scale bar = 50µm.

5. CD41 is induced by RANKL
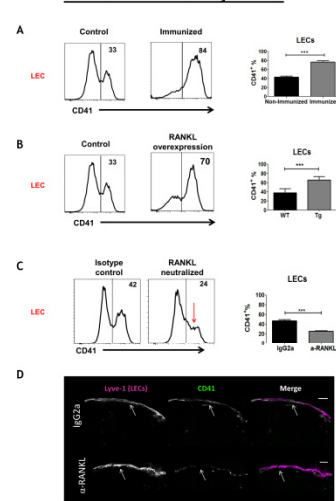
Figure 5 : CD41 expression measured by FACS in LECs of LNs **A:** after immunization with OVA and heat-inactivated *Bordella pertussis*, **B :** from mice overexpressing RANKL, **C :** after treatment with anti-RANKL antibody or isotype control. **D:** Cryosections of a LN from a mouse treated with anti-RANKL antibody or isotype control stained for Lyve 1 (purple) and CD41 (green). Scale bar = 50µm

3. LECs of CD41 -/- mice loose CD41 expression
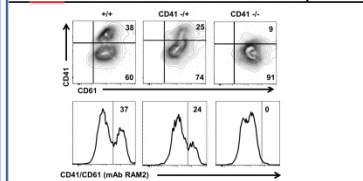
Figure 3 : LN-LECs from WT, CD41 -/+ and CD41 -/- mice were labeled for CD41, CD61 and the CD41/CD61 complex and analysed by FACS.

4. CD41 is required for B cell homeostasis
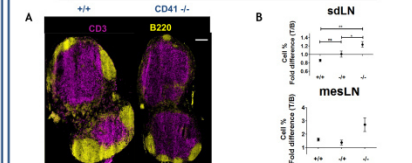
Figure 4 : **A:** Cryosections of LNs from WT and CD41 -/- mice stained for CD3 (purple, T cells) and B220 (yellow, B cells). Scale bar = 300µm **B:** Fold difference of T and B cell proportion in skin draining (sd) and mesenteric (mes) LNs of WT, CD41 -/+ and CD41 -/- mice were determined by FACS.

Conclusion

Our data demonstrate that lymph node LECs express CD41 and CD61. This was shown using a set of different tools: flow cytometry immunohistochemistry with different clonal antibodies, and mice knocked out for the *cd41* gene. LEC CD41 expression is not due to platelet contamination. We could show that, in non-immunized mice, CD41 is expressed by a subset of LECs that reside in the medulla, the cortex and the subcapsular sinus. Interestingly, the subcapsular sinus ceiling LECs lacked CD41. CD41/CD61 would assist in cell anchoring to extracellular matrix and thus participate in B cells homeostasis. We showed that CD41 is a LEC activation marker after immunization and that its expression on LECs is induced by RANKL (TNF superfamily member 11). Preliminary findings show that CD41 is also expressed by human LECs raising a clinically relevant issue of reactivity of anti-GPIIb/IIIa autoimmune antibodies in patients with thrombocytopenia, so far thought to be exclusively directed against platelets and megakaryocytes.

References: [1]Boisset, J. C. et al, 2013, Biology Open; [2]Du and Ginsberg, 1997, Thrombosis and Haemostasis; [3]Debili, N. et al., 2001, The American Society of Hematology, [4]Malhotra, D. et al., 2012, Nat Immunol.

Characterization of two anti-RANK (TNFRSF11a) antibodies with different biological activities

Mélanie Chypre[1,2], Olga Cordeiro[1], Jonathan Seaman[3], Andrew Buchanan[3], Richard C.A. Sainson[3], Pascal Schneider[4], Hideo Yagita[5], Christopher G. Mueller[1]

[1]CNRS, Laboratory of Immunopathology and Chemistry, UPR3572, IBMC, University of Strasbourg, France; [2] Prestwick Chemical, Blvd Gonthier d'Andernach, 67400 Illkirch, France [3] MedImmune, Granta Park, Cambridge CB21 6GH, UK [4] Department of Biochemistry, University of Lausanne, Epalinges, Switzerland [5] Department of Immunology, Juntendo University School of Medicine, Tokyo 113-8421, Japan

Introduction

Receptor activator of NF-kB (RANK) is a member of the TNF-family of receptors. It is engaged by its ligand RANKL but blocked by OPG (osteoprotegerin) that binds to RANKL and prevents it from recognizing RANK.

RANK is known for its role in regulating bone mass but is increasingly recognized as a central player in immune regulation and epithelial cell activation.

However, the study of RANK biology has been hampered by insufficient characterization of antibodies used to detect murine and human RANK. Here, we present a careful description and comparison of two anti-RANK antibodies, RANK-02 obtained by phage display (RANK binding sequence from Newa et al., 2014) and R12-31 generated by immunization (Kamijo et al., 2006). Both antibodies that recognize with high affinity murine and human RANK (KD in the range of 10^{-9} to 10^{-10} M) were analyzed (i) for RANK recognition by flow cytometry, (ii) for receptor trimerization of a RANK-Fas fusion protein leading to cell death, and (iii) for NF-kB signaling using transfected cell lines and reporter plasmids. We find that the antibodies both recognize RANK in transfected and primary cells but differ in biological activities. These tools are likely to help map the distribution and understand the regulation of RANK expression.

Methods

Jurkat JOM2 cell lines :

Seed Jurkat JOM2 cells — 16h 37°C 5% CO_2 +/- treatment — Add 20µl/ well of Celltiter 96 Aqueous one solution (Promega) — 2h 37°C 5% CO_2 — Read absorbance 490nm

Jurkat JOM2 (Fas deficient) / Jurkat JOM2 RANK:Fas
Viable cells / Dead cells
MTS — Formazan — Viable cells

HEK 293 – RANK cell lines:

Seed HEK293-RANK cells — O/N 37°C 5% CO_2 — Transfect the cells with: NF-kB luciferase reporter vector β-galactosidase reporter vector — 24h 37°C 5% CO_2 — Treat the cells with RANKL or anti-RANK antibodies — 16h 37°C 5% CO_2 — Cell lysis — Luciferase assay / β-galactosidase assay

Human skin crawl out:

Human skin ≈ 800 µm — 4 Days — Flow cytometry analysis of crawl out cells (dermal dendritic cells and Langerhans cells)

Results

1. RANK-02 and R12-31 bind to human and mouse RANK extracellular domain

Jurkat JOM2 / Jurkat JOM2 mRANK:Fas / Jurkat JOM2 hRANK:Fas / HEK 293 / HEK 293-mRANK / HEK 293-hRANK

Cell count — RANK (RANK-02)

Cell count — RANK (R12-31)

— Anti-RANK antibody   — Isotype control
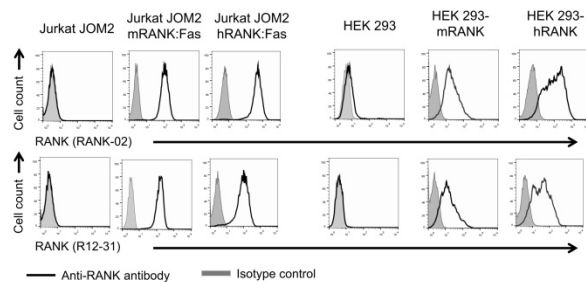
Figure 1 : Flow cytometry on cell lines overexpressing both mouse and human RANK : Jurkat JOM2 RANK:Fas and HEK293-RANK with the two anti-RANK antibodies

3. Only R12-31 is an agonist of mouse RANK

A: Cell viability (% of NT) vs log [R12-31](ng/ml) — JURKAT JOM2, JURKAT JOM2 mRANK:Fas
B: Cell viability (% of NT) vs log [RANK-02](ng/ml) — Jurkat JOM2, Jurkat JOM2 mRANK:Fas
C: Relative NFkB activation (%) — NT, RANKL, Anti-RANK (R12-31)
D: Relative NFkB activation (%) — NT, RANKL, Anti-RANK(RANK-02)
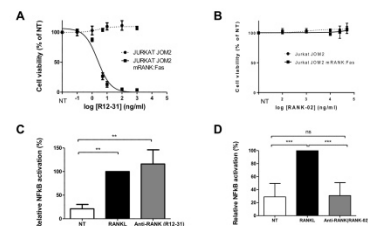
Figure 3. A: Viability assay on Jurkat JOM2 cells expressing or not mRANK:Fas with different concentrations of R12-31 antibody. **B:** same as A but with RANK-02 antibody. **C:** NF-kB reporter gene assay in HEK 293-mRANK cells with RANKL (0.1µg/ml) and R12-31 (25µg/ml). **D:** same as C but with RANK-02 (50µg/ml). Statistical analysis was made using one way ANOVA followed by Bonferroni test ** $P \leq 0.01$, *** $P \leq 0.001$.

2. R12-31 is a strong agonist and RANK-02 a weak agonist of human RANK

A: Cell viability (% of NT) vs log [R12-31](ng/ml) — JURKAT JOM2, JURKAT JOM2 hRANK:Fas
B: Cell viability (% of NT) vs log [RANK-02](ng/ml) — Jurkat JOM2, Jurkat JOM2 hRANK:Fas
C: Relative NFkB activation (%) — NT, RANKL, Anti-RANK (R12-31), Anti-RANK (RANK-02)

Figure 2. A: Viability assay on Jurkat JOM2 cells expressing or not hRANK:Fas with different concentrations of R12-31 antibody. **B:** Same as A but with RANK-02 antibody. **C:** NF-kB reporter gene assay in HEK293-hRANK cells with RANKL (0,1µg/ml), R12-31 (25µg/ml) and RANK-02 (50µg/ml). Statistical analysis was made using one way ANOVA followed by Bonferroni test *** $P \leq 0.001$.

4. RANK-02 and R12-31 recognize activated primary human Langerhans cells

A: Gating strategy — FVD, HLA-DR, DC SIGN, Langerin, Dermal DC, Langerhans cells
B: Cell count — RANK (RANK-02), RANK (R12-31)
C: Cell count — RANK (RANK-02), RANK (R12-31)

— Anti-RANK antibody   — Isotype control
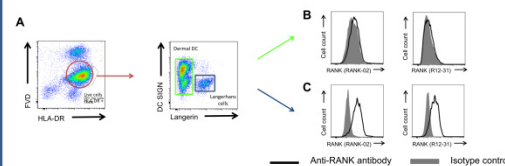
Figure 4. A: Gating strategy for analysis of activated Langerhans cells and dermal dendritic cells (DC) after crawl out from human skin. **B:** RANK staining by RANK-02 and R12-31 antibody on dermal dendritic cells. **C:** Same as B on activated Langerhans cells

Conclusion

Antibodies with high affinity and specificity are important therapeutic reagents and investigative tools. In order to be used adequately, these tools must be well investigated with respect to their affinity, specificity and biological activity. Therefore, we characterized two anti-RANK antibodies, RANK-02 obtained by phage display and R12-31 obtained by immunization. We found that they bind with high affinity to human and mouse RANK but that they differ in their biological activity. Indeed, R12-31 is agonist on both human and mouse RANK while RANK-02 has only a weak agonist effect on human RANK. Both mAbs could be used to recognize activated Langerhans cells after their crawl out from human skin. This shows that R12-31 can be employed to study RANK signaling and that both antibodies will be valuable tools to map RANK distribution in different tissues.

References: Kamijo, S., Nakajima, A., Ikeda, K., Aoki, K., Ohya, K., Akiba, H., Yagita, H., and Okumura, K. (2006). Amelioration of bone loss in collagen-induced arthritis by neutralizing anti-RANKL monoclonal antibody. Biochem. Biophys. Res. Commun. 347, 124–132; Newa, M., Lam, M., Bhandari, K.H., Xu, B., and Doschak, M.R. (2014). Expression, Characterization, and Evaluation of a RANK-Binding Single Chain Fraction Variable: An Osteoclast Targeting Drug Delivery Strategy. Mol. Pharm. 11, 81–89.

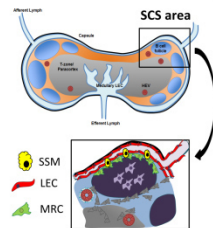Regulation of lymph node macrophage differentiation by RANKL

Mélanie CHYPRE

PRESTWICK CHEMICAL

UNIVERSITÉ DE STRASBOURG

Role of receptor activator of NF-kB ligand (RANKL) in adult lymph node homeostasis and identification of inhibitors

cnrs

Résumé

Le récepteur activateur de NF-κB (RANK), membre de la famille des récepteurs au TNF, est connu pour son rôle dans l'homéostasie de l'os, mais joue aussi un rôle important dans le système immunitaire. J'ai tout d'abord étudié des outils permettant de ciblé RANK/RANKL. J'ai caractérisé et comparé l'activité biologique de deux anticorps anti-RANK. J'ai également criblé une librairie de petites molécules pour identifier des inhibiteurs de l'interaction RANK/RANKL. Dans une deuxième partie, je me suis intéressée au rôle du ligand de RANK (RANKL) dans l'homéostasie du ganglion lymphatique. RANKL joue un rôle dans la différenciation des ostéoclastes mais son rôle dans la différenciation d'autres macrophages n'a pas été étudié. Nous avons étudié des souris déficientes pour RANKL dans les cellules marginales réticulaires (MRC) qui expriment RANKL de manière constitutive dans le ganglion adulte. Nous avons observé une diminution de la population de macrophages sous-capsulaires (SSM). Nous avons également montré que les cellules endothéliales lymphatiques (LEC) expriment l'intégrine alpha 2b (ITGA2b) et que cette expression est sensible à la présence de RANKL.

Mots clés : RANKL,RANK, ganglion lymphatique, macrophages, cellules endothéliales lymphatiques, inhibiteurs

Résumé en anglais

The TNF-family member Receptor Activator of NF-κB (RANK) is known for its role in bone homeostasis and is increasingly recognized as a central player in immune regulation. Firstly I looked for new molecular tools to target RANK/RANKL axis. I characterized and compared the biological activity of two anti-RANK antibodies. Moreover, I screened the Prestwick Chemical Library® of small molecules in order to identify inhibitors of RANK/RANKL interaction. Secondly, I studied the effect of the RANK/RANKL axis in lymph node homeostasis. RANKL is known to promote osteoclast differentiation but whether it also plays a role in the differentiation of other macrophage subsets is not known. We addressed this question by conditionally deleting RANKL from marginal reticular stromal cells (MRCs) that constitutively express RANKL in the lymph node. We observed impaired differentiation of the subcapsular sinus macrophages (SSMs). We also studied lymph node lymphatic endothelial cells (LECs) and showed that integrin alpha 2b (ITGA2b) is expressed by a lymph node subset of LECs and its expression is sensitive to RANKL.

Keywords: RANKL, RANK, lymph node, macrophages, lymphatic endothelial cells, inhibitor